1988

Tests Of A Fractal Model Of Topography

Brian Klinkenberg

List of Figures

NOTICE

The quality of this microform is heavily dependent upon the quality of the original thesis submitted for microfilming. Every effort has been made to ensure the highest quality of reproduction possible.

If pages are missing, contact the university which granted the degree.

Some pages may have indistinct print especially if the original pages were typed with a poor typewriter ribbon or if the university sent us an inferior photocopy.

Previously copyrighted materials (journal articles, published tests, etc.) are not filmed.

Reproduction in full or in part of this microform is governed by the Canadian Copyright Act, R.S.C. 1970, c. C-30.

AVIS

La qualité de cette microforme dépend grandement de la qualité de la thèse soumise au microfilmage. Nous avons tout fait pour assurer une qualité supérieure de reproduction.

S'il manque des pages, veuillez communiquer avec l'université qui a conféré le grade.

La qualité d'impression de certaines pages peut laisser à désirer, surtout si les pages originales ont été dactylographiées à l'aide d'un ruban usé ou si l'université nous a fait parvenir une photocopie de qualité inférieure.

Les documents qui font déjà l'objet d'un droit d'auteur (articles de revue, tests publiés, etc.) ne sont pas microfilmés.

La reproduction, même partielle, de cette microforme est soumise à la Loi canadienne sur le droit d'auteur, SRC 1970, c. C-30.

TESTS OF A FRACTAL MODEL OF TOPOGRAPHY

by

Brian Klinkenberg

Department of Geography

Submitted in partial fulfillment
of the requirements for the degree of
Doctor of Philosophy

Faculty of Graduate Studies
The University of Western Ontario
London, Ontario
May 1988

ISBN 0-315-43299-3

Abstract

This thesis tested a fractal model of topography using a variety of measurement techniques (including the variogram method, the cell counting method, and the dividers method) applied to a range of surface types.. The methods were first tested for reliability and accuracy by applying them to simulated surfaces of known fractal dimensions. Then, the methods were applied to 58 datasets obtained from U.S.G.S. Digital Elevational Models which covered 9 physiographic provinces in the United States.

The fractal model was found to be a valid model. It fit some topographic datasets well but did not consistently fit all datasets. The fractal dimension was found to vary depending on elevation, direction, and sample size. Those methods which were applied to individual contours were found to consistently produce different dimensions than those methods which were applied to the surfaces. However, it was found that the physiographic provinces could be statistically distinguished using the fractal dimension (D). In addition, it was discovered that the intercepts obtained from the variogram analyses could also be used to separate landform types.

An interesting result of this thesis research was that the fractal model analyses brought to light differences within physiographic provinces that were otherwise not visible using traditional morphometric parameters.

New avenues of research have been identified as a result of the findings of this research.

This thesis is dedicated to the memory of my father,
Hans Klinkenberg

Acknowledgements

In the course of my stay at Western many people provided assistance; my thanks go to them all. In particular, my supervisor, Mike Goodchild, provided extensive support in many ways and expert guidance. Special thanks to Terry Van Kessel, Harry Taylor, Jr., Peter Keller, Maria Glieca, Diane Shillington, and to Don Janelle, for their continued support and encouragement. Sincere thanks also to my committee members -- Don Janelle, Brian Luckman and David Mark -- for their rapid reviews of the draft manuscript, and to Tom Poiker for his helpful comments.

This thesis was completed while working at the University of British Columbia, and I would like to extend my thanks and appreciation to the staff and faculty there for their support. In particular, Graham Thomas provided assistance when it was most needed.

Thanks must be extended to the University of Western Ontario, the Government of Ontario, and the Natural Sciences and Engineering Research Council for funding this research during the course of this thesis.

Thank you to my wife Rose, for her support, encouragement and patience throughout this work.

Table of contents

List of tables

List of Figures

Chapter 1

Introduction

1.1 Fractal research -- a new field

This thesis examines the application of fraotals, a recent mathematical concept, to the traditional geomorphological task of describing the form of landscape. The initial development of the concept dates back to the work of the French mathematician Benoit Mandelbrot in the sixties, but the term 'fractal' wasn't coined until 1975 (Mandelbrot, 1984d). In that short time, scientists have discovered a multitude of applications for fractals. Most of these have been in disciplines such as physics and particle science, but major corporations such as Esso and IBM are also studying fractals and are spending portions of their research budgets on the subject (Kadanoff, 1986). In certain fields within physics, the concept of fractals has revolutionized research so much that up to a third of all submissions to some journals relate to fractals in some form or other (Kadanoff, 1986).

The beginnings of this revolution in science can be traced back to a small number of publications, the most important of which is the text **Fractals: Form, Chance and Dimension**, published by Benoit Mandelbrot in 1977. The title of Mandelbrot's 1977 book can be used to explain why the concept of fractals has become so predominant in so many fields. The title - **Fractals: Form, Chance and Dimension** - can also be used to illustrate the various stages of research on fractals. The first stage is the investigation of **dimension**. That is, various methods are developed which allow scientists to determine the fractal dimension of the phenomenon under study. This important first stage of research is necessary, for the fractal dimensions of most aspects of nature are not known.

The second stage of research concerns the development of models which incorporate **chance** constrained within a fractal framework (fractal geometry). In the third stage the **forms** produced by the fractal models are compared to the original phenomenon and, most likely, the research cycles through the three stages until the fractal forms agree sufficiently with the natural phenomenon under study, or the fractal model is rejected.

The numerous fields of investigation which are based on fractals have advanced through various stages of this research cycle. For instance, the fractal models of rain developed by Lovejoy, Swertzer and Mandelbrot represent the results of several cycles. Lovejoy first reported on the fractal dimensions of clouds in 1982. Subsequently, a number of other papers were published which extended Lovejoy's results (Lovejoy and Schertzer; 1985, 1987; Lovejoy and Mandelbrot, 1985). In particular, investigations into the temporal and spatial variability of the fractal dimension allowed Lovejoy and his collaborators to obtain in-depth knowledge of the fractal geometry of rain and rain clouds. This knowledge was then used to guide the development of a fractal model which has allowed them to better understand the behaviour of rain and rain clouds. In developing their model they knew that it must constrain chance in a very specific manner in order to replicate the fractal variation of the rain they observed.

In geophysics, most research is still concerned with the first stage, that of measuring the fractal dimension of various phenomena. For example, Scholz and Aviles (1986) and Power et al. (1987) studied the fractal geometry of faults, and Kagan and Knopoff (1980) have studied the fractal dimensions of earthquake foci.

In geography research has not progressed much past the first stage. Papers by Goodchild (1982) and Mark and Aronson (1984) present the results of a number of investigations into the fractal geometry of terrain, while the papers by Burrough (1983b & c) report on his investigations into the fractal dimension of soils. However, most of the papers published in geography have been concerned with the development of various methods of determining the fractal dimension of cartographic lines, with a few papers on measuring the fractal dimension of terrain per sé. Prior to developing a model which better reflects the characteristics of terrain, the fractal geometry of terrain must be investigated in more detail.

There have been a limited number of investigations into the applicability of fractal geometry to digital models of the landscape, but as yet there has not been an in-depth study of a large number of landscapes from a wide geographic area. One previous study looked at a number of digital landscapes, but used only one analysis technique to test the applicability of the fractal model (Mark and Aronson, 1984). Conversely, a few other studies have used a number of analytic techniques, but then only applied them to one landscape type (e.g., Goodchild, 1982; Roy et al., 1987).

1.2 Fractals in Geomorphology

This thesis examines the application of fractal concepts to geomorphology. "Geomorphology is that science which has for its objects of study the geometrical features of the earth's terrain, an understanding of which has been attempted in the past within clearly definable, but not always clearly defined, spatial and temporal scales..." (Chorley, 1978, 1; his emphasis). If the objects of study exhibit nonintegral fractal dimensions, then processes operating within, or on, those objects should be studied within the framework of that object's fractal geometry (Le Mehaute, 1984, 666), and the precision with which limits to the spatial or temporal scales can be set should be open to question. For example, to properly model a (scaling) fractal phenomenon, the fractal dimension should be used as an integral component in any model of that phenomenon.

Dimensional analyses (e.g., Church and Mark, 1980) should be reconsidered in light of fractal geometry.

Form, or geometry, does not simply mean the topology of an object -- as some mathematicians would define it -- but rather a measure of the 'local' irregularity of the object (Mandelbrot, 1978, 236). The fractal dimension can be used to quantify one aspect of that form. When applying a new concept such as fractals to the study of landscape, a number of major concerns are raised, and these concerns, as expressed by the following questions, are the focus of this thesis.

1) Do the methods used to determine the fractal geometry of landscapes produce consistent results when applied to a variety of landscape types, and
2) are the techniques which have been suggested in the literature commensurate?
3) Are the measurement methods precise, and
4) do the values they return provide a reliable means of differentiating landscape types?

1.3 Structure of the thesis

Because this thesis applies a new concept -- fractal geometry -- to a series of traditional geographical concepts, an overview of both fractals and selected geographical concepts is presented first in chapters two through four. Then the specific applications which are being tested in this thesis, the methods used and the results, are presented in chapters five through seven, the bulk of the thesis. The final chapter, eight, summarizes the material presented in the preceding chapters and outlines new ideas for research.

CHAPTER 2

Concepts in Geomorphology

> As in any scientific study the first requirement in geomorphology is the exact description of what is seen or, in any way, sensed. Description is in some measure objective and lasting, while explanation is subjective and liable to change.
> ....
> Explanation ... should begin only after the phenomena have been described. (Hettner, 1972, 3)

Fractals have provided geomorphologists with a new way of looking at the form of the landscape. In addition, fractals provide a new method of modelling the landscape. However, unlike traditional models, fractal models are scale-independent. In this thesis, fractals are applied to the study of landscape form, and in order to provide a context for the role of fractal models in geomorphology the following methodological framework is presented.

Since form is such an important aspect of fractal research, the role in geomorphology of the study of form will be considered first. This is followed by a brief review of models used in geomorphology. Then, before considering the placement of fractal models in the suite of stochastic models available, two specific concerns will be discussed. First, the random character of nature will be considered in light of the two diametric views of randomness in nature held by geomorphologists. Second, the question of how scale influences perception of the form or process will be addressed.

2.1 Form and process

The dominant theme or theory of a given time governs which measurement techniques are considered appropriate. However, at the same time the measurement techniques available at any given time may constrain which theories are testable, and therefore determines which theories are dominant (see, for example, Chorley, 1972b, 9). Thus, "once a new technique becomes available, the whole scientific process can circle up to a higher level of investigation and explanation" (Goudie, 1981, 10). The changing approaches to the study of form and process in the last 40 years illustrate this point.

Two of the dominant themes in geography are the study of form and the study of process (Pattison, 1964; Amedeo and Golledge, 1975; Haining, 1981), particularly in geomorphology (Pitty, 1971; Small, 1978; Derbyshire, Gregory and Hails, 1979; Thornes, 1979; Evans, 1987). Although the qualitative description of form was a dominant characteristic of geomorphological study for many years (Pitty, 1971; Evans, 1972; Mather, 1972, 1979), it was replaced during the 1950s and 1960s by the study of process. This shift in approach followed the emergence of systems analysis as a basis of study (Pitty, 1971; Mather, 1979; Wrigley and Bennett, 1981, 259).

A dominant method in geomorphology prior to the 1960s was (1) to make inferences about processes based on investigation of form properties (Thornes, 1979, 386). This approach made extensive use of univariate and simple multivariate statistics, statistics which were consistent with the statistical sophistication of the geomorphologists of the time. A more recent method has been (2) to study processes and to make inferences about form and its development through time on the basis of the results of that study (Thornes, 1979, 387). This approach uses statistically complex techniques such as time-series models and entropy-based models (Wrigley and Bennett, 1981), techniques which have become commonplace only since the advent of computers.

Mather (1979) identifies two research approaches which parallel these two methodologies: (1) the functional and (2) the realist. The functional approach relies "on the mainstream logical positivist thesis that real world phenomena can be explained by showing them to be instances of repeated and predictable regularities in which form and function can be assumed to be related" (Mather, 1979, 471). The realist approach is more concerned with the identification of the causal mechanisms that underlie the observed phenomenon. Each approach uses analytical techniques appropriate to its philosophical orientation, as described above. Moreover, it is obvious now that the specific approaches reflected the limitations of the techniques available at the time the approach was in vogue.

Mather (1979) believes that a methodological approach should reflect the philosophical orientation of the researcher. Harvey (1971) states that there is a difference between adopting a particular method as a result of philosophical beliefs, and adopting it because it is an effective and convenient method. That is, a person who philosophically believes in determinism may use probabilistic models, "arguing that our own ignorance and inability was such that we required such an approximation in order to get anywhere with the analysis" (Harvey, 1971, 7). In addition, many observations are open to interpretations that, while opposing, are equally valid interpretations of the phenomenon under observation, and thus could provide support for conflicting philosophical positions. A philosophical position cannot be supported on the basis of a particular method alone, although the converse is possible -- a methodological approach can be upheld as consistent with a philosophical position (Harvey, 1971).

Haines-Young and Petch (1980, 63) state:

> In the same way as it is now found unacceptable that statistical techniques should be used without attention to their underlying assumptions, it seems equally undesirable that a particular methodology be employed without some attention to its underlying philosophical implications.

However, it is obvious that methods can be used independently from any particular philosophical stance -- the acceptance of a philosophical stance does not necessarily restrict the researcher to a particular set of techniques. Whether scientists really hold any particular philosophical stance, in a prescriptive or restrictive sense, is also open to question (Mather, 1979; Haines-Young and Petch, 1980). This is particularly so with the growing group of geomorphologists who belong to neither of the two categories defined by Mather above -- the applied geomorphologists.

This third group is more concerned with applied analyses than has been the case previously (Wheeler, 1978; Derbyshire et al., 1979, 47; Mather, 1979; Wrigley and Bennett, 1981). Partially as a result of this changing emphasis, the study of form is undergoing a renaissance. While the study of form may not provide much ground for theoretical explanations, it does allow for advances in applied techniques (Brunsden and Thornes, 1979; Goodchild, 1983). And, "description coming before theory is the usual pattern of science" (Mandelbrot, 1986, 11).

This revival of research into form itself also relates to the emergence of stochastic process models -- models which include fractal models -- as useful methodological tools in geomorphology (Goodchild, 1980a, 1980b; Culling, 1981; Wrigley and Bennett, 1981, 259). The use of these models may "aid in formulating additional or new problems" (Amedeo and Golledge, 1975, 88), and thereby contribute to theory development. Even in pure mathematics the study of form -- for example, pictures of mathematical functions -- has become a significant innovation which has led to advances in the field (Mandelbrot, 1984c, 1661).

Thus, delving into form is increasingly seen as a viable research priority in and of itself. However, this increased interest in form may be also a result of the disenchantment with systems analyses by some scientists. The more complex the landform studied by the geomorphologist, "the less useful are simple explanatory 'systems models' as aids to understanding and the more useful is a 'statistical' approach" (Pielou, 1977, 4).

> The difficulty of matching necessarily simplified but analytically tractable models with the evolution of complex landforms, from very imperfect knowledge, is most acute when dealing with the evolution of form (Thornes and Brunsden, 1977, 23).

2.2 Models

In geomorphology many researchers are moving away from deterministic to probabilistic modes of explanation. In part, this is a reflection of the maturation of probability theory which occurred in the 1930s and 1940s (Culling, 1981). The development of probability theory presented scientists with the opportunity to develop theories of nature that were not based on a simple deterministic viewpoint. This change of viewpoint reflected the geomorphologists' increasing awareness of randomness in nature, an awareness that has resulted in an increased interest in randomly-occurring phenomena (Thornes and Brunsden, 1977, 3).

Mark and Aronson (1984) present two classes of geomorphic models (see also Woldenberg, 1985). The first class is based on established geomorphic processes. The computer simulation by Davidson-Arnott (1981) of nearshore bar formation, developed after extensive research, represents this type of model. The second class is composed of models that are purely statistical in nature, with no direct links to known physical processes. The main aim of this type of model is to generate values which resemble real data in relation to predefined properties. "The parameters defining its inner form and workings need not have any physical interpretation" (Mather, 1979, 475).

Stochastic models, including fractal models, fit within this second class. In particular, fractal models belong to that class of stochastic model which incorporates the stochastic component directly rather than simply having the stochastic element entered as an external parameter, as in, for example, Monte Carlo techniques or probabilistic simulation models. Models based on simple independent-event random walks and Markov chains belong to the same class of stochastic models as do fractal models.

The emergence of stochastic process models is a reflection of the "recent recognition of randomness and apparent randomness in fluvial processes, geomorphic evolution, hydrology, landmass distribution, [and] geographical shapes..." (Mann, 1970, 95; see also Werritty, 1972, 167). For example, over the last 20 years the rank-size rule, the gravity model, central place hierarchy, and Horton's laws of stream channel form have all been shown to be mathematically consistent with random behaviour (Goodchild, 1983, 12). This reflects the growing awareness that randomness is an integral component of natural processes. A result of this awareness has been a shift in research methods. However, is the randomness inherent in the process, or simply apparent in the form? To answer this question the concepts of randomness and scale must be considered.

2.3 Randomness in nature

There are two dominant diametric views of randomness in nature (Mann, 1970; Krumbein, 1976). One view holds that the physical laws that are observed (e.g., Horton's law of drainage composition) are the result of many independent variables acting together. While the average is reproducible, the individual processes that make up the whole can be considered only in a statistical sense. That is, there is an element of inherent uncertainty in natural processes.

The other view holds that the individual processes are deterministic, but taken together they become a 'complex and undecipherable tangle' (Mann, 1970, 97; Smart and Werner, 1976). Thus, for "complex phenomena deterministic modelling is not always the optimum approach" (Krumbein, 1976, 50), and a statistical approach would be more appropriate.

For each view of the character of randomness in nature there is a rationale for using stochastic models:

1) The 'nature is deterministic' viewpoint. Every process has its characteristic temporal and spatial scale, and to be able to completely explain all of the variability present in the world is unlikely. Therefore, models which do not incorporate some aspect of randomness can never be expected to match the real world. However, "'average' or normative statements, which are of a statistical character, may be made about processes and the outcome of processes" (Thornes and Brunsden, 1977, 155). This is not to say that each process could not be deterministic when considered by itself, it is only when considered in toto that the processes appear random.

2) The 'nature is random' viewpoint. Many systems are composed of events that, for all intents, can be considered as independent random events. For example, the spatial distribution of falling raindrops is random by nature -- the position of each raindrop can be considered independent of the others. However, the pattern can be described in terms of its trend, mean spacing, etc.

In reality there is probably a complete spectrum of concepts. Few would argue that all processes can be predictable with complete certainty. That is, in practice many (deterministic) processes must be considered random because the specific predictors are unknown, and possibly likely never to be known. The concept of statistical determinacy, ranging from high probability to low probability, could apply to most phenomena. Similarly, the concept of randomness "entails only less specificity in nature than the traditional, strict deterministic interpretation" (Mann, 1970, 101). Calling a process random does not necessarily imply that the process is without direction, nor does it imply that it is independent of external environmental parameters (Mann, 1970, 98). If randomness has been recognized in a process or form, the question of why should be considered, along with the question of whether the randomness is truly random, or possibly 'deterministically random'. In response to these questions, various types of models, applicable to the study of random phenomena, have been developed.

2.4 Considerations of scale

The question of scale must be considered when describing a process or event as random. Within defined limits many processes appear random, but when considered at a finer or a coarser scale the same process may appear nonrandom. Consider a storm: the occurrence of a particular storm during a year can be considered as a random event, yet when the time frame is shortened to a few days, the storm is obviously not independent of the weather that preceded it nor that which followed it. Shorten the time scale even further -- to a second of time -- and the distribution of the raindrops appears random (Thornes and Brunsden, 1977). This example illustrates how a single process can be viewed ~~on a~~ continuum which ranges from random to nonrandom, with the process's position on that continuum dependent on the scale at which the process is viewed. The concept of scale is an important one in geomorphology (e.g., Pitty, 1971; Thornes, 1979; Church and Mark, 1980; Goodchild, 1980a & b, 1981), but one that is much less so when working with fractal models (Mandelbrot, 1984d).

The concepts of randomness and determinism are usually considered dependent on the scale at which the process is being analysed. At one scale a deterministic model may provide a complete description of the process, while at another scale the model may be totally inadequate -- at that scale the process may appear to be random. However, if that random process can be described by some probabilistic measure, it can be differentiated from many other random processes (Journel and Huijbregts, 1978). Thus, the use of probabilistic models "both opposes and completes the explanatory aspects of the standard, deterministic [geomorphological] approach" (Journel and Huijbregts, 1978, 1). Consider also that the model itself ~~may~~ be scale dependent, and that the process domains are simply a function of the model's dynamics. A scaling model -- a model that is scale independent -- may reveal consistencies in the process which span the previously observed domains. Models based on fractal concepts are by definition scaling models.

Note that many of the stochastic models which have been developed were developed in response to specific research problems, and are best described as grey or black boxes. "Application is often viewed as following rather than leading pure research, but harsh reality suggests the opposite" (Goodchild, 1985, 13). For example, the field of fractals owes much of its beginnings to research into transmission line noise, an engineering problem that Mandelbrot worked on around 1962. To a 'pure' researcher these models may be anathema, but to an applied scientist, results come first.

2.5 Stochastic models

Stochastic models, by their very nature, can produce extreme results. If a mismatch occurs when the results of the model are compared to the real world example, the question then arises: Does the model's results, or the particular real world example chosen, represent an extreme instance, or does the model misrepresent the problem? The answer to this question is of particular importance, for it is only by comparing the model to the real world example that the appropriateness of the model can be judged (Mather, 1979; Davidson-Arnott, 1981; Mandelbrot, 1983). Furthermore, when using a stochastic model, the success of the model should be judged only on the basis of its aggregate results; the model should not stand or fall on the basis of its component parts (Thornes and Brunsden, 1977, 156). When working with stochastic processes, or models of stochastic processes, the only significant statements are those of a statistical nature.

Why use stochastic models? Stochastic models complement existing methodologies and allow the researcher the opportunity to quantify processes or form in a manner not previously possible. The success or failure of a model also provides direction for further study (Davidson-Arnott, 1981; Kirkby, 1976). The three main concerns of simulation studies, as outlined by Harbaugh and Bonham-Carter (1970), are understanding, prediction, and control. Thornes and Brunsden (1977) further note that a simulation model can accommodate scale changes in time and space, and that a successful model can further our knowledge of the process or form.

Of course, simulation techniques are not without their problems. Few would argue that the components of most processes are completely described (Thornes and Brunsden, 1977), and that variables may be included in the model which are not relevant to the process (Amedeo and Golledge, 1975, 90). There is also the question of how best to judge the 'goodness-of-fit' of the results of the simulation. Some authors advocate numerical comparisons, whereas others claim that "the basic proof of a stochastic model of nature is in the seeing; numerical comparisons must come second" (Mandelbrot, 1982, 581). Attempting to judge the goodness-of-fit also raises the question of what is the proper null hypothesis for the process or simulation model? If an improper null hypothesis is selected, then any conclusions based on the results of statistical tests may be suspect. Finally, there is the problem of equifinality -- any given landform may be the result of a range of causes. "Similarity of form does not imply that those forms have been produced by similar processes" (Mather, 1979, 475). However, many geomorphologists would agree in principle that "if a computer simulation model produces surfaces that are indistinguishable from real terrain, a considerable step toward a quantitative theory of landforms will have been achieved" (Mark and Aronson, 1984, 672).

But, regardless of one's philosophical orientation with respect to randomness, probabilistic models are an important research tool. When using these types of models, the inner workings need not be meaningful. Mandelbrot (1983, 253) argues "that a lack of serious motivation in a model that fits and works well is much preferable to a lack of fit in a model that seems well motivated." However, not all researchers would agree with this. In addition, the statistical nature of the probabilistic models should be stressed; although, again, not all would agree with the viewpoint, as expressed by Mandelbrot, that the 'proof is in the seeing.'

The use of stochastic models has allowed scientists to quantify forms and processes that previously were 'noise' within a system. One such stochastic model -- the fractal model -- has become widely accepted and used in many disparate disciplines. The introduction of fractal concepts has allowed scientists to divide nature into three classes (following McDermott, 1984, 115): order (Euclidean geometry), manageable chaos (fractal geometry), and unmanageable chaos (no apparent geometry).

In the following chapters the concept of fractals will be described, and the uses to which fractal models have been applied reviewed.

CHAPTER 3

Introduction to fractals

For a small number of geographers the subject of fractals has evolved from one of mere curiosity to one of serious scientific pursuit. Because this transition has been restricted to only a few, many geographers are unfamiliar with the overall concept of fractals. Thus, a general introduction to the concept is now presented. Specifically, geometry, dimension and self-similarity, fundamental concepts of fractal research, are given special attention. In addition, the notion of texture, considered from a fractal point of view, is also discussed. Some of the discussion is based on a summary of the content of Mandelbrot's two books, **Fractals: Form, chance and dimension** (1977), and **The fractal geometry of nature** (1983).

Although fractal concepts were first used in a geographical context as far back as 1961 (Mandelbrot, 1967), few geographers in the 1960s and 1970s were aware of them. Only within the last decade have geographers 'discovered' fractals and their uses (for a recent review, see Goodchild and Mark, 1987). A more detailed discussion of some of the more geographical concepts of fractals, and examples of geographical analyses which have used fractals, will be presented in the next chapter.

There are two general classes of fractals: mathematical or nonrandom, and natural or random. Random fractals "are those that generate random patterns like the ones found in nature" (McClure, 1985, 52). They may be most useful in fields which make heavy use of statistics. This is particularly so in geomorphology because most geomorphic processes can never be documented completely. Mandelbrot (1983, 201) considers geomorphology to be a science that makes more use of statistics than most fields, due in part to the complex interactions involved in most geomorphic processes.

Nonrandom fractals, because they do not involve any stochastic component, are shapes which can be exactly replicated using a simple recursive procedure. Peano curves, Sierpinski's gasket, and von Koch's snowflakes are three of the better known nonrandom fractal curves or figures. Shapes such as these were labelled as 'monsters' by turn-of-the-century mathematicians because of their inability to describe them using conventional Euclidean concepts. But using fractal concepts, these monsters have become tamed (Gardner, 1976; Mandelbrot, 1984c). Although nonrandom fractals are used extensively in certain fields such as physics and computer graphics (e.g., Aharony, 1984; Le Mehaute, 1984; Orbach, 1984; Kadanoff, 1986), they are of little direct interest to geomorphologists. Thus, the following discussion relates more to natural fractals than to mathematical fractals.

As the titles to Mandelbrot's two books indicate, the concept of fractals incorporates geometry (or form), chance, and dimension. In order to develop a more complete understanding of fractals, the terms geometry, chance, and dimension will be discussed in detail in this chapter.

3.1 Geometry and dimension

Euclidean geometry -- the geometry of points, lines and areas -- has become so familiar that it is the invisible framework within which most people work. It has become "an article of faith" (Robinson and Petchenik, 1976, 66). The concept of another geometry -- or more explicitly, that there could be dimensions between those implicit in the notions of points, lines and areas -- is a foreign one. "The idea of dimension is fundamental to our view of the real world ... and is implied in most descriptions of the landscape" (Culling and Datko, 1987, 370). With the introduction of fractals the framework of Euclidean geometry is made visible, and many of the implicit notions must be reconsidered. As McDermott (1984, 111) notes: "Fractals delineate a whole new way of thinking about structure and form."

The Euclidean dimension is represented by a positive whole number. This number (E) equals the number of coordinates necessary to define a point. For example, to specify any point on a profile requires two coordinates (x,y), thus a profile has a Euclidean dimension of two. To describe a point on a surface requires three coordinates (x,y,z), therefore a surface has a Euclidean dimension of three. Euclidean geometry is restricted to dimensionally concordant sets, sets for which all dimensions coincide (i.e., all phenomena are assumed to have integer-valued dimensions). Within Euclidean space (R^E, with dimension E) the topological dimension (D_T) coincides most closely with our intuitive sense of dimension. The topological dimension is also always integer valued, and $D_T \leq R^E$. Thus, on a flat piece of paper (E = 2) one can draw a 2-dimensional figure ($D_T = 2$), a 1-dimensional line ($D_T = 1$) and a 0-dimensional point ($D_T = 0$).

In 1977 Mandelbrot formally introduced another dimension: the fractal dimension (D). This dimension need not be an integer, and need not coincide with the topological dimension. Fractals are dimensionally discordant. The relationship between the above three dimensions can be expressed as:

$$0 \leq D_T \leq D \leq E$$

Within Euclidean geometry, D always equals D_T. Within fractal geometry, the fractional dimension D can take on any value which lies between the topological dimension of the phenomenon under study and the Euclidean dimension of the space within which the phenomenon occurs.

Mandelbrot at first defined the fractal dimension in terms of the Hausdorff-Besicovitch dimension (e.g., Mandelbrot, 1983, 15), but he has since disassociated the two terms, feeling that the Hausdorff-Besicovitch dimension is but one representation of the more general fractal dimension (Mandelbrot, 1984b, 909). He goes on to state:

> Today, I use the term "fractal dimensionality" generically, as equally applicable to numerous, but not all, specific definitions of anomalous dimensionality, and I try not to have to define "fractal" (Mandelbrot, 1984b, 928; his emphasis).

Mandelbrot (1984c) has also reversed his previous restriction on the limits of the fractal dimension -- that it must strictly exceed the topological dimension. He now states that in some cases one metric may return a dimension equal to the topological dimension, but yet the phenomenon may still be fractal as determined by some other metric. In the theoretical mathematics literature the property of 'being fractal' may be referred to as erraticism (Adler, 1981, 187).

The topological dimension tells us little about how shapes differ. All coastlines, for example, have the same topological form or dimension ($D_T = 1$). However, not all island coastlines are identical in form. It has been shown (Goodchild, 1980b; Mandelbrot, 1983) that different coastlines generally have differing fractal dimensions. Thus, "differences in fractal dimension express differences in a nontopological aspect of form" (Mandelbrot, 1983, 17, his emphasis). Fractals quantify the metric information in lines and surfaces in a new and unique manner.

The implicit notion of length should be reconsidered in light of fractals. For standard Euclidean curves, such as a circle with a radius of 3 cm, the length can be determined, and there will be little argument that the measurement does, in fact, represent the 'true' length. These curves are defined as rectifiable. However, consider measuring a natural curve, such as a section of the coastline of Newfoundland. If the measurement is made with a 'yardstick' that is 1 km long, and then with a yardstick that is 0.5 km long, and so on until the yardstick is only 1 m long, it will be apparent that for each yardstick a different coastline length is obtained. Stated in a more general way, as the measurements become more precise the length appears to increase without bound (Mandelbrot, 1983, 27). Fractal curves that exhibit this tendency are defined as nonrectifiable. Geographical curves are often nonrectifiable, a fact explicitly considered by Richardson (Mandelbrot, 1967, 1975a). The question of whether geographic lines had 'natural limits' was a subject of debate by cartographers at the turn of the century (Poiker, personal comm., 1988).

Cartographic generalization produces similar results. As the scale of the map decreases, fewer (finer) details of a coastline, for example, can be represented. Thus, as the scale decreases -- as the yardstick increases in length -- the scaled length must decrease. Measurements of complex natural features represented on maps of differing scales are apt to return values which appear to be a function of the scale.

The question then arises: How can one compare curves whose lengths are nonrectifiable? Mandelbrot (1983, 30) shows that the fractal dimension (D) of a curve is theoretically independent of the measurement precision, or, equivalently, of the scale of the map. Thus, D can be used as a measure by which natural curves --fractal curves -- can be compared.

The length of the bounding curve of a shape is often an important component in shape parameterization. Shape indices are used in a wide variety of fields (Boyce and Clarke, 1964; Pavlidis, 1978; Dutton, 1981, 23; Woronow, 1981; Kennedy and Lin, 1986). Consider the indices of length, $(\text{area})^{1/2}$, and $(\text{volume})^{1/3}$. These measures provide alternative descriptions of shape, and the ratio of any two of them should be a unitless shape parameter (Church and Mark, 1980). Thus the relationship

$$(\text{area})^{1/2} = \beta(\text{length}) \qquad [1]$$

holds for circles ($\beta = \frac{1}{2}\pi^{-1/2}$) and squares ($\beta = 1/4$), and all other Euclidean shapes. However, Hack (1957), after measuring the lengths of the main river within a number of drainage basins, found the relationship between length and area to be:

$$(\text{area})^{1/2} \propto (\text{length})^{1/D} \qquad [2]$$

with D = 1.2, which is definitely above the implicit D = 1 in [1]. Since Hack's original study, further tests have been made of this relationship. It has been observed that the empirically derived value of D holds for both short and long rivers, but that for very long rivers within very large drainage basins (area > 10^4 km^2), the value of D approaches one (Mandelbrot, 1983, 111; but see Church and Mark, 1980, 359-364). This implies that maps of short and long rivers, and their associated drainage basins, drawn at different scales such that they would fit within equal areas on a piece of paper, would look the same. However, similar maps of very long rivers would appear to be much straighter.

In conjunction with the question: How long is the coast of Newfoundland, there is the closely associated question: How many islands are there off of its coast? The total number of islands appears to increase with increasing resolution because smaller and smaller shapes are plotted on the larger scale maps. Continuing with this thought, further questions then arise: Is there a theoretical limit to the number of islands, and is there a relationship between the areas of the islands? The second question has been considered and a relationship has been determined -- the 'Korcak empirical relation for islands' (Mandelbrot, 1983, 117). The relationship, which incorporates the fractal dimension D, is represented by this equation:

$$Nr(A>a) = F' a^{-(D/2)} \quad [3]$$

where $Nr(A>a)$ represents the number of islands of greater than known area a, and

F' is simply a positive constant.

From equation [3] it is evident that as the area (a) approaches zero, the number of islands with area greater than area (a) approaches infinity, thus answering the first question posed above. Mandelbrot also concludes that the cumulative area of the very small islands is finite and negligible:

> the largest island's relative contribution to all the islands' cumulative area tends to a positive limit as the islands increase in numbers. It is not asymptotically negligible. (Mandelbrot, 1983, 119, his emphasis)

An additional consequence of the fractal nature of coastlines is that the cumulative length of the coastlines of the smaller islands is infinite. This means that the relative contribution of the coastline length of the largest island to the cumulative length of all coastlines becomes negligible.

These two observations have implications in fields such as biogeography where delimiting the distribution of a species or environmental factor is often a primary research focus. If the research is concerned with interactions across a boundary, then attention must be given to determining all locations where the factor or species occurs. However, if the research is more concerned with an estimation of the population size or resource base, then the benefits of further searching can be continually monitored and the costs weighed against the diminishing returns.

The Korcak empirical relation for islands is theoretically derived from the hyperbolic distribution. If island areas have a hyperbolic distribution, then why not lake areas also? Most researchers would agree that most non-glaciated landscapes contain far fewer lakes than oceans do islands. This fact can be accommodated by the relation through restriction of the prefactor F' to values smaller than those used when working with islands. F' sets the absolute value for the area of the ith island or lake. Thus, if F' is set to a small enough value the area of the $(i,\infty]$ lakes rapidly become negligible. In fact, the areas of the world's larger lakes have been found to follow a hyperbolic distribution (Goodchild and Mark, 1987).

Mandelbrot feels that the hyperbolic probability distribution is the most appropriate distribution with which to model natural phenomena (Mandelbrot, 1983, 262). (A random variable U is called hyperbolic when $P(u) = Pr(U>u) = Fu^{-\alpha}$, where Pr stands for probability.) However, this view of nature is not supported by the many scientists who believe that the lognormal distribution underlies most natural phenomena[1]. In geomorphology, for

---

[1]The statistical model which results in a lognormal distribution is very appealing. In a biogeographical context, the abundance of a species is lognormal if the

example, Speight (1971) expects slopes to display a log-normal distribution, but see O'Neill and Mark (1987). Mandelbrot (1983) indicates that many fractal measures can be derived from the hyperbolic distribution and, in fact, many geographical phenomena have been found to follow a hyperbolic distribution (Goodchild and Mark, 1987). A few other examples include the areas of craters found on the moon, Mars, etc., the rank-size rule of cities, cave lengths, and the spatial distribution of some mineral resources -- all have been found to follow a hyperbolic distribution (Hartmann, 1977; Mandelbrot, 1963, 1983; Goodchild and Mark, 1987).

3.2 Self-similarity and fractional Brownian motion

Randomness does not necessarily imply haphazardness, or complete unpredictability (section 2.3). For example, we can speak of self-constrained chance and of nonconstrained chance. For many geomorphic processes the present outcome is often constrained by the outcome of an earlier stage, and "is strongly self-constrained by the geometry of space" (Mandelbrot, 1983, 203; my emphasis). Although the notion of self-constrained chance is conceptually easy to grasp,

---

number of individuals of that species is the result of a large number of independent causes that are multiplicative in their effect (Pielou, 1977, 47; May, 1975). The log-normal distribution is a reflection of the Central Limit Theorem, although Mandelbrot (1983, 423) would argue that there are other equally valid central limit theories that result in other distributions, such as the hyperbolic.

the development of models that incorporate this type of chance is fairly difficult. Thus, most stochastic models are based on nonconstrained chance.

Consider a map of the eastern coastline of Newfoundland. At one scale, it would appear that a tangent to the coastline could be defined for any given point. However, if the scale were increased, the point at which the tangent was taken would now be composed of a number of curved sections (e.g., bays and spits too small to plot at the smaller scale). This process can be repeated (theoretically) for many rescalings -- leading to the conclusion that the coastline never has a tangent. The coastline is, of course, a continuous curve. When considered jointly, coastlines can be defined as continuous curves which never have tangents. Previous mathematics, based on Euclidean precepts, do not have methods which adequately deal with such curves (Gardner, 1978). However, the concept of fractal geometry allows one to deal effectively with such curves.

Formally, fractals are non-differentiable continuous curves. A curve, or more precisely, a function, is differentiable if, for every point, a tangent exists. In order for a tangent to exist, the function, when taken to the limit (e.g., a segment defined by two points an infinitely small distance apart is considered), must appear smooth or 'flat'. A fractal curve, when taken to its limit, will always (theoretically) exhibit more curves -- it will never be smooth or 'flat', as in the example of the coastline above. Brownian motion is the most common example of a continuous, non-differentiable stochastic process. (A Koch curve, and a Peano curve are two common examples of continuous, non-differentiable nonrandom processes.)

Brownian motion was first described by the botanist R. Brown around 1826, and "together with the Poisson process it constitutes one of the two fundamental species of stochastic processes, in both theory and application" (Chung, 1979, 249, his emphasis). It is the most widely studied Gaussian process, and perhaps the most important (Adler, 1981, 184). (For a formal definition of Brownian motion see Chung, 1979, 250; Mandelbrot, 1983, 351; or Lavenda, 1985.) Unbounded Brownian trails, with $D_T = 1$, have a $D = 2$. That is, considered from $-\infty$ to $+\infty$, a Brownian trail will cover or fill a plane completely. Further characteristics of a Brownian trail are:

1) the probability that a given point will be crossed by the trail is zero,
2) the probability that the trail will pass within a given distance ε of a given point is 1, and
3) a Brownian trail has stationary increments and exhibits statistical self-similarity (figure 3.1).

Informally, self-similarity implies that a portion of the curve (or function), when considered at a reduced scale, would appear similar to the whole curve. The bottom, boxed

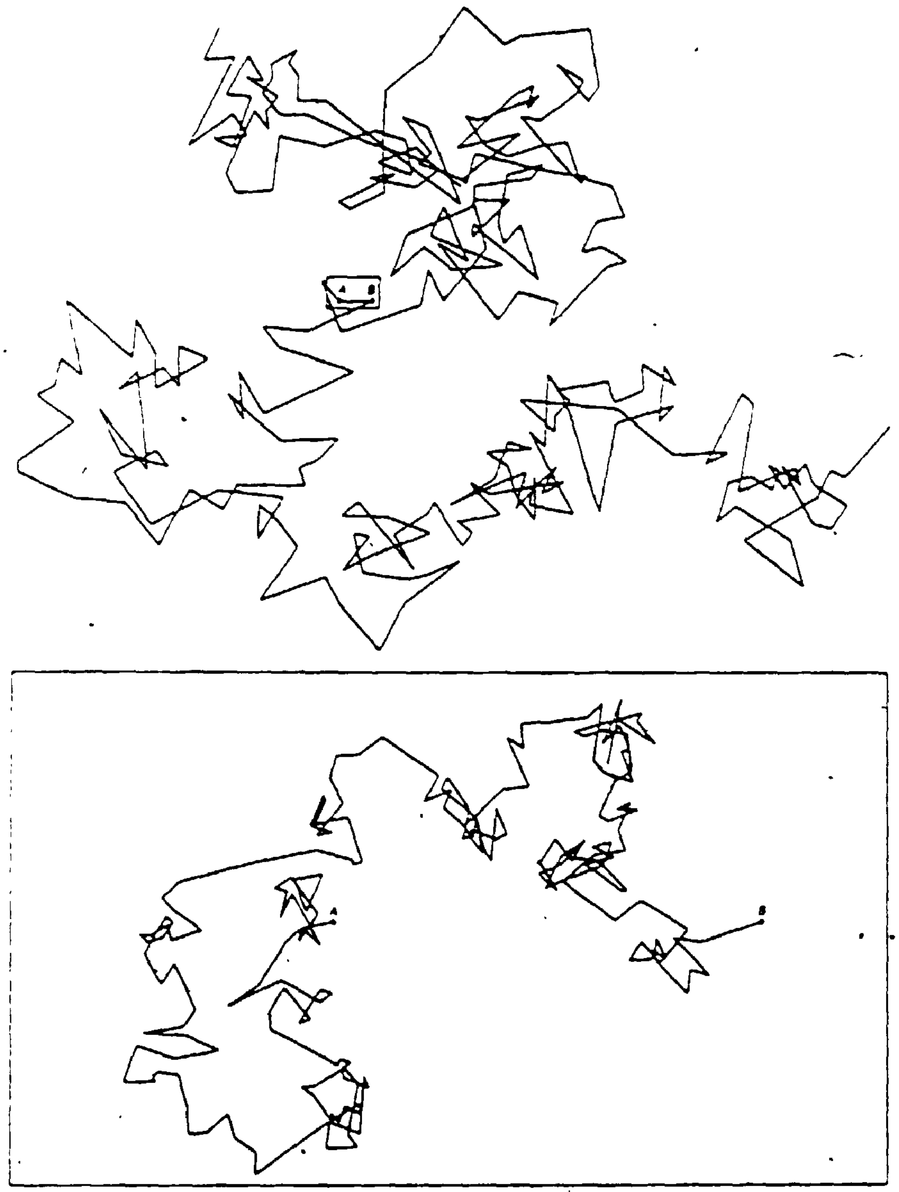

Figure 3.1 Brownian motion.

This figure illustrates the concept of statistical self-similarity. The upper diagram illustrates the motion of a microscopic particle suspended in water. The lower diagram represents the path from A to B -- shown as a straight line in the upper diagram -- magnified 100 times. Source: Lavenda, 1985.

portion of figure 3.1 appears similar to the top portion, yet it represents only that small portion of the top curve from A to B.

For mathematical or non-random fractals, self-similarity can be exact because the mathematical function which defines the fractal ensures that the parts are identical to the whole. For random or natural fractals, self-similarity is considered in a statistical, or visual sense. The visual self-similar nature of maps of river basins was considered previously. Statistical self-similarity can be formally defined as follows.

Given $T < \infty$, $h < 1$, and allowing t to vary from 0 to T, $h^{-1/2}B(ht)$ is statistically identical to B(t) (Mandelbrot, 1983, 236). This can be shown as follows. The displacement vectors of $\Delta B(t)$ are random normal variables, independent and isotropic. Considered over an arbitrary succession of equal time increments Δt, it follows that:

$$\langle \Delta B(t) \rangle = 0 \qquad \text{(where } \langle\rangle \text{ represents the expectation.)} \qquad [4]$$

and

$$\langle [\Delta B(t)]^2 \rangle = |\Delta t|. \qquad \text{(From the formal definition of Brownian motion, as in Chung, 1979, 250.)} \qquad [5]$$

If Δt is scaled by the ratio h, then [4] becomes:

$$\langle h^{-1/2}\Delta B(ht)\rangle = 0 \quad [6]$$

and

$$\langle [h^{-1/2}\Delta B(ht)]^2\rangle = h^{-1}|h\Delta t|$$

$$= |\Delta t| \quad [7]$$

Isosets are defined as sets of constancy of the coordinate functions X(t) and Y(t) of the function B(t). The zeroset is the isoset most often discussed in the literature, and is defined as those instants t for which X(t) = 0 (Mandelbrot, 1983, 236). While the intervals between zeros are independent random variables, the pattern of zeros is distinctly clustered. For example, sea level is a natural zeroset. A height profile along a line of latitude or longitude, and the plane formed by a contour are examples of isosets. If the surface has a dimension (D), then the isoset has a dimension of (D - 1), by definition. For example, if a surface has D = 2.2, an isoset of that surface will have dimension D = 1.2.

Fractional Brownian motion (fBm) is a generalized form of ordinary Brownian motion. Ordinary Brownian motion has independent increments and is a process without persistence -- it does not have a memory. Mandelbrot (1983, 245 & 260) introduces a parameter H [often referred to as the Hurst scaling parameter (Culling, 1986)], which is related to D through the expression D = 3 - H for a surface, and D = 2 - H for a line (i.e., for the phenomenon under consideration, $E = D + H$). By allowing H to vary from 0 to 1, Mandelbrot generalized the concept of Brownian motion. Except for the special case when $H = 1/2$ (which corresponds to ordinary Brownian motion), fBm processes have a memory. When $1/2 < H < 1$, the fBm exhibits persistence, or has positive correlations among the increments, and the one-dimensional trails have dimension D between 1 and 1.5. When $0 < H < 1/2$, the process is antipersistent, with negative correlations, and the trails have dimension D between 1.5 and 2.0. The result is that antipersistent fBm fills the space more slowly than ordinary Brownian motion.

Because of the relationships which exists between H, the dimension of a surface ($2 \leq D \leq 3$), and the dimension of any isoset of that surface ($1 \leq D \leq 2$), the values of H and D which are used in the following chapters are used in a nonrestrictive manner. That is, unless otherwise noted, if the value of D is given as a number between 1 and 2, the value specifically refers to the dimension of an isoset; if the value of the dimension is given as a number between 2 and 3, the value refers to the dimension of a surface. The value of H can be used to define either the dimension of a surface or of an isoset. The context in which the values are used will make it clear whether the value of H should apply to a surface or an isoset. In addition, for ease of comparison in tables and figures, the dimensions obtained from the isosets will often be referred to as if they were obtained from a surface (i.e., the isoset dimensions will have one added to them, so that instead of D having a value between one and two, D will have a value between two and three).

3.3 Fractals and Scale

The question of scale must be considered when describing a process as random (section 2.3). Throughout his book Mandelbrot (e.g., 1983, 27 & 103) indicates that the fractal characteristics of curves, surfaces, or processes may only apply within defined limits or zones. The scale dependence of D is a recurring theme in many of the papers that have been written on fractals. For example, scale dependence is discussed at some length, from a geomorphological viewpoint, in Mark and Aronson (1984). However, work by Lovejoy and others on multifractals may eventually provide a means of accounting for, and eventually modelling, scale-dependent fractal forms (Mandelbrot, 1986b).

3.4 Summary

The discussion up to this point has shown how analyses of many of the planar features of the Earth's surface, such as the length-area relationship for rivers, the number-area rule for islands, and the near infinite aspect of coastline length, have involved the use of fractals. Other aspects of the landscape, such as the scalelessness evident for some features (e.g., profiles of mountains, within defined limits), further reinforce the notion that the Earth's surface may be modelled by a fractal surface. Mandelbrot presented some of the earliest examples of Brownian landscapes in his 1975a paper, and the colour plates in his 1983 text clearly illustrate how close the computer images have come to representing real terrain. Since 1975 computer scientists have spent considerable effort on improving the qualitative aspect of Brownian landscapes (Carpenter, 1980; Fournier, Fussell and Carpenter, 1982a). Few scientists, however, have considered the quantitative fractal aspects of landscapes, with the exceptions of Goodchild (1982), Mark and Aronson (1984) and more recently a few others (e.g., Culling and Datko, 1987; Roy et al, 1987; Anderle, 1987).

In the following chapter a number of studies will be presented which have utilized fractals in a number of innovative ways. These studies provide an indication as to why fractal models are of importance to geography in general, and to geomorphology in particular.

CHAPTER 4

Applications of fractals

In the previous chapter the general concept of fractals was introduced. In this chapter, specific examples of how the concept of fractals has been applied will be reviewed in order to illustrate the broad utility of fractals in geography. Although geomorphological concepts are the main focus of this thesis, the research will also look at related concerns in cartography. Thus, the discussion of why determination of the fractal dimension has attracted so much attention will include sections on cartography and terrain analysis. This overview chapter will be followed by a review of the methods which have been used to determine the fractal dimension (D), and discusses those methods which are evaluated in this thesis and how they are implemented.

4.1 Non-random fractals

There have been a few notable applications of nonrandom fractals (Goodchild and Mark, 1987). Goodchild and Grandfield (1983) were concerned with optimizing raster storage, and felt that an ordering that preserved the spatial relationships present in geographical data theoretically would be of greatest benefit. In light of this, they felt that a Peano-based ordering would best reflect the autocorrelated nature of most natural phenomena better than, for example, conventional row ordering. Goodchild and Grandfield (1983) compared four ordering alternatives, and empirically found that the Peano-based ordering performed the best. However, based on an analytical study none of the four orders produced optimum efficiency, resulting in a mixed result. Mark and Lauzon (1984) and Lauzon et al. (1985) developed a quadtree data structure, known as two-dimensional run encoding (2DRE), based on the deterministic Morton fractal ordering. Arlinghaus (1985) has shown that the geometry of central place theory is a subset of a particular type of mathematical fractal shapes. However, of the two general classes of fractals, random fractals have received the most attention from geographers. Thus, the bulk of this chapter will consider random fractals.

4.2 The fractal dimension as a simple parameter applied to random fractals

The most basic use of random fractals was expressed by Kadanoff (1986, 7): "If two objects are the same they must at least have the same fractal dimension." Thus, determination of **D** is one means of comparing two objects. However, the fractal dimension does not provide a unique identification -- two objects which look different can have identical values of D -- although it can provide a means of distinguishing between objects, as examples below will illustrate.

The use of D as a simple parameter has received some attention. A topographic profile can be described using only D and an amplitude parameter (Fox and Hayes, 1985). The fractal dimension may have "wide application in geomorphology as a well defined comparator of irregular phenomena" (Culling, 1986, 95). Kaye (1985) notes that D provides a useful working concept which we can interpret as being descriptive of the space-filling ability of a phenomenon. In particle science, fractal analysis has emerged as the image analysis technique "most suited to the characterization of rugged or re-entrant particle surfaces" (Clark, 1986, 45). And as Goodchild and Mark (1987, 267) state:

> The numerical value of D may be the most important single parameter of an irregular cartographic feature, just as the arithmetic mean and other measures of central tendency are often used as the most characteristic parameters of a sample.

In soil-covered landscapes, Culling and Datko (1987, 384) note that D can be used to differentiate between surfaces "ostensibly of different evolution and can be used to monitor the progress in the struggle between rejuvenation and degradation." It is important to note that the fractal dimension is a true mathematical 'measure' (Culling, 1986). Because of this, it possesses well defined properties (cf. Lovejoy et al., 1985) which means that determining D is not simply an end to itself; D is an extensible statistic.

Mandelbrot (1983, 130) presents the results of a study that analysed the canopy outlines of the Okefenokee Swamp in Georgia using the Korcak empirical relation for islands. The study found that for cypress trees D ≈ 1.6, while for broadleaf and mixed broadleafed areas D was much closer to one. The investigators felt that analysis and monitoring of the fractal dimension could provide a means of quantifying change to the system (McDermott, 1984, 111). Another related study looked at the fractal dimension of the shape of a coral reef (Bradbury <u>et al</u>., 1983, 1984; Mark, 1984), and found that there were sharp transitions in the observed dimensions of the reef.

The following study on a measurement network further illustrates the use of D as a prescriptive parameter. Lovejoy <u>et al</u>. (1985) determined the fractal dimension of meteorological stations across Canada and found that the Canadian meteorological network has a fractal dimension of 1.5. They further show that, in the case of the Canadian meteorological network, any phenomenon with a dimension less than 0.5 will almost certainly be missed or not detected by the network[2]. Of particular interest to meteorologists are those rare events that are extremely intense -- such as tornadoes. According to work by Lovejoy and Schertzer (1985), these events will have small fractal dimensions

---

[2] A value obtained by subtracting the dimension of the measuring network (D = 1.5) from the Euclidean dimension of the embedding space, (E = 2.0), following a theory in geometry on the intersection of two sets.

(i.e., less than 0.5), possibly accounting for the low number of tornadoes recorded by the meteorological network.

This exclusion of sparse but intense phenomena from the records results in biases in geophysical statistics, difficulties in interpolating measurements, and problems in calibrating instrumentation. Thus, prior to setting up a network of measuring stations, the theoretical fractal dimension of the network could be calculated and the network adjusted so that it exhibited the highest D possible. Similarly, existing networks could be analyzed and new stations added based on this criterion. Such analysis could be important in a wide variety of fields.

The fractal dimension of a phenomenon is not expected to be constant -- it is expected either to apply to a range (through time or space) or to vary continuously according to some function (Scholz and Aviles, 1986; Lovejoy and Schertzer, 1986; Mandelbrot, 1977 and 1984; Kennedy and Lin, 1986). Therefore, findings that a single D does not apply to an object under study are to be expected. As Pentland (1984, 666; his emphasis) states:

> Physical processes do not typically act at all possible scales but rather only over a range of scales. Thus, we should expect that a physical surface (and thus its image) will change its fractal characteristics when we pass from a range of scales dominated by one formative process to a range of scales that was shaped in a different manner.

If most geographical phenomena are the result of the interactions of several processes, each of which is dominant over a different range -- but each of which is also scaling

-- then the dimensional plot of one such phenomenon should show a series of straight-line segments corresponding to the dominance ranges of the different processes. Some examples follow.

In their analyses of terrains, Mark and Aronson (1984) note that the scales at which the dimension changes could be of use in defining homogeneous geomorphological provinces; Fox and Hayes (1985) used a 'province picker' in their spectral analysis of seafloor terrain. The study by Pentland (1984) used a similar rationale to define 'edges' between homogeneous areas in digital images. Kent and Wong (1982), in their study on the fractal nature of the shorelines of lakes on the Canadian shield, felt that the break in the dimensional plots occurred where the dominance from large-scale glacial corrasive processes switched to smaller scale erosional processes.

Kaye (1985, 32), in an analysis of aluminum shot particles, felt that the placement of the break in the dimensional plot was "a measure of the magnitude of the turbulent forces versus the surface tension forces which competed with each other to produce the final shape of the aluminum shot fine particle." Above the break the turbulent forces dominated, below the break the surface tension forces were dominant. Thus, the value at which the dimension changed was an indication of the efficiency of the manufacturing process (the smaller the value the more efficient the process). In a similar study, Kennedy and Lin (1986) deduced that the break represented the change from a description of the gross shape, to one representative of the surface texture. Mandelbrot et al. (1984) have made similar statements with respect to fracture surfaces of metals and its fractal dimension.

4.3 Fractals and cartography

Fractal geometry will play an important role in cartography, as the statement from Goodchild and Mark (1987) quoted at the beginning of this chapter indicates. Many researchers [e.g., Dutton (1981); Shelberg and Moellering (1982); Armstrong and Hopkins (1983); Dell'Orco and Ghiron (1983); Muller (1986, 1987)] have considered the applications of random fractals to cartography. These geographers have addressed concerns such as how to determine the fractal dimension of digitized curves, and how to restore fractal qualities to digitized lines. As an example, Dutton's and Muller's works are discussed in more detail below.

Cartographic or map data follows fractal geometry much more than it follows standard Euclidean geometry (Dutton, 1981). This fact led Dutton to consider that "perhaps it is possible to subject strings of coordinates describing lines on maps to algorithms that modify them according to fractal criteria" (Dutton, 1981, 25). With this aim Dutton developed an algorithm that added detail to digitized lines in a self-similar manner. For certain types of maps, such as precise topographic maps, this technique would be inappropriate. However, for thematic maps and those used in vehicular navigational systems, where appearance may be more of a concern than precise boundary definition (Hill and Walker, 1982), the technique has potential. With suitable algorithms (e.g., Fournier et al., 1982; Jeffrey, 1987) much smaller data bases could be used, while at the same time presenting to the map user an aesthetically correct image (e.g., coastlines would have rugged outlines, rivers suitable meanders) (Hill and Walker, 1982). Of course, many cartographers feel that adding wiggles to any cartographic line is unwarranted cartographic practice.

On standard topographic maps feature generalization is very structured (Gloss, 1972). Most cartographic institutions have well defined criteria by which to judge the accuracy of contour lines (Lawrence, 1979; Muller, 1986). However, the question of judging the results of line generalization -- and in particular automated line generalization techniques -- requires a different, usually subjective, approach (Muehrcke, 1972; Monmonier, 1982; but see Maling, 1968, 153). Muller (1986) suggests the use of the fractal dimension as a means by which to judge line generalization techniques (also see Eastman, 1985). That is, those line generalization methods which best preserve the fractal dimension of the original line would be judged as better than those methods which do not preserve the fractal dimension as well.

Similarly, the fractal dimension of a cartographic line can be used as a predictor of the number of points needed to adequately describe the line (Muller, 1987). Lines with high Ds would require many points to be completely described; lines with low Ds could be described with much fewer points. This notion of using the fractal dimension as a measure by which to judge the benefit or appropriateness of some future action has generated some interest, although it is an area that warrants further research. For example, Mark and Aronson (1984) note that surfaces with high Ds do not lend themselves well to interpolation techniques because of their low autocorrelation. In the same light, Goodchild and Grandfield's (1983) work on data compaction techniques found that on surfaces that had high Ds, no method performed significantly better than any other. Thus, knowledge of the fractal dimension of a phenomenon will provide preliminary assessment of the benefit of data compaction, or the penalty associated with interpolation. In this light, fractal 'landscapes' could be used as the foundation upon which tests of contouring algorithms and line generalization routines could be conducted.

4.4 Fractals and shape indices

As introduced in the previous chapter, the use of D in indices is another area where fractals may have a significant role to play. Using fractals, geographers can develop shape indices that are nondestructive of information

(Pavlidis, 1978; Dutton, 1981). Goodchild (1980a & b) shows how the fractal dimension provides a common framework for the problems of length, area, and point estimation. In a more applied analysis, Woronow (1981) shows how a fractal shape measure can be used to differentiate between classes of ejecta deposits on Mars.

Woronow's analysis, presented below in some detail, represents a type of analysis that could become widely used in geomorphology (c.f., Church and Mark, 1980). Traditional studies of the scaling nature of crater ejecta are usually approached in a different manner -- with multi-parameter non-fractal models (e.g., Housen and Schmidt, 1983). Studies similar to Woronow's have been conducted, including Kent and Wong's (1982) analysis of the traditional morphometric indices used in biology.

In quantitative geomorphological studies the different resolution capabilities of measuring devices, coupled with the different resolutions associated with the physical size of the landform itself, can lead to measurements that are dependent upon the measurement scale (Woronow, 1981). For example, if the perimeters of a number of areal features -- identical in plan outline but of varying size -- are measured, the relationship of their perimeters to their (area)$^{1/2}$ will not be linear. This nonlinearity would be the result of details that were included in the perimeter measurements of the larger features but were too small to be included in the perimeter measurements of the smaller features. This dependency of quantitative measurements on the measuring resolution "can present considerable obstacles to meaningful quantitative description, classification, and modeling of landforms because the data may appear internally inconsistent" (Woronow, 1981, 202).

However, the concept of the fractal dimension allows for the interplay of quantitative measurements, size differences, and the resolution of the measuring device. Woronow (1981) used a fractal measure to determine if genetic relationships exist among craters on Mars. He concluded that the three classes of craters that are observed on Mars are the result of different physical processes, and are not different simply because of their varying sizes.

Woronow's analysis was based on a measure derived from a simple perimeter-area relationship For simple Euclidean shapes the relationship between the area and perimeter is independent of changes in the resolution of the measuring instrument, and can be expressed as:

$$P/A^{1/2} = K \qquad [8]$$

where P is the perimeter, A is the area, and K is a constant. Woronow (1981) developed a similar equation for fractal curves:

$$\frac{P^{1/D}}{A^{1/2}} = K \qquad [9]$$

Using non-linear regression Woronow determined the fractal dimension (D) for the three classes of craters (the dimensions were 1.03, 1.08 and 1.27). He concluded that the fractal dimension "indicates, in a general sense, how crenulated the edge is, while K indicates the overall geometric shape (e.g., circular, elliptical)" (Woronow, 1981, 215). Note that these two parameters are not independent, and thus must be considered jointly in reaching a conclusion.

Although Woronow's analysis dealt with Martian ejecta deposits, his method has wide application in geomorphology. Fractal dimensions "are relevant to problems in geomorphology where the areas and perimeters of features are measured, similar relevance occurs for measurements of lengths (as in shorelines and river courses) and of surface areas (as of plutons and glaciers)" (Woronow, 1981, 215).

Burrough (1981 & 1983a) reviewed a number of studies in fields such as hydrology, climatology, soils, and geology, and considered them in light of the fractal model. He observed that coastlines, topography, river discharges, climatic variation, island and lake size distributions, and soil variation, all share one characteristic: that, on first sight, no single length, area, or time scale can be applied to them. The fractal model did not provide a universal fit, but the application revealed aspects of the data that were not obvious previously (e.g., Burrough 1983b & c). Theoretically, fractals should be most applicable to phenomena that are the result of processes that are scalable -- such as turbulence and wind speed. Conversely, if the processes are structured or non-scalable, greater deviations from the fractal model would be expected (Burrough, 1983a), or possibly, nonrandom fractals could be used.

4.5 Fractals, soils and terrain

Burrough was the first soil scientist to apply fractals to soil variation (Burrough, 1983b & c). Soil should be an ideal candidate for a fractal model as it is the product of complex interactions of parent materials, climate, topography, time, hydrology, and biological activity. Each component acts over a unique spatial scale, and within each soil-forming factor there may be several scales of interaction (Burrough, 1983b, 578).

When the semivariogram is plotted for most soil data, non-zero variance is observed (i.e., the 'best-fit' regression line does not go through the origin) (Burrough, 1983b, 581; see also Krige, 1966 and Journel and Huijbregts, 1978, and section 5.2.3 for a description of variograms). This non-zero variance could be the result of sampling error or the result of very small-scale irregularities in the surface (i.e., white noise). However, it is also known that by increasing the resolution of the analysis, part of what was originally noise becomes signal, or structure. This led Burrough to consider using a fractal model, as it "takes into account the nested, autocorrelated and scale dependent nature of unresolved variation" (Burrough, 1983b, 582).

Soils clearly exhibit fractal-like qualities, especially with respect to the resolution of their scale-dependent spatial variation. However, soils are not ideal fractal surfaces in that the semivariance typically exhibits a step-wise profile -- true fractal surfaces should exhibit a monotonically increasing semivariance with increasing inter-sample distance and area studied (Burrough, 1983b, 593). That is, soils exhibit only partial self-similarity and transition zones are present. These transition zones appear to be related to the geological structure because when the sampling interval was fine enough to reveal the structure, the semivariance differed greatly from that of a fractal. At a coarser sampling interval, however, the semivariance became indistinguishable from that of a fractal (Burrough, 1983a, 9).

By examining the semivariogram Burrough discovered that soils exhibit a value of $H < 0.5$, which indicates that short-range effects dominate the soil-forming process. Landforms, river discharge, geological sediments, and climatic data all tend to exhibit values of $H > 0.5$, which is indicative that long-range effects dominate (remember that $H = E - D$). Burrough then sought to determine the cause for the unusual value of H for soil. From this research he developed a model of soil formation (Burrough, 1983c). Culling (1986) studied the spatial variability of soil-pH and also found that it had a high dimension ($D \approx 1.8$), in agreement with Burrough's results.

Burrough concluded that soils and landforms have nested levels of variation "controlled by the importance and scales of the various geomorphological and soil-forming processes that have been active" (Burrough, 1983b, 594), and thus are not ideal fractional Brownian processes. Burrough's analyses were only concerned with soils; his remarks made with respect to landforms are not supported by any independent research. A number of geographers (e.g., Goodchild, 1982; Mark and Aronson, 1984; Roy et al., 1987; Culling and Datko, 1987; Anderle, 1987) have explicitly considered the fractal nature of landforms, however, and some of those studies will be reviewed below.

Goodchild (1982) determined the fractal dimensions of the shoreline and selected contours and lake outlines found on Random Island, off the eastern coast of Newfoundland, using three different methods. The three methods produced different D values for the same features, but all methods exhibited the same trend of increasing D with elevation. Goodchild (1982) stated that the systematic trend in the fractal dimension was due in part to the different geomorphic processes dominating at different elevations. He concluded:

> Although one would expect geomorphic and geologic controls to produce significant departures from self-similarity at certain scales, there is no clear evidence that this has happened on Random Island over the range of scales used in this analysis (Goodchild, 1982, 1137).

The application of the fractal model to Random Island had mixed success, for while it produced consistent trends among the various relationships studied, the parameters were numerically inconsistent (Goodchild, 1982, 1137).

Mark and Aronson (1984) were also concerned with the fractal geometry of landscape. They noted that, previously, few authors (with the exception of Goodchild, 1982) had considered the 'reasonableness' of the fractal model, or the implications of their work for geomorphology. (Most papers on fractal landscapes had been written by computer scientists or mathematicians.) In particular, they were concerned with the lack of a relationship between the mathematical methods by which fractal surfaces are generated and geomorphic processes.

Mark and Aronson (1984) investigated the fractal nature of 17 digital elevational models. Of the 17 models, only one had a variogram totally consistent with the concept of self-similarity. The other 16 variograms had sections that were straight, with changes in the slope at 'characteristic' scales. That is, within a physiographic province there were consistent distances at which the fractal dimension **D** changed, a reflection of the characteristic slope length and structural control of that province. The lower straight sections had **Ds** ≈ 2.3, while the higher sections had **Ds** ≈ 2.75. The values at which the **D** changes "represent scales at which the relative importance of different processes, of structural effects, and of time scales also change"

(Mark and Aronson, 1984, 681). Therefore, they concluded, both conventional geomorphic wisdom (landscapes have characteristic scales) and the fractal model (geomorphic surfaces are statistically self-similar) are applicable.

Roy et al. (1987) also studied the fractal nature of a digital elevational model (DEM). They found that although the entire DEM exhibited properties of self-similarity, sections and horizontal and vertical slices -- or isosets -- of the DEM exhibited differing characteristics. That is, the fractal dimension appeared to vary spatially within their study area.

As the above mentioned studies illustrate, the study of fractals is the study of form. D is used to quantify one aspect of form (Mandelbrot, 1978), but it differs from other measures of 'roughness' in that it provides a description independent of the sample -- most other measures of roughness are sample dependent (Brown and Scholz, 1985; Scholz and Aviles, 1986; Mark, 1975). That is, scale invariant measures "are expected to have a fundamental physical significance, since the ensemble average of their spatial means do not depend on the scale (or dimension of space) over which they are averaged" (Lovejoy and Schertzer, 1987, 5). Scale invariant -- fractal -- measures allow one to "extrapolate from properties observed at one scale to the properties of a scale which has not been observed" (Gilbert, 1987, 7).

These statements are somewhat at odds with conventional geomorphological philosophy, however. "Scale has long been a fundamental concern in geomorphology. Size and form are inextricably connected through the function and scale of geomorphic systems" (Mark and Aronson, 1984, 672). However, Culling and Datko (1987, 370) note: "We need a measure of landscape form that transcends structure and process, a matter of geometry and dimension." Consider Lovejoy's (1982) work on the fractal dimensions of clouds. This work produced results which were counter to the then current theories of meso-scale atmospheric modelling. Lovejoy's findings have since been confirmed and greatly extended (Lovejoy and Schertzer, 1985; Lovejoy and Mandelbrot, 1985). Thus, it is too early yet to reject the use of fractal concepts in geomorphology, even though they might appear counter-intuitive.

In many fields, such as geomorphometrics, quantitative methods are used to investigate the links between form and process. Physical models of the process must contain the scaling and self-similarity properties inherent in the geometry if they are to be truly functional (Scholz and Aviles, 1986; Lovejoy and Mandelbrot, 1985). Thus, knowing that a phenomenon has a fractal dimension (between certain limits) allows us to make certain assumptions about the physical processes which produced the phenomenon. Knowledge of the fractal dimension will help define the types of questions which might have interesting answers, when looking for the links between form and process (Mark and Aronson, 1984; Kadanoff, 1986). For example, within geomorphology, what is needed is a geomorphologically-derived mathematical link between landform and the mechanics of geomorphic processes (Mark and Aronson, 1984, 672). In the absence of such a link, the use of the fractal model as a method of simulation which produces 'reasonable' results becomes a viable alternative.

As an aside, but still related to the preceding discussion, the following study is reported. Pentland (1984) asked a number of subjects unfamiliar with the concept of fractals to subjectively rank a number of images on a roughness scale from 1 (smooth) to 10 (rough). He reported that "the mean of the subject's estimates of roughness had a nearly perfect 0.98 correlation ($p < 0.001$) with the curve's fractal dimension" (Pentland, 1984, 663). The fractal dimension of an object thus appears to represent perceptual roughness extremely well. This provides another reason for the intuitive appeal of D as a summary statistic, and also provides support for Mandelbrot's (1982, 581) statement that "the basic proof of a stochastic model of nature is in the seeing."

In this chapter a number of studies which involved fractals were presented, with subjects ranging from data storage techniques using non-random fractals to an analysis of perception. Results of these studies have answered some of the initial questions concerning the applicability of fractals to geography, and the question -- are fractals of use in geographic research --was clearly answered in the affirmative. In the following chapter methods which are used to determine the fractal dimension will be discussed in detail. In addition, the data sources used in this thesis will also be discussed.

Chapter 5

Data sources and methodology

In a variety of ways -- from the use of D as a simple statistic, to the use of D as the prime parameter in complex models -- a wide range of disciplines use fractal geometry. Because of this range, it is not surprising that most of them have derived independent methods of working with fractals, methods which integrate easily with their own mathematical `tool box'. In this chapter some of the methods which have been used to determine fractal dimensions are reviewed. In particular, those methods which are evaluated in this thesis, and their implementations, are discussed.

5.1 Data sources

Before discussing the variety of methods used to determine fractal dimensions, descriptions of the data sets used in this thesis are presented. Two different data types were used: one data type was used primarily for testing the measurement methods, the other data type was used for testing the fractal properties of terrain.

5.1.1 Simulated surfaces

The first data source, used for testing the consistency of the methods implemented in this thesis, consists of simulated surfaces of specified fractal dimensions. The method used to generate these surfaces is outlined in Mandelbrot (1975a), wherein it is shown that it is possible to generate fractional Brownian surfaces of arbitrary H, and thus, of arbitrary D (Orey, 1970). Fractional Brownian surfaces produce, arguably, realistic simulations of natural landscapes (Mandelbrot, 1983; Voss, 1985); most certainly they produce the best approximations of real terrain available at present (Mark, 1978, 1979; Goodchild and Mark, 1987).

These simulated fractal landscape surfaces are commonly referred to as fractional Brownian motion (fBm) surfaces. Each simulated surface represents one realization of a fractional Brownian function. Basically, a plane surface is modified "by superimposing very many, very small cliffs, placed along straight faults and statistically independent" (Mandelbrot, 1975a, 3825).

A simplified description of the method used to generate the surface follows:

i) A randomly orientated 'fault' is placed randomly over the plane;

ii) The half planes on either side of the 'fault' are then shifted vertically (one up, the other down) some random amount to form a cliff. The amount of the displacement is a function of H; for surfaces with H = 0.5 the displacement is equal and opposite, for surfaces with other values of H the displacement is not equal. The overall distribution of the cliff heights should follow a normal distribution (of zero mean and finite variance), with the following covariance function:

$$C(\chi.H) = \tfrac{1}{2}[(\chi + 1)^{2H} - 2|\chi|^{2H} + |\chi - 1|^{2H}]$$

where χ is the sampling interval, and $0 < H < 1$ is the scaling function (Burrough, 1985).

iii) This process is continued long enough so that the effect of any one cliff becomes negligible. For the 256 by 256 cell surfaces used in this thesis, a total of 1000 cliffs were generated to ensure a high probability that at least one cliff occurred between every pair of adjacent cells.

By definition, fractional Brownian functions generate surfaces which are self-similar and have isotropic increments. However, as Mandelbrot (1975a, 3827) notes:

> A striking feature of sample Brown surfaces is the invariable presence of clear-cut ridges. They are merely an unexpected consequence of continuity, but their presence expresses that each sample is grossly non-isotropic. Since these ridges have no privileged direction, they are quite compatible with isotropy of the mechanism by which [the surface] is generated.

Thus, since the generation of each surface is based on a stochastic process, one surface may have different properties from another, even though both surfaces may have been defined with similar values of H.

The seven simulated 256 by 256 cell surfaces used in this thesis were generated with values of H ranging from 0.3 to 0.7 in steps of 0.1. Three versions of the H = 0.7 surface were generated because this value of H (D = 2.3) is thought to give the best resemblance to real terrain (Mandelbrot, 1975a, 1983). The simulated surfaces will be referred to as H3, H4, H5, H6, H7A, H7B, and H7C, where H7B refers to one of the surfaces generated with H = 0.7, for example.

5.1.2 Digital Elevational Models

The second data source, used for testing the fractal characteristics of natural terrain, consists of 58 Digital Elevational Models (DEMs). Complete details of the locations of the DEMs used in this thesis are presented in chapter 7 (figure 7.1 and table 7.1). A DEM is composed of a regular array of elevations referenced to mean sea level with a horizontal spacing of 30 metres in both the N-S and

E-W directions, and a vertical resolution of 1 metre (see Elassal and Caruso, 1983, for a complete description of the format and content of a U.S.G.S. DEM).

The unit of coverage for a DEM is a standard U.S.G.S. 7.5 minute quadrangle, and the elevations are referenced to the Universal Transverse Mercator (UTM) coordinate system. Thus, each DEM has a variable number of rows and columns, a result of the variable angle between true north (used as the reference for the quadrangle boundaries), and grid north (used as the reference for the UTM coordinate system). Generally, a standard DEM has many more rows than columns. The following quote indicates how the U.S.G.S. produces DEMs. Only DEMs produced by methods (1) and (2) were used in this thesis.

> The USGS uses three systems to collect the digital elevation data for production of 7.5-minute DEM's: (1) the Gestalt Photo Mapper II (GPM2); (2) manual profiling from stereomodels; and (3) the Digital Cartographic Software System (DCASS).
>
> The GPM2 is a highly automated photogrammetric system designed to produce orthophotos, digital terrain data, and contours. .... The horizontal (x and y) spacing of the elevation points within each patch is ... equivalent to a ground distance of approximately 47 ft., ... these are regridded to form a DEM in the standard format.
>
> The manual profiling systems use stereoplotters, interfaced with electronic digital profile recording modules, for scanning of stereomodels in the photo y direction. The scan speed and slot size (stepover interval) can be selected by the operator, ... which results in elevation profiles spaced approximately 90-m apart. Elevations are normally recorded every 30-m along each profile. The profiled elevation data are reformatted and

> regridded to a regular 30-m UTM spacing, written in standard DEM format.
>
> The DCASS forms a DEM from digitally encoded vector contour data. Stereoplotters, equipped with three-axis digital recording modules, are used to collect vector contour data while the instruments are being used for photogrammetric stereocompilation of 1:24,000-scale quadrangle maps. .... The vector contour data are processed into profile lines and the elevation matrix at a 30-m spacing is formed using a bilinear interpolation between the intersections of the lines with the contour vectors. (Elassal and Caruso, 1983, 2-3)

Further characteristics of the two data sets will be introduced in the following section and chapters when necessary.

5.2 Methodology

The following tables (5.1 and 5.2) provide an overview of some of the methods which have been used in the earth-based sciences (geography, geology, geophysics, meteorology, hydrology) to determine fractal dimensions, and they summarize some of the studies which have been reported. Although attempts were made to document most of the major papers published in geography, the list presented in table 5.2 is not exhaustive.

Several of the methods listed (table 5.1) have received much more attention in Geography than in other fields (table 5.2). This is partially due to the nature of the phenomena that Geographers routinely work with, and partially due to the methodological 'tool box' that Geographers are most

Name of method	Relation	Estimate of D
Area/perimeter relationship	$A = kP^{2/D}$ A = estimated area P = estimated perimeter k = constant	Plot log A against log P, slope is 2/D
Cell counting (or box counting)	$\langle n \rangle \propto b^{-D}$ $\langle n \rangle$ = avg number of boundary cells b = cell size	Plot log $\langle n \rangle$ against log b, slope is -D
Circle relationship	$\langle n(L) \rangle \propto L^{D}$ $\langle n(L) \rangle$ = avg number of points located within distance L	Plot log $\langle n(L) \rangle$ against log b, slope is D
Dividers relationship	$L(\tau) = k\tau^{1-D}$ $L(\tau)$ = length of trail τ = step size k = constant	Plot of log L against log τ, slope is 1 - D
Intersegment angles	$D = \dfrac{\log(2)}{\log(2)+\log[\langle(\frac{c}{ab})^2\rangle]^{0.5}}$ a,b = segment lengths about point j c = distance from pt(j-1) to pt(j+1)	D is obtained directly
Korcak's law (Empirical relation for islands)	$N_r(A>a) = F'a^{-(D/2)}$ $N_r(A>a)$ = number of islands above size a F' = a constant > 0.0	Plot of log $N_r(A>a)$ against log a, slope is -(D/2)
Power spectrum	$P(w) = w^{-(5-2D)}$ P(w) = the power w = the frequency	Plot of log P(w) against log w, slope is -(5-2D)
Variogram	$\langle[(Z_p-Z_q)^2]\rangle = k(d_{pq})^{(4-2D)}$ Z_p, Z_q = elevations at points p and q d_{pq} = distance between p & q k = constant	Plot of log $\langle[..]\rangle$ against log (d_{pq}), slope is (4-2D)

Table 5.1 Methods used to estimate D for geophysical data

(Taken partially from Burrough, 1983a, table 2 and other sources listed in table 5.2)

Author	Method	Applied to	Comments
Goodchild 1982	Area/perimeter	digitized shorelines & contours	D = f(elevation) - increases
Kent & Wong 1982	" "	" "	D constant over scale (5 km to 20 km)
Lovejoy 1982	" "	digital cloud images	D constant between 1 and 1000 km
Skoda 1987	" "	digitized radar echoes of rain	D = f(underlying topography)
Woronow 1981	" "	digital images of craters on Mars	
Albinet et al. 1986	Cell counting	digital models of forest fires	
Goodchild 1980a	" "	theoretical considerations	
Goodchild 1982	" "	digitized contours & shoreline	D = f(elevation) -> increases
Hakanson 1978	" "	lake shorelines	used maps, not concerned with D per se
Lovejoy et al. 1987	" "	radar rain reflectivities	D = f(intensity of rainfall)
Morse et al. 1985	" "	photographs of vegetation	breaks delimited vegetation types
Shelberg et al 1983	" "	DEMs	D relatively constant
Lovejoy & Schertzer 1986	Circle counting	World Meteorological Network	D constant
Kagan & Knopoff 1980	" "	spatial dist of earthquake foci	within limits of continental plates, D constant
Aviles et al 1987	Dividers	digitized fault traces	definite break in D at 1 4 km
Batty & Longley 1986	"	digitized urban boundaries	D relatively constant
Culling & Datko 1987	"	digitized contours	D = f(elevation) -> increases
Goodchild 1982	"	digitized contours and shorelines	D = f(elevation) -> decreases
Kent & Wong 1982	"	digitized shorelines	definite break at 350 m
Laverty 1987	"	line skeletons of cave passages	found cave passages exhibited fractal behaviour
Maling 1968	"	cartographic lines	used physical dividers, not after D per se
Richardson 1961	"	cartographic lines	used physical dividers, not after D per se
Roy et al. 1987	"	digitized contours?	D = f(elevation) -> decreases
Shelberg et al. 1982	"	digitized cartographic lines	tested the method, found it reasonably consistent
Muller 1986 1987	"	digitized cartographic lines	D = f(scale of the map)
Eastman 1985	Intersegment <'s	digitized cartographic lines	results consistent with dividers method
Kent & Wong 1982	Korcak's law	areas of lakes	found D to agree with value obtained from area/perimeter determination, although data was obtained from different sources
Brown & Scholz 1985	Power spectrum	natural rock surfaces	D = f(scale)
Fox & Hayes 1985	" "	digital model of ocean floor	D = f(scale, direction) from 10[illegible] to 10[illegible] m
Kagan & Knopoff 1980	" "	earthquake foci over time	
Power et al. 1987	" "	natural rock surfaces	D = f(scale, direction) from 10[illegible] to 10[illegible] m
Scholz & Aviles 1986	" "	digitized traces of faults	D = f(scale) from 10[illegible] to 10[illegible] m
Steyn & Ayotte 1985	"	DEMs (2)	D = f(direction) for one DEM
Burrough 1981 1985	Variogram	various geophysical phenomena	
Burrough 1983a	"	soil profiles	found very high values of D
Culling 1986	"	soil pH	found very high values of D
Culling & Datko 1987	"	digitized maps (17)	consistently found two regimes
Mark & Aronson 1984	"	DEMs (17)	definite breaks
Roy et al. 1987	"	DEM (1)	D = f(direction, location)

Table 5.2 Studies which have considered the fractal nature of geophysical phenomena

comfortable with. For example, cartographers are traditionally concerned with representation and measurement of linear features (e.g., Perkal, 1966; Maling, 1968). In particular, computerized line-generalization techniques have received much attention lately (Muehrcke, 1972; Monmonier, 1982). Thus it is not surprising that the dividers method has been used extensively by cartographers. In addition, determination of the area of mapped features is a traditional geographical concern (Monkhouse and Wilkinson, 1971; Lawrence, 1979), and grid overlay (cell counting) methods are widely used in the discipline (Gierhart, 1954; Frolov and Maling, 1969; Goodchild, 1980b). When looking at the fractal nature of terrain geographers have preferred to use the variogram method rather than spectral analysis -- the technique used most frequently by geophysicists.

A distinction should be made between digitized cartographic lines and derived lines. In this thesis, all of the 'lines' were derived from the DEMs by an automated contouring package (Precision Visual's DI-3000 contouring subroutine). Most of the tests which have been made on the fractal nature of cartographic lines have been applied to digitized cartographic lines (e.g., Goodchild, 1982; Kent and Wong, 1982; Shelberg, Moellering and Lam, 1982; Muller, 1986, 1987), with the exception of Shelberg, Moellering and Lam (1983) and Roy <u>et al</u>. (1987).

"If cartographic generalization preserves self-similarity, then the source of the data would not affect the estimation of D" (Roy <u>et al</u>., 1987, 72). However, the work of Muller (1985) would suggest that Roy <u>et al</u>.'s assertion is incorrect. Muller (1985, 128) found "a clear reduction of fractal dimension on smaller scale representations" for seven of ten lines tested. Since geomorphic processes act at characteristic scales (as was found to be the case in Kent and Wong, 1982, for example), then the scale of the map from which the data are obtained could influence the dimension obtained. Furthermore, if the cartographic line is not self-similar, then the basic assumption of Roy <u>et al</u>. is invalid.

There are reasons why digitized cartographic lines may or may not have greater fractal dimensions than derived cartographic lines -- the counter arguments indicate that this area requires further research. For example, the derived lines used in this work were purposely not smoothed. A cartographer would have naturally 'rounded the corners', and adjusted the contours to better follow hydrographic features. The contours used in the following analyses were derived independently of the hydrological network.

The elevations used in the analyses were deterministically selected. For every data set, the range of elevations was determined. The range was then divided into seven groups, and the elevations at the middles of each of the five inner groups were selected as the values which were used in all subsequent analyses. These values were chosen in an attempt to avoid the extremes of the data sets, while at the same time providing a reasonable sample of the terrain represented by the data set.

5.2.1 The dividers method

Walking a pair of dividers along a linear feature to determine its length is a long-standing method (Maling, 1968; Steinhaus, 1969). One of the first studies to examine methodically the relationship between the length of a cartographic line and the scale it is plotted at was by Richardson (1961). He was concerned with the variation in the warlike propensity of neighbouring states, and felt that the length of the common border might be a major influencing factor. In his work he analysed the dependency of the border length on the divider's width and illustrated that when the border lengths were plotted against the sampling interval on log-log paper, the data points tended to fall on a straight line with a negative slope. Richardson did not consider further the implications of the negative slopes, but he did empirically derive a formula which describes the relationship between border length and dividers width which included an exponent we now refer to as D. The negative slopes are now recognized as indicative of the fractal nature of coastlines and other cartographic features, as Mandelbrot (1967) subsequently brought to light.

Like Richardson, Maling (1968) was also concerned with the fundamental problem of determining the 'true' length of a cartographic line. Maling quantified the relationship between scale and length, but his work has largely been superceded by that of Mandelbrot (1967, 1975). Although Håkanson (1978) was also explicitly concerned with the problem of line length and measurement scale, he used a variation of the cell counting method. His study will be discussed later in the section on cell counting methods.

The dividers method was used to determine the fractal dimensions of cartographic features for the first time by Goodchild (1982), Kent and Wong (1982), and Shelberg et al. (1982). Mandelbrot (1967) re-analyzed Richardson's (1961) plots -- he did not redo the entire study. Subsequently, there have been a number of studies which have expanded the range of phenomena analysed using this method (table 5.2).

Goodchild (1982) looked at the fractal characteristics of the coastline, the 250 foot and 500 foot contours, and the lake outlines of Random Island, Nfld. The fractal dimensions obtained using the dividers method were consistent with the results obtained by other methods (i.e., cell counting and area-perimeter relationships) applied to the same data. In working with the lake outlines, it was found that some of the lakes had shoreline lengths smaller than the larger step sizes -- this caused the slope to 'flatten' at the larger step sizes, and reduced the overall linearity of the log-log plots.

Kent and Wong (1982) also looked at the representations of shorelines of lakes digitized from NTS map sheets. For one of the lakes they obtained three digitized versions from maps of three different scales (1:50,000; 1:250,000; and 1:500,000). However, they found that they could superimpose the log-log graphs of shoreline length against divider's width from the three scales and still observe a linear trend within the area of overlap. But, Muller (1986, 128) performed a similar analysis, using maps of various scales, and concluded there was a "clear reduction of fractal dimensions on smaller scale representations."

Kent and Wong (1982) also modified the basic method after noting that the measured length was affected by the starting point; they used a number of starting points and took the averages of the trials for each dividers width. The same problem has been addressed by other researchers, such as Schwarz and Exner (1980), Eastman (1985), Batty and Longley (1986), and Kennedy and Lin (1986).

Shelberg et al. (1982) published a 'walking dividers' algorithm and illustrated its use on a number of data sets. They tested their method by analyzing the same coastlines as did Richardson (1961; as subsequently analyzed by Mandelbrot, 1967), and arrived at similar values of D. The algorithm works on digitized strings as follows: An initial step size (dividers width) is selected. Starting at one end of the string, the algorithm tests each successive point until it finds the first point (**n**) which is farther than the step length away from the starting point. Using linear interpolation the program then determines where between points **n** and **n** - 1 the intersection between the step length and the string occurs, and subsequently uses this interpolated point as the new starting point. This procedure is followed until the end of the string is reached. (See below for a discussion of the 'remainder' problem.) Then, the step size is increased by some amount -- usually it is doubled, so that the log of the step size values form an even progression -- and the process repeated. The length of the string is determined by multiplying the number of chords required to completely cover the string times the step size -- note that for every step size there will be a unique string length. The step sizes and corresponding string lengths are then used in a linear regression where the log of the string length is regressed against the log of the step size. The string's fractal dimension is then equal to one minus the slope of the line (table 5.1).

Shelberg et al. (1982) felt that the initial chord length (the smallest) should not be smaller than one-half of the average chord length. This follows a sampling theory which states that c-. should sample (at least) at one-half the average wavelength in order to cover all significant variations. In fact, the theory on the Nyquist frequency states that the highest frequency (shortest wavelength) that can be detected is equal to twice the sampling rate (Davis, 1986; 257). Thus, sampling at only half the average wavelength could miss some of the variation present in the digitized lines.

Shelberg *et al*. (1982) also noted that the log-log plots must be linear. If the plot is not a straight line, then the number of included solution steps should be decreased. The solution which has the highest relative r^2 value should be selected as the most appropriate. Slope values obtained from graphs with fewer than five data points should be considered unreliable, although Shelberg *et al*. (1982) emphasized that linear regression is used primarily as a means of obtaining the slope value; it is not used for making statistical inferences.

Aviles, Scholz and Boatwright (1987) recently analyzed the fractal nature of fault traces using the dividers method. They noted there are actually three variations possible when using the traditional dividers method. These variations arise from how the remainder is treated; almost all trials will result in a non-integer number of dividers being required to completely cover the line. The first variation is to use only those measurements which leave a remainder less than some specified value or tolerance. The second variation is to add the remaining bit as a proportion of a divider -- this is the approach taken by all of the other published papers cited (table 5.2) which used the dividers method. The third variation is to add one to the total count of dividers if any remainder is present. They tested these variations on a number of linear features and found that the first variation gave the smallest scatter, that the second variation produced slightly greater scatter, and slightly higher values of D, and that the third method produced much greater scatter, and much lower values of D. They also noted that at larger divider steps a steep drop in total length was clear (c.f., Goodchild, 1982) -- they subsequently removed the data values associated with the largest step sizes from their analyses.

Gilbert (1987) also reviewed the same three variations to the divider's algorithm, and found that all three methods produced unreliable results. His findings contrast greatly with those of, for example, Muller (1986), Shelberg et al. (1982) and Aviles et al. (1987). Gilbert concluded that spectral methods are the most appropriate to use in the estimation of the fractal dimension. However, Culling (1986, 223) shows that, theoretically, spectral methods are inappropriate methods to use in the estimation of the fractal dimension of terrain.

An alternative to the walking dividers algorithm is the equipaced polygon method (Batty and Longley, 1986) or, as it is known in particle science, the Schwarz and Exner (1980) fast algorithm. One of the problems associated with the traditional dividers method is its computational complexity -- the algorithm performs many linear interpolations while 'walking' the line. In order to increase the efficiency of the dividers method, the equipaced polygon method uses a number of points, say n, to represent the step size. Thus, in this method only those points which define the string are used, and every step is probably of different length.

Starting at the first point, the distance to the nth point is calculated, then the distance from that point to the 2 * nth point is calculated, and so on until the end of the string is reached. The sum of all the 'steps' represents the total string length, and the average step length is obtained by dividing the total length by the number of steps required to cover the string. The value of **n** generally starts at one and progresses in a geometric progression (i.e., 1,2,4,8,...). To reduce the influence of the starting position, the method should start at all possible points (i.e., when the value of **n** is 4, points 1, 2, 3 and 4 should all be selected as starting points) and the average of all runs used. Because this method follows the curve much more closely than the dividers method, the influence of perturbations in the line is much greater than in the traditional method. This has been considered both a benefit of the method (Batty and Longley, 1986) and a serious drawback (Clark, 1986).

5.2.1.1 Implementation

The dividers method was used in three distinct manners in this thesis. The first procedure was to use the dividers method in its traditional implementation (as in Shelberg et al., 1982), applied to the individual contours. The equipaced polygon method was also applied to the individual contours as the second procedure. These two analyses were applied 'blind' to the contour lines. That is, because of the extremely large number of contour lines involved it was not possible to view every log-log graph. The process was automated, and a program written which cycled through the data points -- starting the analyses by including every data point, and then sequentially dropping the smallest dividers width from the regression until only five data points were left. Additionally, to determine if the largest dividers width 'flattened' the curve (as in Goodchild, 1982 and Aviles et al., 1987), when only five data points were left the program retrieved the last removed data point and removed the data point associated with the largest dividers width. The results of every regression were written to a file and the solution with the highest correlation was selected. For a contour line to be included in the analyses, it had to have had at least 32 coordinate pairs. This value was selected to ensure that at least five data points were produced by the dividers method, given that the dividers width increased by a geometric progression. It also ensured that very short contour loops -- of which there were very many -- were excluded from the analyses.

The program proceeded as follows:

i) The data sets were passed to a contouring package which wrote out, for the selected elevations, the strings of coordinates for each contour line generated (the contour lines were not smoothed);

ii) For every contour line with at least 32 coordinate pairs, the two measurement methods were applied to the string, and the data values (measured length and dividers width) passed onto another program;

iii) The data values were analysed, using the method described above.

The third procedure used was to reverse the relationship between the step size and the derived contour lines. In the traditional implementation the step size changes while the scale of the data remains constant. In this implementation the scale of the data was varied, while the step size remained constant. In this implementation the total length of all contour lines for a given elevation was the dependent variable, not the length of each individual contour. The 'step size' for a given scale was equated to the average chord length (total length of all contour lines / total number of coordinate pairs).

The program proceeded as follows:

i) The length of all contour lines, for each selected elevation, was determined at the original scale;

ii) The original 256 by 256 array was sampled deterministically to produce a 128 by 128 array;

iii) The contour line lengths for this new array were determined;

iv) The 128 by 128 array was sampled to produce an array 64 by 64.

v) This sampling/length determination process continued until the array was of size 8 by 8.

Note that from each 'original' array at least four 'new' arrays can be obtained, as illustrated below (figure 5.1).

Suppose that the four corner cells of the original array are labelled A through D. In sampling process any of the four cells can become the new corner cell, for example cell (D_{old}) could become cell (A_{new}) (figure 5.1a). Thus, for the original array only one determination of total length is possible, but for the 128 by 128 array four independent determinations are available; for the 64 by 64 array sixteen independent determinations are available; and for the 8 by 8 array 1024 determinations of length are possible -- using the sampling scheme illustrated (figure 5.1). However, in the actual implementation of the program the number of samples was restricted to only 16 for the arrays of size (64 by 64) and smaller. The average of the totals derived from each sample was used in the log-log regression.

5.2.2 <u>The cell counting method</u>

The cell counting method has long been used in the determination of the area of cartographic features (Gierhart, 1954; Maling, 1968; Steinhaus, 1969). Håkanson (1978) was

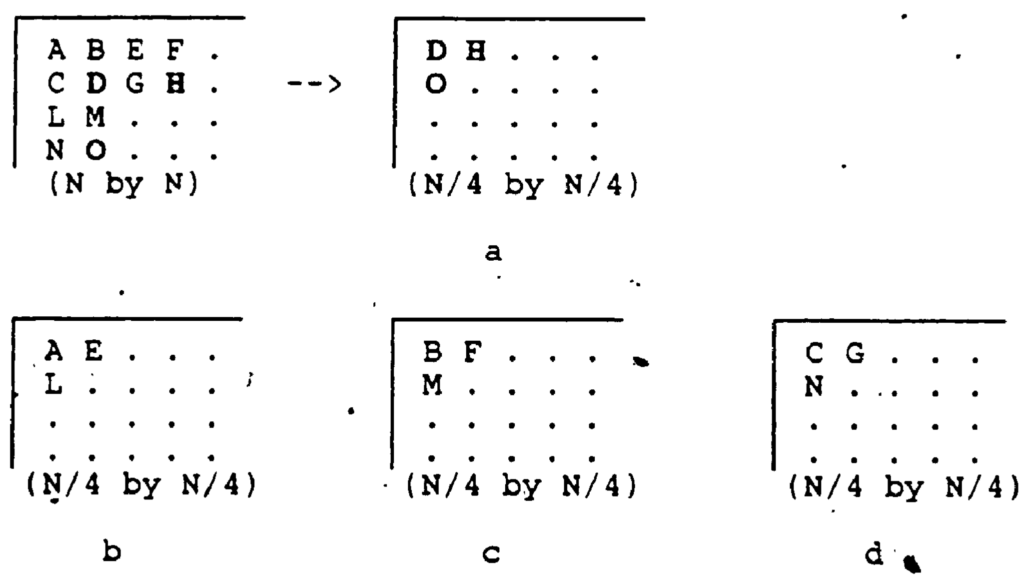

Figure 5.1 Dividers sampling scheme

The four different sampling schemes used when applying the dividers methods to the entire data set. (Size of array = N) one of the first to use this method to examine the relationship between the length of a cartographic line and the measurement scale. However, although aware of Mandelbrot's publications, Håkanson did not place his analyses within the context of fractal geometry. In addition, his implementation of the cell counting method is not directly applicable to research into D. As Goodchild (1980b) noted, Håkanson's method, based on counting the number of intersections of the cartographic line with each cell, is too dependent upon the map construction process -- not simply upon the scale of the map as it theoretically should be. To make the method more appropriate for research into D -- making the results a function of scale -- the number of cells intersected should be determined, not the number of intersections.

The cell counting method can be applied to both linear features, such as cartographic lines, and to representations of surfaces, such as DEMs. When the method is applied to linear features, the method works as follows:

i) lay a grid over the 'map';
ii) count the number of cells intersected by the line;
iii) reduce or enlarge the grid (preferably by a factor of two, so that the log (data points) are evenly spaced);
iv) recount the number of cells intersected.

This process is repeated until enough measurements have been made -- although as a minimum only two measurements need be made, the greater the number of measurements the more confidence one can attach to the results. The maximum number of measurements will be reached when the grid spacing becomes as fine as the resolution of the data, or as large as the feature itself. When the log of the average number of cells intersected is regressed against the log of the cell size the fractal dimension is equal to the slope times minus one (table 5.1).

Albinet, Searby and Stauffer (1986) used a similar method to determine the fractal dimension of the 'front' of a computer model of a forest fire, but they also used eight neighbour (Moore) counts, and 24 neighbour counts. The standard method applied to surfaces looks at only the four neighbours (the Von Neumann neighbourhood). The values of D obtained when using the Moore neighbourhoods were similar to those obtained using the Von Neumann neighbourhoods. The values of D produced when using the 24 neighbour counts were much smaller, however.

The implementation of the cell counting method to a surface is accomplished in the following manner:

i) the surface is sliced by a horizontal plane of a given elevation;

ii) those cells that are above the plane are coded as white, those cells below as black;

iii) a count is made of the number of cells which have a neighbour of the opposite colour;

iv) the cell size is increased by use of a process such as that illustrated in figure 5.1, for example, and the process repeated until the maximum cell size is reached.

The log of the average number of boundary cells is then regressed against the log of the cell size. The fractal dimension of the surface is equal to one minus the slope (table 5.1).

Lovejoy, Schertzer and Tsonis (1987) recently published a paper on 'box counting', a method which is similar to the cell counting method. Box counting involves the successive subdivision of space into 'boxes' that decrease in size by factors of two (i.e., a geometric progression). After each subdivision the number of boxes which contain the phenomena under study is counted, and the fractal dimension is determined from the equation $N(L) \alpha L^{-D}$, where L is the size of the box and N(L) is the number of occupied boxes. This method is simply the extension of the cell counting method to three dimensions, which means that the cell counting method can now be applied to point sets, lines, areas, and even volumes. Lovejoy et al. (1987) note that the box need not be a square, but can be any shape, such as a rectangle. Thus, this method is useful in the study of non-isotropic, multi-dimensional fractals.

2

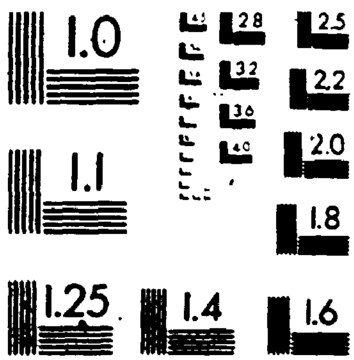

5.2.2.1 Implementation

The cell counting method was implemented as follows:

i) The entire 256 by 256 array was read in, and the starting cell size was set to one;

ii) For all pairs of cells the given cell size apart, and across all rows and columns, the pairs of cells were inspected to determine the relationship of their elevations;

iii) If the cells lay on opposite sides of the given elevation, the counter was incremented by one;

iv) The cell size was doubled (i.e., 1, 2, 4, 8, 16, 32, 64, 128), and the process repeated.

Every possible starting cell was used. For example, when the cell size is 4, cells 1, 2, 3, and 4 are all used as the starting cells in successive runs. The average number of border cells for a given cell size is then used in the subsequent regression analysis of log (average number of border cells) against log (cell size), and the fractal dimension determined using the equation above (table 5.2).

5.2.3 The variogram method

The variogram is one of "the primary tool[s] for examining the spatial characteristics of data" (Green, 1985, 187).

The essence of this graphical method of data analysis is that the statistical variation between samples is some function of the distance between them. The independent variable is the distance between pairs of samples; the dependent variable is the variance of the difference in the data values for all samples the given distances apart. Expressed mathematically, the variogram relationship is:

$$2\tau(d) = E[z(x,y) - z(x+u,y+v)]^2,$$

where $z(x,y)$ and $z(x+u,y+v)$ represent the heights at points (x,y) and $(x+u,y+v)$ respectively, and $d = (u^2 + v^2)^{½}$.

The use of variograms as one component of the process of kriging (Krige, 1966) has received wide attention in many fields, especially geology (e.g., Journel and Huijbregts, 1978; Agterberg, 1982) and soil science (e.g., Burgess and Webster, 1980a, b; Burrough, 1983b; Armstrong, 1986; McBratney and Webster, 1986). Note that the semivariogram is simply $\tau(d)$. In geography the technique has received relatively little attention as an interpolation technique, however. When a variogram is used as such the detection and removal of non-stationarity in the data is an important consideration (Cressie and Hawkins, 1980). However, when using a variogram as a means of testing the fractal model, detection of non-stationarity is part of the analysis (Armstrong, 1986), and therefore it should not be removed.

(This is one of the problems spectral analysis techniques have -- some initial trend removal is always necessary.)

Mandelbrot (1975b) and Mandelbrot and van Ness (1968) have shown that fractional Brownian surfaces have variograms which have the property that:

$$\tau(d) = d^{2H},$$

where $0 < H < 1$, and

$D = 3 - H$ (Mandelbrot, 1975b, 3827; Orey, 1970).

For a profile, the expression becomes: $D = 2 - H$.

By making the assumption that the fractional Brownian surface model is a valid mathematical approximation of terrain, and that terrain has statistical properties similar to that of the model, it is possible, therefore, to determine the fractal dimension of terrain through use of the variogram (table 5.1, and discussion in the section Data sources -- Simulated surfaces). Culling and Datko (1987, 384) state:

> A Brownian surface is ergodic. This means that points sufficiently spaced apart are independent and this implies the existence of time and space means and their equivalence and hence supplies a theoretical justification for measurement on the landscape surface.

Lovejoy and Schertzer (1987) note that the fractional Brownian surface model is a mono-dimensional model, and that (unspecified) multi-dimensional models might provide a more reasonable fit.

Although the idea of using variograms as a method for determining fractal dimensions has been known for many years (e.g., Mandelbrot, 1975b, 1977), little work has been reported in the geographic literature on the use of this method. Burrough (1981) was able to calculate the fractal dimensions of many phenomena by re-examining the published results of a number of studies which made use of variograms. Nevertheless, Burrough's studies of the spatial variation in soil (Burrough, 1983b, c) were the first in geography to make direct use of variograms to obtain the fractal dimension of the phenomena under study. Mark and Aronson (1984) were the first geographers to investigate the fractal nature of terrain using variograms. Roy, Gravel and Gauthier (1987) and Culling and Datko (1987) recently reported on the results of similar studies.

The method used by Mark and Aronson (1984) was to select randomly 32,000 pairs of points within their study areas and record the distance and elevational differences for every pair. The distances were then placed into one of 100 equal distance classes, and the variance of the height differences in each class was determined. Distance classes which contained less than 64 observations were not used in the subsequent analyses. A variogram was produced, and the fractal dimension was obtained by <u>manually</u> measuring the slope of the curve.

The data used in their analyses were obtained from U.S.G.S. DEMs. To avoid directional bias in their analyses, because of the greater number of rows in the standard DEM, the study areas as defined by Mark and Aronson (1984) were restricted to those elevations enclosed by the largest circle which could be drawn within the DEM.

Roy et al. (1987) based their study on Mark and Aronson's (1984), but with some substantial changes. They noted that by defining equal distance classes before taking the logarithm Mark and Aronson (1984) ended up with an uneven progression of distance classes in log space, and in particular they noted that the larger distance classes were over-represented. Thus, Roy et al. (1987) defined the distance classes using a geometric progression so that in log space the classes would be evenly spaced. They also used a sampling design that ensured that every distance class contained a predetermined number of samples. A number of sampling schemes were used in order to test different facets of the DEM they studied. These sampling schemes included: the entire DEM; fixed profiles along the rows, columns and diagonals of the DEM to test for anisotropies; three selected subsamples of the full DEM to test for local variation in D; and dividers tests applied to the contours.

As in the analyses by Mark and Aronson (1984) and Roy et al. (1987), most of the analyses performed in this thesis used U.S.G.S. DEMs as their data source. However, rather than define the sample area as the largest inscribed circle, the sample areas in this thesis were a consistently selected 256 by 256 array of elevations from each DEM. Various sampling schemes were then applied to the array of elevations:

i) the entire array was sampled;

ii) samples were constrained to fall along rows or columns;

iii) samples were constrained to fall within one of six angular classes;

iv) samples were constrained to fall within one of the four quarters of the entire array (i.e, the 256 by 256 array was divided into four 128 by 128 arrays).

The general arrangement of the sampling schemes is illustrated below (figure 5.2).

The various sampling schemes were devised to address a number of preliminary concerns. Sampling schemes (i) and (iv) would test the question of whether terrain is (mono-dimensionally) fractal, or more specifically, whether terrain exhibits behaviour consistent with fractional Brownian models. Sampling scheme (iv) tests the fractal properties of smaller samples, samples which would limit the number of possible landscape 'types' present in the data set. Sampling scheme (iii) was included to test the anisotropic nature of the fractal dimension of terrain, following work by Fox and Hayes (1985), in particular. An angular range of 30° was selected following Green (1985,

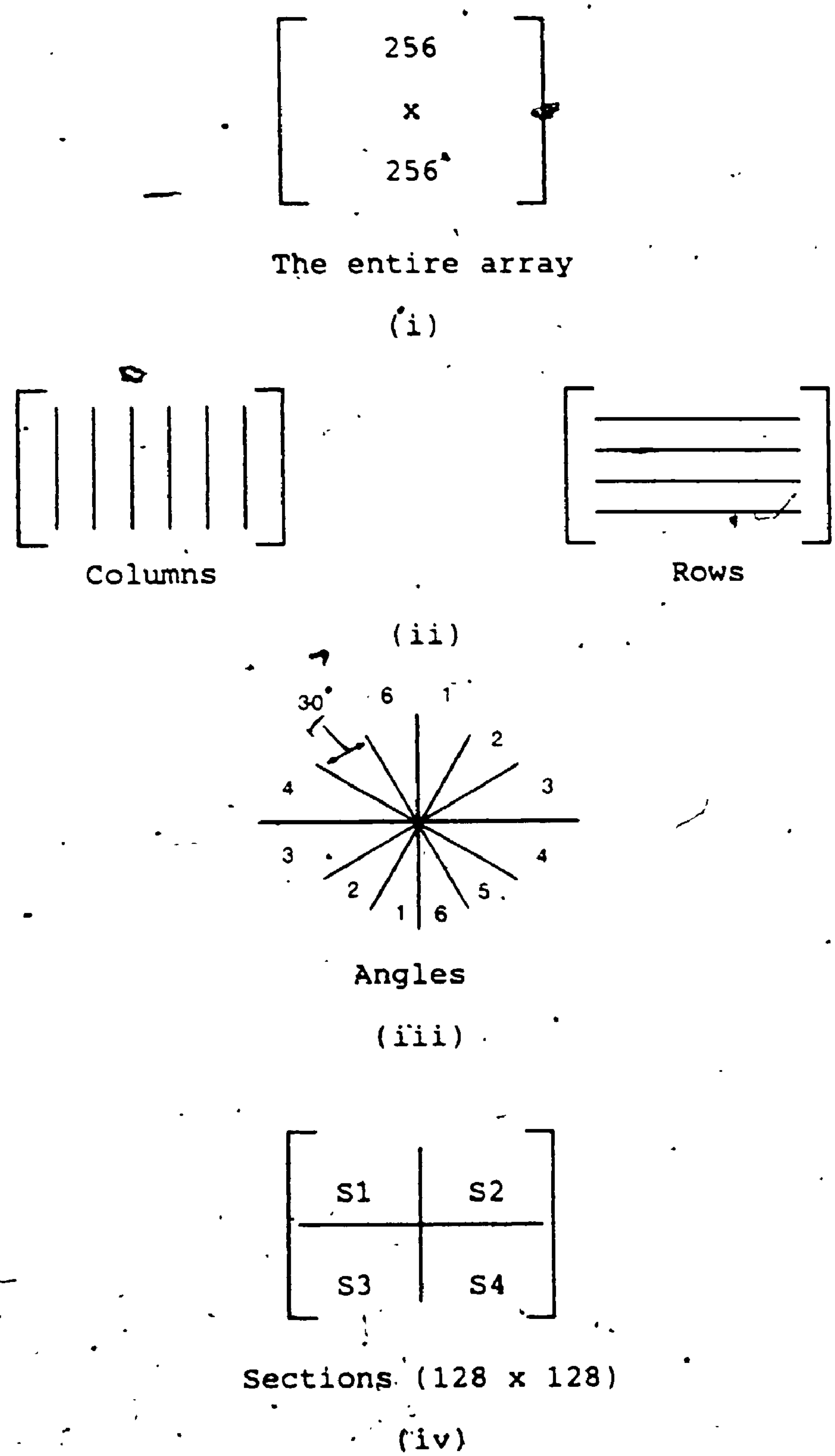

Figure 5.2 Variogram sampling schemes

190) and McBratney and Webster (1986, 630). Terrain exhibits anisotropies, but few studies on the fractal nature of terrain have directly addressed this question (e.g, Roy et al., 1987). Note that the dividers and the cell counting methods as implemented in this thesis cannot be used to test the anisotropic nature of terrain.

Sampling scheme (ii) was included to determine if the methods by which the U.S.G.S produces DEMs has some effect on their fractal dimensions. Two out of every three columns of elevations produced by the manual profiling system are interpolated values. Thus, it might be expected that the fractal dimensions of the rows and columns might be different.

5.2.3.1 Implementation

The variogram method used in this thesis on all of the sampling schemes outlined above was as follows:

i) The maximum distance contained with the input array was determined;

ii) This distance was divided into 30 distance classes using a geometric progression, such that the difference between the natural logs of the widths of each distance class was the same. The mid-point of each distance class was used in the subsequent regressions. For the sampling schemes which looked at the quarters of the DEMs, the number of distance classes was increased to 100. However, because of the scale limitations of the data, the first 50 distance classes were grouped into only 5 major classes (0-10, 10-20, 20-30, 30-40, 40-50).

iii) Within each distance class, 100 random samples were taken (200 samples in the row/column variograms). The sample pairs were obtained by:

a) A random point was selected from the entire array;

b) A vector, with a random length (constrained to fall within the limits of the selected distance class) and random direction, was used to determine the coordinates of the second point (all points that fell outside of the array bounds were rejected). For the directional-based variograms, the direction of the vector was also constrained to fall within the appropriate angular limits.

iv) The averages of the deviations of the elevations were determined for each distance class, and used in the subsequent regression analyses.

For all of the analysis methods described, the slopes of the lines were determined using conventional least-squares regression. Except as otherwise noted, the graphs were visually inspected and the breaks in the slopes determined for each interval. The best-fitting regression within each interval was then calculated and plotted. If any non-linearity then became obvious, a new set of limits was selected and the process repeated. Only regression lines with an r value greater than 0.90 are used in the analyses presented in this thesis. Although the use of least-squares regression and a 0.90 correlation cut-off point can be considered arbitrary, they are objective measures.

In the following chapter the results of investigations which used the methods discussed in this chapter, and applied them to fractal surfaces of known dimensions, are presented. In the subsequent chapter the results of the selected methods applied to the Digital Elevation Models are presented.

Chapter 6

Simulated surfaces results

In this chapter the results of the analyses performed on the simulated fractal surfaces are presented. There are three components to these results. The first, and most important, relates to the consistency of the methods used to determine the fractal dimensions of surfaces. The second component looks at the relationship between selected morphometric parameters and the fractal dimension of the surfaces. The third component considers the results of the measurement methods in light of the a priori specifications of the dimensions of the surfaces.

6.1. Results: Measurement methods

Those methods which use the surface "as is" produce results consistent with each other, while those methods which use the contour lines obtained from a surface produce very different results (table 6.1). Also, given the concerns of Gilbert (1987) and Aviles *et al*. (1987), as mentioned in the previous chapter, the results of the dividers methods applied to the contour lines are considered separately. Thus, the discussion of the measurement methods is divided into two subsections -- in the first subsection the results of the methods which used the surface "as is" are presented, while in the second subsection the results of the methods applied to the contour lines are presented.

6.1.1. Results: Surface methods

The average values for those methods which 'looked at' the entire surface are fairly consistent (table 6.1). The main exception is the cell counting method which produces values much higher than the overall averages for those surfaces with D_{avg} > 2.5. However, the cell counting method produces results consistent with the other methods for those surfaces having an average fractal dimension below 2.5. When the individual values are considered --rather than the averages -- it is clear that considerable variation may exist within a particular method, and that the pattern of this variation is not consistent across all methods (figures 6.1.1, 6.1.2, 6.1.3).

In order to test the consistency of the variogram method, variograms for the entire surface were computed four times for two of the surfaces: H3[3] and H7C. All four variograms for the H3 surface produce identical values for

[3] The surfaces are referred to by their values of H, rather than by their values of D, because no one value of D fits the surface, and because H is the parameter specified in the simulation model. (D = 3 - H)

the surface's fractal dimension, while the fractal dimensions obtained from the H7C surface are 2.19, 2.20, 2.20 and 2.21. It was concluded that the sample size used by the variogram methods is adequate.

Method	Surface H3	H4	H5	H6	H7A	H7B	H7C
Variogram							
• All	2.79	2.62	2.53	2.30	2.08	2.14	2.20
• Sector	2.79	2.64	2.53	2.27	2.07	2.15	2.21
• Angles	2.76	2.62	2.50	2.27	2.09	2.13	2.21
• R/C	2.79	2.61	2.50	2.26	2.11	2.13	2.21
Cell	2.90	2.75	2.59	2.28	2.06	2.10	2.14
Dividers	2.79	2.64	2.49	2.25	2.05	2.10	2.12
Average	2.81	2.66	2.53	2.27	2.08	2.12	2.17
Cont. Lines							
• Dividers	1.25	1.22	1.22	1.17	1.04	1.08	1.10
• Equipaced	1.37	1.34	1.30	1.27	1.10	1.16	1.18
(N)	(74)	(75)	(65)	(14)	(5)	(7)	(12)

Table 6.1

Simulated surfaces' average results

(N = # of contour lines analysed)

The spread of the dimensions produced by the variogram methods (the variance) appears to be inversely related to the fractal dimension of the surface. That is, as the apparent fractal dimension of the surface decreases, the surface appears more heterogeneous (figures 6.1.1 and 6.1.2). On the other hand, the variance of the cell counting and dividers methods appears to be directly related to the fractal dimension of the surface; the two methods

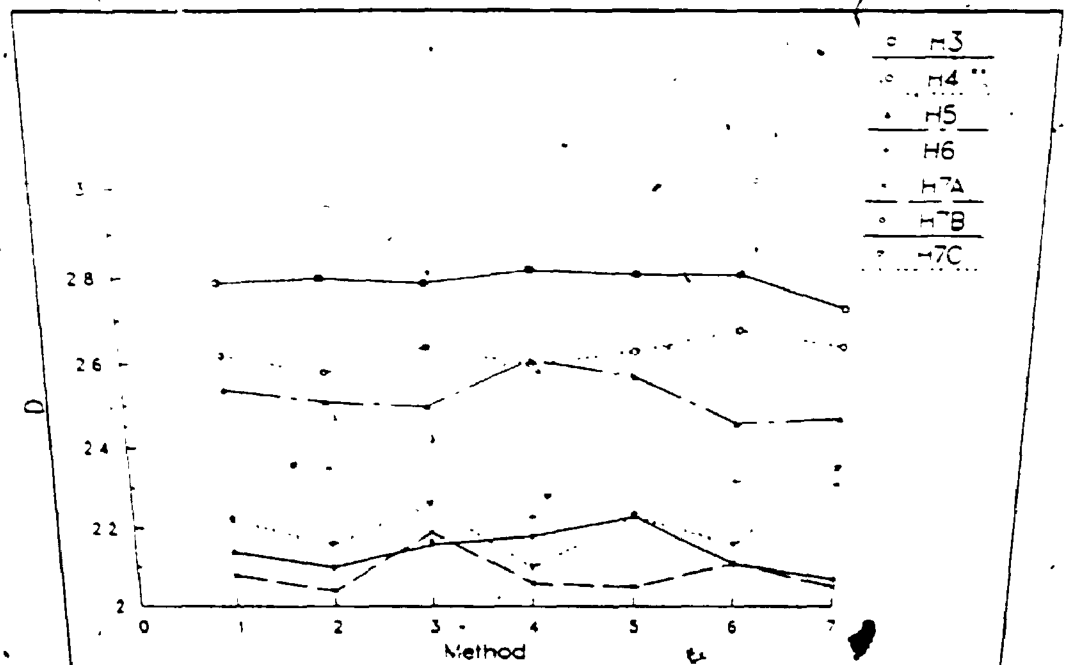

	ALL	ROW	COL	S1	S2	S3	S4
H3	2.79	2.80	2.79	2.82	2.81	2.81	2.73
H4	2.62	2.58	2.64	2.60	2.63	2.68	2.64
H5	2.54	2.51	2.50	2.61	2.57	2.48	2.47
H6	2.23	2.35	2.17	2.23	2.24	2.32	2.31
H7A	2.08	2.04	2.19	2.06	2.05	2.11	2.05
H7B	2.14	2.10	2.16	2.18	2.23	2.11	2.07
H7C	2.22	2.16	2.26	2.10	2.23	2.16	2.35

Figure 6.1.1 Simulated surface results

Note: Lines are drawn for illustrative purposes only, they are not intended to signify any relationship between the points.

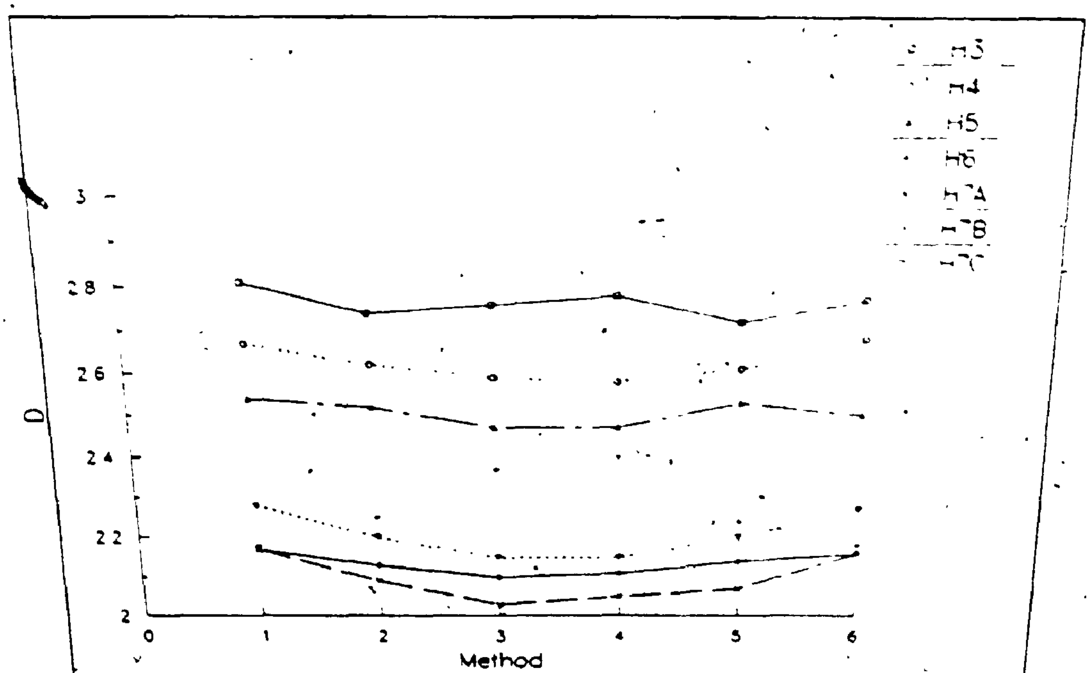

	A1	A2	A3	A4	A5	A6
H3	2.81	2.74	2.76	2.78	2.72	2.77
H4	2.67	2.62	2.59	2.58	2.61	2.68
H5	2.54	2.52	2.47	2.47	2.53	2.50
H6	2.18	2.25	2.37	2.40	2.24	2.18
H7A	2.17	2.09	2.03	2.05	2.07	2.16
H7B	2.17	2.13	2.10	2.11	2.14	2.16
H7C	2.28	2.20	2.15	2.15	2.20	2.27

Figure 6.1.2 Simulated surface results

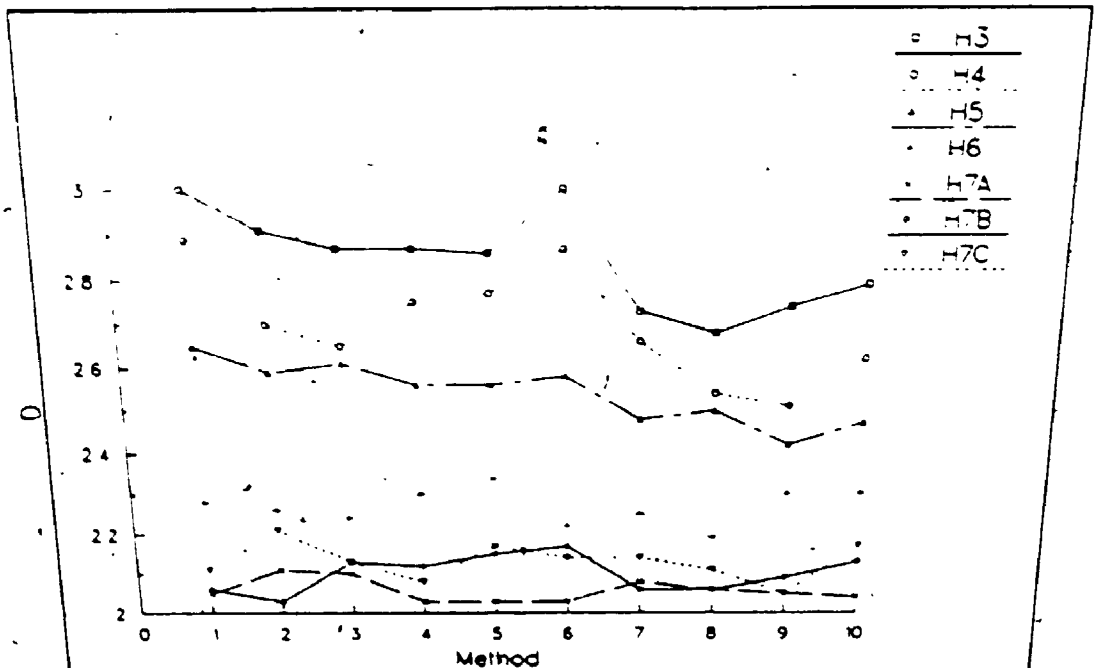

	CC1	CC2	CC3	CC4	CC5	DI1	DI2	DI3	DI4	DI5
H3	3.00	2.91	2.87	2.87	2.86	3.00	2.73	2.68	2.74	2.79
H4	2.89	2.70	2.65	2.75	2.77	2.87	2.66	2.54	2.51	2.62
H5	2.65	2.59	2.61	2.56	2.56	2.58	2.48	2.50	2.42	2.47
H6	2.28	2.26	2.24	2.30	2.34	2.22	2.25	2.19	2.30	2.30
H7A	2.05	2.11	2.10	2.03	2.03	2.03	2.08	2.06	2.05	2.04
H7B	2.06	2.03	2.13	2.12	2.15	2.17	2.06	2.06	2.09	2.13
H7C	2.11	2.21	2.13	2.08	2.17	2.14	2.14	2.11	2.05	2.17

Figure 6.1.3 Simulated surface results

produced more consistent results the lower the surface's fractal dimension (figure 6.1.3). These results are explained below.

Consider the question of the anisotropic nature of a generated surface. For surfaces with higher fractal dimensions, profiles taken in any direction would appear statistically very similar (figure 6.2.1). For surfaces with lower fractal dimensions, directional profiles would appear statistically different (with respect to their lower order moments) because of the presence of long-term trends in the surface (figure 6.2.2). Conversely, when horizontal sections (slices) of the surfaces are considered, the higher the surface's D value, the greater the variance in the characteristics of those slices. The problem of working with a closed system compounds the interpretation of these results, however. That is, since the dimensions are constrained to fall between 2.0 and 3.0, the possible variance of the dimensions obtained from a surface which has a mean of 2.08 will be very different from the possible variance obtained from surface which has a mean of 2.5 (c.f. Zar, 1984).

Even when working with surfaces which are known to be fractal, the plots used in the determination of the fractal dimensions sometimes exhibited data points that had to be excluded from the analysis. That is, some points were obvious outliers. This is to be expected, because the data sets have both an upper scale limit, and a lower scale

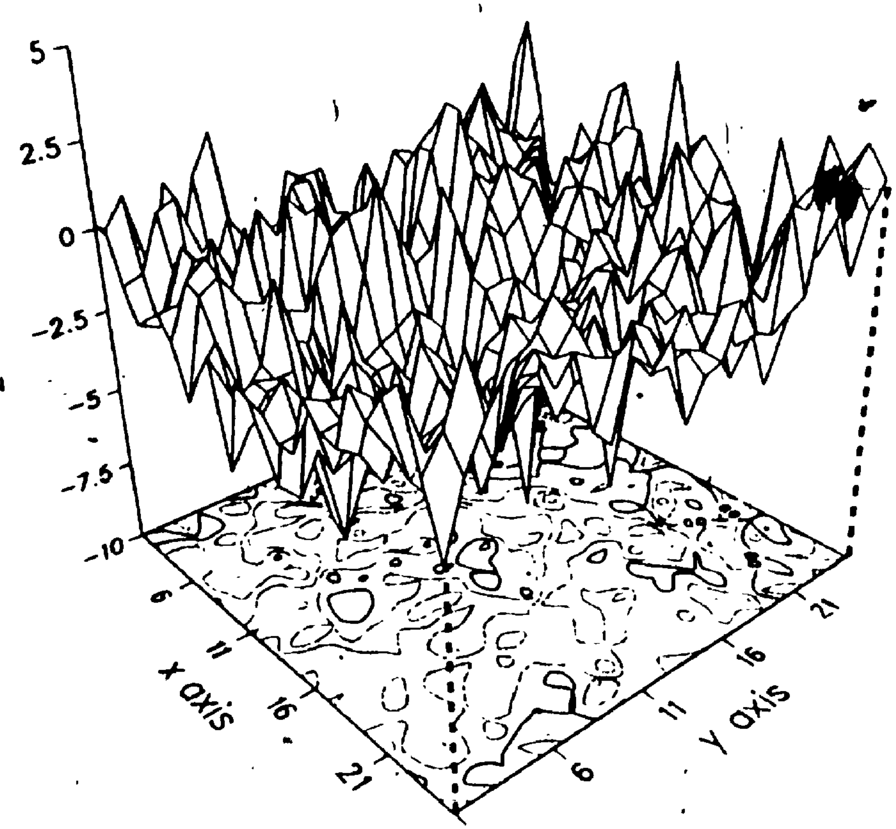

Figure 6.2.1 Simulated fractal surface, H = 0.3
(Note the equal z ranges on the x and y axes)

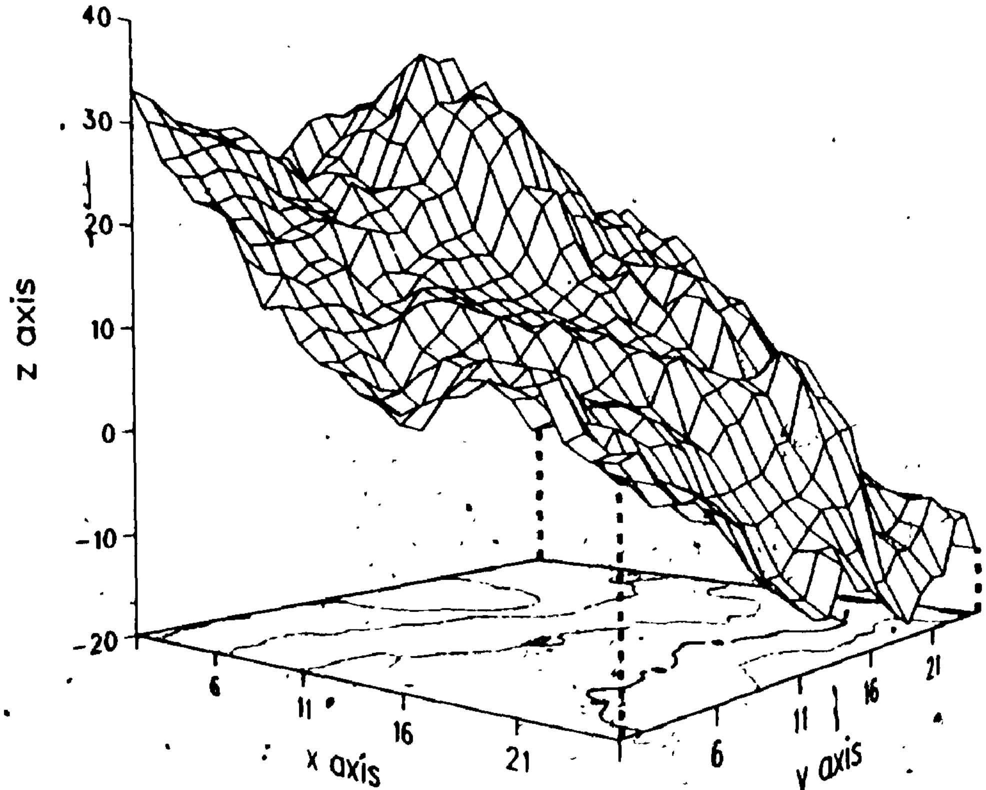

Figure 6.2.2 ,Simulated fractal surface, $H = 0.7$
(Note the unequal z ranges on the x and y axes)

limit. The variogram methods required the least amount of data culling, only a few of the plots associated with surfaces H3 and H5 required some data points to be removed. Generally one or two data points associated with the shortest distance classes were removed, and occasionally it was necessary to exclude some of the data points associated with the longest distance classes. Overall, the data point associated with the first distance class -- cells one distance unit apart -- exhibited much lower variance than expected in the majority of the variograms.

When looking at the plots of the cell counting method no data points were excluded when analysing the H3, H4 and H5 surfaces, while for the remaining surfaces in most instances the data point associated with the largest (128) cell size had to be excluded. When the graphs of the dividers method were analysed all surfaces had at least one graph with at least one data point removed -- generally the data point associated with the smallest array size of 16 (or conversely, the largest cell size). The majority of these outliers occurred because at the largest cell size the surfaces appeared smoother (of lower D) than they did at the smaller cell sizes. When viewing the graphs associated with the dividers method, the overall impression was that the data points exhibited more curvature as the fractal dimension decreased (i.e., the surfaces appeared less like true fractal surfaces as their dimension decreased). This could be a result of using only a very limited sample of the surface when contouring the smaller array sizes.

A selection of the plots associated with the analyses carried out on the simulated surfaces, are included here (figure 6.3). The selection includes some examples of the 'best' plots (very linear) and some examples of the 'worst' plots, with much curvature and/or scatter evident.

6.1.2. Results: Contour line methods

The two methods which used the individual contour lines to determine the fractal dimensions of the surfaces -- the dividers method and the equipaced polygon method -- produce results, on those surfaces with fractal dimensions greater than 2.5, which differ greatly from those produced by the methods which used the surface "as is" (table 6.1). On surfaces with $D_{avg} > 2.5$, both methods underestimate the fractal dimensions of the surfaces by large amounts; on surfaces with $D_{avg} < 2.5$, the equipaced polygon method produces results which agree with those of the surficial methods, while the dividers method continues to produce values which are consistently lower than all others. The dividers methods -- whether applied to the surfaces or to the contour lines -- consistently produce estimates of the fractal dimensions which are below the overall average values.

The relationship between the results of the dividers method and the cell counting method (table 6.1) parallels

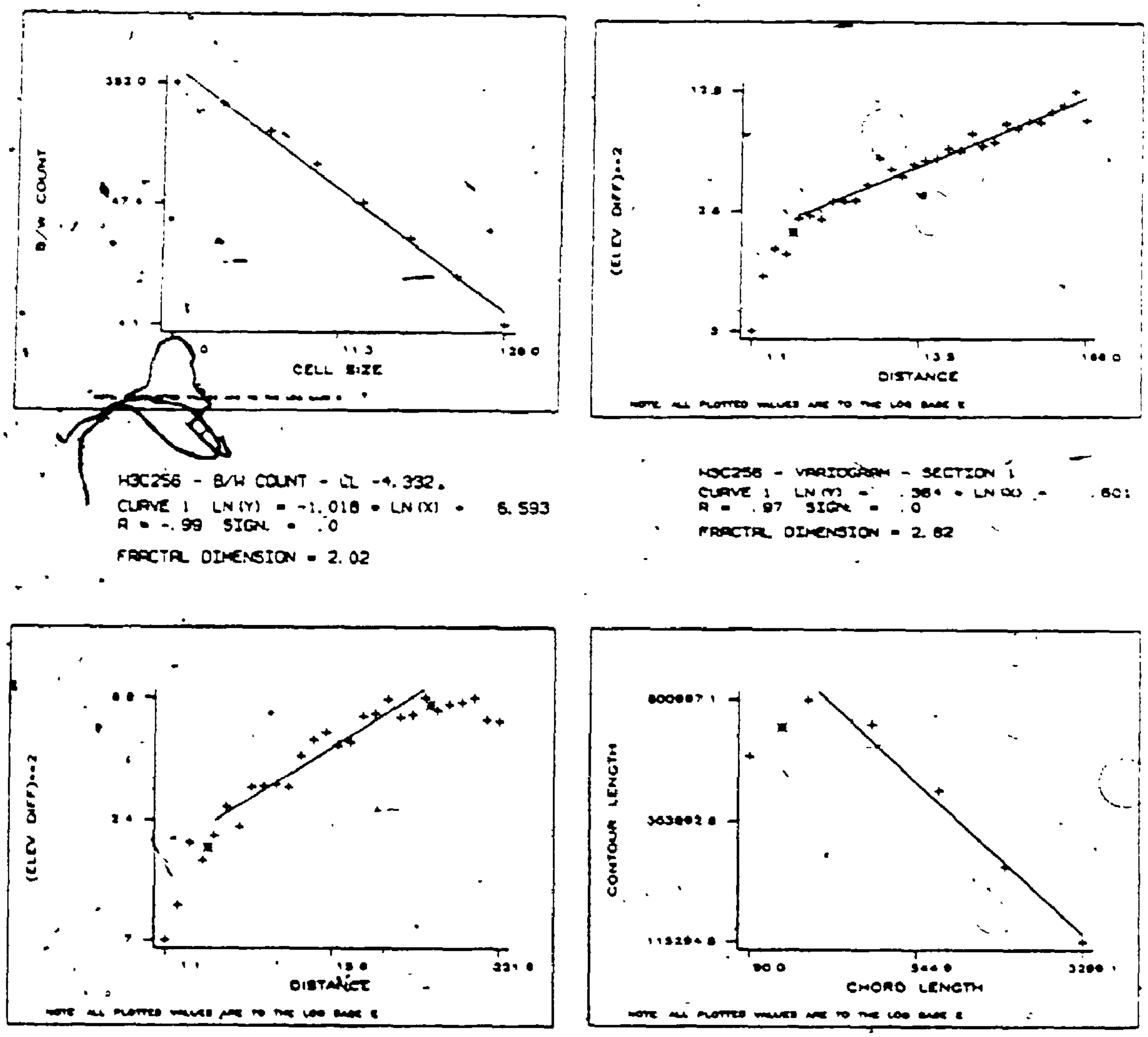

H3C256 - B/W COUNT - CL -4.332.
CURVE 1 LN(Y) = -1.018 * LN(X) + 6.593
R = -.99 SIGN. = .0
FRACTAL DIMENSION = 2.02

H3C256 - VARIOGRAM - SECTION 1
CURVE 1 LN(Y) = .384 * LN(X) + .601
R = .97 SIGN. = .0
FRACTAL DIMENSION = 2.82

H3C256 - VARIOGRAM - COLUMN DATA
CURVE 1 LN(Y) = .415 * LN(X) + .515
R = .95 SIGN. = .0
FRACTAL DIMENSION = 2.79

H3C256 - DIVIDERS METHOD - CL 0.769
CURVE 1 LN(Y) = -.880 * LN(X) + 17.210
R = -.99 SIGN. = .0
FRACTAL DIMENSION = 1.88

Figure 6.3 Examples of regression plots

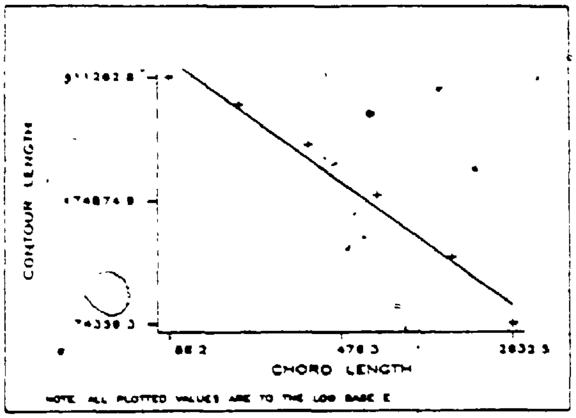

HSC256 - DIVIDERS METHOD - CL 3.151
CURVE 1 LN(Y) = -.499 * LN(X) + 15.278
R = -.99 SIGN. = .0
FRACTAL DIMENSION = 1.50

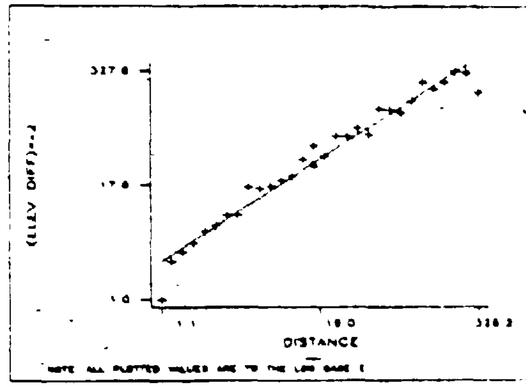

HSC256 - VARIOGRAM - ALL DATA 2
CURVE 1 LN(Y) = .910 * LN(X) + .856
R = .98 SIGN. = .0
FRACTAL DIMENSION = 2.54

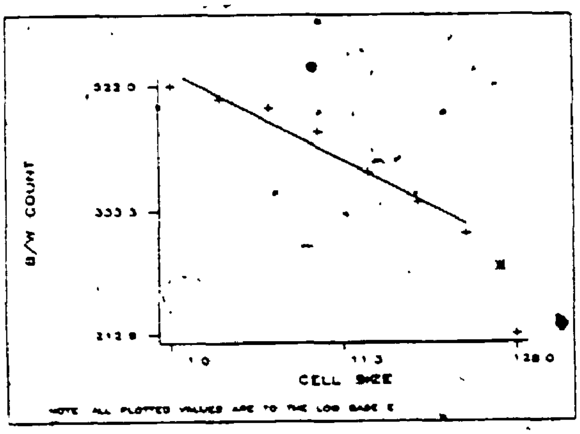

H7C2568 - B/W COUNT - CL 134.332
CURVE 1 LN(Y) = -.132 * LN(X) + 6.312
R = -.98 SIGN. = 0
FRACTAL DIMENSION = 1.13

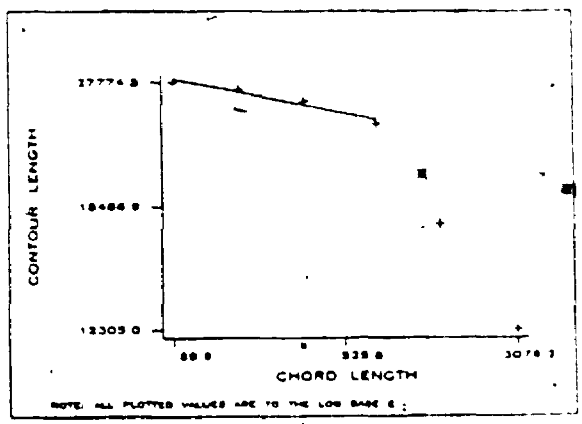

H7C2568 - DIVIDERS METHOD - CL 80.234
CURVE 1 LN(Y) = -.064 * LN(X) + 10.032
R = -.97 SIGN. = 0
FRACTAL DIMENSION = 1.06

Figure 6.3 (continued) Examples of regression plots the results presented in Goodchild (1982, table I). There it is also evident that the dividers method produces values which are consistently lower than those produced by the cell counting method. Additionally, in that study the differences between the dimensions calculated by the two methods increases as the average dimensions increase, similar to the results presented here (table 6.1). It appears that the cell counting method produces values which are an increasing function of the actual fractal dimension of the surface.

When the average estimates of the fractal dimensions produced by the two individual contour line methods for each slice of the surface are plotted (figure 6.4), it is clear there is a large variance even within one surface. This raises the question of the reliability of the fractal dimension obtained from single isolines (e.g., single coastlines), and the subsequent application of that dimension to the entire surface. As an example, the values associated with each mid-elevation contour line of the surface H3 are presented below (table 6.2). With such variance the accuracy of dimensions obtained from single isolines should always be questioned. It should be kept in mind that the values produced by the equipaced polygon method represent averages of all possible starting positions, and therefore are expected to be more consistent than the dividers methods estimates. Note also that the results illustrated (table 6.2) are representative of all results produced by the contour line methods.

Figure 6.4 Dividers methods results

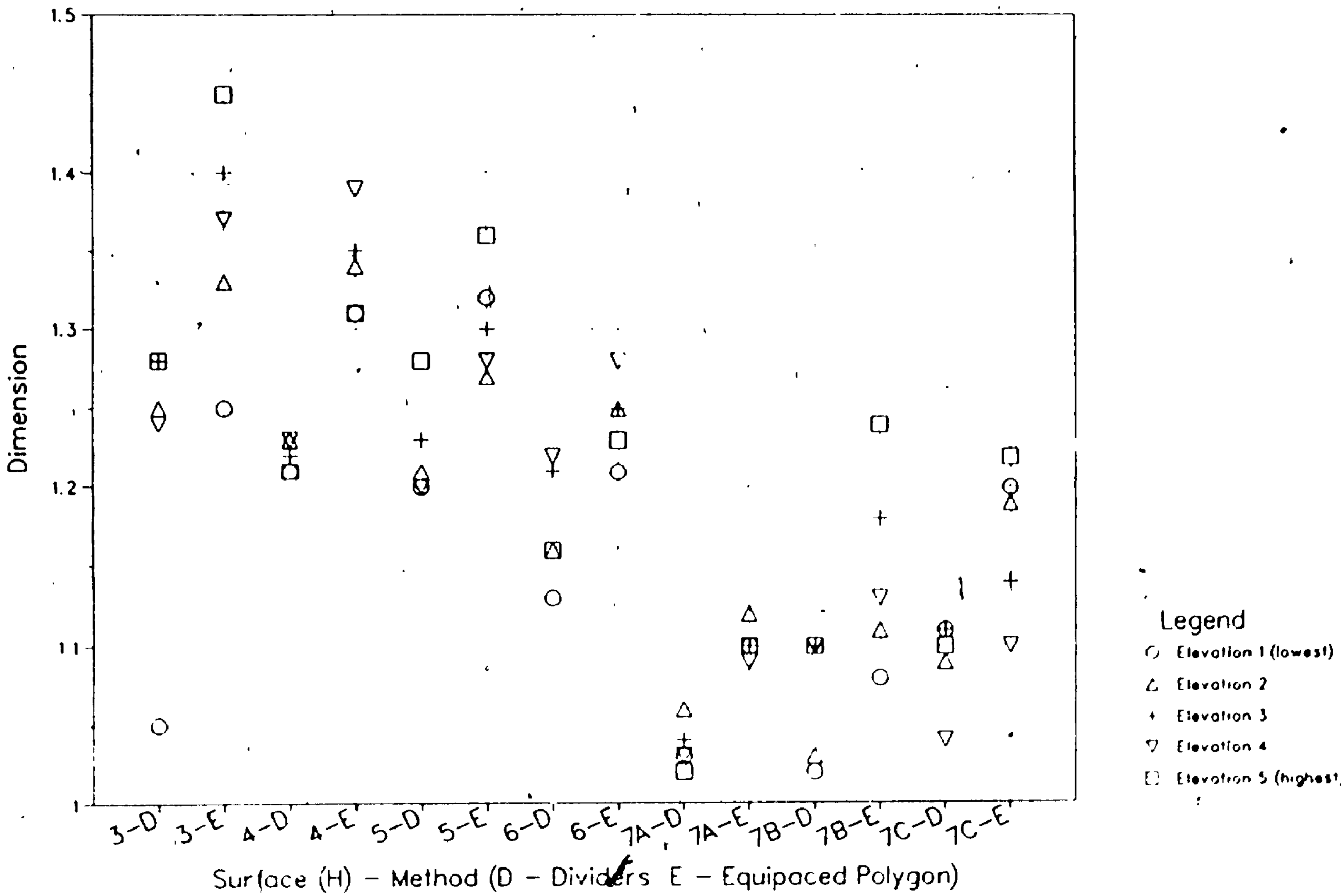

Contour Line	Dividers D	Dividers intercept	Equipaced D	Equipaced interc't
1	1.36	11.15	1.42	11.60
2	1.29	10.76	1.63	12.99
3	1.34	13.47	1.48	14.61
4	1.51	13.74	1.61	14.51
5	1.19	9.21	1.17	9.13
6	1.27	11.44	1.49	13.19
7	1.27	9.13	1.21	8.99
8	1.21	11.29	1.33	12.20
9	1.23	9.15	1.33	9.78
10	1.33	13.29	1.49	14.41
11	1.29	10.91	1.41	11.69
12	1.21	9.15	1.35	9.92
13	1.33	11.94	1.56	13.54
14	1.11	8.50	1.25	9.25
15	1.27	10.34	1.28	10.53
Mean	1.28	10.90	1.40	11.76
Std.	0.09	1.64	0.14	1.99
Max	1.51	13.74	1.63	14.61
Min	1.11	8.50	1.17	8.99

Table 6.2

Individual contour line results
for the H3 surface

As mentioned previously (chapter 5), the dividers method outlined in Shelberg et al. (1982) was used in this thesis. Because the results produced by this method are at odds with the results produced by the other methods, a second algorithm was used as a check to determine the relationship between the divider's width and the number of dividers necessary to cover the line. This alternative algorithm, based on the caliper's method implemented in the PLUSX subroutine PCCULL (Goodchild, 1981), produces results very similar to those produced by the Shelberg et al. (1982) algorithm. Thus, the fractal dimensions produced by the dividers method appear independent of the particular implementation of the method.

In order to test what effect contour line smoothing would have on the results, an additional set of contour lines were generated for the H7A surface. For this additional set <u>only</u>, the contour lines were smoothed using the default parameters supplied by the DI-3000 contouring package. The individual contour lines are all slightly shorter in length, and the average fractal dimension for the surface is only 2% smaller than the average produced when using the unsmoothed contour lines. Thus, smoothing of the contours does not appear to influence the fractal dimensions of the contour lines. This provides support for Roy <u>et al</u>.'s (1987) contention concerning the source of cartographic lines and the influence on the fractal dimension.

6.2. Results: Morphometric parameters

Using the simulated surfaces, some preliminary investigations were made to see what relationships exist between the fractal dimensions of the surfaces and some selected morphometric parameters. It has been emphasised previously that the fractal dimension quantifies one aspect of form. It is, therefore, interesting to see which of the traditional form parameters it most closely approximates, if any. The morphometric parameters selected for these analyses were picked as representative parameters following work by Evans (1972, 1986) and Mark (1975), and should capture some of the surfaces' characteristics. There are, of course, many other morphometric parameters which could have been selected (such as those relating to slope), but as the emphasis of this work is on fractal geometry the selection was purposely kept limited. The parameters selected are listed in table 6.3.

Some of the morphometric parameters are scale dependent (table 6.3; table 6.4). The simulated surfaces were generated by Mandelbrot's method, as described in the previous chapter, and were used as is. That is, they were not standardized to have, for example, equal ranges. As mentioned previously, the fractal dimension is a measure of the persistence of the first derivatives. High fractal dimensions ($D > 2.5$) correspond to antipersistent derivatives, with negative correlations among the increments, while low fractal dimensions ($D < 2.5$) correspond to persistent derivatives, with positive correlations among the increments. Thus, surfaces with a high fractal dimension would exhibit a small overall range but would be rough everywhere, whereas surfaces with a low fractal dimension would have a very large range but appear relatively smooth.

Therefore, the correlations between those morphometric parameters which are scale dependent and the fractal dimension are meaningless. Thus, only those correlations

Parameter	Description
Mean	Mean elevation over all 65 536 cells
Sd	Standard deviation of the elevations; representative of the relief of the topography.
Skew	Skewness -- measures the degree to which the distribution of the elevations follows a normal distribution. A positive value indicates that more of the elevations fall below the mean, with most of the extreme values greater than the mean; a negative value indicates the reverse. The closer the value is to zero, the more 'normal' is the distribution. (the third moment)
Kurt	Kurtosis -- measures the relative peakedness or flatness of the distribution of the elevations. A normal distribution receives a value of 3. Values below 3 indicate that the distribution of elevation is tending towards a more uniform distribution, whereas values above 3 indicate that the elevations are clustered around the mean.
Cd	Coefficient of dissection -- reflects the distribution of the landmass with elevation. Strahler (1952) concludes that values above 0.6 indicate that the landscape is in a 'youthful', inequilibrium stage, values between 0.65 and 0.35 indicate a landscape in a 'mature' or equilibrium stage, and values below 0.35 indicate that the area is in an 'old age' stage with monadnock masses present. The formula used is: $cd = \frac{z_{Avg} - z_{min}}{z_{max} - z_{min}}$

Table 6.3 Morphometric parameter descriptions

between the skewness, kurtosis and coefficient of dissection are presented in table 6.5.

Surf	Skew	Kurt	C.d.
H3	0.094	3.262	0.541
H4	-0.057	2.541	0.521
H5	0.177	2.599	0.468
H6	-0.202	4.163	0.531
H7A	0.166	2.209	0.511
H7B	-0.731	3.359	0.583
H7C	0.655	2.695	0.393

Table 6.4

Morphometric parameters of the simulated surfaces

The variables of skewness, kurtosis and the coefficient of dissection must reflect very different aspects of the surfaces, as reflected by their very low correlations with the fractal dimensions. However, actual interpretation of these parameters will be left to the following chapter, where the morphometric parameters have been applied to the DEMs, and their values have geomorphic significance.

Parameter	R^2	Significance
Skewness	0.01	0.85
Kurtosis	0.06	0.59
C.d.	0.02	0.77

Table 6.5

Correlations between selected morphometric parameters and D

6.3. Surfaces: Dimensions and expectations

From the previous discussions it can be seen that the fractal dimensions calculated for the surfaces differ from the dimensions as specified by the parameter H (table 6.1). There are at least two explanations for this observation. The measurement methods may be inaccurate, and may return the incorrect values for the dimensions of the surfaces. However, it is unlikely that this explanation is correct given the agreement among the various methods and the results of previous studies which have independently arrived at the same fractal dimension for selected features (e.g., the west coast of Britain). Alternatively, the method used to produce the simulated surfaces may not produce surfaces with the expected dimension. That is, although the parameter H is specified as 0.7, for example, the simulated surface may be found to have a fractal dimension of 2.1 rather than its expected dimension of 2.3. This explanation is the more likely.

The algorithm which produces the simulated surfaces is based on a generalization of a technique used to generate Brownian surfaces (H = 0.5), which by definition have a fractal dimension of 2.5. Thus, although the method is known to produce Brownian surfaces with the correct dimension (and was found to do so here), very little work has been conducted on the generalization of the technique to the production of fractional Brownian surfaces and the relationship between the expectation --associated with the parameter H, and the realization -- associated with the parameter D.

In this chapter some preliminary investigations were carried out to test the consistency of the methods used to determine the fractal dimensions of surfaces. It is evident that for surfaces with fractal dimensions below 2.5, most of the methods tested should produce reasonably consistent values, given the differences between those methods which used the surface "as is" and those methods which used the contour lines. Of course, these conclusions are based on investigations of surfaces which are known to have fractal properties -- it remains to be seen whether the various methods behave similarly when applied to natural surfaces. In the following chapter this question will be considered.

Chapter 7

Digital elevation model results

In the following sections the results of the investigations into the fractal nature of the digital elevation models (DEMs) are considered. In the first section the locations of the DEMs, and their assignment to physiographic provinces, are considered. Following this, an overall summary of the results will be made in light of the impressions obtained from the analyses performed on the fractal surfaces. As noted in chapter 5, the USGS uses a number of methods to produce their DEMs. The affirmative answer to the question 'Does the method of generation of the DEM influence the fractal characteristics of the DEM' will be presented in the third section. The bulk of this chapter is contained in the fourth section, wherein the results of the investigations on the fractal nature of the DEMs are considered. Comparisons between the results of previous investigations and the results obtained here are made in the fifth section. The chapter concludes with a summary of the material presented.

7.1 DEM Locations

The USGS is far from completing its task of producing a DEM for every 1:24,000 quad sheet that covers the United States, and the existing coverage varies widely -- from areas such as Florida which have very few models completed, to areas which have almost a complete coverage, such as the state of Wyoming (Anonymous, 1985). In order to make valid statistical tests of the consistency of the fractal dimension, a random sample of all potential DEMs, stratified by physiographic province (section 7.1.1), would be the preferred sampling scheme. However, constraints on data acquisition precluded the taking of such a sample. Therefore, the datasets used in the following analyses were those which were freely available. Forty DEMs were obtained from Dr. J. Carter (University of Tennessee); twenty DEMs were obtained from Dr. D. M. Mark (SUNY at Buffalo). As they had obtained the DEMs for their own research purposes, the majority of the DEMs are from the eastern United States, with 28 of the DEMs from the state of Tennessee alone (figure 7.1).

The DEMs obtained from Dr. Carter are labelled DEM1 to DEM40, while those obtained from Dr. Mark are labelled DM1 to DM20 (table 7.1). Two of the original sixty datasets were removed from the analyses: DEM15 because of problems in reading the data from the computer tape, and DM19 because it was found to be a duplicate of DEM21. While conducting the preliminary analyses the locations of the individual DEMs were purposely left out so as not to bias the analyses

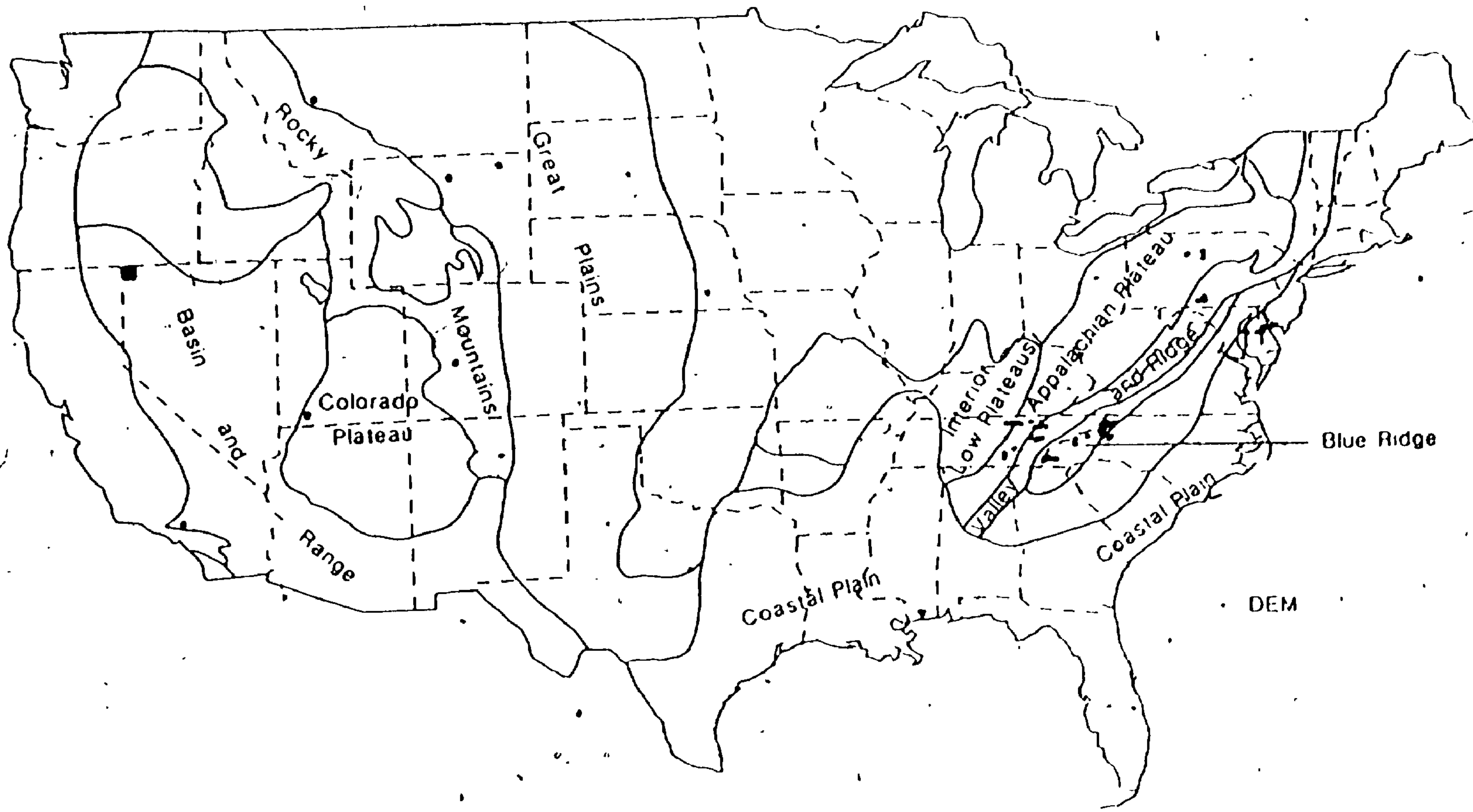

Figure 7.1 DEM locations within the physiographic provinces

DEM Name	QUAD Name	State	Physio Region	Method of Production	Accuracy (M rms)	Longitude (W) ° ' "	Latitude (N) ° ' "
DEM21	Barbara	MS	1	Stereoplotter	0-3	89 00 00	30 52 30
DEM22	Benndale SE	MS	1	Stereoplotter	0-3	89 00 00	30 37 30
DEM23	Benndale SW	MS	1	Stereoplotter	0-3	88 52 30	30 37 30
DEM9	Krone Ranch	MO	5	GPMII	0-7	112 15 00	47 07 30
DEM35	Shining Rock	NC	2	GPMII	8-15	82 52 30	35 15 00
DEM34	Silvers Bald	NC	2	GPMII	8-15	83 37 30	35 30 00
DEM40	Sylavorth	NC	2	GPMII	8-15	83 15 00	35 22 30
DEM13	Billingsley Gap	TN	4	GPMII	0-7	85 15 00	36 37 30
DEM3	Duncan Flats	TN	4	GPMII	8-15	84 22 30	36 07 30
DEM18	Grassy Cove	TN	4	GPMII	0-7	85 00 00	35 45 00
DEM10	Herbert Domain	TN	4	GPMII	0-7	85 15 00	35 45 00
DEM14	Jelicoest	TN	4	GPMII	0-7	84 15 00	36 30 00
DEM4	Lake City	TN	4	GPMII	8-15	84 15 00	36 07 30
DEM1	Loudon	TN	3	GPMII	0-7	84 15 00	36 37 30
DEM17	Madisonville	TN	3	GPMII	0-7	84 15 00	36 30 00
DEM2	Meadow	TN	3	GPMII	0-7	84 15 00	36 37 30
DEM12	Melvine	TN	4	GPMII	0-7	85 07 30	36 37 30
DEM5	Norris	TN	3	GPMII	8-15	84 07 30	36 07 30
DEM38	Oswald Dome	TN	3	GPMII	8-15	84 37 30	36 07 30
DEM20	Pattie Gap	TN	3	GPMII	0-7	84 37 30	36 37 30
DEM19	Pennine	TN	4	GPMII	0-7	85 00 00	36 37 30
DEM8	Sampson	TN	6	GPMII	0-7	85 22 30	36 37 30
DEM7	Spenser	TN	6	GPMII	0-7	85 30 00	36 37 30
DEM36	Tallassee	TN	3	GPMII	8-15	84 07 22	36 30 00
DEM15	Vandover	TN	4	GPMII	0-7	85 07 30	35 15 00
DEM16	Vonore	TN	3	GPMII	0-7	84 22 30	36 30 00
DEM6	Welchland	TN	6	GPMII	0-7	85 37 30	35 37 30
DEM37	Whiteoak Flats	TN	2	GPMII	8-15	84 07 30	35 22 30
DEM29	Eagan	TN/KY	4	GPMII	8-15	84 00 00	36 30 00
DEM28	Jellico East	TN/KY	4	GPMII	8-15	84 07 30	36 30 00
DEM32	Cades Cove	TN/NC	2	GPMII	8-15	83 52 30	35 30 00
DEM39	Davy Crockett Lake	TN/NC	2	GPMII	8-15	82 52 30	36 00 00
DEM31	Hot Springs	TN/NC	2	GPMII	8-15	82 52 30	35 52 30
DEM33	Thunderhead Mt.	TN/NC	2	GPMII	8-15	83 45 00	35 30 00
DEM30	Unicoi	TN/NC	2	GPMII	8-15	82 22 30	36 07 30
DEM24	Cedar BreaksNW	UT	8	Ortho	0-5	113 00 00	37 37 30
DEM25	Cedar Breaks SW	UT	8	Ortho	0-2	113 00 00	37 30 00
DEM26	Cedar BreaksNE	UT	8	Ortho	0-4	112 52 30	37 37 30
DEM27	Cedar Breaks SE	UT	8	Ortho	0-2	112 52 30	37 30 00

Table 7.1 DEM locations and method of production

DEM Name	QUAD Name	State	Physio Region	Method of Production	Accuracy (M rms)	Longitude (W) ° ' "	Latitude (N) ° ' "
DM17	Pacifico Mountain	CA	9	GPMII	0-7	118 07 15	34 22 30
DM20	Grand	CO	7	GPMII	7-15	107 00 00	39 00 00
DM9	Adel	OR	9	Stereoplotter	0-9	120 00 00	42 07 30
DM1	Calderwood Resevoir	OR	9	Stereoplotter	0-4	119 52 30	42 07 30
DM2	Coleman Lake	OR	9	Stereoplotter	0-6	119 52 30	42 00 00
DM6	Collins Rim	OR	9	Stereoplotter	0-6	120 07 30	42 00 00
DM7	Crump Lake	OR	9	Stereoplotter	0-11	119 52 30	42 15 00
DM5	Drake Peak	OR	9	Stereoplotter	0-10	120 07 30	42 15 00
DM3	May Lake	OR	9	Stereoplotter	0-3	120 00 00	42 00 00
DM8	Priday Resevoir	OR	9	Stereoplotter	0-10	120 00 00	42 15 00
DM4	Sage Hen Butte	OR	9	Stereoplotter	0-7	120 07 30	42 07 30
DM11	Augwick	PA	3	GPMII	0-7	77 52 30	40 15 00
DM13	Blain	PA	3	GPMII	0-7	77 37 30	40 15 00
DM12	Blairs Mills	PA	3	GPMII	0-7	77 45 00	40 15 00
DM14	McCoysville	PA	3	GPMII	0-7	77 37 30	40 22 30
DM10	Keating Summit	PA	4	GPMII	0-7	78 15 00	41 37 30
DM16	Lee Fire Tower	PA	4	GPMII	7-15	77 37 30	41 30 00
DM15	Marshlands	PA	4	GPMII	7-15	77 37 30	41 37 30
DM18	Big Horn	WY	5	Ortho	0-5	107 00 00	44 37 30

Table 7 : continued DEM locations and method of production

in any way. For example, if it was known that the four datasets DEM24, DEM25, DEM26, and DEM27 were located adjacent to each other, it might have led to searching for common patterns in their variogram plots, patterns that may or may not exist.

7.1.1 Physiographic regions

The datasets were placed into groups which reflect their overall physical characteristics. The results of previous analyses on the fractal characteristics of terrain (Mark and Aronson, 1984) were also considered with respect to a natural classification scheme. The division of the United States into natural regions has been intensely researched (e.g., Hunt, 1974, Thornbury, 1965). "Each province has characteristics peculiar to itself -- a distinctive structural framework giving rise to distinctive landforms expressing their structure..." (Hunt, 1974, 3). It is expected that the morphometric characteristics of the DEMs would be consistent with this classification scheme; however, it remains to be seen whether the fractal characteristics are consistent also. However, the fractal dimension has been found to be closely tied into visual qualities of roughness (Pentland, 1983, 1984), so some agreement is expected.

"The natural regions of the United States and Canada" (Hunt, 1974) was used as the primary source for defining the physiographic divisions used in this work. The physiographic provinces to which most datasets belonged was generally easy to determine. However, some datasets were located close to the borders of their province, and some provinces borders are gradational over a wide area (Hunt, 1974). In order to correctly assign the datasets to their respective physiographic province, a small scale map (Raisz, 1957) was used for this step. Nonetheless, for those DEMs which straddled the boundaries, their placement into the appropriate province was sometimes difficult (e.g., DEM7 and DEM8 into the Interior Low Plateaus, rather than into the Appalachian Plateau).

The 58 DEMs represent nine of the twenty-four physiographic provinces which make up the coterminous United States. The distribution of the DEMs into the nine provinces varies greatly, from the Rocky Mountains physiographic province which is represented by only one DEM, to the Appalachian Plateaus province which is represented by fourteen DEMs. The physiographic provinces which are represented, and the numbers of DEMs which represent them, are presented below (table 7.2). In the following tables and figures, the provinces will be referred to either by their physiographic region number or by their name.

Physiographic		Number of DEMs
Region	Province	
1	Coastal Plain	3
2	Blue Ridge	10
3	Valley and Ridge	12
4	Appalachian Plateaus	14
5	Great Plains	2
6	Interior Low Plateaus	3
7	Rocky Mountains	1
8	Colorado Plateau	4
9	Basin and Range	10

Table 7.2

Physiographic Province Representation

In order to determine how well the physical characteristics of the datasets follow the physiographic classification scheme, a discriminant analysis was performed using a limited selection of the morphometric parameters obtained from each DEM as the discriminating variables (table 7.3). Four of the seven morphometric parameters are used in this analysis: the mean elevation, the standard deviation and kurtosis of the elevations and the coefficient of dissection. These four variables have correlations with each other of less than ± 0.15, with the exception of the correlation between the mean and standard deviation, which is 0.50.

The sole aim of this analysis is to determine the adequacy of the classification scheme and the relative consistency of the morphometric parameters -- as expressed

CANONICAL DISCRIMINANT FUNCTIONS

FUNCTION	EIGENVALUE	PERCENT OF VARIANCE	CUMULATIVE PERCENT	CANONICAL CORRELATION	AFTER FUNCTION	WILKS' LAMBDA	CHI-SQUARED	D F	SIGNIFICANCE
					0	0 0059291	258 96	32	0 0000
1*	36 81248	94.42	94 42	0 9866883	1	0 2241941	75 510	21	0 0000
2*	1 29417	3 32	97 74	0 7510747	2	0 5143402	33 576	12	0 0008
3*	0 80305	2 06	99 80	0 6673706	3	0 9273799	3 8073	5	0 5775
4*	0 07831	0 20	100 00	0 2694811					

* MARKS THE 4 CANONICAL DISCRIMINANT FUNCTIONS WHICH REMAINED IN THE ANALYSIS

STANDARDIZED CANONICAL DISCRIMINANT FUNCTION COEFFICIENTS

	FUNC 1	FUNC 2	FUNC 3	FUNC 4
MEAN	1 17718	-0 13854	0 07273	-0 00227
KURT	0 02807	0 35373	0 43214	0 88893
CD	-0 60001	0 63791	0 81011	-0 28605
SD	-0 16144	0 99593	-0 37405	0 00666

CLASSIFICATION RESULTS

ACTUAL GROUP	NO. OF CASES	PREDICTED GROUP MEMBERSHIP 1	2	3	4	5	6	7	8	9
GROUP 1 Coastal Plain	3	3 100 0%								
GROUP 2 Blue Ridge	9		8 88 9%	1 11 1%						
GROUP 3 Valley and Ridge	12			11 91 7%	1 8 3%					
GROUP 4 Appalachian Plateaus	14			2 14 3%	10 71 4%		2 14 3%			
GROUP 5 Great Plains	2					2 100 0%				
GROUP 6 Interior Low Plateau	3				1 33 3%		2 66 7%			
GROUP 7 Rocky Mountains	1							1 100 0%		
GROUP 8 Colorado Plateau	4								4 100 0%	
GROUP 9 Basin and Range	10									10 100 0%

PERCENT OF "GROUPED" CASES CORRECTLY CLASSIFIED 87 93%

Table 7 3

Discriminant analysis using the morphometric parameters by the percent of cases correctly classified -- not to examine which of the morphometric parameters maximize the differences between groups. It is recognized that the inequality of the sample sizes does not allow for valid statistical inferences to be made. The results are also dependent upon the ability of the selected morphometric parameters to capture the distinctive nature of each physiographic region.

Using the SPSS (SPSS Inc.) discriminant procedure, and accepting all of its defaults such as direct entry of all discriminating variables, 50 or 86% of the cases are assigned to their correct group (table 7.3). Seven of the eight mis-assigned cases involve the Appalachian Plateau province, and in particular, four of those cases also involve the adjacent Interior Low Plateau province. Altogether, five of the mis-assigned cases occur along the border of their assigned province, and the remaining three cases involve datasets located well within their assigned province.

Based on the results of the discriminant analysis, and a careful re-examination of the assignment of the datasets to their respective physiographic provinces, it is concluded that the original assignation is adequate, and that the placement of the 58 datasets into the nine physiographic provinces is reasonable. It is also apparent that even among the more traditional morphometric parameters some intra-provincial variation exists which can be as great as or greater than the inter-provincial variation.

7.2 First Impressions

7.2.1 Surficial methods

It is apparent that the analyses on the DEMs produce results which differ according to the physiographic region (figure 7.2), and that the relationships among the results differ from those obtained from the analyses on the fractal surfaces. This is particularly noticeable with the results of the variogram analyses (compare figure 7.2, tables 7.4 and 7.5 with table 6.1), wherein the sectional variograms generally produce dimensions consistently different from the other variogram methods. However, it must be stressed that the dimensions shown in figure 7.2 are those dimensions associated with the first segments only. As is evident in table 7.5, the averages of the second dimensions are not significantly different (see also Roy *et al.*, 1987, 74). The results are presented in full in appendix 1.

The major difference between the results of the methods when applied to the fractal surfaces and when applied to the DEMs is that many of the DEMs exhibit more than one fractal dimension -- many are bi- or even tri-dimensional. This means that many of the datasets have more than one linear segment present in the graph used to determine the fractal dimension, irrespective of the method used. The only method

Figure 7.2 Results grouped by physiographic province

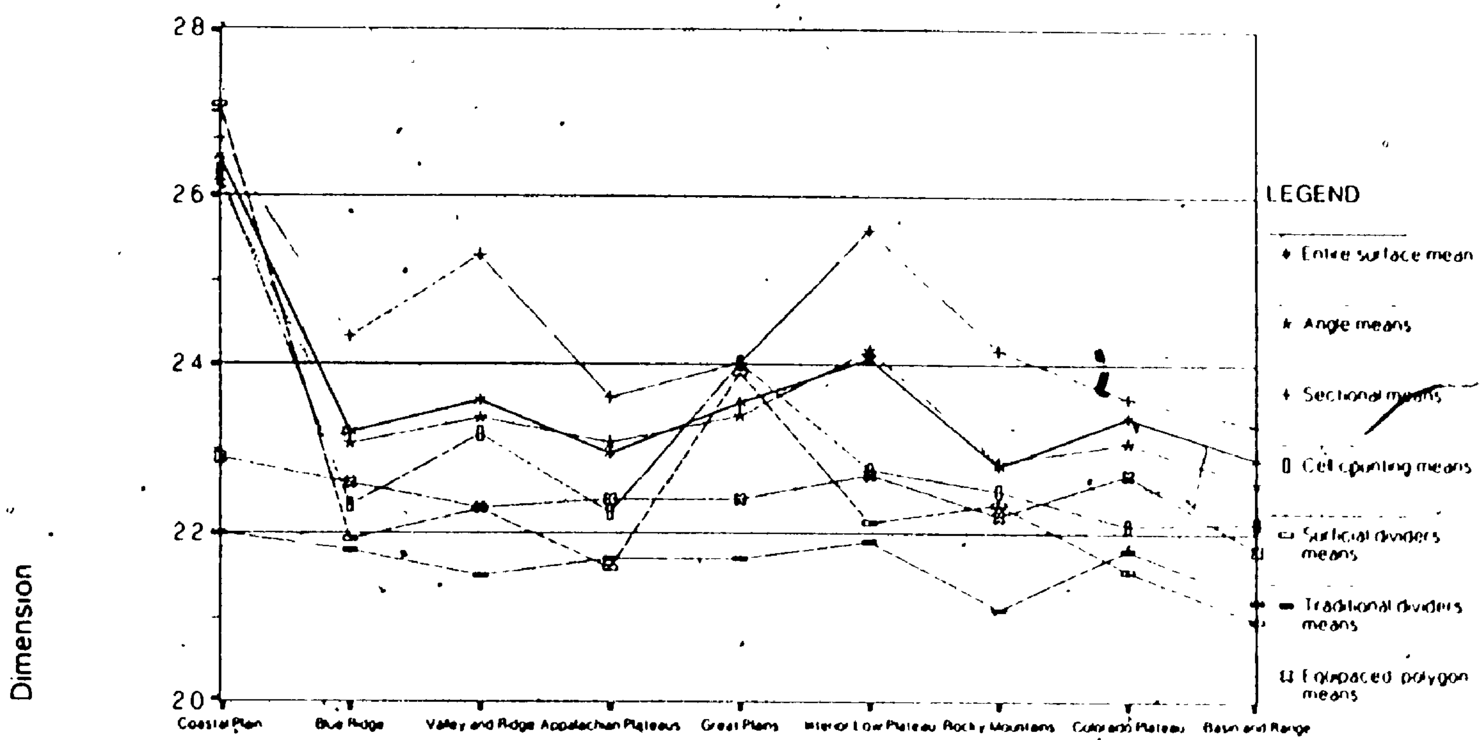

Physiographic region

NOTE All dimensions have been adjusted to fall between 2.0 and 3.0 to aid in comparing the results

Physio region	VALLD	VALLI	Diff V-S	Mean sect	S d sect	Mean angle	S d angle	Skew-ness	Kurt-osis	Coef dis	S d elev	Mean cc D	S d cc D	Mean div D	S d div D
C Pl	2 647	2 391	0 06	2 665	0 070	2 616	0 119	0 454	603	0 448	3 619	2 668	0 178	2 629	0 102
B R	2 320	4 830	0 10	2 422	0 093	2 306	0 059	0 479	0 260	0 395	13 789	2 193	0 066	2 233	0 070
V&R	2 357	3 415	0 17	2 524	0 122	2 337	0 083	0 643	0 286	0 355	7 170	2 228	0 115	2 318	0 087
A P	2 295	3 862	0 10	2 378	0 125	2 308	0 074	- 562	1 808	0 492	9 236	2 159	0 095	2 226	0 088
G P	2 355	2 840	0 04	2 397	0 107	2 339	0 048	0 085	453	0 383	6 937	2 390	0 115	2 396	0 102
I L P	2 407	2 911	0 19	2 452	0 136	2 417	0 083	-1 166	4 651	0 683	6 199	2 213	0 143	2 276	0 130
R M	2 280	4 304	0 07	2 352	0 194	2 285	0 059	1 118	0 375	0 285	14 446	2 234	0 091	2 245	0 037
C Pt	2 337	4 525	0 04	2 321	0 088	2 308	0 040	- 393	0 590	0 370	12 773	2 155	0 056	2 209	0 085
B&R	2 289	3 309	0 08	2 326	0 128	2 253	0 078	0 907	1 601	0 320	10 145	2 097	0 038	2 212	0 043

Table 7 4

Regional summary of the results

Variable descriptions (All variables represent the average over all datasets within the province)

- VALLD - Entire-surface variogram D
- VALLI - Entire-surface variogram Intercept
- Diff V-S - Average absolute difference between VALLD and each of the four sectional variograms D
- Mean sect - Mean D of the four (or less) sectional variograms
- S d sect - Standard deviation of the sectional variograms Ds
- Mean angle - Mean D of the six angle variograms
- S d angle - Standard deviation of the angle variograms Ds
- Skewness - Skewness of the distribution of the elevations
- Kurtosis - Kurtosis of the distribution of the elevations
- Coef dis - Coefficient of dissection
- S d elev - Standard deviation of the elevations
- Mean cc D - Mean D of the cell counting method
- S d cc D - Standard deviation of the cell counting methods Ds
- Mean div D - Mean D of the surficial dividers method
- S d div D - Standard deviation of the dividers methods Ds

that consistently has mono-dimensional results is the surficial dividers method. The surficial cell counting method's results have the greatest number of bi-dimensional results -- 45 or 78% of the DEMs have at least one elevation with a bi-dimensional result. Overall, the results of the cell counting method, especially when compared to the results of the surficial dividers method, are not very satisfactory. The number of bi-dimensional results produced by the other methods are as follows: 20 or 34% of the variograms for the entire surfaces produced bi-dimensional results; 24 or 40% of the surfaces had at least one bi-dimensional sectional variogram result; and 40 or 70% of the surfaces had at least one bi-dimensional angle variogram result. The dimensions associated with the longer distances are, on average, very much higher than the dimensions associated with the shorter distances (table 7.5). The second dimensions, on average, are remarkedly consistent.

The relationships of the two surface contour methods to each other, and to the variogram results, are not as expected (cf. chap. 6). The cell counting method generally produces dimensions[4] below those of the dividers method -- the reverse of the situation with respect to the fractal surfaces -- and there does not appear to be any relationship between the dimensions produced by these two methods and the

[4] References to the dimension of a dataset which is bi-dimensional are to the first dimension -- the dimension which applies to the shorter distances or lags -- rather than to the second dimension -- the dimension which applies to the longer distances or lags -- unless otherwise noted.

relative value of that dimension. That is, unlike the results published previously and discussed in section 6.1.2, the differences between the Ds produced by the two methods does not appear to be an increasing function of D. However, because the dividers method produced only mono-dimensional results, while the cell counting method produced mainly bi-dimensional results, interpretation of the relationships between these two methods, and the others, is difficult.

Method	Mean/s.d. 1st dim.	Mean/s.d. 2nd dim.
Variogram		
• All	2.34/0.123	2.66/0.220
• Sector	2.42/0.133*	2.68/0.167
• Angles	2.33/0.101	2.70/0.080
• Row/Col	2.32/0.101	2.68/0.134
Cell counting	2.21/0.162*	2.71/0.200
Dividers	2.27/0.126*	- / -

* Significantly different from D_{All} (1st segment) using a standard T-test.

Table 7.5

Average dimensions over all datasets by method.

The patterns in the variances of the dimensions produced by the various methods follows the patterns evident in the simulated surfaces results. The intra-dataset standard deviations[5] of the sectional variograms' Ds have a

[5] The standard deviations considered in this paragraph are the **intra-dataset** standard deviations, obtained by considering the deviations of the dimensions for that particular surface / method combination about the mean dimension for that same combination.

slight negative correlation with the average dimension of the surface, while the standard deviations of the Ds of the surficial contour methods (cell counting and dividers) have significant positive correlations with the average dimensions of the datasets (0.49 and 0.44, respectively). Thus, as the dimension of the dataset increases, the sectional variograms are more likely to produce more similar dimensions for the different sections whereas the surficial contour methods are more likely to produce dissimilar dimensions for each contour. The standard deviations of the angle variograms' Ds have a significant positive correlation (0.41) with the average dimensions of the datasets, opposite to the trend evident in the fractal surface results. This indicates that surfaces with higher Ds appear slightly more anisotropic than do surfaces with lower Ds. This result is contrary to expectations (e.g., see figures 6.1 and 6.2).

The sectional variograms produce higher first-segment dimensions on average than the other variogram methods. Since the sectional variograms are 'looking at' the DEMs at a larger scale than either the entire surface variograms or the angle variograms, and since the first-segment dimensions of the sectional variograms apply to much shorter distances on average (i.e., the mean breakpoints for the four sectional variograms are 2995, 3108, 2843 and 2755 m, whereas the mean breakpoint for the entire surface variogram is 5255 m), the physical natures of the datasets, as represented by the fractal dimensions, are different at larger scales than they are at the smaller scales. Note, however, that within some physiographic provinces the differences in the dimensions produced by each method are very small, whereas in others they are very large (figure 7.2). Further discussion on the differences between the results of the sectional variograms and the variograms which looked at the entire surface will be found in chapter 8.

7.2.2 Contour line methods

The two methods which analysed the individual contour lines -- the traditional dividers method and the equipaced polygon method -- produce dimensions very dissimilar to those produced by all of the other methods (figure 7.2). These results are expected, given the relationships observed among the results of the various methods on the simulated fractal surfaces (table 6.1). Comparing the dimensions obtained from the H = 0.4 fractal surface with the average dimensions obtained from the DEMs located within the Coastal Plain Physiographic province illustrates that the methods act similarly on both simulated and 'real' surfaces (table 7.6), and that the differences in the dimensions reflect differences among the methods, not differences between the two types of surfaces. Similar comparisons also could be made between other simulated and real datasets.

Method	H=0.4 Surface	Coastal Plains DEMs
Variogram		
• All	2.62	2.65
• Sector	2.64	2.67
• Angles	2.62	2.62
Cell c'ting	2.75	2.67
Dividers	2.64	2.63
Contours		
• Dividers	1.22	1.20
• Equipaced	1.34	1.29

Table 7.6

The Coastal Plain's results
contrasted with the H = 0.4 results

The average dimensions produced by the two individual contours methods vary little across the physiographic provinces -- they provide little discriminating power. This lack of variation by province disallows using these methods to generate unique statistics, unlike the dimensions produced by the variogram methods which do differentiate between the physiographic provinces. The constancy in the dimensions produced by these two methods, and their consistent low values, also could explain why most studies which have used the dividers method have found low values for the fractal dimensions of cartographic lines (e.g., Muller, 1986, table 6; of 46 dimensions reported, all are below 1.25 and almost half are below 1.10).

The correlations between the dimensions produced by the individual contours methods - whether considered on an individual basis or as averages -- and the entire surface variogram dimensions are all very low (less than 0.40), as are the correlations with the two surficial contour methods (all correlations are below 0.50). Correlations between the average dimensions of the four methods which looked at the surfaces on an elevational basis reveals that (i) the two surficial methods produced results consistent with each other (r = 0.61), (ii) the individual contours methods' results are consistent with other (r = 0.62), but (iii) the cross-correlations are lower (r < 0.4).

When the correlations between the two sets of contour-based methods are considered on an elevational basis some interesting results appear. The highest correlation between the two individual contours methods occurs at the mid-elevational level (r = 0.88), the correlation decreases to either side (i.e., from the lowest to highest elevations the correlations are 0.50, 0.82, 0.88, 0.70, 0.15). This indicates that the two methods are not stable -- that the dimensions returned are not independent of the characteristics of the lines. In contrast, the two surficial contour methods consistently have high correlations, with the correlations not a function of the elevation.

These results suggest that the characteristics of the contour lines differ at the higher and lower elevations from those at the middle elevations, at least when considered on an individual contour line basis. That is, the characteristics of the contour lines are such that at the middle elevations both methods produce similar results, but at the elevational extremes (and in particular at the highest elevations) the characteristics of the contour lines are such that the two methods produce dissimilar results. Thus, not only do the two methods produce results which differ on average, but they also produce results which differ as a function of the elevation. These results are also a reflection of the confidence which can be associated with each elevationally-dependent dimension. That is, since there are more mid-elevational contours than there are contours at either the higher or lower elevations, the average dimension at the mid-elevation will be more stable (representative) than the dimensions at either the higher or lower elevations. Because of the the elevational dependency of the results, and the lack of variation in the dimensions, in the discussions which follow on the dimensions of the physiographic provinces the individual contour lines methods' results will not be considered.

7.3 Row / Column Tests

As mentioned in section 5.1.2, the USGS uses three different methods to generate their DEMs. Most of the DEMs used in this thesis were produced using the Gestalt Photomapper II (GPMII) (41 or 71%), the remaining DEMs were produced using either a Wild C8 stereoplotter (12 or 21 %) or in conjunction with the production of an orthophotograph (5 or 8 %) (table 7.1). Thus, only two of the three methods are represented by the datasets, for both the orthophoto and the stereoplotter datasets are representatives of the manual profiling system.

The dimensions of the datasets as calculated from the rows (D_{row}) plotted against the dimensions as calculated from the columns (D_{col}) should be randomly distributed about the line $D_{row} = D_{col}$. However, it is apparent that while the values associated with the DEMs produced by the GPMII system do appear to be randomly distributed about that line, the values derived from the manual profiling system are not (figure 7.3). To test whether the means associated with the rows and columns are significantly different when the method of production is considered, a t-test was performed (table 7.7). This confirms the suspicion that the manual profiling system produces biased results.

The GPMII DEM elevations are produced with an initial ground spacing of approximately 14 m which is regridded to the final DEM spacing of 30 m. Thus, there should not be any differences in the row or column profiles, for both profiles are derived from equivalent data distributions. The manual profiling system produces the 30 m DEMs in the following manner: First, elevations are recorded every 30 m or so along north-south running profiles which are spaced approximately 90 m apart. Second, the intervening elevations are produced using a bilinear interpolation algorithm which first interpolates along the rows (i.e., in an east-west direction) and then along the columns (i.e., in a north-south direction) (Elassal and Caruso, 1983). Thus,

Figure 7.3 Row and column variogram dimensions

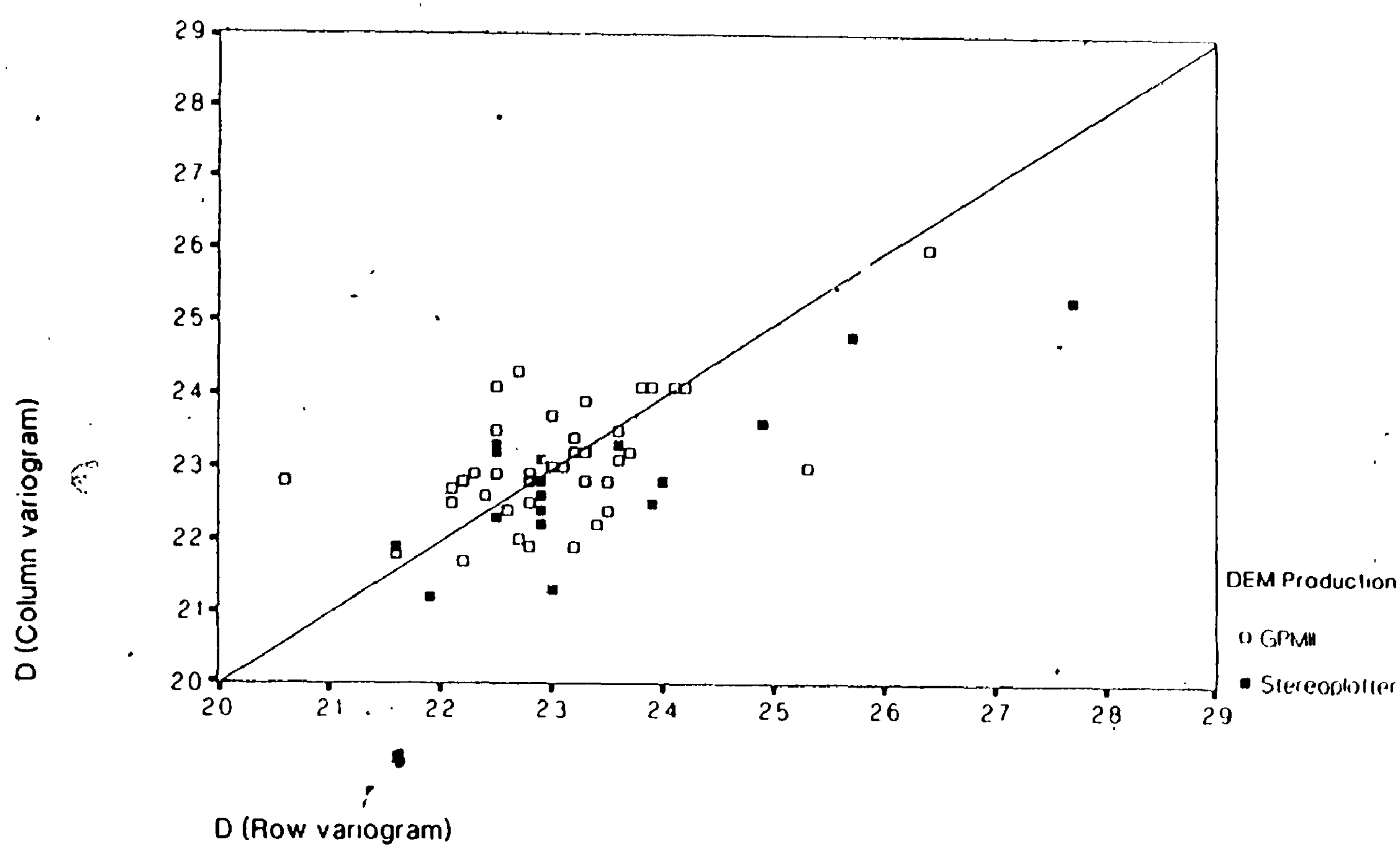

Method (n)	Direction	Mean/SD	T-value
Stereoplotter (17)	Row	2.358/0.177	2.55 (sig)
	Col	2.286/0.106	
GPMII (41)	Row	2.326/0.103	1.11 (n.s.)
	Col	2.311/0.087	

Table 7.7 Row / column t-test results

profiles of elevations taken along the columns of a DEM produced in this manner would be expected to be smoother than those taken along the rows, for the column values are interpolated last. Most of the dimensions associated with datasets produced by the manual profiling system fall below the line ($D_{row} = D_{col}$). This confirms that the dimensions produced by the column variograms are in fact smaller than the corresponding dimensions produced by the row variograms -- that the column profiles appear smoother than do the row profiles.

Because the dimensions of the row and column variograms were obtained primarily as a means of testing whether or not the method of production has an influence on the dataset dimensions, the results of the row and column variograms are not considered in the discussions below. Note, however, that the results of the row and column variograms are subsumed in the angle variogram results. Of course, the dimensions produced by the angle variograms (i.e., angles 1, 3, 4 and 6; see figure 5.2) would be affected by the method of generation also. However, the effect would be tempered somewhat, in that the angle variograms (1 & 6, and 3 & 4) include off-column and off-row values, respectively.

7.4 Dimensional Analyses by Physiographic Region

The results of the investigations on the fractal nature of terrain will now be considered in detail. The DEMs have been placed within groups -- physiographic provinces -- and the results will be considered on a province by province basis. It is apparent (Mark and Aronson, 1984; figure 7.2; table 7.4) that the fractal dimension varies considerably **between** physiographic provinces. The nature of the variations of the fractal dimensions within each province is the main subject of this section. The physiographic provinces appear in the order that they are presented in table 1.1 of Hunt, 1974. An overview of the average characteristics of the nine physiographic provinces is presented in table 7.4; all of the data is presented in the appendices (appendix 1).

Using the fractal dimension of the entire dataset as the dependent variable, and the physiographic region as the categorical variable, a way-one analysis of variance was used to test whether the datasets from the physiographic provinces could be distinguished solely by their fractal dimension. The results (table 7.8) indicate that it is possible to distinguish, as a group, the physiographic provinces' datasets simply by considering their fractal dimensions. However, using both the fractal dimensions and the intercepts provides a better means of differentiating among the provinces, as will be shown.

In the discussions on the physiographic provinces which follow the terms **scaling**, **homogeneous** and **isotropic** will be used with the following meanings. The provincial average of the absolute differences between the dimensions obtained from the entire-surface variogram, and the dimensions obtained from the four sectional variograms, provides some

Source	D.F.	Sum of Squares	Mean squares	Ratio	Prob.
Between groups	8	.3612	.0451	4.4090	.0005
Within groups	49	.5017	.0102		
Total	57	.8629			

Group	Mean	S.d.	Error	Min.	Max.	95% conf int for mean
Coastal Plain	2.6467	.0751	.0433	2.5600	2.6900	2.4602 to 2.8331
Blue Ridge	2.3200	.0684	.0228	2.1800	2.4200	2.2674 to 2.3726
Valley & Ridge	2.3575	.1367	.0394	2.1200	2.5600	2.2707 to 2.4443
Appalachian Plat.	2.2950	.0800	.0214	2.1700	2.4600	2.2488 to 2.3412
Great Plains	2.3550	.0919	.0650	2.2900	2.4200	1.5291 to 3.1809
Interior Low Plat	2.4067	.2082	.1202	2.2400	2.6400	1.8895 to 2.9238
Rocky Mountains	2.2800					
Colorado Plat.	2.3375	.0236	.0118	2.3200	2.3700	2.2999 to 2.3751
Basin & Range	2.2890	.0867	.0274	2.1400	2.4300	2.2270 to 2.3510
TOTAL	2.3395	.1230	.0162	2.1200	2.6900	2.3071 to 2.3718

Table 7.8

Analysis of variance of D by physiographic province indication of the scaling nature of the surfaces. The closer the two values are, the more scaling are the datasets. The average of the intra-dataset standard deviations of the dimensions of the sectional variograms provides some indication of the 'homogeneity' of the dataset -- the greater the value the more dissimilar are the results of the sectional variograms, and the less homogeneous the surface appears. The provincial average of the standard deviation of the angle variogram dimensions provides some indication of the isotropic nature of the surfaces. The lower the intra-dataset variance the more isotropic the surfaces appear.

7.4.1 Coastal Plain Physiographic Province

Three datasets (DEM21, DEM22, DEM23) are centrally located within the East Gulf section of the Coastal Plains Province (figure 7.1; table 7.1). This province has low topographic relief, a reflection of its origins as a sea bottom. The East Gulf section consists of dissected, belted coastal plain with a series of cuestas and lowlands forming the dominant physiographic features (Hunt, 1974). The three datasets have similar morphometric parameters, and all display little topographic relief -- note the very small range of their elevations, and the very low standard deviations of their elevations (table 7.4). All three datasets have similar, equilibrium coefficients of dissection (appendix 1) (Strahler, 1952).

Somewhat unexpectedly, these DEMs produce the highest Ds found in this study, and rank first (highest **D**) in all of the surface analyses (table 7.4; figure 7.2). Although all three DEMs exhibit similar behaviour across all methods, the two DEMs located adjacent to each other, DEM22 and DEM23, appear very similar (figures 7.4.1.1, 7.4.1.2, 7.4.1.3).

The datasets from this province produce the highest average fractal dimensions, while the average intercepts associated with those dimensions are the lowest (table 7.4, appendix 1). The vertical axis of a variogram represents {expected difference in elevation}^{2}. The lower the value of the intercept, the lesser the expected difference in elevation between two points a unit distance apart. Remember that the data values are derived in log-log space. Therefore the intercept occurs when log{expected difference} = 0, or at a unit distance in antilog space. Thus, although these surfaces would be classified as the 'roughest' surfaces encountered in this study (as represented by their fractal dimensions), the **magnitude** of that roughness was the least of all surfaces encountered, as represented by their intercepts. Fox and Hayes (1985, 18) also refer to a scaling factor for the roughness -- for a given **D** they note that the amplitude is a function of the scaling factor. Although their study used spectral techniques to determine the fractal characteristics of the seafloor, the concepts -- magnitude and a scaling parameter -- are similar.

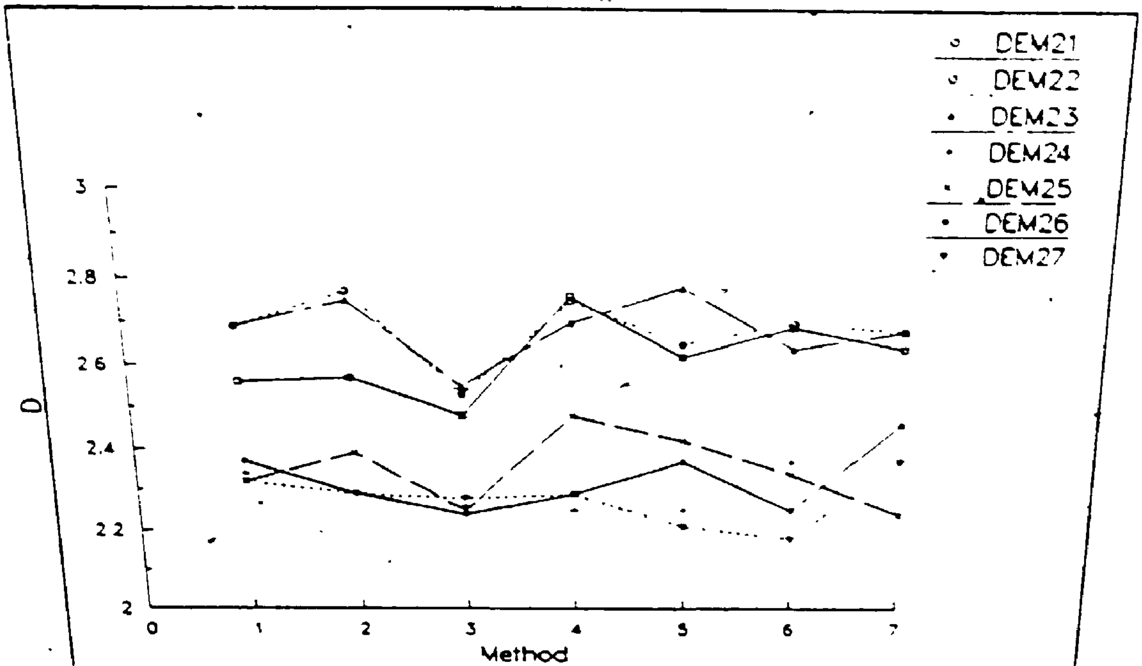

	ALL	ROW	COL	S1	S2	S3	S4
DEM21	2.56	2.57	2.48	2.76	2.62	2 69	2.64
DEM22	2.69	2.77	2.53	2.75	2.65	2 70	2 68
DEM23	2.69	2.75	2.55	2.70	2.78	2.64	2.68
DEM24	2.34	2.29	2.26	2.25	2 25	2.37	2.37
DEM25	2.32	2.39	2.25	2.48	2.42	2.34	2 24
DEM26	2.37	2.29	2.24	2.29	2.37	2.25	2.46
DEM27	2.32	2.29	2.28	2.29	2 21	2.18	2 37

Figure 7.4.1.1 Coastal Plain and Colorado Plateau results

Note: Lines are drawn for illustrative purposes only, they are not intended to signify any relationship between the points.

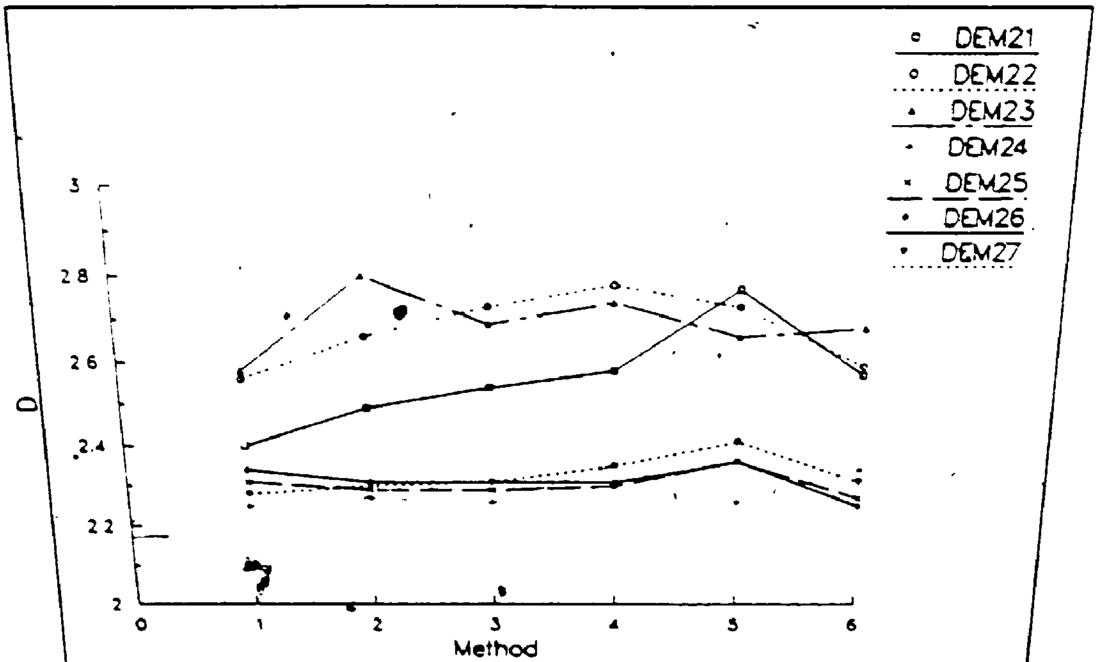

	A1	A2	A3	A4	A5	A6
DEM21	2.40	2 49	2.54	2.58	2.77	2.57
DEM22	2.56	2.66	2.73	2.78	2.73	2.59
DEM23	2.58	2.80	2.69	2.74	2.66	2.68
DEM24	2.25	2.27	2.26	2.35	2.26	2.34
DEM25	2.31	2.29	2.29	2.30	2.36	2.27
DEM26	2.34	2.31	2.31	2.31	2.36	2.25
DEM27	2.28	2.30	2.31	2.35	2.41	2.31

Figure 7.4.1.2 Coastal Plain and Colorado Plateau results

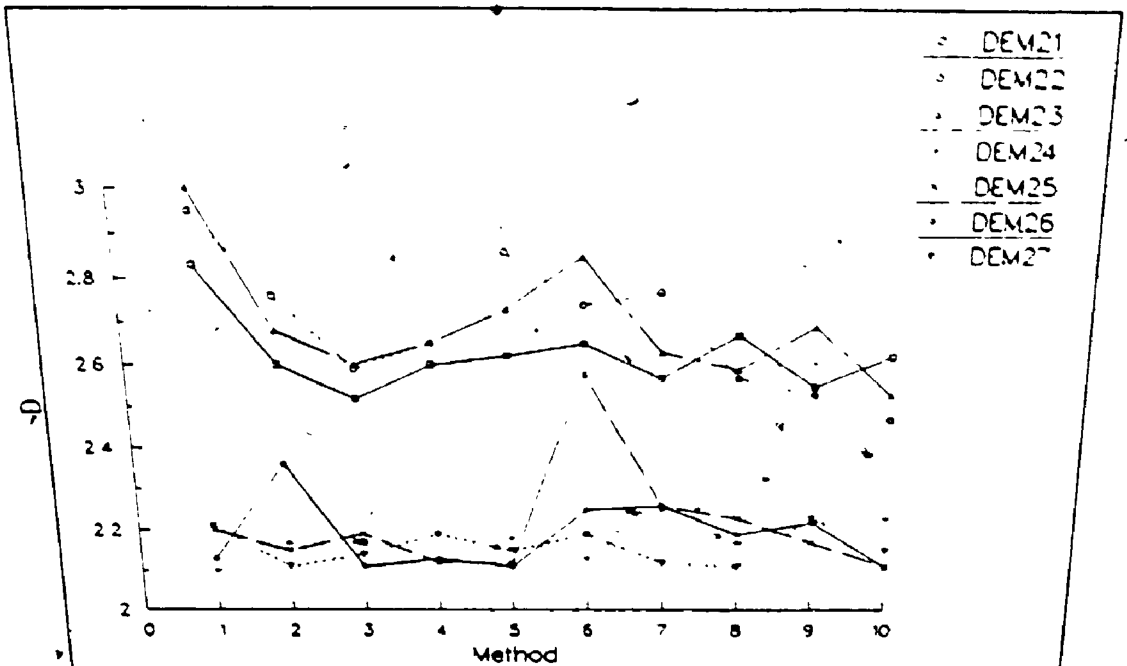

	CC1	CC2	CC3	CC4	CC5	DI1	DI2	DI3	DI4	DI5
DEM21	2.83	2.60	2.52	2.60	2.62	2.65	2.57	2.67	2.55	2.62
DEM22	2.95	2.78	2.59	2.65	2.86	2.74	2.77	2.57	2.53	2.47
DEM23	3.00	2.68	2.60	2.65	2.73	2.85	2.63	2.59	2.69	2.53
DEM24	2.10	2.17	2.11	2.12	2.18	2.13	2.25	2.17	2.22	2.23
DEM25	2.20	2.15	2.19	2.12	2.12	2.58	2.26	2.23	2.17	2.11
DEM26	2.13	2.36	2.11	2.13	2.11	2.25	2.26	2.19	2.22	2.11
DEM27	2.21	2.11	2.14	2.19	2.15	2.19	2.12	2.11	2.23	2.15

Figure 3.4.1.3 Coastal Plain and Colorado Plateau results

Overall, the fractal model appears to fit these datasets well. Most variograms produce mono-dimensional results which fit the entire scale of the variogram plot (from ≈.1 km to 9.8 km). Slight patterning was evident in only a few of the variograms. The surficial methods (i.e., the entire surface variograms, the sectional and angle variograms, the cell counting and dividers methods) produce dimensions more consistent with each other than in any of the other physiographic provinces.

The average intra-dataset standard deviations of the sectional dimensions is the lowest of all physiographic provinces (table 7.4), which indicates that this province has the most homogeneous datasets of all. The very small average absolute differences between the overall entire-surface dimensions and the average sectional dimensions indicates that this province also has the most scaling datasets. However, this province would be considered very anisotropic because the angle dimension's intra-dataset standard deviations are high.

All three datasets follow a similar pattern with respect to the dimensions associated with the angle variograms: the fractal dimension and the distance to which the dimension applies (i.e., the break point in the graph) both peak in the direction of angle 4 - 5. That is, the highest Ds and the longest linear segments are associated with those directions, directions which would run parallel to the cuesta slopes of the Southern Pine Hills -- the physiographic features which occur within the area of these DEMs (Thornbury, 1965, 56). The contour plots of these datasets do not exhibit any obvious topographic features (e.g., ridges or slopes as indicated by parallel contour, therefore the variograms are picking up detail that is not visible (see appendix 2).

The angle variograms from this province have very high significant correlations between their dimensions and associated intercepts (table 7.9). The high positive value indicates that as the dimensions increase, so do the values of the intercepts. This means that the rougher the surface -- as represented by its fractal dimension -- the greater the magnitude of that roughness. These results indicate that the magnitude of the roughness is greater when looking perpendicular to the slope than when looking up the slope.

The intra-dataset variance of the cell counting techniques is fairly high, although a consistent pattern in that variation is present. The fractal dimension decreases from a very high value associated with the lowest contours, to a low value associated with the middle contours, and then increases to the highest contours. The results of the dividers method are not as consistent, the intra-dataset variance of the results is very high. Overall, the relation between D and elevation is slightly negative -- the general trend is that D decreases with elevation.

Physiographic Region	Dataset	Pearson's r	Sign.
Coastal Plain	DEM21	.93	Y
" "	DEM22	.93	Y
" "	DEM23	.84	Y
Blue Ridge	DEM30	.55	N
" "	DEM31	.95	Y
" "	DEM32	.76	N
" "	DEM33	.94	Y
" "	DEM34	.98	Y
" "	DEM35	.97	Y
" "	DEM37	.54	N
" "	DEM39	.68	N
" "	DEM40	.99	Y
Valley & Ridge	DEM1	.80	N
" "	DEM2	.63	N
" "	DEM5	.75	N
" "	DEM16	.97	Y
" "	DEM17	.09	N
" "	DEM20	.48	N
" "	DEM36	.60	N
" "	DEM38	-.70	N
" "	DM11	-.96	Y
" "	DM12	-.88	Y
" "	DM13	-.95	Y
" "	DM14	-.06	N
Appalachian Plat.	DEM3	.47	N
" "	DEM4	.54	N
" "	DEM10	.92	Y
" "	DEM11	.61	N
" "	DEM12	.68	N
" "	DEM13	.59	N
" "	DEM14	.47	N
" "	DEM18	.89	Y
" "	DEM19	.85	Y
" "	DEM28	.88	Y
" "	DEM29	.90	Y
" "	DM10	.90	Y
" "	DM15	.97	Y
" "	DM16	.97	Y
Great Plains	DEM9	-.67	N
" "	DM18	-.36	N
Interior Low Plat.	DEM6	.58	N
" " "	DEM7	.96	Y
" " "	DEM8	.98	Y
Rocky Mountains	DM20	.69	N
Colorado Plat.	DEM24	.93	Y
" "	DEM25	.41	N
" "	DEM26	.98	Y
" "	DEM27	.33	N
Basin and Range	DM1	.79	N
" " "	DM2	.29	N
" " "	DM3	.96	Y
" " "	DM4	.89	Y
" " "	DM5	1.00	Y
" " "	DM6	-.68	N
" " "	DM7	.53	N
" " "	DM8	.74	N
" " "	DM9	.68	N
" " "	DM17	.94	Y

Table 7.9

Correlation of D with the intercepts from the angle variograms

(Y - significant at the 0.05 level
N - not significant at the 0.05 level)

7.4.1.1 Summary

All of the surface methods consistently produce very high D values when applied to the DEMs from the Coastal Plains physiographic province and, with the exception of the sectional variograms, exhibit very high intra-dataset variance. These DEMs are good examples of homogeneous scaling surfaces -- because the sectional variograms exhibited very little variance, and their average dimensions are very close to that of the entire surfaces' dimensions -- but they are not isotropic surfaces, because of the large intra-dataset angle variance.

7.4.2 Blue Ridge Physiographic Province

There are nine DEMs scattered throughout the southern half of the Blue Ridge Physiographic Province (figure 7.1; table 7.1). This province has been subjected to strong folding and faulting, and its physiography ranges from a single ridge in the north to a complex of closely spaced ridges in the south. The southern part is generally higher in elevation that the northern part, and the highest peaks in the Appalachian provinces are found within this province. Although the southern section of this province does not display the same lineation of topography as does the northern section, the western part of the southern section -- where most of the DEMs are located -- does display some lineation similar to the northern section (Thornbury, 1965, 103; Hunt, 1974). The interprovincial boundaries between this province and the Piedmont Plateau to the east, and the Valley and Ridge to the west, are well defined.

Some of the morphometric parameters clearly reflect the very high topographic relief present within this area of the Blue Ridge province: the range and the average standard deviation of the elevations are very large (table 7.4). Most of the datasets are at an equilibrium stage, judged by their coefficients of dissection. However, three datasets (DEM30, DEM35 and DEM39) have value below equilibrium ('monadnock phase', Strahler, 1952; appendix 1).

Although all datasets fit the fractal model well, some fit the model much better than others, notably DEM31 and DEM32. Some slight patterning was evident in many dataset's variogram plots, especially at the longer distances. In particular, the results from DEM40 display the most patterned plots. As a group, however, most of the datasets are mono-dimensional, especially when compared to the datasets from the other Appalachian provinces which much more consistently have bi-dimensional results.

Although the three physiographic provinces from the Appalachian Division have similar fractal dimensions, as derived from their entire surface variograms (figure 7.2), the intercepts and breakpoints clearly differentiate among the three (table 7.4). The Blue Ridge province has the largest average intercept, a reflection of its greater relief; it also has the longest average breakpoint, which indicates that the fractal model fits the datasets within this province much better (or, at least, over greater distances) than it does the datasets from the other two Appalachian provinces.

Based on the aggregate statistics, these datasets are both homogeneous and isotropic, but not scaling. The average intra-dataset standard deviation of the sectional dimensions is very low, as is the average intra-dataset standard deviation of the angular dimensions, but the average dimension associated with the sectional variograms is much higher than the overall entire-surface dimension. The cell counting and dividers methods also produced dimensions which were consistent across all elevations.

The average intercept for the entire surface variograms is the largest of all physiographic provinces. Thus, although the surfaces have a relatively low fractal dimension, the magnitude of their 'roughness' is very high. The Blue Ridge province is the mountainous region of the Appalachian Division, and compared to the lone dataset from the Rocky Mountains, the datasets from this province display a greater roughness, and a greater magnitude to that roughness.

No obvious patterns appear in the sectional variograms (figure 7.4.2.1). With the exception of the DEM30 and DEM39, all datasets have fairly consistent dimensions and break points across all four sectional variograms. However, the overall average first segment D for the sectional variograms is much higher than the D of the surface as a whole. This indicates that the datasets from this province appear to have three domains: at shorter distances the surfaces have a high dimension (≈ 2.52), at medium distances the surfaces have a lower fractal dimension (≈ 2.36), while at longer distances they exhibit a higher dimension again (≈ 2.69).

The results of the angle variograms appear more consistent as a group than do the results of the sectional variograms (figure 7.4.2.2). Although the average D across all angles is fairly stable, the intra-provincial variance of D peaks at angle three, and decreases to either side of that angle (appendix 1). The overall directional trend of the ridges within this province is northeast-southwest (corresponding to angles two and three), and the highest average D is also associated with the angle 2 and 3 variograms. These results reflect the variability in the physiography that each DEM captures. That is, the greatest variability in the physical nature of the DEM is expected in the direction of the ridges, which may or may not be expressed within any one DEM. Five of the datasets have significant, very high correlations between their angle variograms dimensions and their intercepts. The remaining four datasets have lower, non-significant correlations (table 7.9). The two groups are spatially intermixed, so regional differences cannot be used to explain these differences.

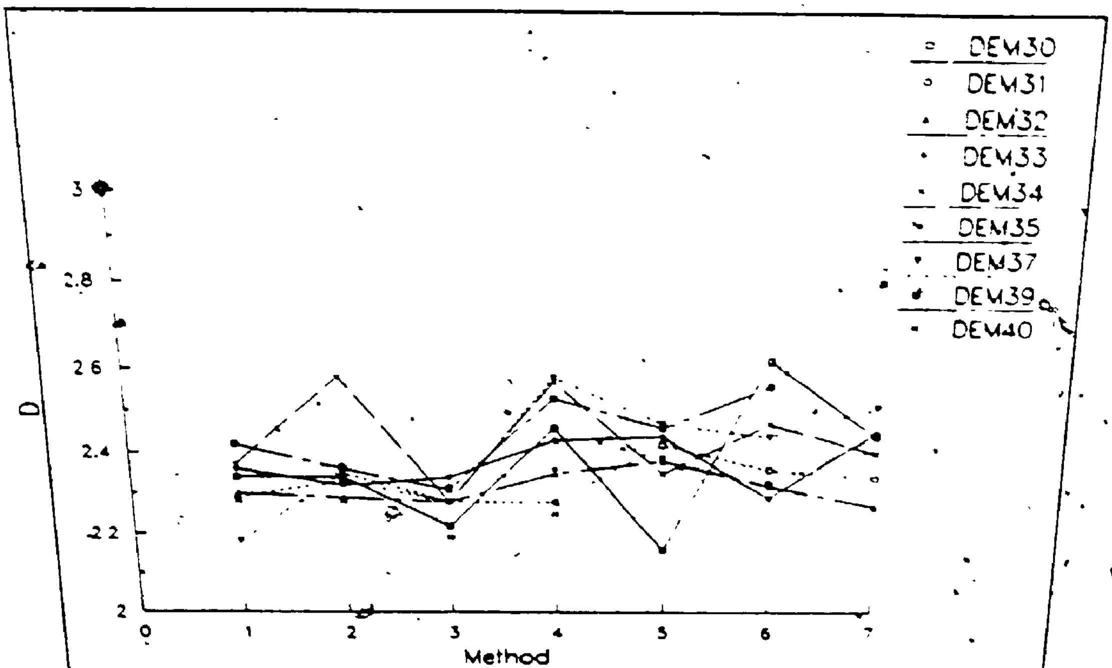

	ALL	ROW	COL	S1	S2	S3	S4
DEM30	2.34	2.34	2.22	2.46	2.16	2.62	2.44
DEM31	2.29	2.33	2.28	2.28	2.42	2.36	2.34
DEM32	2.30	2.29	2.28	2.35	2.38	2.32	2.27
DEM33	2.34	2.37	2.32	2.36	2.43	2.33	2.51
DEM34	2.37	2.58	2.28	2.57	2.35	2.4[illegible]	2.40
DEM35	2.36	2.32	2.34	2.43	2.44	2.29	2.45
DEM37	2.18	2.35	2.28	2.58	2.47	2.44	2.51
DEM39	2.42	2.36	2.31	2.53	2.46	2.56	2.80
DEM40	2.28	2.28	2.19	2.25	2.39	2.32	2.44

Figure 7.4.2.1 Blue Ridge results

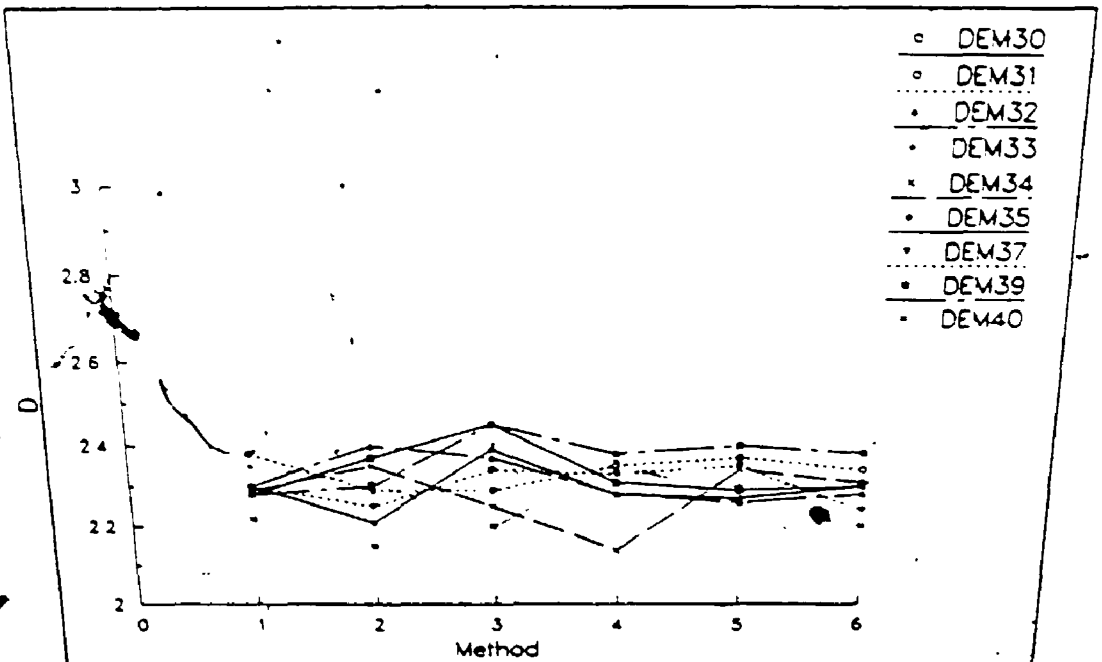

	A1	A2	A3	A4	A5	A6
DEM30	2.28	2.37	2.45	2.31	2.29	2.30
DEM31	2.38	2.29	2.29	2.35	2.37	2.34
DEM32	2.30	2.40	2.37	2.28	2.26	2.28
DEM33	2.35	2.31	2.20	2.34	2.30	2.31
DEM34	2.29	2.35	2.25	2.14	2.34	2.31
DEM35	2.30	2.21	2.39	2.28	2.27	2.30
DEM37	2.30	2.25	2.34	2.33	2.35	2.24
DEM39	2.28	2.30	2.45	2.38	2.40	2.38
DEM40	2.22	2.15	2.20	2.36	2.26	2.20

Figure 7.4.2.2 Blue Ridge results

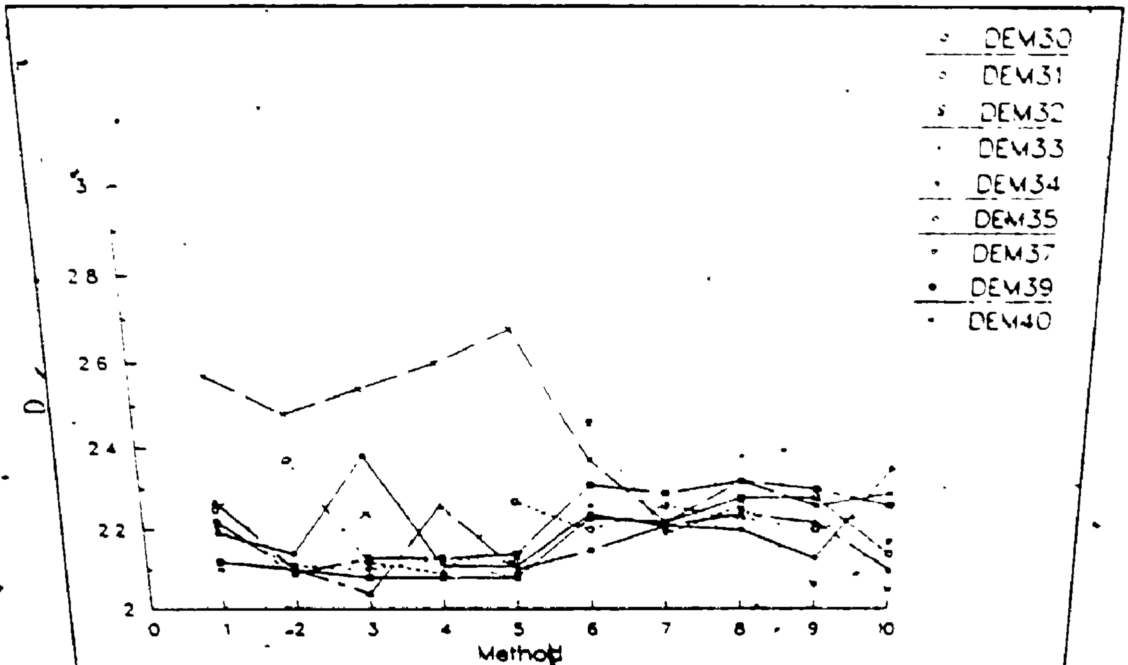

	CC1	CC2	CC3	CC4	CC5	DI1	DI2	DI3	DI4	DI5
DEM30	2.12	2.10	2.08	2.08	2.08	2.23	2.22	2.28	2.28	2.14
DEM31	2.25	2.37	2.12	2.09	2.27	2.20	2.26	2.23	2.20	2.26
DEM32	2.27	2.10	2.04	2.26	2.10	2.15	2.21	2.24	2.22	2.10
DEM33	2.12	2.11	2.12	2.09	2.09	2.26	2.20	2.38	2.26	2.10
DEM34	2.57	2.48	2.54	2.60	2.68	2.37	2.22	2.32	2.26	2.29
DEM35	2.19	2.14	2.38	2.11	2.11	2.24	2.21	2.20	2.13	2.35
DEM37	2.20	2.11	2.10	2.13	2.12	2.46	2.19	2.26	2.06	2.17
DEM39	2.22	2.09	2.13	2.13	2.14	2.31	2.29	2.32	2.30	2.26
DEM40	2.10	2.11	2.24	2.12	2.08	2.15	2.21	2.25	2.21	2.05

Figure 7.4.2.3 Blue Ridge results

The two surficial contour methods display a relatively small amount of intra-dataset variance (table 7.4; figure 7.4.2.3). There does not appear to be any trend in the results of the cell counting method. The dimensions are scattered without any definite pattern, although the inter-dataset standard deviations do increase monotonically as the elevation increases. This implies that the lower areas of the datasets are slightly more similar to each other in their fractal characteristics than are the higher areas. Within this province, most datasets, when analysed using the cell counting method, appear bi-dimensional, and the second dimension is usually greater than 2.50. DEM34 stands out by having a relatively high average dimension of 2.58; its row variogram dimension is also much higher than expected. However, the contour plot of this DEM does not reveal any features which appear unique. Subjectively, DEM34's contour plot looks very similar to DEM33's plot, and DEM33's results are consistent with the other datasets results. Why DEM34 stands out is not apparent.

With the dividers results, no trend is apparent in the dimensions, nor is one present in the standard deviations (figure 7.4.2.3 ; appendix 1). Note that DEM34 does <u>not</u> stand out when looking at the dividers results. It would appear that the fractal dimensions of most of the datasets within this physiographic province decrease only slightly with elevation. This possibly indicates that similar processes act over all elevations, or at least that no physical process dominates at any particular elevation.

7.4.2.1 Summary

In summary, the datasets from the Blue Ridge physiographic province fit the fractal model reasonable well. None of the surficial methods varied systematically across the surface, and the break points of the variogram graphs occurred generally at longer distances. However, the datasets could not be classed as scaling, because the sectional variograms consistently produced much higher dimensions than did the other surficial methods, and at longer distances higher dimensions were also evident among the results of some datasets.

7.4.3 Valley and Ridge Physiographic Province

The twelve datasets which fall within this physiographic province span the entire region, from east to west and north to south (figure 7.1; table 7.1). The province is aptly named, for it is composed of a great number of fold mountains. The longest scale folding produced synclines 200-250 miles wide, "interrupting this are broad upfolds (anticlinoria) and downfolds (synclinoria) about 25 miles wide, on the flanks of which there are individual anticlines and synclines 1 to 5 miles wide" (Hunt, 1974, 262). As each dataset encompasses relief up to 6 miles wide, it is likely that an individual DEM can exhibit considerable relief, and may include from one to several valleys and ridges. The range in the standard deviations of the elevations of the datasets which occur within this province is fairly large -- an indication that some datasets contain considerable relief whereas others contain much less.

More than half of the datasets have coefficients of dissection below 0.35. This indicates that they are in the late mature stage (Strahler, 1952). The remaining datasets have equilibrium coefficient of dissection values (appendix 1). There is a "marked parallelism of ridges and valleys, commonly in a northeast-southwest direction" (Thornbury, 1965, 109) throughout this province, and many of the DEMs' contour plots have definite ridges/valleys running in that general direction (i.e., DEM2, DEM5, DEM17, DEM20, DEM36 and DEM38, and DM11, DM12, DM13, and DM14).

Datasets DM11, DM12, DM13 and DM14 all occur within the northern section of the province, while the remaining datasets occur within the southern, eastern Tennessee section. The northern section lacks the predominant longitudinal ridges and the major drainage occurs longitudinally rather than transversely -- features characteristic of the southern section, and the area was glaciated, unlike the southern section (Thornbury, 1965, 113). From this it is expected that the four datasets from the northern section will stand out from the group as a whole. Their morphometric parameters appear somewhat distinctive, with larger elevational standard deviations and skewness values than the majority of the other Valley and Ridge datasets. The two datasets which occur close to the boundary between this physiographic province and the adjacent Blue Ridge province (DEM36 and 38) also have larger than average standard deviations, values more characteristic of the Blue Ridge province. This illustrates that the boundaries between the physiographic provinces are not always distinct.

Although the province is generally composed of parallel valleys and ridges, little direct evidence of this parallelism is present in the variograms. Only a few datasets had patterns present in their variogram plots, and the patterning was restricted to the angle variogram plots. About 20% of all variogram plots had areas with very scattered data points.

The datasets do not fit the fractal model all that well. A large number of results are bi-dimensional, some are even tri-dimensional. Among the bi-dimensional results the average dimension associated with the shorter distances is about 2.35, while the average dimension associated with the longer distances is around 2.75 (appendix 1). The sectional variograms, of which almost all are mono-dimensional, have dimensions which lie between those two dimensions. The intra-dataset variance in the sectional variogram dimensions is above average, and the intra-dataset variance of the angle variogram dimensions is among the highest of all provinces. Thus, the datasets from this province are not scaling, homogeneous, or isotropic. These results reflect the physical nature of the Valley and Ridge province (e.g., the definite isotropism present), and the way in which the DEMs capture that physiographic variation.

The results of these datasets are also of note because of the large variance of the dimensions across datasets (appendix 1). This province is the most variable with respect to its overall average fractal dimension and, even when the two regions of the province are considered separately (the northern and southern parts), considerable variation exists within the datasets' dimensions. As mentioned, the range of the relief present in this province is such that a single DEM may contain only one dominant ridge/valley, or it may contain several. That the fractal characteristics of the DEMs vary considerably is, therefore, simply a reflection of the variance of the region's physiography.

The differences between the sectional variogram dimensions and the dimensions associated with the other variogram methods are the largest of all provinces (table 7.4, figure 7.4.3.1). The most noteworthy results from the sectional variograms are those from DEM1. Two of the sections (S1 and S2) are tri-dimensional: 2.43 - 2.60 - 2.30, and 2.39 - 2.61 - 2.39, respectively. Some feature of the landscape occurs within a relatively narrow band (between ≈ 0.4 km and ≈ 1.4 km) which dramatically increases the fractal dimension within that band, yet it does not appear to influence the overall fractal characteristics of the DEM.

The plots showing the angle variogram results (figure 7.4.3.2) are not as explanatory as they could be, a consequence of the large number of bi-dimensional results. The averages of the second dimensions -- representative of the longer distances -- for five of the six angular swaths are remarkably consistent, having values very close to 2.75. Angle 2 is the lone exception; the average Ds for the first, shorter distance dimension, peak at angle 2. The lowest variance in D is also associated with angle 2. This is the direction of orientation of most of the valleys and ridges (Thornbury, 1965). The distances to the first breakpoints in the graphs of the angle 2 variogram plots are also much longer -- six times longer on average than the breakpoint distances of the angle 5 plots, the angle which is perpendicular to the ridges and valleys. The breakpoint distances within angle 5 are very variable, however, and possibly reflect the variance in the spacing of the ridges and valleys present within any one dataset.

Almost all of the southern datasets have non-significant positive correlations between the angle dimensions and the intercepts (table 7.9). The northern datasets all have negative correlations, and three of the four datasets' correlations are very large and significant. These results clearly distinguish between the two geographic groups, and suggest that regional differences might account for the differences in the correlations. Which of the regional differences -- the lack of predominant longitudinal ridges, the longitudinal drainage, or the effects of glaciation -- account for the reversal in the correlations is unknown at present.

The two surficial contour methods produced very different results (figure 7.4.3.3). The average dividers' D is much closer to the entire surface mean, while the average D for the cell counting method falls 0.13 below it. The averages and standard deviations of the dimensions produced by the cell counting method decrease as the elevation increases, the breakpoint also decreases as the elevation increases (from ≈ .5 km at the lowest elevation to ≈ .2 km at the highest elevations, see appendix 1). This indicates that, with respect to increasingly shorter distances, the terrain becomes more similar as the elevation increases and appears less 'rough'. However, the dividers results are not so clear. Although the dimension generally declines as the elevation increases, the highest elevations generally have a higher dimension than the second highest elevations. The standard deviations of the dimensions also generally decrease as the elevation increases. These results reinforce the conclusion that the terrain appears smoother and more alike as the elevation increases.

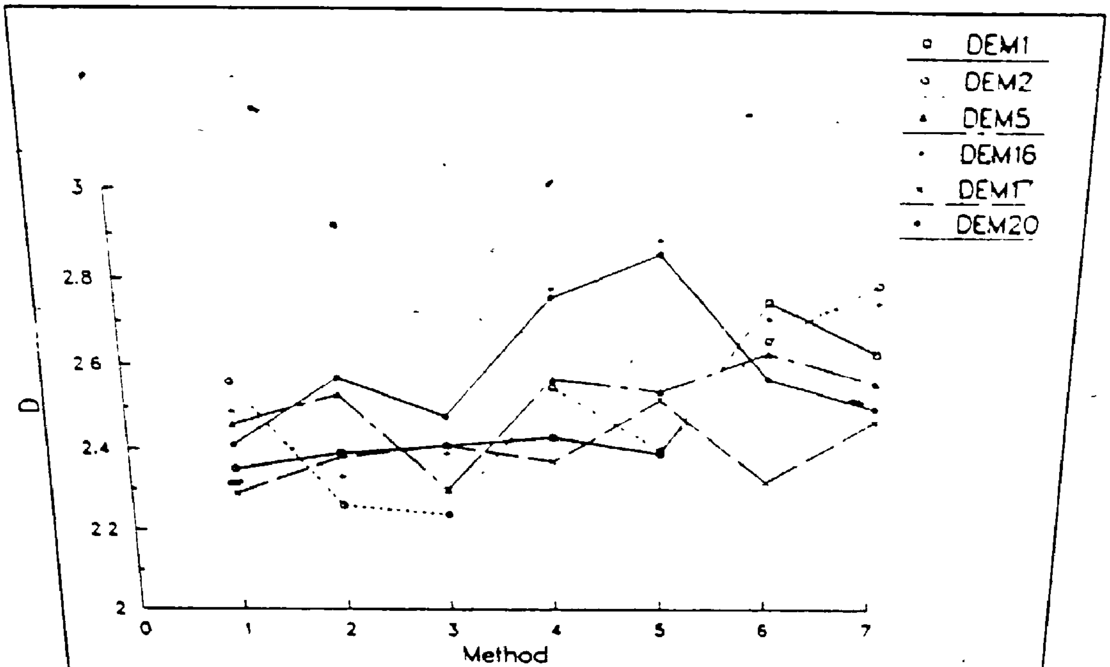

	ALL	ROW	COL	S1	S2	S3	S4
DEM1	2.35	2.39	2.41	2.43	2.39	2.75	2.63
DEM2	2.56	2.26	2.24	2.55	2.40	2.66	2.79
DEM5	2.46	2.53	2.30	2.57	2.54	2.63	2.56
DEM16	2.49	2.33	2.39	2.78	2.89	2.71	2.75
DEM17	2.29	2.38	2.41	2.37	2.52	2.32	2.47
DEM20	2.41	2.57	2.48	2.76	2.86	2.57	2.50

Figure 7.4.3.1 Valley and Ridge results

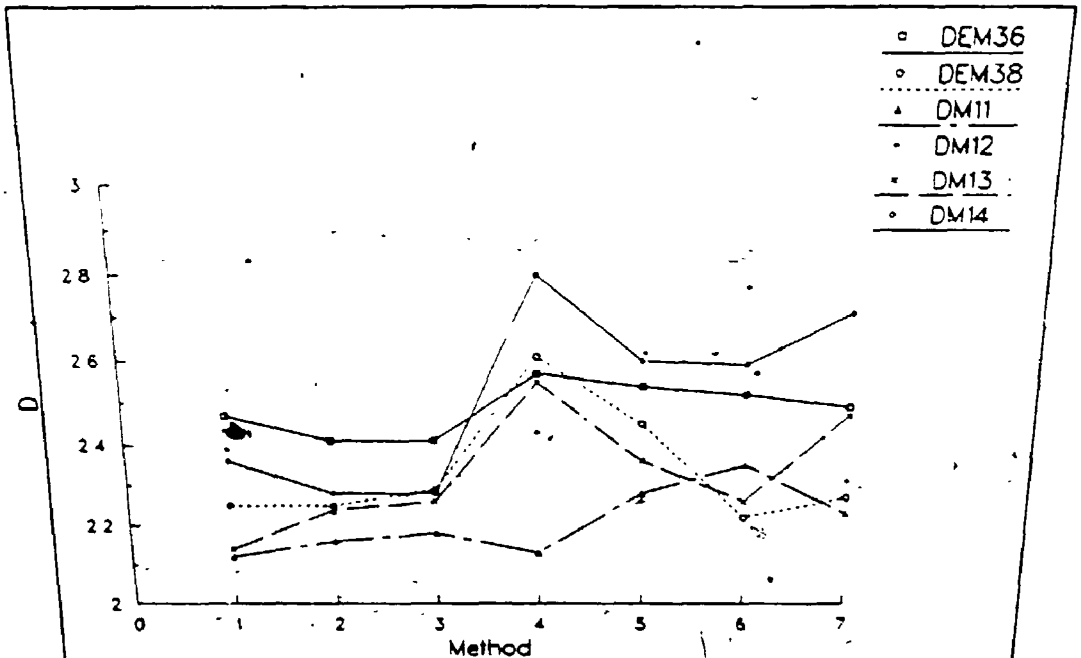

	ALL	ROW	COL	S1	S2	S3	S4
DEM36	2.47	2.41	2.41	2.57	2.54	2.52	2.49
DEM38	2.25	2.25	2.29	2.61	2.45	2.22	2.27
DM11	2.12	2.16	2.18	2.13	2.28	2.35	2.23
DM12	2.39	2.23	2.29	2.43	2.26	2.77	2.31
DM13	2.14	2.24	2.26	2.55	2.36	2.26	2.47
DM14	2.36	2.28	2.28	2.80	2.60	2.59	2.71

Figure 7.4.3.1 (continued) Valley and Ridge results

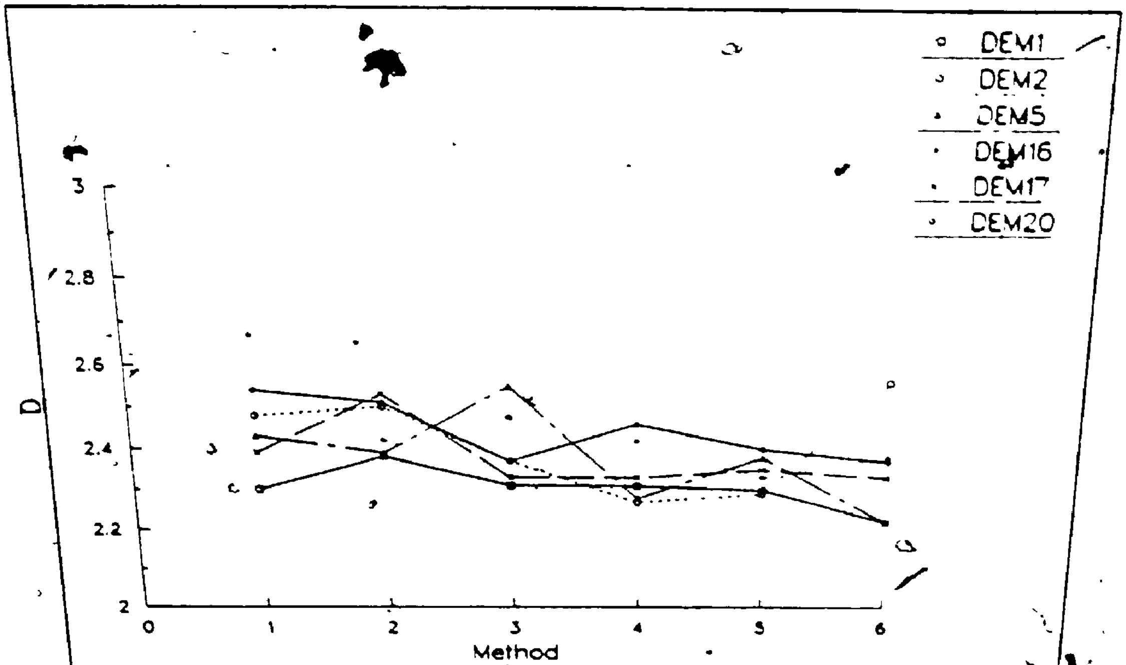

	A1	A2	A3	A4	A5	A6
DEM1	2.30	2.38	2.31	2.31	2.30	2.22
DEM2	2.48	2.50	2.37	2.27	2 29	2 56
DEM5	2.43	2.39	2.55	2.28	2.38	2.22
DEM16	2.67	2.42	2 33	2.42	2 33	2 38
DEM17	2.39	2.53	2.33	2.33	2.35	2.33
DEM20	2.54	2.51	2.37	2.46	2.40	2.37

Figure 7.4.3.2 Valley and Ridge results

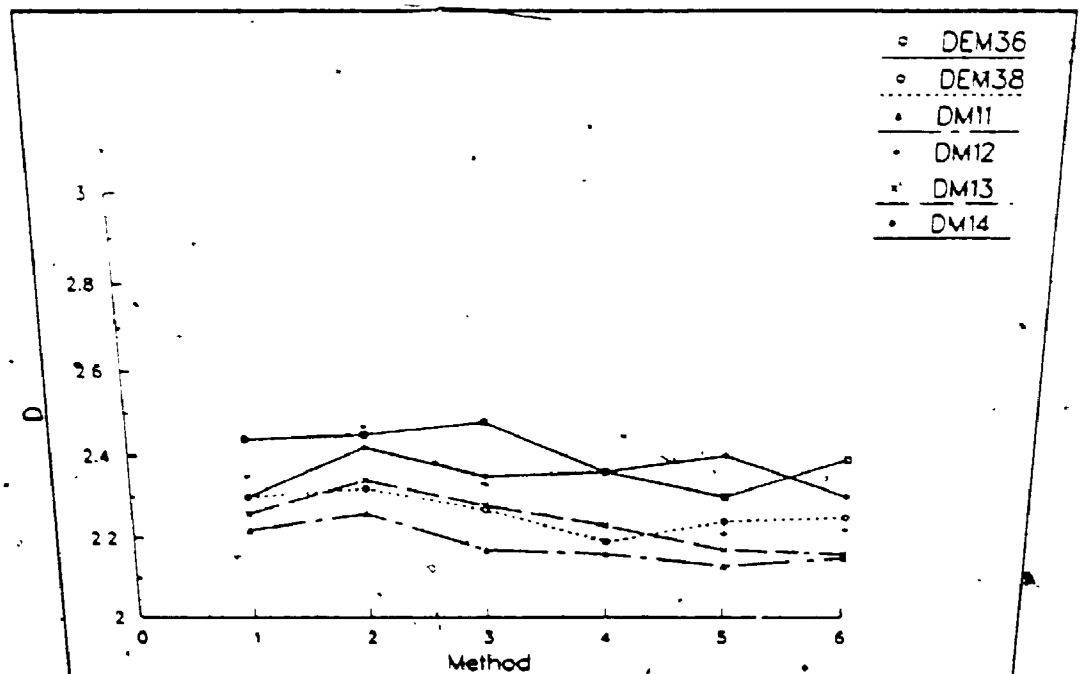

	A1	A2	A3	A4	A5	A6
DEM36	2.44	2.45	2.48	2.36	2.30	2.39
DEM38	2.30	2.32	2.27	2.19	2.24	2.25
DM11	2.22	2.26	2.17	2.16	2.13	2.15
DM12	2.35	2.47	2.33	2.19	2.21	2.22
DM13	2.26	2.34	2.28	2.23	2.17	2.16
DM14	2.30	2.42	2.35	2.36	2.40	2.30

Figure 7.4.3.2 (continued) Valley and Ridge results

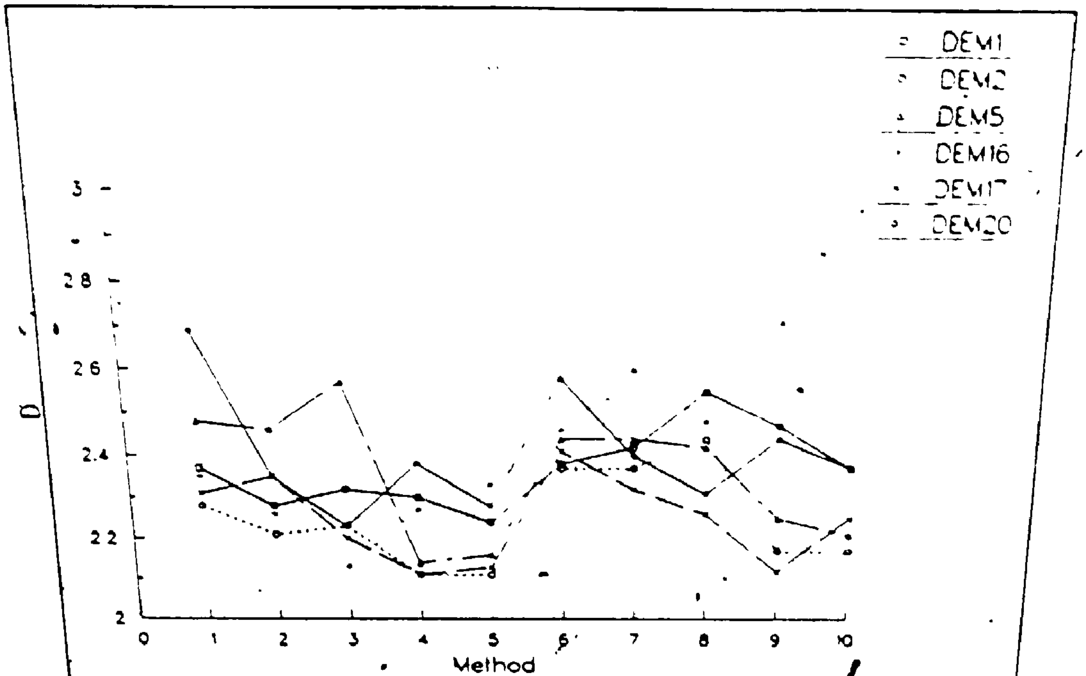

	CC1	CC2	CC3	CC4	CC5	DI1	DI2	DI3	DI4	DI5
DEM1	2.37	2.28	2.32	2.30	2.24	2.38	2.42	2.55	2.47	2.37
DEM2	2.28	2.21	2.23	2.11	2.11	2.37	2.37	2.44	2.17	2.17
DEM5	2.48	2.46	2.57	2.14	2.16	2.44	2.44	2.42	2.25	2.21
DEM16	2.35	2.26	2.13	2.27	2.33	2.46	2.60	2.48	2.71	2.96
DEM17	2.31	2.35	2.20	2.11	2.13	2.41	2.32	2.26	2.12	2.25
DEM20	2.69	2.35	2.23	2.38	2.28	2.58	2.40	2.31	2.44	2.37

Figure 7.4.3.3 Valley and Ridge results

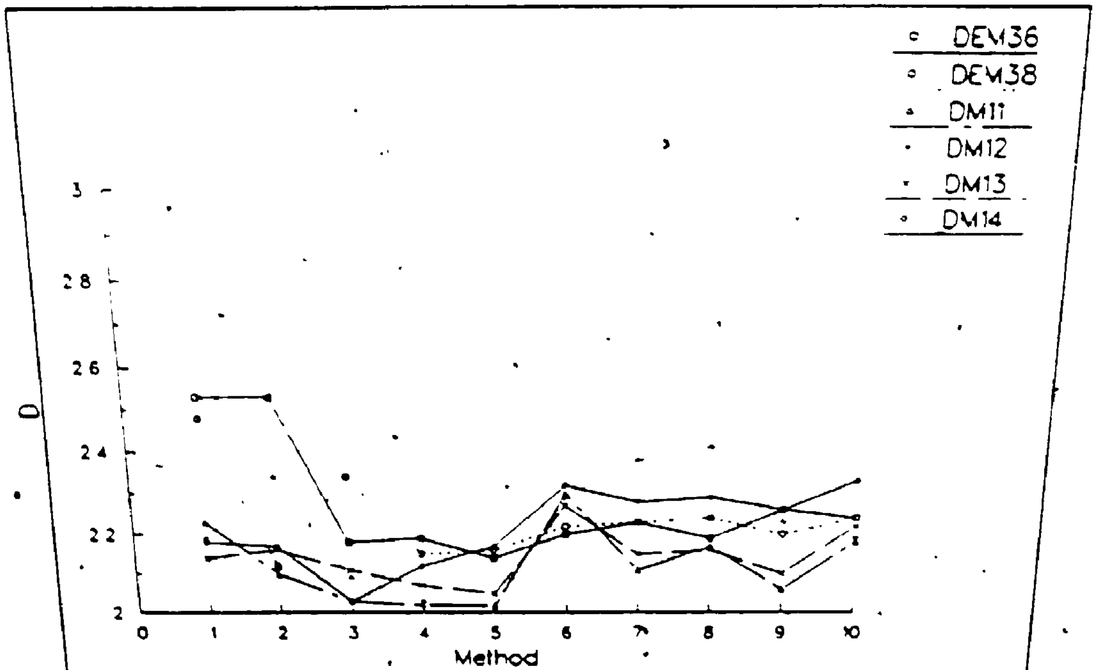

	CC1	CC2	CC3	CC4	CC5	D11	D12	D13	D14	D15
DEM36	2.53	2.53	2.18	2.19	2.14	2.20	2.23	2.19	2.26	2.24
DEM38	2.48	2.12	2.34	2.15	2.16	2.22	2.23	2.24	2.20	2.24
DM11	2.23	2.10	2.03	2.02	2.02	2.30	2.11	2.17	2.06	2.18
DM12	2.19	2.34	2.09	2.03	2.01	2.29	2.38	2.41	2.23	2.19
DM13	2.14	2.16	2.11	2.07	2.05	2.27	2.15	2.16	2.10	2.22
DM14	2.18	2.17	2.03	2.12	2.17	2.32	2.28	2.29	2.26	2.33

Figure 7.4.3.3 (continued) Valley and Ridge results

7.4.3.1 Summary

Although the intra-dataset variation within any one measurement method (e.g., the angle variograms) is not very large, the inter-dataset variation is consistently very large. This indicates that there is considerable variation, as measured by the fractal dimension, across the Valley and Ridge province. Overall, the results indicate that the predominant ridges and valleys of this region can be detected with the short breakpoints, especially in the direction perpendicular to the dominant trend of the ridges/valleys, the large number of bi-dimensional results, and the pattern present in the angle variogram dimensions, serving as indicators.

7.4.4 Appalachian Plateaus Physiographic Province

The majority of the fourteen datasets which fall within the Appalachian plateaus physiographic province occur in the southern (Tennessee) section of the province. Only three of the datasets (DM10, DM15 and DM16) occur in the northern section (table 7.1, figure 7.1). This province is characterized by deeply incised valleys with steep hillsides and considerable local relief (Hunt, 1974). The average standard deviation of the elevations is near the medium value for all of the provinces looked at, so in that sense the province does not stand out. This province has coefficients of dissection which span the entire range --

from values characteristic of early youth or inequilibrium (DEM11, DEM13, DEM19 and DM16) through to full maturity, or equilibrium, and finally, some at old age (DEM3 and DEM4).

The northern section of the province differs from the southern section only in that it was glaciated; otherwise the sections differ little (Hunt, 1974, 262). However, considerable physiographic differences do exist within the province, as "some areas are deeply dissected with closely spaced valleys between narrow ridges ...; others may be equally deeply dissected but by widely spaced valleys that are separated by broad, open uplands" (Hunt, 1974, 263). Thus, considerable inter-dataset variation is expected, and is reflected in the coefficients of dissection. For example, DEM11 represents one of the broad, open uplands, while DEM3 represents a deeply dissected area (appendix 2). In addition, many of the DEMs occur near the boundaries of the physiographic province, and their morphometric parameters reflect the influences of their neighbouring physiographic province, and exhibit considerable variation (appendix 1).

On a number of the contour plots definite ridges/valleys are present. In particular DEM4, 12, 13, and 14 have ridges/valleys running in a northeast-southwest direction (corresponding to angle 2) and DEM10, DEM19 and DM15 and DM16 have valleys running in a northwest-southeast direction (corresponding to angle 5). The remaining contour plots have numerous ridges and valleys running in all directions (appendix 2).

There is considerable variation in the fits of the fractal model to the datasets. Even within a single dataset the variation in fit can be considerable. Eight of the variogram plots have noticeable patterns present (i.e, relating to cycles of the ridges/valleys). Many of the sectional variograms produce bi-dimensional results, notable because in the majority of the other physiographic provinces' sectional results most datasets appear mono-dimensional. One dataset (DM10) stands out because of its extremely poor fit to the fractal model. One of its sectional variograms (S2) lacks any portion that can be considered linear, while its other three sectional vario-grams have only very short linear sections. This lack of fit was also observed in some of the angle variograms of DM10.

Of all of the datasets from the Appalachian provinces, the datasets from this province produce the lowest average fractal dimensions (table 7.4). Generally the intra-dataset variation in the dimensions was equal to or slightly less than that present in the Valley and Ridge datasets. Thus, this province appears to be somewhat more homogeneous and isotropic than the Valley and Ridge province. Given the small difference between the overall mean dimension of the sectional variograms and the overall mean dimension of the entire surface variogram, this province's datasets are also the most scaling of the three Appalachian provinces' datasets.

The most notable aspect of the sectional variogram results is the number of datasets which are bi-dimensional (appendix 1). If the value of D = 2.12 from S2 of DEM10 is ignored, the average dimension for the longer distances is 2.74, which is much higher than the average dimension of 2.38 associated with the shorter distance dimensions (figure 7.4.4.1). A similar greater-distance dimension is also present in the Valley and Ridge results. These two provinces are also similar in having a fractal dimension between 2.3 - 2.4 apply to the shorter distances (≈ 1 km or less apart).

Many of the angle variograms from the Appalachian Plateaus province are bi-dimensional, similar to those obtained from the Valley and Ridge datasets (figure 7.4.4.2; appendix 1). Of particular note, DEM19 is tri-dimensional in three directions, and the set of tri-dimensions (with one exception) does not vary by much. This indicates that while this landscape is scaleless, in the sense that a more or less constant fractal dimension applies at all scales, the 'roughness' (the range of the elevations) is a function of the scale.

In examining those datasets which have definite ridges or valleys running through them, some patterns do emerge in the results of the angle variograms. Datasets DEM4, DEM13 and DEM14 have their highest dimensions associated with the second angle (30° to 60°) -- the ridges/valleys predominantly run in a northeast-southwest direction in these datasets (figure 7.4.4.2; appendix 2). The ridge present in DEM12 runs in a more northerly direction, and its peak dimension also occurs in the first angle. Other datasets, DEM10, DEM19 and DM15, which have dominant ridges/valleys running in a northwest-southeast direction, also have their peak dimensions occurring in the corresponding angular swaths. These patterns are complicated somewhat by the occurrence of lesser ridges and valleys which run in other directions, however. For example, DEM10 also has an obvious valley running in an east-west direction, and the variograms associated with angles 3 and 4 (which correspond to that direction) both produced bi-dimensional results, with the dimension associated with the longer distances being around 2.78.

The remaining datasets do not display any consistent pattern, although individual cases do follow the expected pattern. For example, DEM3, which has a predominant north-south ridge, has a peak dimension at angle 1 and the lowest dimension occurring at angle 4, the angle 90° to that ridge. The range of physiographic differences present in this province prevent any dominant patterns from emerging; unlike, for example, the results of the Valley and Ridge datasets.

Six of the datasets have non-significant correlations between the angle variogram's Ds and the intercepts; the remaining eight datasets have significant, high correlations (table 7.9). The three northern datasets all have large positive correlations. The major physiographic difference between the northern and southern datasets is that the northern section was glaciated. This suggests that glaciation does not account for the negative correlations observed in the Valley and Ridge province's results.

No obvious trends appear among the results of the cell counting analyses (figure 7.4.4.3, appendix 1). However, the dimensions across most of the datasets are much more consistent than was the case in either of the other two Appalachian provinces. In particular, the dimensions associated with the first three elevations (those at the average elevation and below) are similar for the majority of the datasets (an average of around 2.11 if the obvious outliers are ignored). In some of those datasets which have dominant ridges/valleys a trend does appear (DEM13, 19 and DM15, 16, and to a lesser extent DEM10). In these datasets the dimensions exhibit a 'U' shaped pattern -- decreasing from the lowest elevation to the mid-elevational (or so) value, and then increasing to the highest elevation.

The results of the dividers method appear much less consistent across all datasets than do those of the cell counting method (figure 7.4.4.3). However, those datasets which have a 'U' shaped pattern in their cell counting dimensions also have a similar pattern in their dividers results. In addition, many datasets exhibit a slight

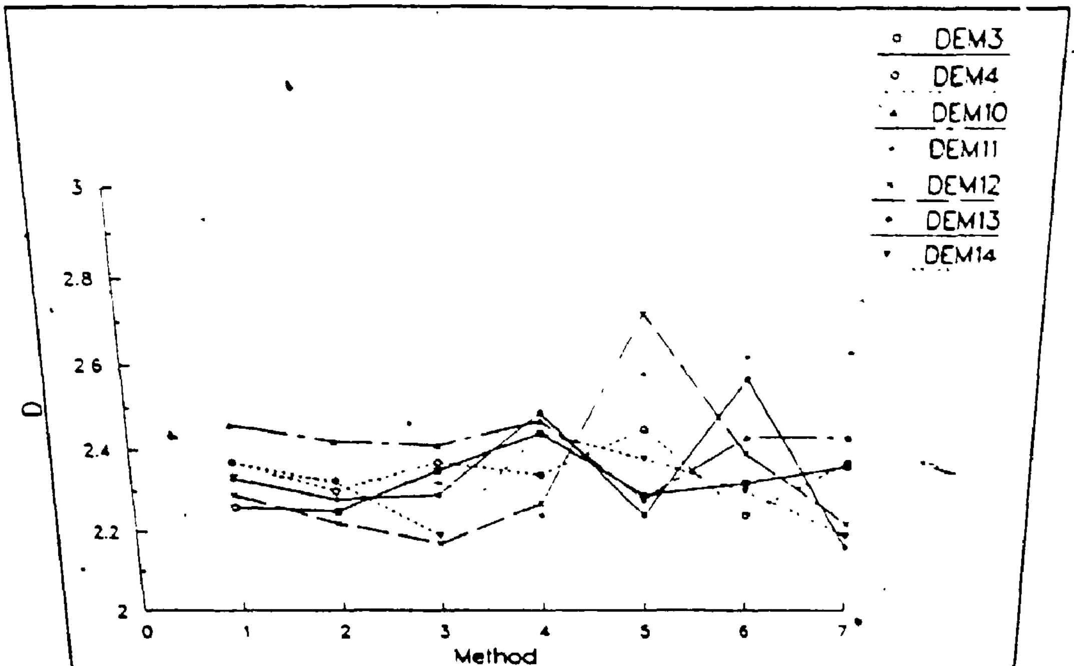

	ALL	ROW	COL	S1	S2	S3	S4
DEM3	2.26	2.25	2.35	2.44	2.29	2.32	2.36
DEM4	2.37	2.30	2.37	2.34	2.45	2.24	2.37
DEM10	2.46	2.42	2.41	2.47	2.28	2.43	2.43
DEM11	2.34	2.33	2.32	2.24	2.58	2.62	2.63
DEM12	2.29	2.22	2.17	2.27	2.72	2.39	2.22
DEM13	2.33	2.28	2.29	2.49	2.24	2.57	2.16
DEM14	2.37	2.32	2.19	2.44	2.38	2.30	2.19

Figure 7.4.4.1 Appalachian Plateaus results

Note: Lines are drawn for illustrative purposes only, they are not intended to signify any relationship between the points.

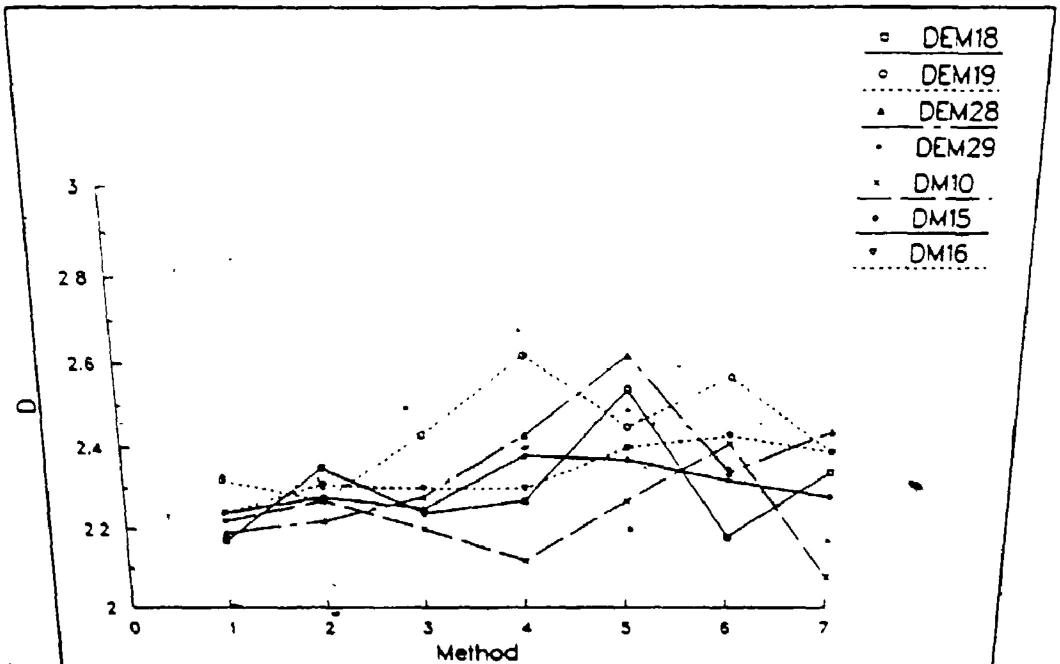

	ALL	ROW	COL	S1	S2	S3	S4
DEM18	2.17	2.35	2.24	2.27	2.54	2.18	2.34
DEM19	2.32	2.27	2.43	2.62	2.45	2.57	2.39
DEM28	2.19	2.22	2.28	2.43	2.62	2.34	2.44
DEM29	2.33	2.30	2.30	2.40	2.49	2.35	2.17
DM10	2.22	2.27	2.20	2.12	2.27	2.41	2.08
DM15	2.24	2.28	2.25	2.38	2.37	2.32	2.28
DM16	2.24	2.31	2.30	2.30	2.40	2.43	2.39

Figure 7.4.4.1 (continued) Appalachian Plateaus results

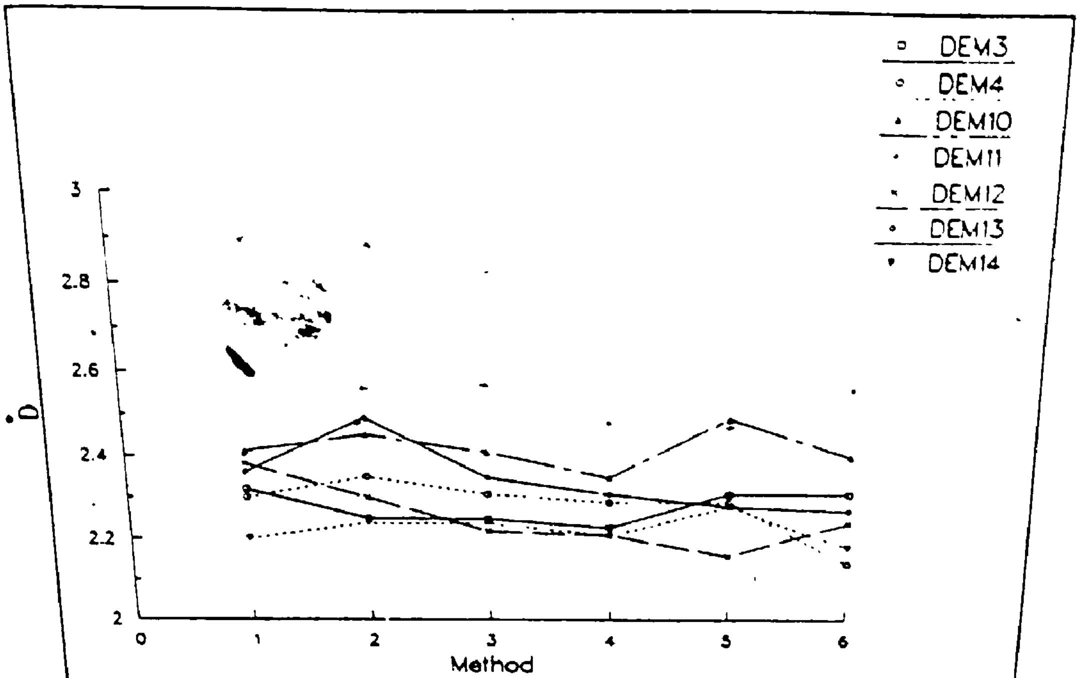

	A1	A2	A3	A4	A5	A6
DEM3	2.32	2.25	2.25	2.23	2.31	2.31
DEM4	2.30	2.35	2.31	2.29	2.29	2.14
DEM10	2.41	2.45	2.41	2.35	2.49	2.40
DEM11	2.40	2.56	2.57	2.48	2.47	2.56
DEM12	2.38	2.30	2.22	2.21	2.16	2.24
DEM13	2.36	2.49	2.35	2.31	2.28	2.27
DEM14	2.20	2.24	2.24	2.21	2.28	2.18

Figure 7.4.4.2 Appalachian Plateaus results

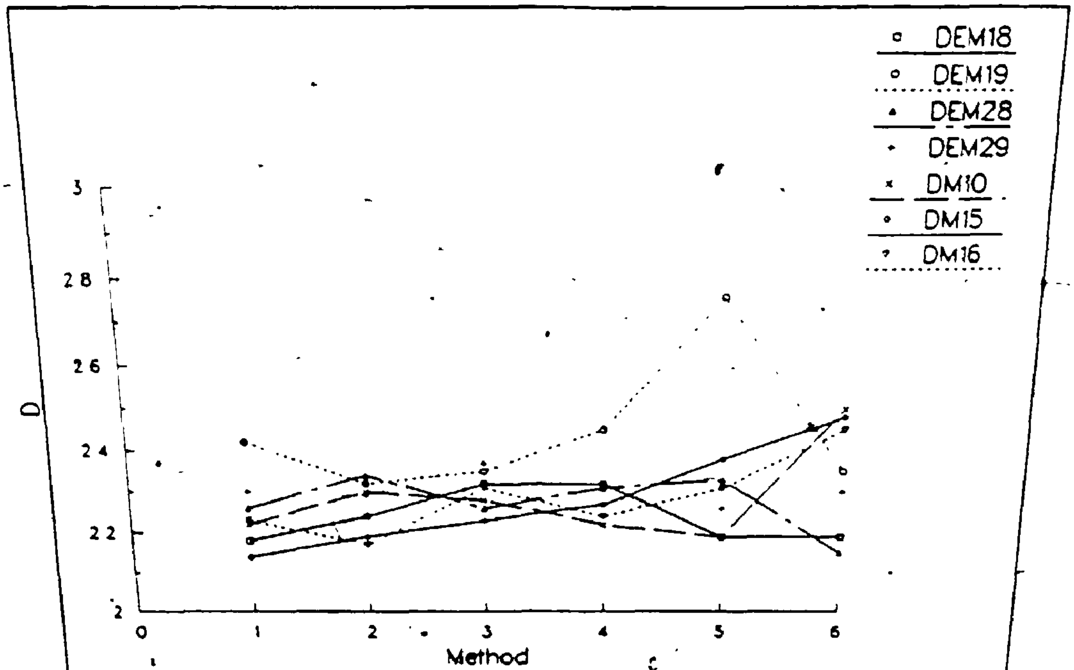

	A1	A2	A3	A4	A5	A6
DEM18	2.18	2.24	2.32	2.32	2.19	2.19
DEM19	2.42	2.32	2.35	2.45	2.78	2.35
DEM28	2.26	2.34	2.26	2.31	2.33	2.15
DEM29	2.30	2.29	2.37	2.27	2.26	2.30
DM10	2.22	2.30	2.28	2.22	2.19	2.50
DM15	2.14	2.19	2.23	2.27	2.38	2.48
DM16	2.23	2.17	2.31	2.24	2.31	2.45

Figure 7.4.4.2 (continued) Appalachian Plateaus results

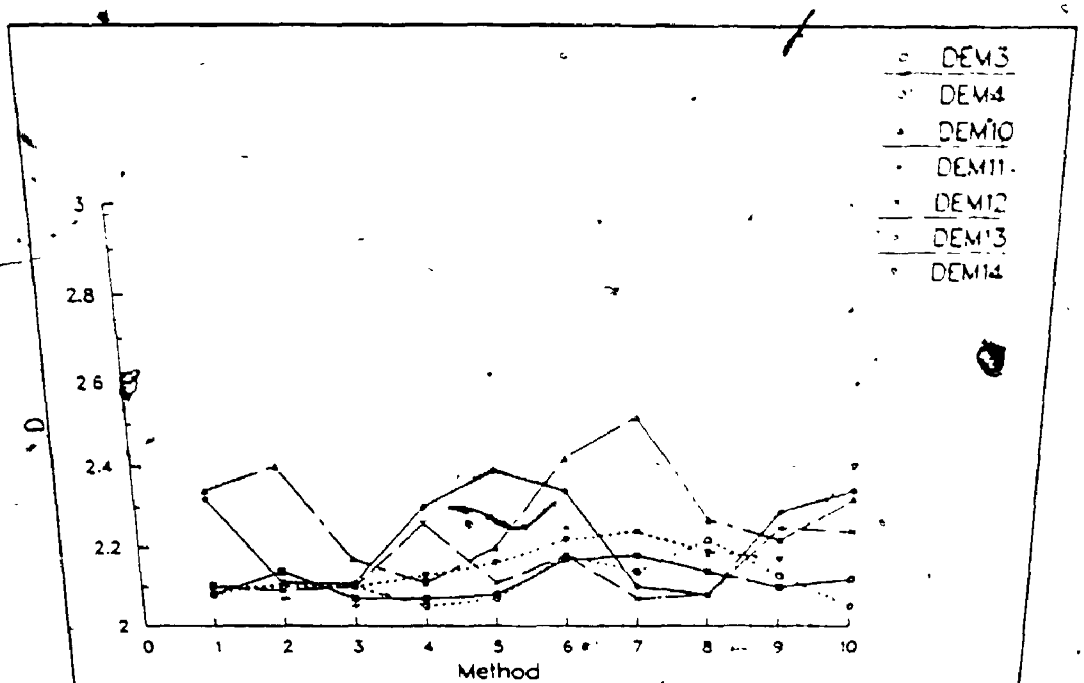

	CC1	CC2	CC3	CC4	CC5	DI1	DI2	DI3	DI4	DI5
DEM3	2.08	2.14	2.07	2.07	2.08	2.17	2.18	2.14	2.10	2.12
DEM4	2.10	2.10	2.10	2.05	2.07	2.18	2.14	2.22	2.13	2.05
DEM10	2.34	2.40	2.17	2.11	2.20	2.42	2.52	2.27	2.22	2.32
DEM11	2.11	2.07	2.05	2.12	2.62	2.25	2.24	2.18	2.29	2.60
DEM12	2.10	2.09	2.10	2.26	2.11	2.18	2.07	2.08	2.25	2.24
DEM13	2.32	2.11	2.11	2.30	2.39	2.34	2.10	2.08	2.29	2.34
DEM14	2.08	2.11	2.10	2.13	2.16	2.22	2.24	2.19	2.17	2.40

Figure 7.4.4.3 Appalachian Plateaus results

3

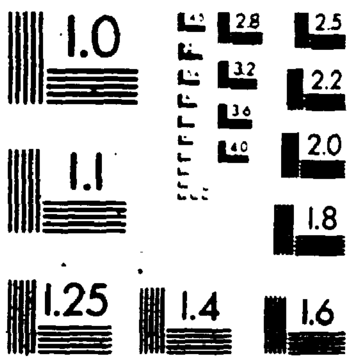

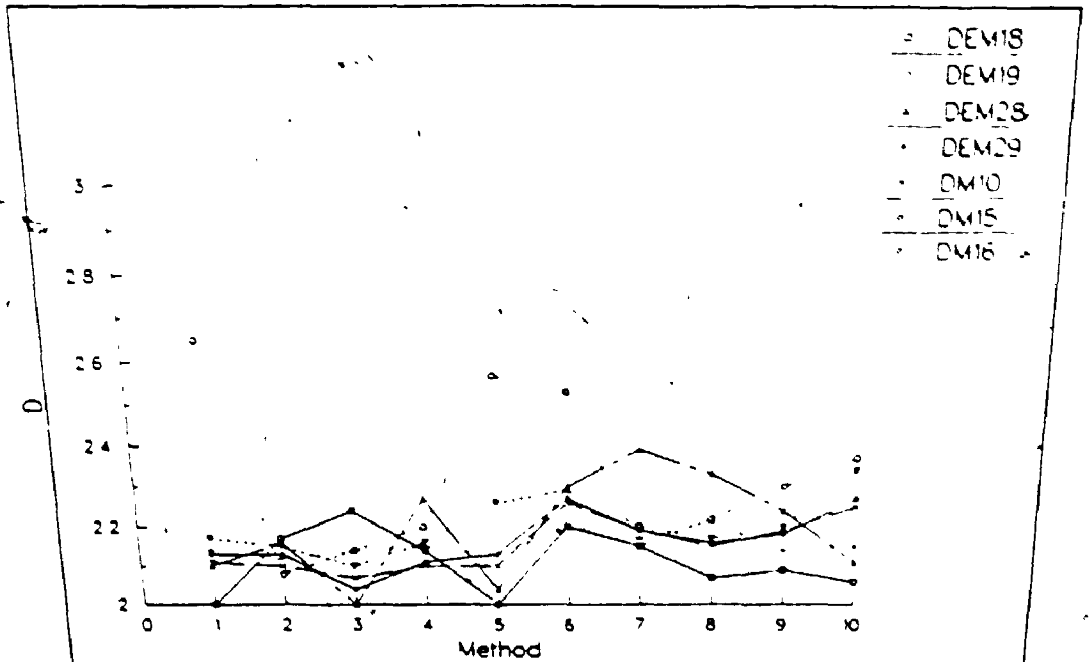

	CC1	CC2	CC3	CC4	CC5	DI1	DI2	DI3	DI4	DI5
DEM18	2.00	2.17	2.24	2.14	2.00	2.20	2.15	2.07	2.09	2.06
DEM19	2.65	2.08	2.14	2.20	2.57	2.53	2.15	2.22	2.30	2.37
DEM28	2.10	2.16	2.00	2.27	2.04	2.30	2.39	2.33	2.24	2.11
DEM29	2.14	2.12	2.14	2.15	2.13	2.20	2.17	2.21	2.14	2.15
DM10	2.11	2.10	2.07	2.10	2.10	2.26	2.19	2.15	2.19	2.25
DM15	2.13	2.13	2.04	2.11	2.13	2.27	2.19	2.16	2.18	2.27
DM16	2.17	2.15	2.10	2.16	2.26	2.29	2.20	2.17	2.20	2.34

Figure 7.4.4.3 (continued) Appalachian Plateaus results

positive relationship between D and the elevation -- as the elevation increases, D also tends to increase. This form of the relationship between D and elevation is not observed to such an extent in either of the other two Appalachian provinces results.

7.4.4.1 Summary

The Appalachian Plateaus province contains a diversity of physiography and the datasets appear to have captured some of that diversity. Thus, no overall conclusion can be reached from the analyses. Nonetheless, in those datasets which contain dominant ridges/valleys consistent patterns emerge from the angular variogram analyses, and from the results of the surficial contour analyses. When contrasted with the two other provinces from the Appalachian provinces, the datasets from this province are the most homogeneous and scaling, and only slightly less isotropic than the datasets from the Blue Ridge province.

7.4.5 Great Plains Physiographic Province

The two DEMs that are from this province are located near the northwestern edge of the Great Plains (figure 7.1; table 7.1). The Plains are described as a broad plateau sloping eastward from the relatively high elevations at the foot of the Rocky Mountains to the lower elevations of the central lowlands. In the northern part of this province the rivers can be entrenched a few hundreds of feet into the plateau, and dome mountains can rise 1500 to 2000 feet above it. Between the dome mountains are broad anticlines and synclines, with cuestas clearly marking their limits (Hunt, 1974; Thornbury, 1965). The two DEMs from this province have low standard deviations and small ranges in their elevations, reflections of low topographic relief. In that sense, these DEMs have only captured a small portion of the range of relief present in this province. Both datasets have equilibrium coefficients of dissection (appendix 1).

Although the two DEMs are located some distance apart, they appear to share similar morphometric characteristics. Both datasets fit the fractal model reasonably well, DM18 slightly more so than DEM9. The datasets do not stand out as having either low or high dimensions, and the results across all methods are in fairly close agreement with each other (figure 7.2). The average absolute difference in dimension produced by the sectional and entire-surface variograms is very low, as are the standard deviations of the sectional and angle variogram results. Thus, the Great Plain datasets would be described as scaling, homogeneous and isotropic.

Both datasets have one sectional variogram which produces bi-dimensional results and, in both cases the dimension associated with the longer distances is approximately 2.60 (figure 7.4.5.1; appendix 1). DEM9 exhibits much more variation in the sectional variogram results than DM18, and its dimensions generally do not extend across as great a distance as they do for DM18. That is, the breakpoints in the variogram plots occur consistently at the shorter distances.

Both DEM9 and DM18 are bi-dimensional in the direction of angle 3, the first dimension being relatively low (2.34 & 2.33) while the second dimension being much higher (2.95 and 2.77, respectively). The contours within DEM9 (appendix 2) generally run in a northwest-southeast direction, and the highest dimension, the longest linear segment, and the lowest intercept all occur in the results of angle 5, the angle parallel to that general trend of the contours (figure 7.4.5.2). No trend appears in the contours of DM18, and no trend appears in the angle variogram results of DM18. Thus, both datasets which exhibit similar bi-dimensional angle 3 variograms cannot be attributed to obvious elevational trends, but must be a result of less apparent factors. Although both datasets have non-significant correlations between the angle variograms' D and the intercepts, the more northern dataset, DEM9, has a fairly large negative correlation.

This is the only physiographic province in which the surficial contour methods produce average dimensions greater than the entire variogram and the angle variograms dimensions (figure 7.2). The two datasets display opposite trends in their results when the cell counting method is used. For DEM9 D generally declines as the elevation increases,

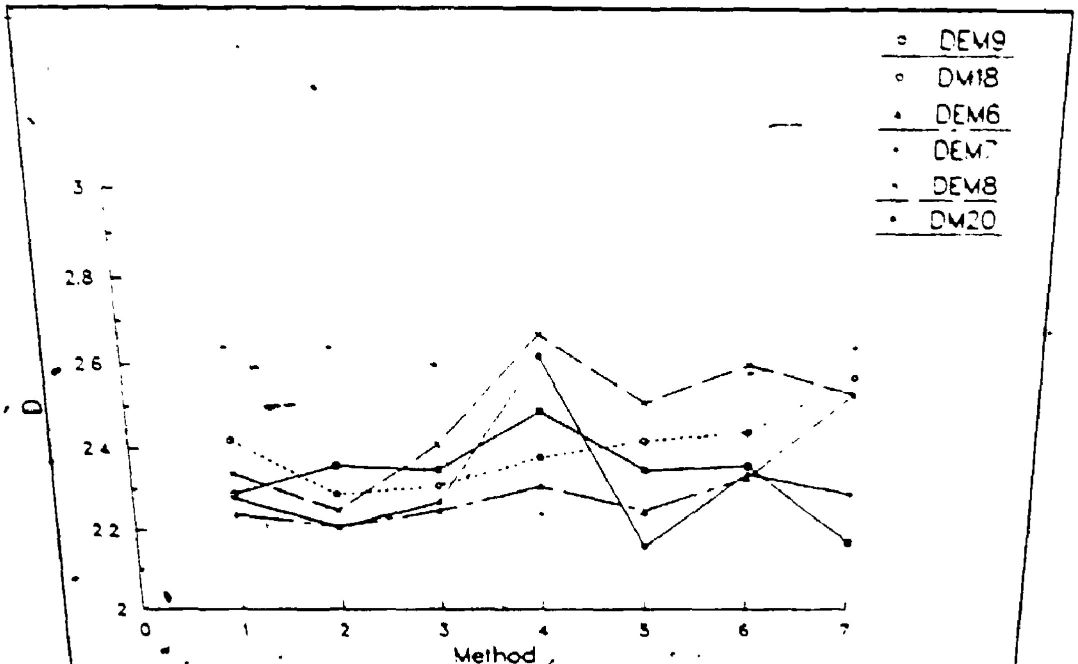

	ALL	ROW	COL	S1	S2	S3	S4
DEM9	2.29	2.36	2.35	2.49	2.35	2.36	2.17
DM18	2.42	2.29	2.31	2.38	2.42	2.44	2.57
DEM6	2.24	2.21	2.25	2.31	2.25	2.33	2.53
DEM7	2.64	2.64	2.60	2.24	2.24	2.58	2.64
DEM8	2.34	2.25	2.41	2.67	2.51	2.60	2.53
DM20	2.28	2.21	2.27	2.62	2.16	2.34	2.29

Figure 7.4.3.1 Great Plains, Interior Low Plateaus, and Rocky Mountains results

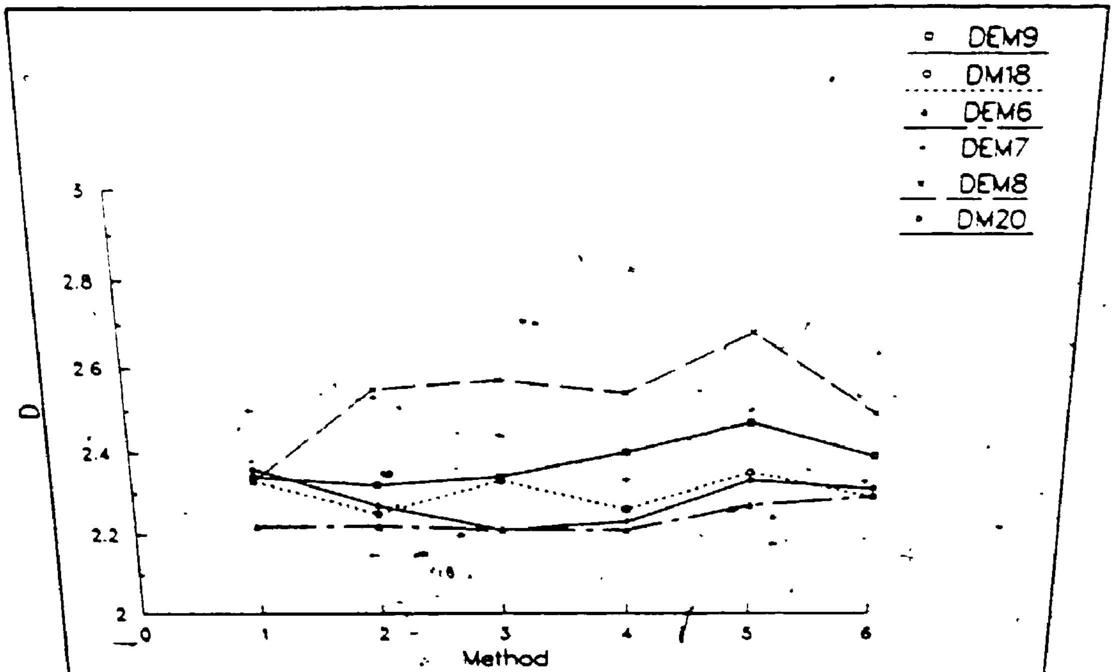

	A1	A2	A3	A4	A5	A6
DEM9	2.34	2.32	2.34	2.40	2.47	2.39
DM18	2.33	2.25	2.33	2.26	2.35	2.29
DEM6	2.22	2.22	2.21	2.21	2.27	2.29
DEM7	2.50	2.53	2.44	2.33	2.50	2.63
DEM8	2.33	2.55	2.57	2.54	2.68	2.49
DM20	2.36	2.27	2.21	2.23	2.33	2.31

Figure 7.4.5.2 Great Plains, Interior Low Plateaus, and Rocky Mountains results

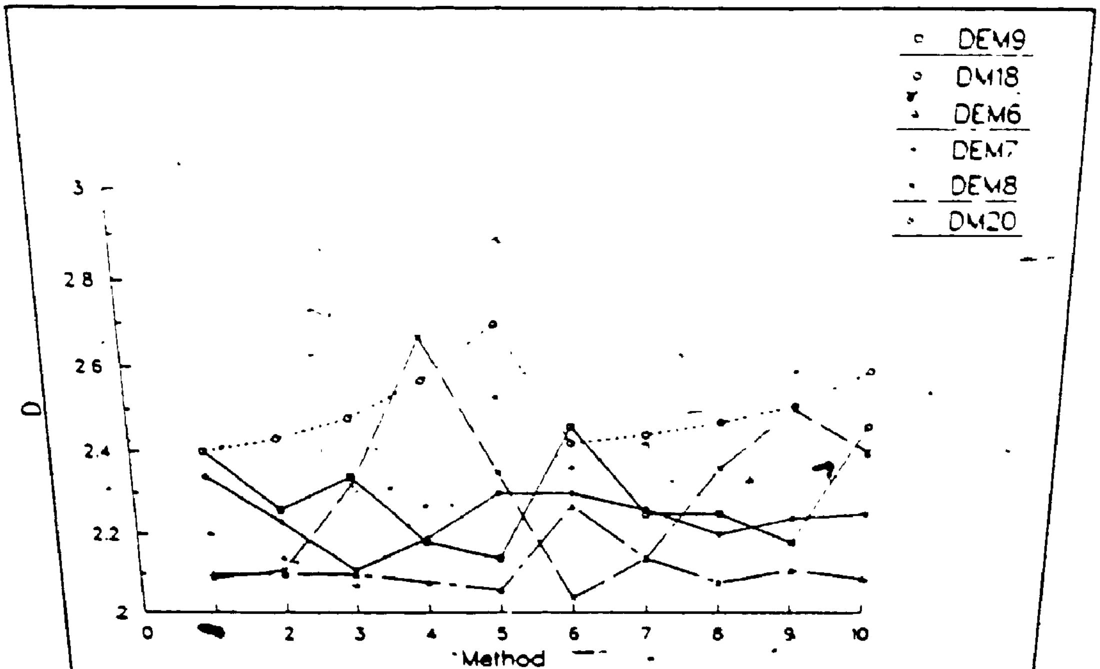

	CC1	CC2	CC3	CC4	CC5	DI1	DI2	DI3	DI4	DI5
DEM9	2.40	2.26	2.34	2.18	2.14	2.46	2.25	2.25	2.18	2.46
DM18	2.40	2.43	2.48	2.57	2.70	2.42	2.44	2.47	2.51	2.59
DEM6	2.10	2.10	2.10	2.08	2.06	2.27	2.14	2.08	2.11	2.09
DEM7	2.20	2.14	2.07	2.27	2.53	2.36	2.42	2.25	2.59	2.39
DEM8	2.09	2.11	2.32	2.67	2.35	2.04	2.14	2.36	2.50	2.40
DM20	2.34	2.23	2.11	2.19	2.30	2.30	2.26	2.20	2.24	2.25

Figure 7.4.5.3 Great Plains, Interior Low Plateaus, and Rocky Mountains results

whereas with DM18 D increases as the elevation increases (figure 7.4.5.3). DEM9 has bi-dimensional results associated with the two highest contours, so the difference between the dimensions of DEM9 and DM18 are not as great as they appear in figure 7.4.5.3.

The dividers results of DM18 parallel those of its cell counting results, with D increasing as the elevation increases. The dividers results of DEM9 also generally parallel the cell-counting results, except that the dimension associated with the highest contour value is much higher than the value associated with the second highest contour. This breaks up the general monotonic decline in dimension with elevation. Why the two datasets exhibit generally opposite trends with respect to their dimensions is not apparent in their contour plots (appendix 1), or in any of their similar morphometric parameters.

7.4.5.1 Summary

Although the two datasets from the Great Plains province have similar morphometric parameters, the results of the surficial contour methods clearly indicate that the two datasets are different. The datasets appear relatively homogeneous, scaling and very isotropic.

7.4.6 Interior Low Plateaus Physiographic Province

The three DEMs assigned to this province (figure 7.1; table 7.1) are all located close to the eastern edge of the province. The Interior Low Plateaus province incorporates a considerable range of physiographic features, with steep-walled streams and smoothly rounded hills, as well as areas of well developed karst topography alongside areas of non-karst topography. The three datasets capture some of this physiographic variation. The westernmost dataset (DEM6) has a deeply incised stream running north-south through it and exhibits considerable relief. However, the easternmost dataset (DEM8), although exhibiting considerable elevational range, is not marked by any significant feature (appendix 2). Nonetheless, the three datasets do appear to form a recognizable group (table 7.2). For example, all three datasets have high coefficients of dissection, which indicates that they are all in the inequilibrium stage (appendix 1; Strahler, 1952).

All three datasets exhibit a poor fit to the fractal model. Scatter in the variogram plots is evident at the longer distances. In particular, the variogram plots produced by DEM8 often have only a very short linear section from which to determine the fractal dimension. Many of the results are also bi- and tri-dimensional, and the intra- and inter-dataset variation in the dimensions is considerable (figures 7.4.5; appendix 1). For example, the results associated with the variograms of the entire dataset vary considerably. DEM8 has a fractal dimension of 2.34, which applies only to short distances (< 0.6 km), while DEM6 has a slightly lower fractal dimension of 2.24 which extends through to a slightly longer distance (< 2.5 km), and DEM7 has a high fractal dimension (2.64) derived from a graph which was linear throughout its entire length. Considering the number of bi-dimensional results, this province appears to be non-scaling, definitely anisotropic, and not homogeneous (table 7.4).

The sectional variograms produce very variable results. All four sections of DEM8 produce dimensions which are above 2.5 (figure 7.4.5.1), three of the four sections of DEM6 have dimensions around 2.3. Two of the sections of DEM7 (S1 and S2) are bi-dimensional, with dimensions of 2.24 in both cases at the shorter distances, and dimensions above 2.70 at the longer distances (appendix 1).

The angle variograms for DEM6 are fairly consistent, especially with respect to the breakpoint (2.49 km) in the variograms from the first four angles. The dimensions associated with the fifth and sixth angle variograms are slightly higher and those angles correspond to the direction of the valley which runs through the dataset (figure 7.4.5.2). Five of the six angle variograms from DEM7 produce bi-dimensional results, with the average breakpoint between the two dimensions around 0.8 km. The patterns of the two associated Ds are opposite to each other. While the shorter distance's Ds generally decline to a low at the fourth angle, and then increase, the longer distance's Ds increase to angle 4, and then decrease. This may be an indication that processes are operating preferentially in one direction at one scale. For example, at some time in the past the surface might have been subjected to a process which increased its dimension in one direction (e.g., faulting). Subsequently, and as a result of the first process, a gradational process, which reduced the dimension at the shorter scales, could be operating preferentially on the most exposed surfaces (those with the higher D).

Two of the datasets have large, significant correlations between the angle variograms' fractal dimensions and the associated intercepts (table 7.9). DEM6, which has a smaller, non-significant correlation, has a deeply incised stream running through it, the other two datasets are relatively featureless. Whether the stream accounts for the differences in the correlations, and how it would influence the relationships, is not known.

No consistent patterns in the dimensions emerged from either the cell counting or the dividers results (figure 7.4.5.3). Almost all of the cell counting graphs produce bi-dimensional results, with the dimensions associated with the shorter distances usually falling below 2.20 where there is an associated second dimension, and the dimensions associated with the longer distances being either above 2.70 (for DEM7 and 8), or else around 2.3 (for DEM6). The dividers results present no consistent pattern (figure

7.4.5.3). The dimension generally increases with elevation for DEM8, decreases with elevation for DEM7, and varies greatly from elevation to elevation for DEM7.

7.4.6.1 Summary

It is difficult to decipher any consistent pattern from the results other than to conclude that two process domains exist. One domain is associated with a low fractal dimension at the shorter distances, and the other domain is associated with much higher dimensions at the longer distances. The Interior Low Plateaus datasets are neither scaling, homogeneous, nor isotropic.

7.4.7 Rocky Mountains Physiographic Province

Only one DEM, DM20, is located within the Rocky Mountains physiographic province, near its eastern edge (figure 7.1; table 7.1). The lone dataset occurs in the White River Plateau area of the southern Rocky Mountains, which borders the Colorado Plateau. The White River Plateau is a lava-covered, uplifted area, and is not a true mountainous region. The anticlinal structure of the White River Plateau, a structure typical of the southern Rocky Mountains, identifies this plateau as part of the southern Rockies (Thornbury, 1965; Hunt, 1974). A high range in elevations, high topographic relief, and a low coefficient of dissection are some of the morphometric parameters associated with DM20. This dataset has a low coefficient of dissection which would place it in the old age stage (appendix 1).

The fractal model fits extremely well for most of the results, with the variogram plots being linear throughout their entire distance range. The intra-dataset variation in the sectional variogram results is high; conversely, the intra-dataset variation of the angle variograms is low. This indicates that the dataset appears isotropic but not homogeneous. The difference between the average sectional results and the entire-surface and angle variogram results indicates that the area is reasonably scaling.

Although all four sections of the contour map (appendix 2) appear visually similar, the dimensions associated with the sectional variograms vary widely (figure 7.4.5.1) -- even though three of the four variogram plots were linear throughout. The one section that stands out (S3) has a variogram plot with only a short linear segment with a dimension of 2.34.

The angle variogram's dimensions do vary slightly by direction, with the lowest D obtained from angle 3 and the highest from angle 1 (figure 7.4.5.2). There is a trend in the elevations within the DEM, from lower elevations on the western edge to higher elevations on the eastern edge. The lower dimension is produced when looking up slope, the higher dimension is produced when looking more or less perpendicular to that slope. The correlation between the dimensions and the intercepts is not significant or very high (table 7.9).

The results of the cell counting method and the dividers method are similar (figure 7.4.5.3). There is a definite 'U' shaped pattern to the dimensions, which start off with a high value in the lower elevations, decrease to a low value at the mid-elevations, and then increase to the higher elevations.

7.4.7.1 Summary

Although the dataset from the Rocky Mountains physiographic province fit the fractal model well (e.g., most of the plots were linear thoroughout), this dataset would not be considered homogeneous. It does appear reasonably isotropic and scaling, however.

7.4.8 Colorado Plateau Physiographic Province

Four DEMs are located near the western edge of the Colorado Plateau in the high plateau section (Hunt, 1974, 426) (figure 7.1; table 7.1). This province contains the highest plateaus in the continent, with extensive igneous structures and steep-walled canyons. In the high plateau section lava capped plateaus are separated by wide, flat-bottomed north-south tending valleys. These fault-related features are found in this section of the province more than in any other part. In addition, "angularity of topography is conspicuous as a result of the arid climate and horizontality of the rocks" (Thornbury, 1965, 405).

All four datasets display considerable topographic relief, with both large standard deviations and a high range in their elevations. Although the coefficient of dissection is also similarly high for all four datasets, with two of the datasets definitely in the inequilibrium stage (appendix 1), the remaining morphometric parameters vary considerably.

The fractal model fits well, and most of the variogram plots are linear throughout. Based on the physiographic description of this province, these results are unexpected. In a few of the angle variograms of DEM25 and DEM27 some slight patterning is present in angles 3 and 4, however. The overall impression is that all four datasets have similar fractal characteristics, although some inter-dataset variation is present in the sectional variograms. These surfaces are scaling: note the small difference between the sectional variogram dimensions and the entire surface variogram dimensions. They are also homogeneous -- note the small intra-dataset variation in the sectional variograms, and isotropic -- the angle variograms display low intra-dataset variation (table 7.3).

All four datasets have a bimodal distribution with respect to their sectional variogram dimensions (figure 7.4.1.1). The sections which have high dimensions tend to be located close to each other: S3 and S4 of DEM24 are located closest to S1 and S2 of DEM25; S2 of DEM27 is close to S2 of DEM25. Most of the sectional variogram plots were linear throughout their entire range. Two of DEM27's sections are bi-dimensional, however, as is one of DEM24's (appendix 1). The contour plots do not provide any insight as to why the dimensions are bimodal, or why certain sections have higher dimensions than others.

Three of the four datasets display similar patterns in the dimensions obtained from the angle variograms; the dimensions rise to a peak value in angle 5 (figure 7.4.1.2). The contour plots (appendix 2) exhibit a slight trend in the elevations, which appear to increase from generally lower values in the southwest to higher values in the northeast. Thus the higher dimensions are associated with the angular swath which runs parallel to the general direction of the contours, as expected. In two datasets the largest intercepts occur in the cross-slope angle variogram results, similar to the Rocky Mountain physiographic province's results. Two of the datasets have fairly high, significant correlations between D and the intercepts (table 7.9), while the other two have fairly low, non-significant correlations. None of the morphometric parameters, or of the contour plots, display a similar breakdown, so the differences cannot be attributed to any obvious characteristics.

No distinctive patterns appear in the dimensions produced by either the cell counting or dividers methods (figure 7.4.1.3). Most of the cell counting results produce typical cell counting bi-dimensional results, with a low dimension associated with distances shorter than 0.5 km and a much higher dimension (mean D > 2.5) associated with the longer distances. The dividers plots are linear only to a ground distance of between 0.5 km and 1 km, and produce a slightly higher overall dimension for the surface.

7.4.8.1 Summary

The Colorado Plateau physiographic province's results are good examples of homogeneous, scaling, and isotropic datasets. A slight trend is present in the directional dimensions, but no trends appear when looking at elevational dimensions.

7.4.9 Basin and Range Physiographic Province

Nine of the ten datasets which are from the Basin and Range physiographic province occur adjacent to each other in the extreme northwest corner of the province (figure 7.1; table 7.1). The remaining dataset (DM17) is located near the southwestern edge of the province in southern California. Although the overall characteristics of this province are distinctive, its boundaries are generally gradational (Hunt, 1974). This suggests that, as DM17 occurs adjacent to the Pacific Border Province and as the remaining datasets are adjacent to the Columbia Plateau, there might be some noticeable morphometric differences between DM17 and the others. Note, however, that in the discriminant analysis (section 7.1.1) DM17 is correctly assigned to the Basin and Range province.

The mountains which make up this province "are typically isolated, subparallel ranges that rise abruptly above adjacent desert plains" (Thornbury, 19656, 471). In general, the axes of the ranges run north-south. The nature of the valleys -- they are structural rather than erosional features -- are distinctive features of this province (Hunt, 1974), and might be expected to influence the fractal dimensions.

The nine northern datasets fall within the Land and Lake portion of the Great Basin area of this province (Hunt, 1974, 496). This portion is "a block-faulted lava plateau with numerous high volcanic cones. .... The topographic grain ... has much less linearity than the other parts of the Great Basin because of the thick, extensive lava flows" (Hunt, 1974, 498). The remaining dataset, DM17, is located in the Sonoran Desert section, but it clearly reflects some characteristics of the adjacent mountainous province. That is, the range of the elevations associated with DM17 is much larger than expected in this area of the Basin and Range province, but it is consistent with the adjacent Pacific Border province. The Basin and Range province has datasets with coefficients of dissection which span the entire range. One of the datasets, DM8, is in the inequilibrium stage, five are in equilibrium, while four (DM1, DM2, DM5, and DM7) are definitely in the old age phase, with coefficients all below 0.20 (appendix 1; Strahler, 1952). The standard deviations of the elevations are above the overall average, but not exceptionally so. These values follow from the physiographic description of this province.

In a study by O'Neill and Mark (1985, 1987) on slope frequency distributions, they noted in particular the wide range of values in the skewness and kurtosis of the slope angles they obtained from these same nine datasets. They also commented upon the bi-modal nature of the slope populations, a reflection of two distinct physiographies present in the datasets: steep fault-scarp slopes and canyon walls, and gently sloping valley floors and uplifted fault block surfaces. These results are further evidence of the large inter-dataset variability captured by the DEMs from this province.

Overall, the fractal model fits these datasets only partially. Many of the sectional variogram plots display scattered plots; in particular DM1, DM2, DM4, DM7 and DM8 all have sectional variogram plots which show so much scatter that it is not possible to obtain any best-fit line from the graphs (i.e., no dimension was obtained in those cases). Each method produces slightly different results (figure 7.1) -- something not observed to this extent in any of the other physiographic province's results. The intra-dataset variations of the variogram methods are slightly above average (table 7.4), while the surficial contour methods have low intra-dataset variation. Thus, while the surfaces are not homogeneous nor isotropic, they are scaling.

As mentioned above, the most notable feature of the sectional variogram results is the number of plots (6) which are so scattered that they preclude regression. This did not occur with any other datasets in any other province. Inspection of the contour plots (appendix 2) provides some clues as to why this might occur. With the exception of DM4's, all of the contour plots for the aberrant datasets display a concentrated, narrow band of contours. This indicates that most of the elevational change is restricted to a relatively small area (an expression of the basin and range topography).

The sectional variogram results (figure 7.4.6.1; appendix 1) indicate that considerable inter-dataset variation exists within this province. Many of the datasets have fractal dimensions which apply throughout the entire range of the plots, which is an indication that the fractal model fits these sections of the datasets well. Thus, the sectional variogram results provide illustrations of some of the best fits to the fractal model, and some of the worst. The best example is DM1: two of its sectional variogram plots lack any linear section, whereas the other two plots are linear throughout.

No obvious pattern emerges from the results of the angle variograms (figure 7.4.6.2, appendix 1). A few of datasets are bi-dimensional; in particular DM8 is tri-dimensional in two directions. The results of DM8 in the second and fourth angles indicate that at medium distances (from ≈ 1 km to ≈ 3 km) the dimension is higher than at either the shorter distances or at the longer distances (2.16, 2.70, 2.14; 2.10, 2.47, 2.35; respectively). There is nothing notable in the contour plot for DM8 which could provide an explanation for this behaviour.

However, when the dimensions of the shorter and longer domains are considered in light of the escarpments present in several of the datasets, one pattern does appear (appendix 2). For example, on DM1, DM2 and DM7 a north-south escarpment appears on the contour plots. In all three cases the datasets are bi-dimensional in the direction of angle 5 -- the direction perpendicular to the escarpment. The dimensions associated with the longer distances are fairly high (2.57, 2.85 and 2.80, respectively), while the dimensions associated with the shorter distances are much lower (2.08, 2.15, and 2.22, respectively). Thus, at shorter distances (which would occur for the most part within the respective plains) the surfaces appear relatively smooth, while at the longer distances (distances which could cross the escarpment) the surfaces appear much rougher.

Six of the ten correlations between the angle variograms' fractal dimensions and the intercepts are non-significant (table 7.9). The most noteworthy result is the negative correlation associated with DM6 -- a non-significant value of -0.68. DM6 is located at the southwest corner of the block of nine datasets, and consistently has among the lowest intercepts in the physiographic province, so it is possible that the physiography in this dataset is different from the adjacent datasets' physiography (it has one deep canyon and is otherwise a rolling plateau).

The cell counting results show little intra- and inter-dataset variations (figure 7.4.6.3, appendix 1). Almost every dataset is bi-dimensional, but unlike most of the other bi-dimensional results, the dimension associated with the longer distances is often below 2.5. The most notable result is the different behaviour of DM17. It stands out by having an average dimension of 2.30, which is 0.20 higher than this province's overall average cell counting dimension. This provides the first indication that this dataset differs from the other datasets. DM17 is also mono-dimensional, with the linear portions of the plots extending from .96 to 1.9 km. This differs from the typical linear segments for the remaining datasets which fall around .24 to .48 km. Thus, it is the fractal nature of DM17 at distances less than 2 km that distinguishes it from the other datasets within this province.

The cell counting results of two other datasets are worth mentioning - DM4 and DM5. Both datasets have a much higher dimension associated with the middle elevation, and the linear portions of the graphs associated with these elevations are also much longer than average (0.96 km). These two datasets do not have similar morphometric para-

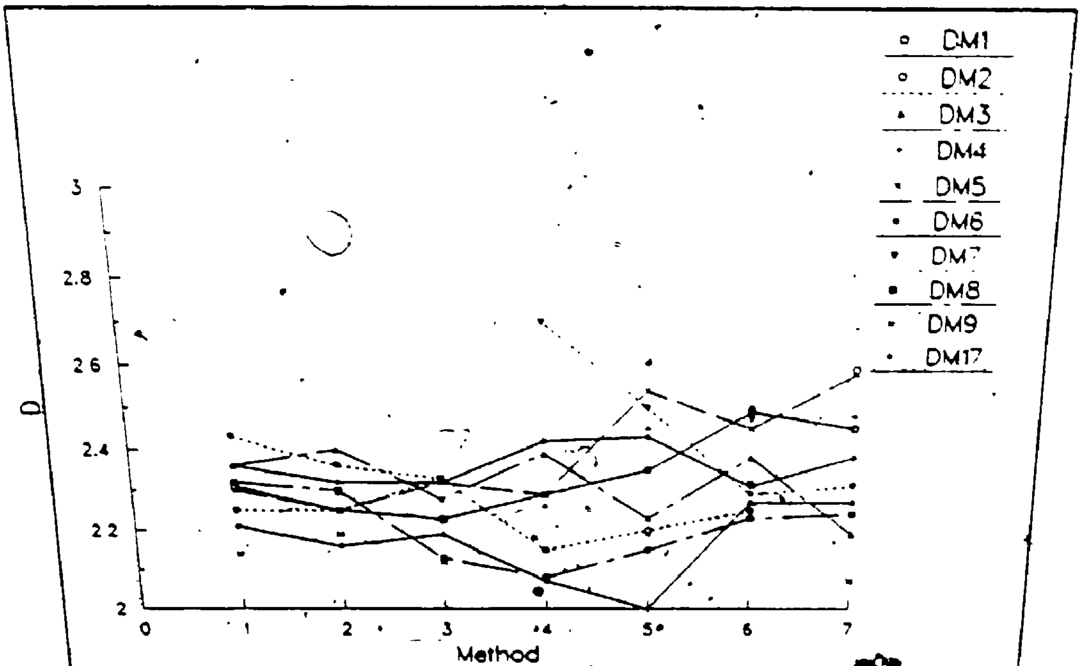

	ALL	ROW	COL	S1	S2	S3	S4
DM1	2.31	2.25	2.23	2.29	2.35	2.49	2.45
DM2	2.25	2.25	2.33	2.15	2.20	2.25	2.59
DM3	2.36	2.40	2.28	2.39	2.23	2.38	2.19
DM4	2.21	2.29	2.22	2.26	2.45	2.48	2.48
DM5	2.30	2.25	2.32	2.29	2.54	2.45	2.58
DM6	2.21	2.16	2.19	2.07	2.00	2.27	2.27
DM7	2.43	2.36	2.33	2.70	2.50	2.29	2.31
DM8	2.32	2.30	2.13	2.08	2.15	2.23	2.24
DM9	2.14	2.19	2.12	2.29	2.19	2.32	2.07
DM17	2.36	2.32	2.32	2.42	2.43	2.31	2.38

Figure 7.4.6.1 Basin and Range results

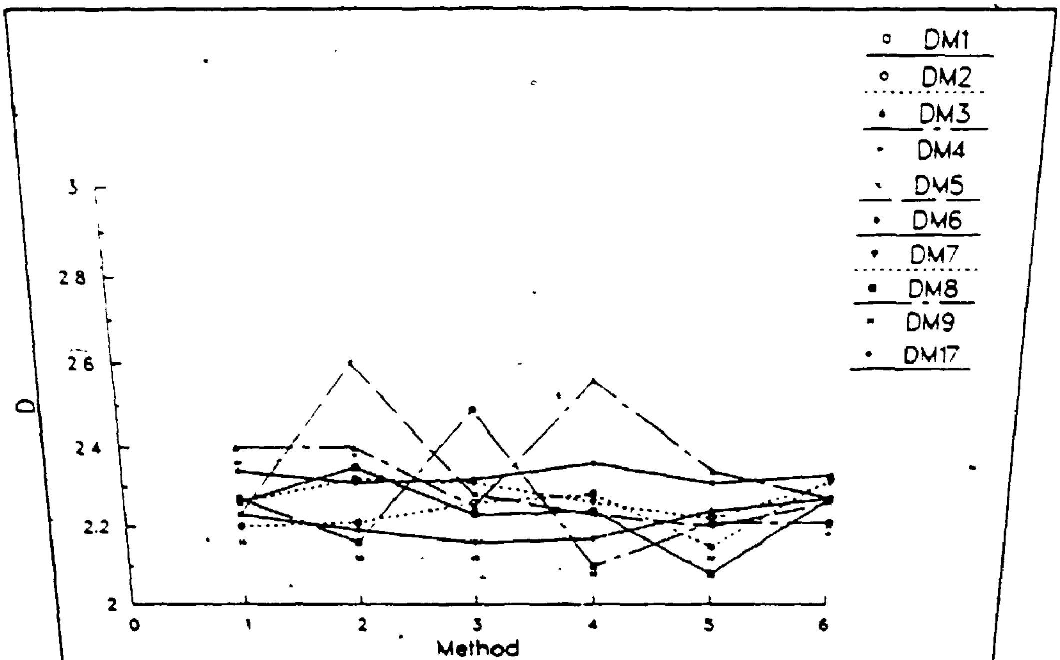

	A1	A2	A3	A4	A5	A6
DM1	2.26	2.35	2.23	2.24	2.08	2.27
DM2	2.20	2.21	2.28	2.28	2.15	2.32
DM3	2.40	2.40	2.25	2.56	2.34	2.27
DM4	2.36	2.38	2.16	2.29	2.23	2.18
DM5	2.23	2.60	2.28	2.23	2.20	2.26
DM6	2.23	2.19	2.16	2.17	2.24	2.27
DM7	2.26	2.32	2.31	2.26	2.22	2.31
DM8	2.27	2.16	2.49	2.10	2.21	2.21
DM9	2.16	2.12	2.12	2.08	2.12	2.20
DM17	2.34	2.31	2.32	2.36	2.31	2.33

Figure 7.4.6.2 Basin and Range results

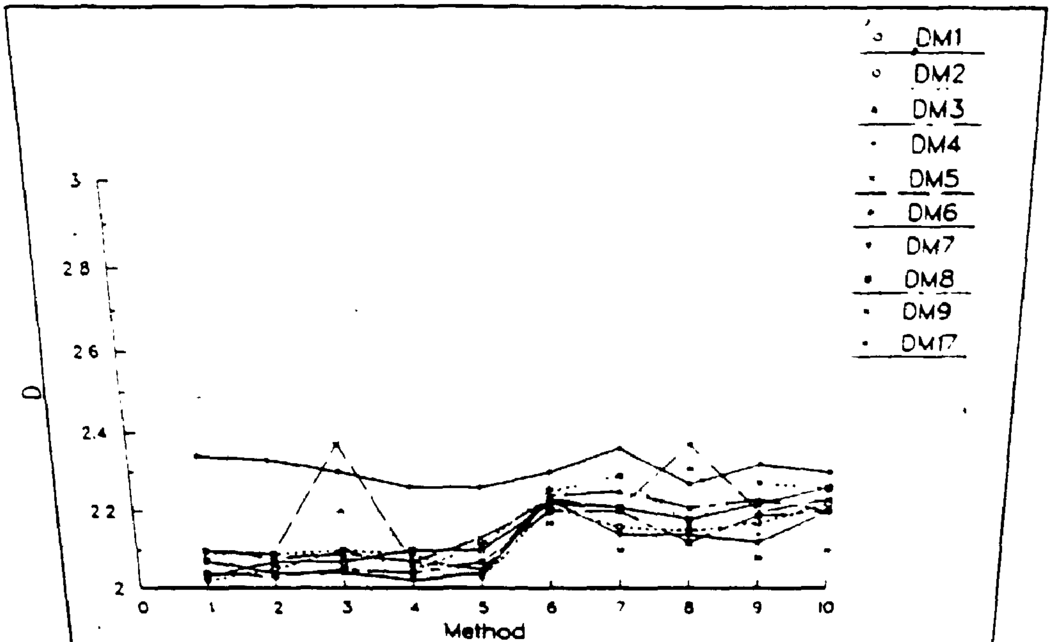

	CC1	CC2	CC3	CC4	CC5	DI1	DI2	DI3	DI4	DI5
DM1	2.03	2.07	2.07	2.10	2.10	2.22	2.21	2.18	2.22	2.26
DM2	2.02	2.05	2.10	2.09	2.03	2.21	2.16	2.15	2.17	2.22
DM3	2.10	2.08	2.09	2.07	2.05	2.24	2.25	2.21	2.23	2.20
DM4	2.08	2.08	2.20	2.06	2.03	2.26	2.15	2.31	2.14	2.25
DM5	2.10	2.09	2.37	2.07	2.13	2.23	2.21	2.37	2.20	2.23
DM6	2.07	2.04	2.04	2.02	2.04	2.23	2.14	2.14	2.12	2.20
DM7	2.09	2.09	2.10	2.05	2.11	2.25	2.29	2.17	2.27	2.26
DM8	2.04	2.03	2.05	2.04	2.07	2.20	2.20	2.12	2.19	2.20
DM9	2.07	2.06	2.04	2.03	2.04	2.17	2.10	2.16	2.08	2.10
DM17	2.34	2.33	2.30	2.26	2.26	2.30	2.36	2.27	2.32	2.30

Figure 7.4.6.3 Basin and Range results

meters, nor do their contour plots offer any evidence as to why their behaviour is so different at the middle elevations.

The dividers method's dimensions are much closer to those of the variogram methods than are the dimensions of the cell counting method, and the difference in the average dimensions between the two surficial contour methods is the largest observed (0.11). Like the cell counting results, however, these results also show little intra- and inter-dataset variation. DM17 does not stand out quite as mucn as it did in the previous results, but it still has the highest overall dimension (2.31, similar to its cell counting dimension). An anomolously high dimension is associated with the middle elevation of DM4; this deviation is not present in the results of DM5.

7.4.9.1 Summary

The datasets from the Basin and Range province provide some of the best and worst fits to the fractal model. No dominant trends or patterns appear in any of the results. The change in the intra-dataset variation, from above average in the variogram methods to much below average in the surficial contour methods, is notable, however. The extent of, and relative placement of, the transition from a basin to a range can have considerable effect on the fractal dimension when the surface is considered as a 'whole', as happens with the variogram methods. However, the transition zone between a basin and a range appears similar from dataset to dataset, and as the contours are concentrated within that transition zone, the fractal dimensions of the contours will appear relatively stable.

7.5 A comparison with previous studies

Mark and Aronson (1984) looked at a number of the datasets which were analysed in this study, but only used an entire-surface variogram to analyse them. A comparison of the results obtained in that study with those obtained in this study is presented below (table 7.10). Some results, such as those of DM20 and DM14, are close. About half of the results agree reasonable well, with differences in their dimensions generally less than 0.10. The results of DM7 are included in this group, for example. Some of the other results, however, are substantially different. In particular, those of DM2 differ by 0.36 in their fractal dimension.

The methodology used by Mark and Aronson (1984) in their study might explain some of the differences in the results. They determined the breaks in the slopes by visual inspection, the 'best fitting' lines were hand drawn, and the slopes determined by careful measurement. In this study, the breaks in the slopes were determined visually, but least squares regression was used to determine the slopes of the lines. Therefore, it is not surprising that there are some differences in the values of the slopes, and

Physiographic Region Dataset	Shorter scale D	Break km	Middle scale D	Break km	Longer scale D
Appal. Plt.					
DM10	2.45	0.74	2.75	4.8	
	2.22	0.46	2.84	6.7	—
DM16	-	0.60	2.73	5.2	
	2.24	0.63	2.85	9.8	
DM15	2.14	0.58	2.75	3.3	2.65
	2.24	0.93	2.53	5.5	
Ridge & Valley					
DM13	2.24	1.00	2.74	6.4	
	2.14	0.40	2.61	9.8	
DM12	2.48	1.80	2.83	7.8	
	2.39	4.50			
DM14	(2)	0.60	2.72	-	
	2.36	0.90	2.73	8.1	
DM11	2.04	0.80	-		
	2.12	1.70	-		
Basin & Range					
DM9	2.03	0.65	2.4	4.6	2.79
	2.14	1.70	2.72	9.8	
DM1	-	0.35	2.39	7.5	
			2.31	9.8	
DM2	(2)	1.30	2.61	7.2	
			2.25	9.8	
DM6	-	1.00	2.40	-	
		0.30	2.21	9.8	
DM7	(2)	0.90	2.53	8.8	
	(2)	0.30	2.43	9.8	
DM5	2.20	1.50	2.65	3.8	2.36
			2.30	9.8	
DM3	(2)	0.33	2.49	7.2	
			2.36	9.8	
DM8	(2)	0.40	2.46	8.3	
			2.32	9.8	
DM4	2.11	0.40	2.77	4.6	2.46
	2.21	0.76	2.79	6.7	
Rocky Mountains					
DM20	2.28				
	2.28	9.8			

Table 7.10 Comparison with the results of Mark and Aronson (1984)

DM•• Mark and Aronson's results
Thesis results

thus in the dimensions. Mark and Aronson used most of the DEM in their analyses, whereas a 256 by 256 cell sample is used in this analyses -- this might also account for some of the differences. That is, the smaller samples might be more homogeneous in their physiographic characteristics, and therefore fit the fractal model better.

Mark and Aronson used 100 equal distance classes in their plots. As a result, the density of the points increases with increasing distance (in log-log space), which might increase the perception of changes in slope at greater distances. In addition, small changes in log-log space in the locations of the breaks of the slopes will appear to be greater in anti-log space, which explains why most of the breaks are at different lengths.

Some of the conclusions that Mark and Aronson (1984) made can be tempered somewhat when considered in light of the results presented above (section 7.4). For example, Clarke (1987) cites Mark (personal comm.) as stating that the results associated with DM20 might be in error; however, the results obtained in this thesis agree well with Mark and Aronson's results. A large number of the datasets they investigated were found to have poor fits to the fractal model. When considered in light of the larger number of datasets analysed in this thesis, it can be seen that the fractal model does provide a reasonable fit to a large majority of the datasets. Thus, the conclusions reached by Mark and Aronson can be seen to represent the results of their limited sample. Furthermore, consideration of the physiographic nature of the province can provide a reasonable explanation for the lack of fit in those cases where the fractal model is found to be deficient.

Roy et al. (1987) analysed one DEM in the White Mountains of New Hampshire. Using the variogram method they obtained an overall surface dimension of 2.15, a dimension which applied to a distance lag of 2.0 km. At greater distances the dimension was much higher, D = 2.82. The average dimensions of the derived contours, obtained using an unknown form of the dividers technique, was found to be 1.09, although ~~the~~ range was high, from 1.01 to 1.28. The results presented in this thesis follow their results.

In their study they also found that D generally decreased with height. They reasoned that "the crenulations associated with fluvial erosion" decrease with increasing elevation (Roy et al., 1987, 75). In order to test if similar trends were present in the elevationally-dependent dimensions derived in this study, the slopes of the dimensions from the cell counting, surficial dividers, traditional dividers and equipaced polygon methods were regressed against elevation order. The range in the slope values is low (0.12), but the mean slopes for all four methods are negative. A negative slope indicates that as the elevation increases the dimension decreases. For the four methods approximately 58% of all slopes were negative, and only 28% of the slopes were positive. Thus although the fractal dimension generally declines with elevation, it does not necessarily do so. Goodchild (1982) also found that D increased with elevation on Random Island, Nfld.

Only ten datasets have (D against elevation) slopes which are positive or equal to zero across all four methods: **DEM7**, DEM8, DEM11, **DEM12**, **DEM13**, **DEM14**, **DEM16**, DM1, DM8, **DM16**. (Those datasets which are **bolded** exhibit definite 'U' shaped trends in the dimensions produced by the surficial contour methods.) Five of these datasets are located adjacent to each other, but in different physiographic provinces (DEM11, **DEM12**, **DEM13** in the Appalachian Plateaus; **DEM7** and DEM8 in the Interior Low Plateaus), which indicates that there might be some physical reason for the relationship between the dimension and elevation. Two other datasets also are located in the Appalachian Plateaus province (DEM11 and DM16), although in separate areas.

One dataset (DM12) was analysed by Steyn and Ayotte (1985) using a standard two-dimensional discrete Fourier transform software package. Although not explicitly concerned with fractals, their results can be compared with those obtained in this analysis. In their study they were particularly concerned with the degree of directionality in the terrain. Figure 1b in Steyn and Ayotte's paper illustrates that the amplitude spectrum shows marked asymmetry in the northeast to southwest direction -- this finding corresponds to the direction of anisotropy identified in the angle variogram results in this study.

Direction	Angle variogram D_1	D_2	Fourier transform D
1	2.35	-	2.47
2	2.47	-	2.27
3	2.33	-	2.65
4	2.19	2.76	2.47
5	2.21	2.87	2.52
6	2.22	2.87	2.55
Average (Entire-surface)	2.39		2.45

Table 7.11

Comparison of DM12's angle variogram results with those of Steyn and Ayotte (1985)

Furthermore, it is possible to transform Steyn and Ayotte's (1985) results to a form directly compatible with those obtained in this thesis (table 7.11). Although the overall average dimensions agree fairly well, the individual directional dimensions do not. However, if the averages of those three angular swaths which are bi-dimensional are computed (2.47, 2.54, 2.54, respectively), then those three angle's Ds agree very closely. This agreement reinforces the correctness of the statement make by Steyn and Ayotte (1985, 2889) that "the variograms and associated fractal scales ... seem more capable of detecting the scale breaks in topographies...." Based on these limited results, it would appear that spectral analysis, even when considered on a directional basis, produces values which are spatial averages. (It should be noted that Steyn and Ayotte explicitly mention that only one of the 12 spectral plots they analysed appeared to have two spectral domains. Thus the absence of any scale dependency in the dimensions obtained from the spectral analysis is not from a lack of looking for any dependency.)

7.6 Morphometric parameters

Correlations between the morphometric parameters and the fractal parameters (the fractal dimensions, the break-points and the intercepts derived from all of the variogram analyses) indicates that the fractal dimensions and the breakpoints are not similar to any of the measured morphometric parameters (e.g., the correlations between the variogram dimension obtained from the entire surface variogram and the morphometric parameters are all less than ± 0.45). On the other hand, there are fairly high significant correlations (generally > 0.70) between the variogram intercepts and the standard deviations of the elevations. This indicates that the value of the intercept reflects the variability of the surfaces, and captures components of the DEMs not reflected by their fractal dimensions. This aspect of the intercept was noted in the previous sections which considered the results on a province by province basis, and these results confirm the impression noted in those sections -- that the intercepts reflect the magnitude of the roughness of the surface, while the fractal dimension reflects the form of that roughness.

None of the morphometric parameters derived in this study relate to slopes. However, O'Neill and Mark (1987) determined the slope frequency distributions for 18 of the DEMs analysed in this work (DM1 to DM18). Of the 19 variables they reported on in their study, five were selected for analysis in this study (table 7.12). The variables selected are:

1) mean slope,
2) standard deviation of the slopes,
3) the proportion of the slopes below 10°,
4) the proportion of the slopes below 5°,
5) the proportion of the slopes below 2°.

It is apparent that the distributions of the slope-related variables are bimodal. Thus, determining Pearson correlation coefficients between those variables, and the variables determined in this study, is not appropriate. However, Spearman's rho, a rank-order correlation coefficient, is an appropriate statistic, and it was determined for the selected group of variables (table 7.13).

The correlations between the fractal dimensions and the slope variables are all low, while the variogram intercepts have fairly high correlations with the slope variables. In addition, there is a high negative correlation between the mean slope and the breakpoints. These results indicate that the greater the mean slope, the shorter the first linear

Physio. region	Data-set	Mean slope	S.d. slope	Slope < 10	Slope < 5	Slope < 2
3	DM11	13.58	6.51	32.10	8.70	2.20
3	DM12	12.96	6.11	34.10	8.80	2.20
3	DM13	12.28	5.94	38.40	10.50	2.60
3	DM14	11.72	5.59	40.90	11.30	2.90
4	DM10	13.87	6.54	31.50	9.40	2.50
4	DM15	13.67	6.00	29.30	7.90	2.00
4	DM16	14.08	7.61	35.00	10.30	2.60
5	DM18	6.08	4.45	79.30	48.70	24.50
9	DM1	3.59	4.73	90.30	72.50	57.60
9	DM2	5.28	5.89	82.60	63.60	42.00
9	DM3	6.51	6.90	77.60	57.60	34.30
9	DM4	5.72	5.42	79.80	59.20	33.80
9	DM5	6.45	6.05	77.10	56.10	29.00
9	DM6	4.64	3.86	89.20	64.20	33.80
9	DM7	5.75	7.65	78.80	66.40	53.10
9	DM8	5.31	6.62	86.20	72.80	37.40
9	DM9	7.68	8.75	73.70	62.00	32.70
9	DM17	14.60	8.38	39.60	26.00	21.10

Table 7.12 Slope variables from O'Neill and Mark (1987)

	Mean Slope	Sd of Slope	Slope < 10	Slope < 5	Slope < 2
D Entire-Surface	-.1139	.0725	.2123	.2020	.2728
Break dist. Entire-surf.	-.5732	-.0486	.6627*	.6384*	.6571*
Intercepts Entire-surf.	.7792*	.8039*	-.6801*	-.4675*	-.4568*
Mean elevation	-.6078*	-.0175	.6925*	.7358*	.6656*
S.d. of the elevations	.0506	.4923*	.0114	.1620	.0724
Skewness of the elevations	-.4448*	-.3457	.3478	.2962	.3659
Kurtosis of the elevations	-.4654*	-.2012	.4448*	.4572*	.4662*
Coefficient of Dissection	.3787	.2632	-.3209	-.2879	-.3773
S.d. of the Angle Ds	.0526	-.0196	-.1806	-.1785	-.1747
S.d. of the Sectional Ds	-.3189	-.0526	.1476	.2178	.2315
S.d. of the Cell count. Ds	.3922	-.2623	-.4804*	-.6740*	-.6065*
S.d. of the Dividers Ds	.3505	-.0343	-.4779*	-.5368*	-.6004*

Table 7.13 Spearman correlation coefficients of the slope variables

(* Significant at the 0.05 level, n = 18) segment in the variogram plot but the greater the value of the intercept. The relationship between the slopes and the intercepts is also reflected in the decreasing correlations between the intercepts and the percentages of slopes less than 10°, 5° and 2° respectively. It is difficult to explain why the intercepts and the standard deviations of the slopes have such a high correlation, although it could be related to the inter-relationships among the standard deviations of the slopes, the standard deviations of the elevations, and the intercepts.

The relationships between the standard deviations of the dimensions produced by the two surficial contours methods and the percentages of the slopes less than 10°, 5° and 2° are also of interest. These values indicate that the greater the percentage of slopes under 5°, the more similar are the dimensions produced by those two methods, but that this relationship decreases in strength as areas of greater slope are included.

7.7 Alternative strategies to grouping the datasets

The datasets used in this thesis were placed into groups on the basis of their geographic location (i.e., into physiographic provinces). The purpose of that grouping was to see if insight into the fractal dimensions, and the methods which produced those dimensions, could be obtained if the results were considered on a physiographic basis. However, there are a large number of *a posteriori* groups which also could be defined. The purpose of results-based classification schemes would be to lead to further research, research into why the groups differed. For example, in what way do the physical characteristics of the a posteriori groups differ, and in what way do they agree?

A large number of classification schemes could be developed, based on the large number of variables determined. However, the purpose of this section is not to examine all possible classifications, but rather to briefly review the possibilities. For example, one dichotomous classification scheme could be based on the relationship between the fractal dimension and the elevation: in some cases D decreases with elevation, in others it increases. Questions which relate to this breakdown are: what are the common elements (physiographic features) among each group, and what process(es) results in the opposite relationship between D and elevation? Another dichotomous grouping could be based on the relationship between the fractal dimensions and the intercepts produced by the angular variograms. Again, with some datasets a positive relationship exists -- as D increases, so does the intercept; in others a negative relationship exists -- as D increases, the intercept decreases. Again, what are the common elements (physiographic features) among each group, and what process(es) results in the opposite relationship between D and the intercepts?

Cluster analysis is the traditional method used in searching for group structure. The results of one such investigation will be presented, using the variability of the dimension in each dataset as the characteristic used to define the group structure. It is evident that some datasets have dimensions which are dependent on direction, and some (possibly the same) datasets have dimensions which are dependent upon location. Using the intra-dataset standard deviations of the angle variograms **D**s, and of the sectional variograms **D**s, a cluster analysis was performed (SPSS* cluster analysis routine with the following characteristics: squared euclidean distances as the similarity measure, and average linkage between groups as the clustering method).

Because the group structure present at four groups is easily interpretable, and each group has sufficient members to make the results of interest, the four group result will be considered in detail. The characteristics of the four groups (table 7.14) indicate that they roughly correspond to:

1) datasets with a low variance in **D** when considered either on a directional basis, or on a locational basis (the low-low group);
2) datasets with a high variance in **D** on a directional basis, but with above average variance in **D** on a locational basis;

3) datasets with a high directional variance in D and a low locational variance; and

4) datasets with both a high directional and locational variance in D (the high-high group).

Using the four group membership as the grouping variable, a discriminant analysis indicates that this four group structure is stable -- all 58 datasets are correctly assigned to their original four groups (using the two variables which were used in the classification analysis as the discriminant variables), and the group means are significantly different. The first discriminant function, which accounts for 65% of the overall variance, correlates most highly with the standard deviations of the sectional variograms Ds, while the second discriminant function, which accounts for the remaining 35% of the variances, correlates most highly with the standard deviations of the angle variograms Ds. Thus, the sectional variations of the datasets better discriminate among them than do their directional variations, when both aspects are considered jointly.

Membership in the four groups does not follow any geographic pattern. For example, all four groups have members from the nine datasets which occur in the Basin and Range province. The three Coastal Plains datasets belong to two different groups; only the Colorado Plateaus four datasets remain as a cohesive group.

Group (n)	S.d. of the Angle Ds (mean/s.d.)	S.d. of the Sectional Ds (mean/s.d.)
1 (27)	0.05/0.015	0.09/0.025
2 (14)	0.07/0.022	0.19/0.028
3 (9)	0.11/0.021	0.06/0.016
4 (8)	0.12/0.020	0.12/0.029
mean	0.07/0.033	0.12/0.055

Table 7.14

Characteristics of the four groups identified by the cluster analysis

A second analysis of variance was conducted on a number of selected variables, using membership within the four group structure as the discriminating variable. Those results which have significant between groups differences in the means are presented in table 7.15. Variables analysed but not found to have significant between group differences are the entire-surface variogram break distances, the mean elevation, the skewness, the kurtosis, and the coefficient of dissection.

The low-low cluster group has a below average entire-surface dimension, and above average intercepts and standard deviations of the elevations. On the other hand, the high-high cluster group has above average entire-surface dimensions and below average intercepts and standard deviations of the elevations. Thus, the low-low group would appear to consist of those datasets which are relatively smooth, but with a large regional trend, whereas the high-high group consists of rougher surfaces with relatively smaller magnitudes to that roughness.

Group	Entire-surface D	Entire-surface Intercept	S.d. of the elevation
1	2.30	4.10	11.21
2	2.34	3.57	9.34
3	2.42	3.25	6.31
4	2.40	3.23	7.44
Mean	2.34	3.72	9.48

Table 7.15

Group means of variables with significant ANOVAs, using the four group structure

A less traditional method of grouping the datasets, but a method more in the spirit of 'fractals', is to visually group the datasets. Symbols are an efficient and effective means of portraying the relationships of many variables (Chambers et al,. 1983) and, for the angle variograms Ds, allow for the display of all 12 possible dimensions and their relationships on a single figure (figure 7.5).

It is apparent that several visually distinct groups exist:

1) those mono- or bi-dimensional datasets with small dimensions in all directions (small tight circles

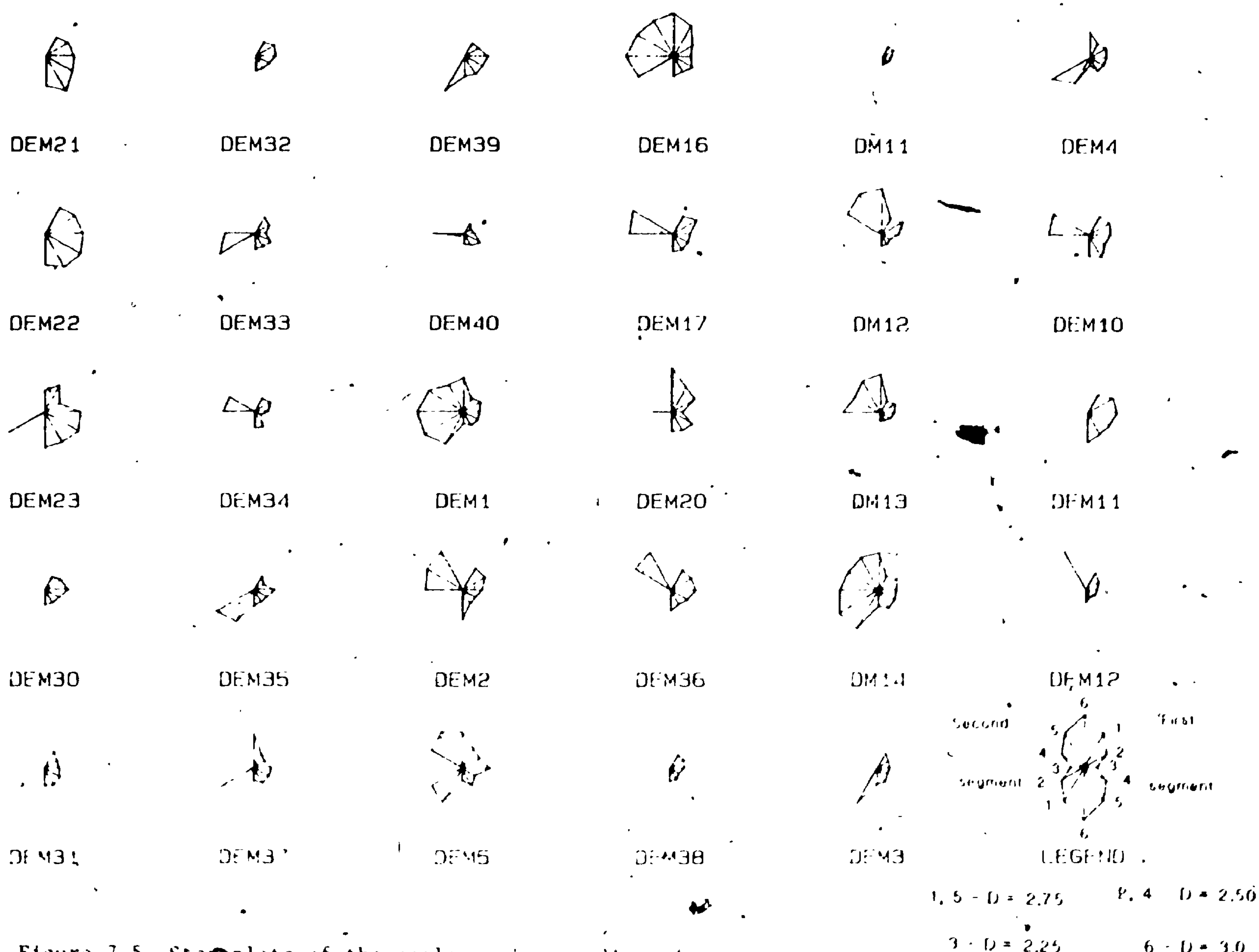

Figure 7.5 Star plots of the angle variogram dimensions

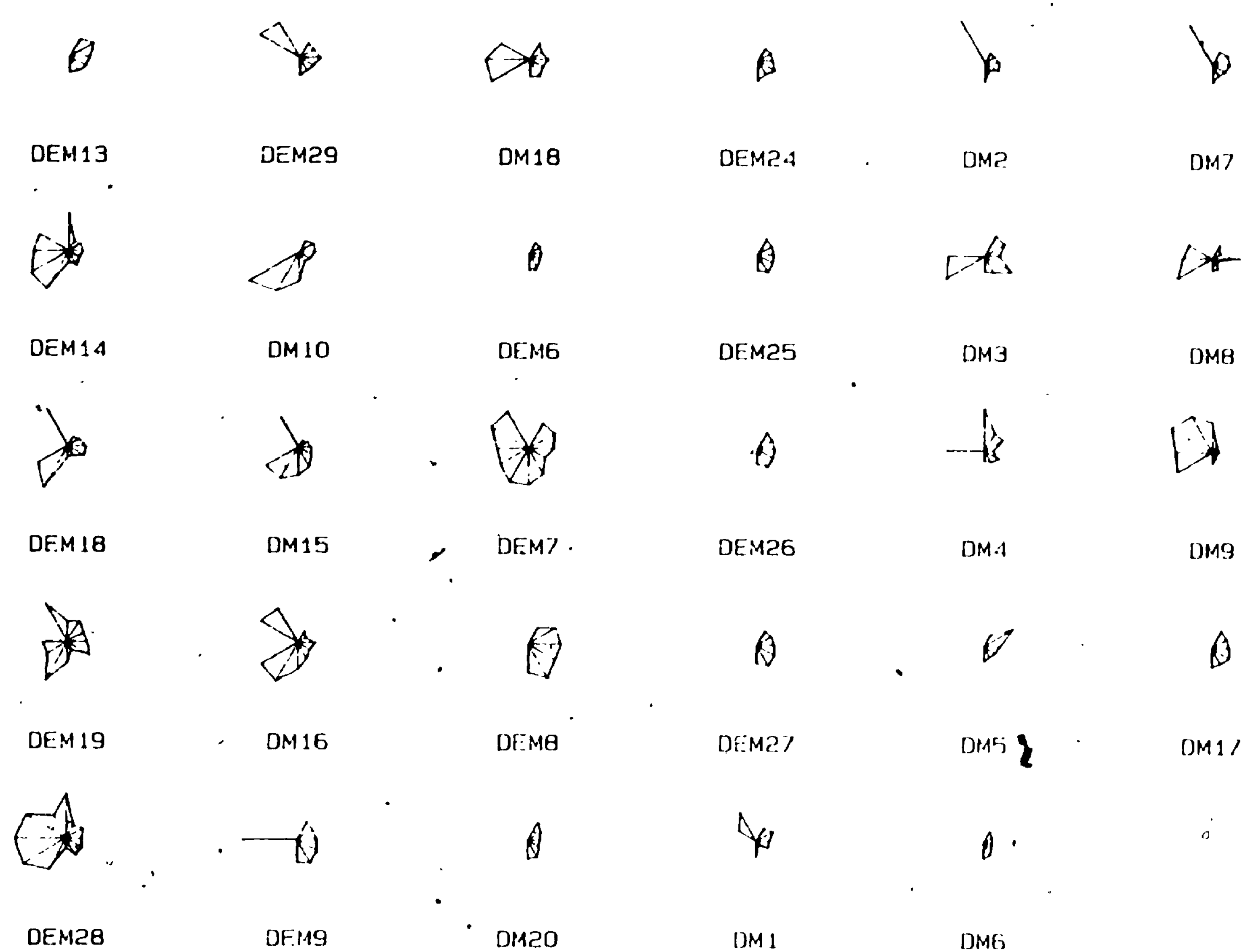

Figure 7.5 (continued) Star plots of the angle variogram dimensions

or semicircles): DEM6, DEM13, DEM24, DEM25, DEM26, DEM27, DEM30, DEM31, DEM32, DEM38, DM5, DM6, DM11, DM17 and DM20;

2) those mono-dimensional datasets with larger dimensions (large semicircles): DEM8, DEM11, DEM20, DEM21, DEM22, DEM23;

3) those bi-dimensional datasets with medium to large dimensions (approaching full circles): DEM1, DEM7, DEM16, DEM28, DM9, DM14;

4) those datasets with one large second dimension and small first dimensions (small semicircle with a single spike): DEM9, DEM12, DEM37, DEM40, DM2, DM7;

5) the remaining datasets which fit into none of the above groups.

Using the five groups visually identified, an analysis of variance was performed on a number of selected variables. The group means of those variables which have significant between group differences are presented in table 7.16. Those variables which did not have significant between groups differences are the skewness, the kurtosis and the coefficient of dissection.

Not surprisingly, given that the groups are identified partially on the basis of the magnitude of the angle dimensions, the analysis of variance (anova) found significant between groups differences with the entire-surface dimensions. The group which contains those datasets not explicitly placed into any of the other groups tends to have values close to the overall average for most of the variables analysed. The other groups appear to have some unique characteristics, however.

Group	Entire-surface D	Break (km)	Interc't	Mean elevation (m)	S.d. of the elevations
1	2.29	0.74	4.11	1560	12.25
2	2.50	0.37	2.45	256	4.30
3	2.36	0.22	3.41	575	7.10
4	2.29	0.62	3.73	1070	11.07
5	2.34	0.48	3.85	770	9.25
Mean	2.34	0.52	3.72	930	9.48

Table 7.16

Group means of variables with significant ANOVAs, using the five group structure

For example, those mono- or bi-dimensional datasets with small dimensions have a low entire-surface D, as expected, but they also have large intercepts, high standard deviations in their elevations, and the highest average break distances. If fit to the fractal model is judged on the linearity of the variogram plot, then this group should be considered as having the best fit to the fractal model among these five groups. Conversely, those mono-dimensional datasets with larger dimensions have an above average entire-surface dimension, much smaller average break distances, and below average intercepts. This group should be considered as having the poorest fit to the fractal model because these datasets only have a short linear portion in their variogram plots.

The five visual groups do not follow the physiographic breakdown any more closely than does the four group cluster analysis structure. Group 1 contains datasets from seven physiographic provinces, but includes all of the Colorado Plateau's datasets; group 2 contains all of the Coastal Plains datasets plus single datasets from three other provinces. Groups 3 and 4 each contain a mixture of datasets from 4 different provinces, while group 5 contains datasets from 5 different physiographic regions, but does include the majority of the Appalachian Plateaus' datasets (10), and half of the Valley and Ridge province's datasets (6). Looking at the geographic distribution of the groups does not provide any further insight into the causes for the differences between the groups.

7.8 Summary of results

Applying the fractal model to a variety of landscape types produces a range of results -- from cases where the model fits the landscape well, to cases where the model fails to fit the landscape at all. The use of the fractal dimension as a morphometric parameter was found to provide some discriminating power. However, in conjunction with the intercept (in the case of the variogram methods), the two parameters would appear to provide a unique descriptor of the landscape.

The various techniques used to determine the fractal dimension of the landscape were also found to have a wide range of results. The variogram methods provide reasonably consistent results, and have the added benefit that the intercept itself is a meaningful statistic. The individual contours methods did not provide meaningful results, in that the dimensions determined by these methods did not vary even though a wide variety of landscape types were looked at. The surficial contours methods produced results which lie in between the individual contours results and the variogram results. That is, although the dimensions produced do vary when the techniques are applied to different landscape types, the results were not as interpretable as those obtained from the variogram methods.

In the following concluding chapter the results of all of the analyses will be summarized, and an outline of future research directions presented.

Chapter 8

Conclusions

As described in the first chapter, research on the fractal nature of natural phenomena can be classified into three main stages. Geographers, at present, are concerned with stage one, the study of the dimensions of natural phenomena. An integral part of that study is consideration of the goodness-of-fit of the fractal model to the form of a particular phenomenon. In order to adequately assess goodness-of-fit, researchers must work with robust measurement techniques that have well-known characteristics.

Determination of the fractal dimension of natural landscapes forms the core of this thesis. However, because at present there is a lack of standardized robust measurement techniques for determining the fractal dimensions of natural landscapes, this thesis compared the behaviour, over a variety of surfaces, of an assortment of measurement techniques which have been identified in the literature. In addition, the dimensions of a number of landscapes representative of a wide range of physiographic provinces were determined, and the goodness-of-fit of the fractal model to those surfaces was analysed.

In this concluding chapter the results of these two investigative themes are summarized. In addition, the appropriateness of the specific fractal model used in this thesis is assessed, and the possible development of a more appropriate model is discussed. Finally, the question of future research directions will be considered.

8.1 Overview of the measurement techniques

It is hard to judge the overall accuracy of the measurement techniques used in this thesis because there are two possible explanations for the difference between the dimensions produced by the techniques and the dimensions specified for the simulated surfaces. Either the method of simulating the fractal surfaces does not produce surfaces with the dimensions as specified, or the methods produce inaccurate values even although the surfaces may have been created with the proper dimension. The first explanation is the more likely.

Those methods which looked at individual contours produced results which were very unsatisfactory. Even those methods that looked at the entire surface on an elevational basis produced results which differed from those produced by the variogram methods. These differences can be interpreted in a number of ways. The simplest interpretation is that the contour or elevationally-dependent methods are not robust methods, and that the dimensions they produce are not representative of the dimensions of the surfaces. However, Mandelbrot (1984b) has recently discussed how isosets need not have dimensions equivalent to the dimensions of the surfaces (i.e., a dimension one less than that of the surface). This means that the dimensions produced by the contour methods may in fact be valid dimensions. However, further research into the relationship between the dimensions of isosets of natural surfaces and the dimensions of the surfaces themselves is required before this can be accepted as the reason for the differences in the dimension. At the very least, the representativeness of the results of investigations of individual contours should be questioned.

The results obtained from the angle variograms, on average, agree very well with the results obtained from the entire-surface variograms. Thus, future investigations need only perform angle variogram analyses, rather than both angle and entire-surface analyses. In addition, the results of the angle variograms can be used to resolve the isotropic nature of the landscape. Although it is possible to determine the effects of anisotropic variation in the landscape using 30° swaths, a more refined view could be obtained if the angle swaths were smaller, say 5°. Using the results of these finer angular classes, the development of techniques capable of automatically detecting the dominant (and subdominant) directions of the anisotropy present in the landscape could be considered (cf., Fox and Hayes, 1985).

Because of the differences observed between the results of Mark and Aronson (1984) and the results obtained in this thesis, smaller distance classes than those used in this thesis should be used in future research in order to capture more of the variation present in the landscape. This would also allow for more detailed analyses of the scaling nature of natural landscapes.

In the analyses of the datasets derived from the DEMs it was found that the sectional variograms produced dimensions significantly different from those obtained by the entire-surface variograms. This means that the natural surfaces could have fractal characteristics dependent upon distance. However, based on concerns raised with respect to Fourier transforms, another, possibly more appropriate reason, for the anomalous behaviour of the sectional variograms can be postulated.

Consider the relationship between the variance in elevation and the distance between the points. When a surface has a dimension of exactly 2.5, the relationship remains constant regardless of the scale. However, when a surface has a dimension other than 2.5 the relationship does not remain constant. On surfaces with dimensions below 2.5, the variance at longer distances increases <u>relative</u> to the variance at the shorter distances (the surfaces appear smoother, with a large regional trend present). On surfaces with dimensions above 2.5, the reverse occurs and the variance at the shorter distances increases <u>relative</u> to the variance at the longer distances (the surfaces appear rougher, with no regional trends apparent).

The sectional variograms are based upon a sample that is half the length of the entire-surface variograms. By working with this sample the data tend to exhibit a greater amount of shorter-distance variance than that which actually exists in the data (Bracewell, 1978; Fox and Hayes, 1985). Elevational differences between points located relatively far apart tend to be under-represented because (truncated) parts of the longer-term variance are included as part of the shorter-distance variance. Thus, it is not surprising that the sectional variograms produce higher dimensions for the surfaces than do the entire-surface variograms. That is, the variance at the shorter distances has increased relative to that at the longer distances, and the surfaces appear to be of higher dimension. This implies that all dimensions will be inflated by some amount. This may account for the consistently high second dimensions of most bi-dimensional results.

Fox and Hayes (1985, 18) also note that an overestimation of the amplitude tends to occur when analysing samples, as was found to occur here. The intercepts produced by the sectional variograms are significantly higher than those produced by either the entire-surface or the angle variogram analyses.

The simulated fractal surfaces are free of distance-dependent variance, and therefore the variogram methods do not produce consistently different dimensions when analysing those surfaces.

8.2 Overview of the dimensional analyses

The results of the analyses of the dimensional characteristics of the physiographic provinces ranged from very satisfactory to very unsatisfactory. The fractal model generally fits those datasets from the Coastal Plain, the Great Plains, the Rocky Mountains, and the Colorado Plateau physiographic provinces well. The fractal model generally does not fit those datasets from the Valley and Ridge, and the Interior Low Plateaus physiographic provinces. And then there are some provinces, such as the Appalachian Plateaus and the Basin and Range, which have mixed results. Thus, it is not possible to provide blanket statements about the overall fit of the fractal model. Based on overall impressions of the physiographic provinces obtained from the variogram analyses, the apparent dependence of the fractal dimension on direction, distance and location is summarized in table 8.1.

The fractal model fits the three datasets from the Coastal Plain very well, particularly since all surficial methods returned very similar values. These datasets also provided the most surprising results because the fractal dimension was found to be extremely high. Conceptually, one would expect 'plains' to have a much lower dimension, and mountainous areas, such as the Rockies or even the

Physiographic Province	Dependence of D
Coastal Plain	D α f(**direction***)
Blue Ridge	D α f(distance)
Valley and Ridge	D α f(**distance, direction**, location)
Appalachian Plateaus	D α f(**distance**, direction)
Great Plains	D α f(direction,location)
Interior Low Plateaus	D α f(**distance**, direction, location)
Rocky Mountains	D α f(**location**, direction)
Colorado Plateau	D α f(**location**, direction)
Basin and Range	D α f(**location**, direction)

Table 8.1

Fractal characteristics of the physiographic provinces

***Bolded** names indicate that the relationship between D and the characteristic **bolded** is perceived as stronger than the relationship between D and the nonbolded characteristics.

Appalachian provinces, to have the higher dimensions. By comparing the results of the Coastal Plain with those of the nine datasets from the Blue Ridge, the importance of considering both the dimension and the intercept is highlighted. The highest fractal dimensions are associated with the Coastal Plain datasets, but the highest-valued intercepts are associated with the Blue Ridge datasets. Very low-valued intercepts are associated with the Coastal Plain. Thus, although the Coastal Plain datasets have the rougher 'form', the magnitude of that form is much smaller than that associated with the Blue Ridge. Without considering the intercept, these results would have been much harder to interpret.

The variance of D increases with increased elevation in the Blue Ridge datasets, which suggests that the lower areas are more similar to each other than are the higher areas. A similar relationship also occurs in the fourteen Appalachian Plateaus datasets. However, the variance of D decreases with elevation in the twelve datasets from the Valley and Ridge province, a relationship opposite to that observed in the other two Appalachian provinces. This illustrates one of the ways that areas from adjacent physiographic regions can be differentiated.

The fractal model fits the datasets from the Valley and Ridge province the least well of the three groups of datasets from the Appalachian provinces, and these datasets exhibit large inter-dataset variation. However, the datasets in the Valley and Ridge province can be subdivided into two groups according to the sign of the correlations between D and the angle variogram intercepts. The two groups correspond to the geographic location of the datasets -- those in the northern portion exhibiting negative correlations, while those in the southern portion exhibit positive correlations. This illustrates that regional differences, even within a province, can be distinguished (although, as of yet, the reasons behind those differences remain unknown). When considering only the fractal dimensions, the two groups of datasets do not appear to be all that different.

A similar regional differentiation is observed in the ten datasets from the Basin and Range physiographic province. Although nine of the datasets are located immediately adjacent to each other, and the remaining dataset occurs in a distant and distinct region of the province, the results of the variogram methods do not provide a ready means of separating the two groups. However, the results of the surficial contour methods do provide a means of distinguishing between the two groups, as the results clearly indicate that there are diffefences in the fractal characteristics of the two groups.

The two Great Plains datasets are the only ones in which the surficial contours methods produce values of D which are greater than the dimensions produced by the entire-surface and angle variogram methods. Why this should occur only with the datasets from this province is unknown and requires further investigation. The average dimension of the two datasets from this province is similar to that of the datasets from the Blue Ridge, but the intercept is approximately half -- further reinforcing the notion that both parameters must be considered if a complete description of a physiographic province is to be obtained.

8.3 The fractal model

A model can be judged on the basis of completeness, uniqueness, and simplicity (Frederiksen et al., 1985). The fractal model was found to provide a very good fit for some landscapes, but an imperfect fit for some others. Thus, it cannot be considered a universal model although it does provide a fairly complete description of some landscapes. It would appear to be a unique model and, given that only two parameters are needed to fully describe it (the fractal dimension and some measure of the relative magnitude such as the intercept), it also appears to be a relatively simple one.

Hobson (1972) notes that a morphometric parameter should be conceptually descriptive, easily measurable and suitable at a variety of scales. The fractal model satisfies all three of Hobson's concerns. For example, Pentland's (1984) work has shown how well the fractal dimension coincides with our perception of roughness. Most of the measurement techniques can be implemented with very little operator intervention, and the fractal model is, by definition, applicable to all scales of investigation.

Evans (1986, 105), in discussing the morphometry of specific landforms, notes that measures are required for (1) position, (2) direction, (3) size, (4) gradient, (5) shape, and (6) context (density, spacing and pattern). Fractal-based measures can be used to meet several of his requirements. For example, from the results of investigations based on angle variograms, measures related to direction (the variation of D and the intercept by direction), size, gradient (the value of the intercept, relative to the value of D, provides an indication of the size or gradient of the feature), and shape (D itself) can be derived. With further investigation, fractal-based measurements could meet more of his requirements.

Various authors have attempted to relate differences observed in the fractal dimension of various surfaces, and within various surfaces, to a number of geomorphic factors. Culling (1986), Culling and Datko (1987), and Ahnert (1984) feel that a general diffusion-degradation regime will tend to smooth the landscape and thereby decrease D. On the other hand, they consider that drainage systems will tend to add irregularity to the landscape through incision and rejuvenation, phenomena that will generally increase the value of D. Fox and Hayes (1985) considered two landform types -- tectonic and sedimentary -- and noted that each would exhibit contrasting behaviour. With tectonic features, the entire rough surface is formed (with a high D) and then erosional and sedimentary processes begin smoothing the surface -- the small features first, progressing to the larger features through time. On the other hand, sedimentary landforms, being relatively smooth at first, would have their roughness increased by erosional processes at the shortest distances first (the higher spatial frequencies), progressing to the longer distances (lower frequencies) through time.

It can be seen that erosional processes act on the fractal dimension of landscape in two conflicting ways depending on the particular landscape. On landscapes with high fractal dimensions (e.g., those created by tectonic forces), erosion will tend to decrease the dimension. Conversely, landscapes with an initially low fractal dimension (e.g., those created as a result of sedimentary processes), will have their fractal dimension increased as a result of erosional processes. Thus, a landscape may be the result of a number of opposing processes, with eaoh process resulting in a specific fractal domain.

8.4 Future research directions

There are two independent streams of research which flow naturally from this thesis. One of these involves further investigation into the specific results reported on in section 7.4; the other involves development of more appropriate measurement techniques and the development of a better fractal model.

Based on the type of analyses discussed in section 7.7 (the classification experiments), more detailed morphometric analyses should be carried out in order to determine the geomorphic similarity among those groups identified on the basis of differences in their fractal characteristics. Numerical classification of terrain has attracted some attention (Hettner, 1972; Scott and Austin, 1971; Zevenbergen and Thorne, 1987); in particular Pike (1986; 1987a, b, c) has written extensively on the subject of geometric signatures for landscapes.

The areas used for the analyses in this thesis were arbitrarily selected from a number of DEMs and, therefore, likely contain a variety of physiographic features. Thus, the approach taken in this thesis has been one of general geomorphometry, rather than specific geomorphometry (Evans, 1986; Mark, 1975a). In particular, each area probably contains components of a number of drainage basins. However, drainage basins have been identified as a fundamental areal unit in geomorphology (Chorley, 1969). Taking that into consideration, the following research strategy, based on specific geomorphometric principles, is suggested.

A study area, such as a DEM, first should be analysed by a subroutine which identifies and numbers individual drainage basins (following Douglas 1986, or Band 1986, for example). Then, using the drainage basin numbers as indices, variograms should be prepared for each individual basin, as well as for the entire surface (incorporating those distance pairs which fall into two drainage basins). In addition, the fractal dimensions of the drainage networks and of the drainage divides should be determined using, for example, routines outlined in O'Callaghan and Mark (1984) for identifying the drainage networks. Finally, within each drainage basin elevationally-dependent methods should be used to determine the elevational dependency of **D**.

This research strategy could be implemented in such a way that very little operator intervention would be necessary. The results of such structured investigations should much more clearly indicate the appropriateness of the fractal model, and the results would more directly address the question of the elevational dependency of **D**. By restricting the elevationally-dependent methods to single drainage basins, the analysis would not incorporate elevations from several drainage basins -- elevations that in one drainage basin could be near the base of the basin, whereas in another basin the same elevation could be near the divide. If **D** should decrease with elevation -- because the crenulations associated with the drainage system decrease in magnitude as one increases in elevation (as hypothesized by Roy et al., 1987) -- then results which corroborate this statement can only be obtained if the analyses are restricted to single drainage basins.

Mandelbrot (1978) hypothesized that a drainage network should possess a fractal dimension which is greater than the dimension of the divide in which the network is embedded. This statement, yet to be tested, does have intuitive appeal. It could be tested easily using the research strategy outlined above. It may be found, for example, that within physiographic regions definite relationships exist between the fractal dimension of the drainage divide and that of the drainage network. Areas of similar lithology would be expected to have similar relationships (c.f. Hobson, 1972). And, since D is a true mathematical measure, geometric theories on the relationships between sets become potential avenues of further investigation (Miyazima and Stanley, 1987). Note that although Culling and Datko (1987) state that they determined the fractal dimension of the drainage networks in their study areas, they do not mention how they obtained those dimensions. Given that Culling and Datko used only a single traverse across each map sheet that they analysed, and that they explicitly mention that they adjusted their traverses to avoid major valleys and a floodplain, how they determined the dimensions of the drainage networks is unknown. Nonetheless, they do report that the drainage network does have a higher dimension than the landscape in which it is embedded.

Given that a suitable fractal model for terrain exists, and that appropriate, robust measurement techniques are available, the following research strategy, based on general geomorphometric principles, could be implemented. First, determine the directional and the scaling fractal characteristics of a representative area from a specific physiographic region. In addition, determine selected morphometric parameters for that same area -- the target area. Then,

1) generate forms with similar fractal dimensions;
2) condition the simulation such that it best represents the other morphometric characteristics of the target area,
3) use the conditioned values as the basis upon which numerical simulations of topographically-dependent processes can be run;
4) cycle through steps 1) through 3) enough times such that the statistics of the models can be determined (c.f., Diaconis, 1983).

The techniques which are possible candidates for a research strategy such as this include mesoscale climatic modelling (Skoda, 1987; Young and Pielke, 1983) drainage simulation (Goodchild et al., 1985), comparisons of interpolation techniques, building models for the detection of blunders in measurements (Frederiksen et al., 1985), and investigating the radiometric characteristics of landscape types (Hobson, 1972; Fox and Hayes, 1985).

8.5 Landscape models

The method used to generate the simulated fractal surfaces analysed in this thesis produces reasonable approximations of natural landscapes. However, in certain ways the method fails to simulate natural terrain. For example, natural landscapes contain scale-dependent features whereas the fractal simulations are completely scale free.

Given these concerns, the approach taken by Clarke (1987) would appear to be an appropriate one to take. A suitable model of the landscape should simulate both scale-dependent and scale-independent processes. Thus, Clarke suggested using spectral analysis to model the scale-dependent aspects of the landscape, and a fractal model to simulate the scale-independent aspects. Fox and Hayes (1985, 37) present a sophisticated spectral analysis-based model which allows for the simulation of anisotropic terrain. Using their method, the larger-scale deterministic features of the landscape could be modelled. Then, the scale-independent features of the landscape could be added using a fractal model such as the one used in this thesis.

The study of the fractal nature of landscapes is a growing field that crosses several disciplines. As new discoveries are made, and the methods are fine-tuned, fractal research will contribute significantly to many fields.

Appendix 1

Data derived from the DEMs

Physio-graphic Region	DEM Name	Min	Max	Mean	s d	Skewness	Kurtosis	r d
1	DEM21	8 00	98 00	47 69	4 408	425	- 991	441
	DEM22	-2 00	61 00	26 37	3 212	525	- 285	450
	DEM23	9 00	66 00	34 88	3 237	412	- 531	454
MEAN		5 0000	75 0000	36 3133	3 61924	45426	- 60251	44815
STDEV		6 0828	20 0749	10 7320	68316	06167	35849	00669
2	DEM30	569 00	1546 00	843 80	13 730	1 288	1 464	281
	DEM31	385 00	1124 00	744 60	12 958	323	610	487
	DEM32	527 00	1453 00	969 90	15 440	- 141	-1 138	478
	DEM33	725 00	1676 00	1182 00	14 146	014	- 777	481
	DEM34	749 00	1785 00	1298 00	14 321	- 353	- 419	530
	DEM35	703 00	1723 00	1057 00	14 384	1 002	331	347
	DEM37	317 00	1304 00	695 40	12 853	522	080	383
	DEM39	374 00	923 00	475 20	9 168	2 115	4 502	184
	DEM40	632 00	1834 00	1094 00	17 103	186	-1 062	384
MEAN		553 4444	1485 333	928 8778	13 78916	47871	26018	39509
STDEV		163 4137	313 9658	261 5381	2 16194	83873	1 78610	11223
3	DEM1	246 00	357 00	303 70	4 562	- 296	527	519
	DEM2	233 00	408 00	303 90	5 315	313	- 176	405
	DEM5	244 00	408 00	303 90	5 535	518	- 309	365
	DEM16	225 00	373 00	270 60	4 769	712	049	308
	DEM17	252 00	369 00	291 60	4 063	837	1 167	338
	DEM20	249 00	392 00	315 80	4 925	- 053	- 722	467
	DEM36	190 00	724 00	342 30	9 027	1 047	1 448	285
	DEM38	220 00	928 00	466 20	12 309	667	- 048	348
	DM11	171 00	612 00	346 50	10 203	669	- 627	398
	DM12	199 00	604 00	324 90	9 330	1 041	516	311
	DM13	199 00	612 00	310 80	9 091	1 040	783	271
	DM14	157 00	463 00	233 10	6 906	1 205	1 881	249
MEAN		215 4167	520 8333	317 7750	7 16952	64342	28637	35535
STDEV		31 9245	177 8037	55 7784	2 71103	45924	86423	08087
4	DEM3	399 00	1011 00	606 70	11 336	697	- 029	339
	DEM4	256 00	1084 00	440 50	13 450	-3 515	18 261	223
	DEM10	481 00	646 00	558 70	5 780	489	845	471
	DEM11	343 00	633 00	575 50	5 558	-2 034	8 015	802
	DEM12	255 00	777 00	461 20	12 570	038	-1 717	395
	DEM13	250 00	640 00	507 40	9 652	-1 458	947	660
	DEM14	282 00	697 00	453 30	10 159	069	-1 244	413
	DEM18	426 00	930 00	618 90	10 116	615	- 487	383
	DEM19	255 00	612 00	503 10	7 979	-1 732	3 013	695
	DEM28	284 00	712 00	437 90	8 325	140	083	360
	DEM29	298 00	761 00	471 30	9 631	378	- 557	374
	DM10	434 00	760 00	615 50	7 560	243	- 124	557
	DM15	427 00	771 00	631 50	8 549	- 371	- 648	594
	DM16	288 00	701 00	546 60	8 335	- 912	649	626
MEAN		334 1429	766 7857	530 5786	9 23105	56214	1 80833	43224
STDEV		81 9314	144 6019	71 4425	2 28122	1 22617	5 32433	16483

Physio-graphic Region	DEM Name	Min	Max	Mean	s d	skew-ness	kur-tosis	c d
5	DEM9	1266 00	1529 00	1374 00	6 602	027	- 354	409
	DM18	1200 00	1491 00	1304 00	7 271	142	553	357
MEAN		1233 000	1510 000	1339 000	6 93672	08454	- 45327	38301
STDEV		46 6690	26 8701	49 4975	47299	08111	14050	03656
6	DEM6	248 00	580 00	456 70	10 055	- 464	-1 202	629
	DEM7	427 00	587 00	545 80	4 094	-1 098	4 255	743
	DEM8	367 00	620 00	538 40	4 447	-1 934	10 899	677
MEAN		347 3333	595 6667	513 6333	6 19874	-1 16863	4 65087	68286
STDEV		91 1062	21 3620	49 4443	3 34417	73710	6 06000	05722
7	DM20	2460 00	3430 00	2736 00	14 446	1 118	375	285
MEAN		2460 000	3430 000	2736 000	14 44645	1 11840	37497	28468
STDEV								
8	DEM24	1984 00	3046 00	2589 00	15 238	- 396	- 515	570
	DEM25	2248 00	3169 00	2650 00	11 895	651	600	437
	DEM26	2523 00	3454 00	3134 00	11 756	-1 059	2 404	656
	DEM27	2446 00	3163 00	2889 00	12 202	- 766	- 128	617
MEAN		2300 250	3208 000	2815 500	12 77295	- 39257	59033	57022
STDEV		240 5582	173 4993	248 6879	1 65400	74661	1 29466	09554
9	DM1	1361 00	1691 00	1416 00	8 532	1 176	- 027	165
	DM2	1356 00	1756 00	1406 00	8 784	2 328	5 068	126
	DM3	1367 00	1618 00	1548 00	9 797	- 086	- 433	401
	DM4	1551 00	1939 00	1733 00	7 520	518	813	470
	DM5	1687 00	2295 00	1800 00	10 237	1 553	1 935	187
	DM6	1640 00	2167 00	1839 00	9 759	1 071	801	378
	DM7	1356 00	1743 00	1395 00	8 519	2 775	7 642	100
	DM8	1431 00	2086 00	1837 00	10 517	- 715	1 627	620
	DM9	1364 00	2051 00	1651 00	13 932	- 127	-1 258	418
	DM17	1069 00	2066 00	1407 00	13 849	582	- 163	339
MEAN		1418 200	1961 200	1603 200	10 14468	90743	1 60066	32032
STDEV		175 6757	203 3398	190 5978	2 17218	1 10386	2 74782	17002
TOTAL		717 4138	1228 603	930 3300	9 47841	18650	1 05304	42483
STDEV		682 3476	865 5302	762 7736	3 53682	1 07189	2 31283	15499

Physio-graphic Region	DEM Name	D All	Break point	Inter cept	D All	Break point	Inter cept
1	DEM21	2 56	6648	2 174			
	DEM22	2 69	3687	2 590			
	DEM23	2 69	9843	2 408			
MEAN		2 6467	6726	2 39067			
STDEV		0751	3079	20854			
2	DEM30	2 34	9843	4 783			
	DEM31	2 29	3030	4 506	2 71	9843	8 051
	DEM32	2 30	6648	4 919			
	DEM33	2 34	4488	5 257			
	DEM34	2 37	8088	5 375			
	DEM35	2 36	9843	5 058			
	DEM37	2 18	630	4 415	2 50	9843	6 015
	DEM39	2 42	9843	4 031			
	DEM40	2 28	5463	5 127			
MEAN		2 3200	6431	4 83011	2 6050	9843	7 03300
STDEV		0684	3310	43950	1485	00	1 43967
3	DEM1	2 35	348	2 135	2 79	3687	4 348
	DEM2	2 56	9843	3 237			
	DEM5	2 46	516	3 406	2 79	9843	5 522
	DEM16	2 49	426	3 618	2 80	9843	4 990
	DEM17	2 29	630	1 628	2 96	9843	5 805
	DEM20	2 41	765	3 136	2 76	5463	4 760
	DEM36	2 47	3687	4 770	2 11	9843	194
	DEM38	2 25	3687	4 150			
	DM11	2 12	1680	3 643			
	DM12	2 39	4488	4 363			
	DM13	2 14	426	3 175	2 61	9843	5 752
	DM14	2 36	930	3 714	2 73	8088	5 870
MEAN		2 3575	2285	3 41458	2 6933	8307	4 65512
STDEV		1367	2812	87680	2547	2428	1 88197
4	DEM3	2 26	2490	4 611			
	DEM4	2 37	9843	4 554			
	DEM10	2 46	6648	2 606			
	DEM11	2 34	630	2 287	2 42	9843	1 929
	DEM12	2 29	9843	3 936			
	DEM13	2 33	9843	3 230			
	DEM14	2 37	3687	4 715			
	DEM18	2 17	1134	3 582	2 75	9843	7 684
	DEM19	2 32	1134	3 766	2 18	9843	985
	DEM28	2 19	237	4 197	2 64	3000	5 940
	DEM29	2 33	1680	4 645			
	DM10	2 22	426	3 925	2 84	6648	7 187
	DM15	2 24	930	3 789	2 53	5463	4 795
	DM16	2 24	630	4 224	2 85	9843	7 751
MEAN		2 2950	3511	3 86193	2 6014	7788	5 18157
STDEV		0900	3816	71337	2442	2776	2 76988

Physio graphic Region	[illegible] Name	D All	Break point	Inter cept	D All	Break point	Inter cept
5	DEM9	2 29	1380	2 674	2 82	9843	6 562
	DM18	2 42	9843	3 006			
MEAN		2 3550	5611	2 84000	2 8200	9843	6 56200
STDEV		0919	5984	23476			
6	DEM6	2 24	2490	3 656			
	DEM7	2 64	9843	2 985			
	DEM8	2 34	630	2 091			
MEAN		2 4067	4321	2 91067			
STDEV		2082	4872	78514			
7	DM20	2 28	9843	4 304			
MEAN		2 2800	9843	4 30400			
STDEV							
8	DEM24	2 34	9843	5 087			
	DEM25	2 32	5463	4 266			
	DEM26	2 37	9843	4 550			
	DEM27	2 32	9843	4 197			
MEAN		2 3375	8748	4 52500			
STDEV		0236	2190	40461			
9	DM1	2 31	9843	2 579			
	DM2	2 25	9843	2 285			
	DM3	2 36	9843	3 721			
	DM4	2 21	765	2 885	2 79	6648	6 761
	DM5	2 30	9843	3 237			
	DM6	2 21	9843	2 038			
	DM7	2 43	9843	3 929			
	DM8	2 32	9843	3 443			
	DM9	2 14	1680	3 839	2 72	9843	8 587
	DM17	2 36	9843	5 137			
MEAN		2 2890	8119	3 30930	2 7550	8245	7 67400
STDEV		0867	3641	91751	0495	2259	1 29118
TOTAL		2 3395	5256	3 71714	2 6650	8349	5 47440
STDEV		1230	4022	96022	2199	2312	2 24898

Physiographic Region	DEM Name	D Row	Break point	Intercept	D Row	Break point	Intercept	D Column	Break point	Intercept	D Column	Break point	Intercept
1	DEM21	2 57	4488	2 418				2 48	4188	1 389			
	DEM22	2 77	5463	3 044				2 53	3687	1 527			
	DEM23	2 75	2490	2 650				2 36	630	792	2 55	5463	1 361
MEAN		2 6967	4147	2 70400				2 4567	2935	1 2[illegible]	2 5500	5463	1 36100
STDEV		1102	1916	31647				0871	2036	39066			
2	DEM30	2 34	3030	4 593				2 22	2016	4 167	2 76	5463	8 900
	DEM31	2 33	3687	4 729				2 28	4488	4 530			
	DEM32	2 29	5463	4 740				2 28	5463	4 979			
	DEM33	2 37	4488	5 323				2 32	4488	5 183			
	DEM34	2 58	5463	6 656				2 28	4488	5 065			
	DEM35	2 02	5463	4 771				2 34	5163	4 973			
	DEM37	2 35	5463	4 866				2 28	1380	4 776	2 88	5463	9 052
	DEM39	2 36	1680	3 748				2 31	930	3 967			
	DEM40	2 28	1134	5 019	2 49	5463	5 984	2 19	5463	4 797			
MEAN		2 3578	3986	4 93833	2 4900	5463	5 98400	2 2778	3801	4 74967	2 8200	5463	8 97600
STDEV		0886	1711	77115				0171	1833	31567	0849	00	10748
3	DEM1	2 39	426	2 396	2 64	5463	3 117	2 41	348	2 454	2 66	5463	3 471
	DEM2	2 26	132	2 346	2 68	5463	4 315	2 24	195	2 586	2 66	5463	4 288
	DEM5	2 53	3687	3 625				2 30	426	3 091	2 76	5463	5 278
	DEM16	2 33	237	3 418	2 83	2490	5 258	2 39	318	3 496	2 73	5463	4 606
	DEM17	2 38	1380	1 839				2 41	1380	2 268	2 93	5463	5 759
	DEM20	2 57	4488	2 418				2 48	4188	1 389			
	DEM36	2 41	1680	4 565				2 41	3030	4 584			
	DEM38	2 25	3687	4 383				2 29	5463	4 118			
	DM11	2 16	1680	3 994				2 18	2490	3 547			
	DM12	2 23	1380	3 817	2 82	5463	8 187	2 29	3030	3 836			
	DM13	2 24	1380	3 250				2 26	288	4 610	2 63	5463	6 099
	DM14	2 28	630	3 348	2 63	5463	5 015	2 28	630	3 550	2 66	5463	5 376
MEAN		2 3358	1732	3 28325	2 7200	4868	5 18440	2 3283	1843	3 21075	2 7186	5463	4 98243
STDEV		1245	1456	86775	0977	1330	1 87553	0891	1825	89207	1038	00	91291
4	DEM3	2 35	2490	4 798				2 35	3687	4 704			
	DEM4	2 30	5463	4 604				2 37	5463	4 658			
	DEM10	2 42	1134	2 546				2 41	4488	2 635			
	DEM11	2 33	630	2 363	2 26	5163	774	2 32	630	2 357	2 57	5463	2 645
	DEM12	2 22	5463	3 725				2 17	2046	3 221			
	DEM13	2 28	5463	3 130				2 29	5463	3 176			
	DEM14	2 02	3030	4 444				2 19	633	4 284	2 70	5463	7 190
	DEM18	2 35	5463	4 263				2 24	2046	3 946			
	DEM19	2 27	1380	3 528	2 31	5463	2 691	2 43	1380	4 059	2 60	5463	4 755
	DEM28	2 22	888	4 116	2 69	5463	6 227	2 48	288	4 103	2 71	5463	6 569
	DEM29	2 30	1134	4 565				2 30	1680	4 581			
	DM10	2 27	630	4 140	2 95	5463	8 025	2 20	426	3 742	2 78	5463	6 764
	DM15	2 28	1134	3 873				2 25	318	3 893	2 61	3687	5 781
	DM16	2 31	930	4 414	2 64	5463	6 113	2 30	930	4 351	2 81	5463	7 548
MEAN		2 2943	2174	3 8[illegible]	2 570[illegible]	5463	4 76[illegible]	2 [illegible]	2107	3 83711	2 [illegible]	5209	5 89314
STDEV		[illegible]24	2086	[illegible]5916	[illegible]	00	2 [illegible]	[illegible]	1649	[illegible]	1016	6[illegible]	1 [illegible]

Physiographic Region	DEM Name	D Row	Breakpoint	Intercept	D Row	Breakpoint	Intercept	D Col (mm)	Breakpoint	Intercept	D Col (mm)	Breakpoint	Intercept
5	DEM9	2 36	3030	2 804				2 35	2490	3 074			
	DM18	2 29	630	2 863	2 67	5163	4 860	2 31	5463	2 270			
MEAN		2 3250	1830	2 83950	2 6700	5463	4 86000	2 3300	3976	2 67200			
STDEV		0195	1697	04172				0283	2102	56851			
6	DEM6	2 21	2490	3 634				2 25	2046	3 719			
	DEM7	2 64	5463	2 823				2 60	5463	2 623			
	DEM8	2 25	426	2 036	2 75	4488	4 340	2 41	426	2 620			
MEAN		2 3667	2793	2.83100	2 7500	4488	4 34000	2 4200	2645	2 59733			
STDEV		2376	2532	79903				1752	2571	67[illegible]			
7	DM20	2 21	5463	4 128				2 27	1380	4 311			
MEAN		2 2100	5463	4 12800				2 2700	1380	4 31100			
STDEV													
8	DEM24	2 29	4488	4 908				2 26	3030	4 768			
	DEM25	2 39	3687	4 684				2 25	4488	3 904			
	DEM26	2 29	5463	4 036				2 24	1680	4 054	2 56	5463	6 292
	DEM27	2 29	4488	3 948				2 28	5463	4 166			
MEAN		2 3150	4571	4 39400				2 2575	3665	4 22300	2 5600	5463	6 29200
STDEV		0500	726 8	47447				0171	1069	37886			
9	DM1	2 25	3687	2 704				2 23	4488	1 666			
	DM2	2 25	5463	2 716				2 33	3687	1 466			
	DM3	2 40	5463	4 055				2 28	5463	3 174			
	DM4	2 29	1134	3 184				2 22	1380	2 869	2 67	4488	5 878
	DM5	2 25	5463	3 048				2 32	4488	3 315			
	DM6	2 16	5463	2 083				2 19	5463	1 572			
	DM7	2 36	5463	3 337				2 33	3687	2 419			
	DM8	2 30	5463	3 356				2 13	5463	2 000			
	DM9	2 19	3687	3 996				2 12	2046	3 755			
	DM17	2 32	3030	4 971				2 32	5463	4 988			
MEAN		2 2770	4432	3 34500				2 2470	4163	2 72210	2 6700	4488	5 87800
STDEV		0730	1503	82228				0814	1478	1 12584			
TOTAL		2 3353	3167	3 72033	2 6431	5159	4 99531	2 3034	2900	3 47305	2 6942	5318	5 66379
STDEV		1283	1958	98477	1953	846 1	2 05620	0911	1918	1 13251	1083	451 8	1 92959

Physiographic Region	DEM Name	D A1	Break point	Intercept	D A1	Break point	Intercept	D A1	Break point	Intercept
1	DEM21	2 40	6648	939						
	DEM22	2 56	3030	1 918						
	DEM23	2 58	6648	1 715						
MEAN		2 5193	5442	1 52400						
STDEV		0987	2089	51669						
2	DEM30	2 28	3030	4 593						
	DEM31	2 38	6648	4 718						
	DEM32	2 30	6648	4 966						
	DEM03	2 35	6648	5 335						
	DEM34	2 29	4488	5 051						
	DEM05	2 30	1134	4 744	2 70	6648	7 706			
	DEM37	2 30	930	4 836						
	DEM39	2 28	630	3 776	2 76	6648	6 557			
	DEM40	2 22	6648	4 901						
MEAN		2 3000	4089	4 76889	2 7300	6648	7 13150			
STDEV		0450	2696	43024	0424	00	81247			
3	DEM1	2 30	195	2 265	2 70	2490	3 738	2 17	9843	1 628
	DEM2	2 48	6648	2 797						
	DEM5	2 43	516	3 206	2 75	6648	5 015			
	DEM16	2 [illegible]	4488	4 182						
	DEM17	2 39	1680	1 854						
	DEM20	2 54	6648	3 067						
	DEM36	2 44	3030	4 626						
	DEM38	2 30	6648	3 949						
	DM11	2 22	3030	3 167						
	DM12	2 35	4488	3 660						
	DM13	2 26	2046	3 384						
	DM14	2 30	630	3 488	2 84	6648	6 583			
MEAN		2 3900	3337	3 30208	2 7633	5262	5 11200	2 1700	9843	1 62800
STDEV		1286	2436	77566	0709	2401	1 42498			
4	DEM3	2 32	3030	4 679	2 79	6648	8 316			
	DEM4	2 30	1134	4 265	2 57	6648	5 469			
	DEM10	2 41	6648	2 536						
	DEM11	2 40	1680	2 317						
	DEM12	2 38	6648	3 964						
	DEM13	2 36	6648	3 270						
	DEM14	2 20	516	4 274	2 76	6648	7 600			
	DEM18	2 18	1134	3 650	2 83	6648	8 153			
	DEM19	2 42	426	4 039	2 76	6648	6 900			
	DEM28	2 26	348	4 384	2 61	3030	5 838			
	DEM29	2 30	1680	4 432						
	DM10	2 22	516	3 [illegible]	2 78	[illegible]	6 855			
	DM15	2 14	237	3 618	2 6[illegible]	6648	5 818			
	DM16	2 [illegible]	426	4 [illegible]	[illegible] 76	4488	7 [illegible]			
MEAN		2 [illegible]	2219	3 82743	2 7[illegible]	[illegible]	6 [illegible]			
STDEV		[illegible]	25[illegible]	[illegible]	[illegible]	[illegible]	1 0[illegible]			

Physio-graphic Region	DEM Name	D A1	Break point	Inter cept	D A1	Break point	Inter cept	D A1	Break point	Inter cept
5	DEM5	2 34	2046	3 161						
	DM18	2 33	6648	2 414						
MEAN		2 3350	4347	2 78750						
STDEV		0071	3254	52821						
6	DEM6	2 22	1680	3 605						
	DEM7	2 50	765	2 240	2 66	6648	2 860			
	DEM8	2 33	426	2 262						
MEAN		2 3500	957 0	2 70233	2 6600	6648	2 86000			
STDEV		1411	648 7	78181						
7	DM20	2 36	6648	4 685						
MEAN		2 3600	6648	4 68500						
STDEV										
8	DEM24	2 25	6648	4 659						
	DEM25	2 31	5463	4 300						
	DEM26	2 34	6648	4 392						
	DEM27	2 28	6648	4 231						
MEAN		2 2950	6352	4 39550						
STDEV		0387	592 5	18764						
9	DM1	2 26	6648	2 050						
	DM2	2 20	6648	1 425						
	DM3	2 40	6648	4 088						
	DM4	2 36	6648	3 261						
	DM5	2 23	1134	3 086						
	DM6	2 23	6648	2 025						
	DM7	2 26	6648	2 432						
	DM8	2 27	6648	3 155						
	DM9	2 16	2046	3 819						
	DM17	2 34	6648	5 063						
MEAN		2 2710	5836	3 04040						
STDEV		0748	2143	1 09798						
TOTAL		2 3278	3866	3 56990	2 7260	5986	6 24093	2 1700	9843	-1 62800
STDEV		1056	2672	1 06879	0805	1426	1 54668			

Physiographic Region	DEM Name	D A2	Break point	Intercept*	D A2	Break point	Intercept	D A2	Break point	Intercept
1	DEM21	2 49	5463	1 924						
	DEM22	2 66	3687	2 631						
	DEM23	2 33	159	1 666	2 80	6648	3 100			
MEAN		2 4933	3103	2 07367	2 8000	6648	3 10000			
STDEV		1650	2700	49961						
2	DEM30	2 37	3687	4 586						
	DEM31	2 29	8088	4 565						
	DEM32	2 40	9843	5 181						
	DEM33	2 31	1380	5 120	2 80	9843	8 772			
	DEM34	2 35	4488	5 236						
	DEM35	2 21	426	4 568	2 84	6648	8 236			
	DEM37	2 25	630	4 462	2 74	9843	7 747			
	DEM39	2 30	930	3 469						
	DEM40	2 15	348	4 639	2 11	930	3 920	2 17	9843	3 722
MEAN		2 2922	3313	4 61733	2 6225	6816	7 16875	2 1700	9843	3 72200
STDEV		0792	3548	53554	3441	4203	2 20591			
3	DEM1	2 38	426	2 260	2 87	9843	4 664			
	DEM2	2 50	9843	2 679						
	DEM5	2 39	630	2 821	2 68	9843	4 151			
	DEM16	2 42	348	3 396	2 78	9843	4 737			
	DEM17	2 53	9843	1 800						
	DEM20	2 51	4488	2 810						
	DEM26	2 45	9843	4 473						
	DEM38	2 32	5463	3 858						
	DM11	2 26	3687	2 769						
	DM12	2 47	6648	3 542						
	DM13	2 34	9843	2 884						
	DM14	2 42	630	3 253	2 88	9843	6 401			
MEAN		2 4158	5141	3 04542	2 8025	9843	4 98825			
STDEV		0822	4037	71486	0932	00	97726			
4	DEM3	2 25	2490	4 591						
	DEM4	2 35	2490	4 299	2 84	9843	8 292			
	DEM10	2 45	5463	2 575						
	DEM11	2 56	9843	2 547						
	DEM12	2 30	9843	3 472						
	DEM13	2 49	6648	3 461						
	DEM14	2 24	516	4 113	2 76	9843	7 346			
	DEM18	2 24	1380	3 807	2 60	9843	6 044			
	DEM19	2 32	930	3 516	2 40	2046	3 652	2 30	9843	1 729
	DEM28	2 34	630	4 368	2 87	9843	7 733			
	DEM29	2 29	765	4 606						
	DM10	2 30	930	4 044	3 00	3030		2 21	9843	1 198
	DM15	2 19	288	3 689	2 65	1380	6 054	2 50	4488	4 491
	DM16	2 17	516	4 070	2 73	3030	6 987			
MEAN		2 3207	3952	3 79700	2 7312	6107	6 58686	2 3367	8758	2 44267
STDEV		1121	3453	64827	1843	4029	1 53566	1484	3992	1 80088

Physio-graphic Region	DEM Name	D A2	Break point	Inter cept	D A2	Break point	Inter cept	D A2	Break point	Inter cept
5	DEM9	2 32	1380	3 120						
	DM1[illegible]	2 25	765	2 516	2 76	9843	5 753			
MEAN		2 2850	1073	2 81800	2 7600	9813	5 75300			
STDEV		0495	434 9	42709						
6	DEM6	2 22	2490	3 644						
	DEM7	2 53	930	2 365	2 56	9843	1 968			
	DEM8	2 55	4488	2 930						
MEAN		2 4333	2636	2 87967	2 5600	9843	1 96800			
STDEV		1850	1783	64094						
7	DM20	2 27	9843	4 568						
MEAN		2 2700	9843	4 56800						
STDEV										
8	DEM24	2 27	9843	4 718						
	DEM28	2 29	4488	4 300						
	DEM26	2 31	9843	4 251						
	DEM27	2 30	9843	4 300						
MEAN		2 2925	8504	4 39225						
STDEV		0171	2677	21839						
9	DM1	2 35	3687	3 398						
	DM2	2 21	9843	2 245						
	DM3	2 40	1380	4 113	2 80	5463	7 366			
	DM4	2 38	6648	3 241						
	DM5	2 60	9843	5 392						
	DM6	2 19	9843	2 203						
	DM7	2 32	9843	3 246						
	DM8	2 16	930	3 079	2 70	4488	6 703	2 14	9843	1 407
	DM9	2 12	1680	3 425	2 70	9843	8 148			
	DM17	2 31	2046	4 985						
MEAN		2 3040	5574	3 53270	2 7333	6508	7 40567	2 1400	9843	1 40700
STDEV		1420	4005	1 03988	0577	2852	72332			
TOTAL		2 3438	4366	3 61705	2 7214	7346	6 08448	2 2640	8772	2 49140
STDEV		1199	3774	95243	1859	3351	1 93823	1450	2395	1 51524

Physiographic Region	DEM Name	D A3	Break point	Intercept	D A3	Break point	Intercept	D A3	Break point	Intercept
1	DEM21	2 54	6648	2 277						
	DEM22	2 73	6648	2 989						
	DEM23	2 69	1380	2 460						
MEAN		2 6533	4892	2 57533						
STDEV		1002	3041	36975						
2	DEM30	2 45	6648	5 097						
	DEM31	2 29	3687	4 562						
	DEM32	2 37	6648	4 998						
	DEM33	2 20	237	4 896	2 59	4488	6 829			
	DEM34	2 25	426	4 988	2 61	6648	6 882			
	DEM35	2 39	6648	5 079						
	DEM37	2 34	6648	4 695						
	DEM39	2 45	6648	4 001						
	DEM40	2 20	426	4 838	2 60	6648	6 763			
MEAN		2 3267	4224	4 79467	2 6000	5928	6 82467			
STDEV		0973	3050	34574	0100	1247	05962			
3	DEM1	2 31	348	2 112	2 90	2040	4 825	2 63	9843	2 778
	DEM2	2 37	426	2 404	2 73	6648	2 388			
	DEM5	2 55	3687	3 606						
	DEM16	2 33	195	3 313	2 93	6648	6 008			
	DEM17	2 33	1380	1 343	2 85	6648	4 909			
	DEM20	2 20	288	2 566	2 37	765	2 856	2 79	6648	5 309
	DEM36	2 48	6648	4 740						
	DEM38	2 27	5463	4 197						
	DM11	2 17	2046	3 710						
	DM12	2 33	3687	3 802						
	DM13	2 28	1680	3 045	2 72	6648	6 372			
	DM14	2 35	516	3 354	2 76	6648	5 696			
MEAN		2 3308	2197	3 18267	2 7514	5150	4 72200	2 7100	8245	4 04350
STDEV		1053	2193	94761	1874	2585	1 54381	1131	2259	1 78969
4	DEM3	2 25	2490	4 731						
	DEM4	2 31	6648	4 367						
	DEM10	2 41	348	2 430	2 78	6648	4 729			
	DEM11	2 57	6648	3 134						
	DEM12	2 22	6648	0 519						
	DEM13	2 35	6648	3 263						
	DEM14	2 24	630	4 295	2 62	6648	6 505			
	DEM18	2 32	6648	3 947						
	DEM19	2 35	930	3 926	2 43	2046	3 923	2 31	6648	2 350
	DEM28	2 26	516	4 203	2 90	6648	7 931			
	DEM29	2 37	1680	4 779						
	DM10	2 28	765	4 180						
	DM15	2 23	630	3 857						
	DM16	2 31	930	4 450						
MEAN		2 3193	3011	3 93436	2 6825	5497	5 77200	2 3100	6648	2 35000
STDEV		0919	2863	65614	2037	2301	1 79863			

Physio-graphic Region	DEM Name	D A3	Break point	Inter cept	D A3	Break point	Inter cept	D A3	Break point	Inter cept
5	DEM9	2 34	1680	3 028	2 95	6648	7 906			
	DM18	2 33	348	3 137	2 77	6648	5 632			
MEAN		2 3350	1014	3 08250	2 8600	6648	6 76900			
STDEV		0071	941 9	07707	1273	00	1 60796			
6	DEM6	2 21	2490	3 715						
	DEM7	2 44	765	2 172	2 55	6648	1 947			
	DEM8	2 57	6648	3 020						
MEAN		2 4067	3301	2 96900	2 5500	6648	1 94700			
STDEV		1823	3024	77276						
7	DM20	2 21	6648	4 248						
MEAN		2 2100	6648	4 24800						
STDEV										
8	DEM24	2 26	6648	4 745						
	DEM25	2 29	2490	4 314						
	DEM26	2 31	6648	4 200						
	DEM27	2 31	6648	4 173						
MEAN		2 2925	5608	4 35800						
STDEV		0236	2079	26514						
9	DM1	2 23	6648	2 409						
	DM2	2.26	6648	2.825						
	DM3	2 25	765	3.589	2.66	6648	5 973			
	DM4	2.16	426	2 650	2 68	6648	5 703			
	DM5	2 28	6648	3 240						
	DM6	2 16	6648	2 055						
	DM7	2 31	6648	3 119						
	DM8	2.49	159	3 660	2 52	6648	5 174			
	DM9	2.12	2046	3 634	2 64	6648	7 855			
	DM17	2.32	2046	4 980						
MEAN		2 2580	3868	3 21610	2 6250	6648	6 17625			
STDEV		1054	2991	82362	0719	00	1 16733			
TOTAL		2 3309	3464	3 67352	2 6933	5827	5 56219	2 5767	7713	3 47900
STDEV		1257	2781	93169	1600	1837	1 70405	2444	1845	1 59921

Physio-graphic Region	DEM Name	D A4	Break point	Inter cept	D A4	Break point	Inter cept	D A4	Break point	Inter cept
1	DEM21	2 58	6648	2 397						
	DEM22	2 76	6648	2 961						
	DEM23	2 74	6648	2 680						
MEAN		2 7000	6648	2 67933						
STDEV		1058	00	28200						
2	DEM30	2 31	6648	4 533						
	DEM31	2 35	3030	4 701						
	DEM32	2 28	6648	4 708						
	DEM33	2 34	4388	5 296						
	DEM34	2 14	288	4 776	2 56	3687	6 671			
	DEM35	2 28	6648	4 671						
	DEM37	2 33	6648	4 879						
	DEM39	2 38	6648	3 727						
	DEM40	2 36	6648	5 412						
MEAN		2 3078	5299	4 74478	2 5600	3687	6 67100			
STDEV		0716	2287	48185						
3	DEM1	2 31	348	2 128	2 78	1134	4 133	2 49	9843	2 069
	DEM2	2 27	348	2 543	2 80	3030	5 066			
	DEM5	2 28	426	3 018	2 69	2490	5 007			
	DEM16	2 42	348	3 598	2 81	6648	5 104			
	DEM17	2 33	1134	1 729	2 89	6648	5 418			
	DEM20	2 46	930	3 446						
	DEM36	2 36	630	4 557	2 80	6648	7 387			
	DEM38	2 19	2046	4 193						
	DM11	2 16	1380	4 214						
	DM12	2 19	930	3 886	2 76	6648	7 758			
	DM13	2 23	1680	3 546	2.58	6648	5 515			
	DM14	2 36	765	3 862	2 68	6648	5 638			
MEAN		2 2967	913 7	3 35333	2 7544	5171	5 66956	2 4900	9843	2 06900
STDEV		0944	558 9	87555	0911	2268	1 16638			
4	DEM3	2 23	1680	4 639						
	DEM4	2 29	6648	4 597						
	DEM10	2 35	426	2 328	2 79	6648	5 051			
	DEM11	2 48	6648	2 739						
	DEM12	2 21	6648	3 701						
	DEM13	2 31	6648	3 432						
	DEM14	2 21	516	4 224	2 59	3030	6 579			
	DEM18	2 32	6648	4 028						
	DEM19	2 45	6648	4 248						
	DEM28	2 31	630	4 348	2 82	6648	7 432			
	DEM29	2 27	930	4 537	2 81	6648	7 952			
	DM10	2 22	516	4 075						
	DM15	2 27	1134	3 906						
	ΓM16	2 24	348	4 184	2 74	6648	6 812			
MEAN		2 2971	3291	3 92757	2 7500	5924	6 76520			
STDEV		0836	3036	68271	0946	1618	1 09869			

Physio-graphic Region	DEM-Name	D A4	Break point	Inter cept	D A4	Break point	Inter cept	D A4	Break point	Inter cept
5	DEM9	2 40	6648	2 772						
	DM18	2 26	930	2 552	2 57	6648	4 058			
MEAN		2 3300	3789	2 66200	2 5700	6648	4 05800			
STDEV		0990	4043	15556						
6	DEM6	2 21	2490	3 448						
	DEM7	2 33	348	1 884	2 74	6648	3 6/3			
	DEM8	2 54	6648	2 714						
MEAN		2 3600	3162	2 68200	2 7400	6648	3 66900			
STDEV		1670	3203	78249						
7	DM20	2 23	6648	4 075						
MEAN		2 2300	6648	4 07500						
STDEV										
8	DEM24	2 35	6648	5 102						
	DEM25	2 30	2490	4 137						
	DEM26	2 31	3687	4 261						
	DEM27	2 35	6648	4 060						
MEAN		2 3275	4868	4 39000						
STDEV		0263	2112	48183						
9	DM1	2 24	288	2 474	2 36	6648	3 137			
	DM2	2.28	6648	2 734						
	DM3	2 56	6648	5 242						
	DM4	2 29	1680	3 215						
	DM5	2 23	6648	3 074						
	DM6	2.17	6648	1 944						
	DM7	2 26	4488	2 667						
	DM8	2 10	630	2 611	2 47	2046	4 535	2 35	6648	3 652
	DM9	2 08	1680	3 703	2 82	6648	9 556			
	DM17	2 36	6648	5 150						
MEAN		2 2570	4201	3 28140	2 5500	5114	5 74267	2 3500	6648	3 65200
STDEV		1369	2805	1.11195	2402	2657	3 37561			
TOTAL		2 3179	3618	3 69424	2 7030	5424	5 82390	2 4200	8245	2 86050
STDEV		1318	2803	96830	1381	1972	1 64869	. 0990	2259	1 11935

Physiographic Region	DEM Name	D A5	Break point	Intercept	D A5	Break point	Intercept
1	DEM21	2 77	9843	3 085			
	DEM22	2 73	6648	2 667			
	DEM23	2 66	9843	2 124			
MEAN		2 7200	8778	2 62533			
STDEV		0557	1845	48185			
2	DEM30	2 29	9843	4 815			
	DEM31	2 37	2490	4 679			
	DEM32	2 26	5463	4 830			
	DEM33	2 30	4488	5 230			
	DEM34	2 34	5463	5 272			
	DEM35	2 27	6648	4 744			
	DEM37	2 35	9843	5 036			
	DEM39	2 40	9843	4 233			
	DEM40	2 26	5463	6 143			
MEAN		2 3156	6616	4 88689			
STDEV		0513	2664	32663			
3	DEM1	2 30	348	2 188	2 57	5463	2 999
	DEM2	2 29	237	2 814	2 83	3030	5 358
	DEM5	2 38	426	3 389	2 80	9843	5 646
	DEM16	2 33	195	3.402	2 78	9843	4 868
	DEM17	2 35	1134	2 093			
	DEM20	2 40	516	3 385			
	DEM36	2 30	516	4 468	2 82	9843	7 533
	DEM38	2 24	3030	4 462			
	DM11	2 13	1380	4 129			
	DM12	2 21	930	4 109	2 87	9843	8 636
	DM13	2 17	516	3 683	2 68	4488	6 649
	DM14	2 40	930	4 088	2 70	8088	5 991
MEAN		2 2917	646 5	3 51750	2 7562	7555	5 96000
STDEV		0887	780 3	.80967	0990	2815	1 71264
4	DEM3	2 31	3030	4 781			
	DEM4	2 29	9843	4 617			
	DEM10	2 49	9843	2 911			
	DEM11	2 47	9843	3 028			
	DEM12	2 16	3687	3 484	2 83	9843	9 717
	DEM13	2 28	9843	3 330			
	DEM14	2 28	1680	4 586			
	DEM18	2 19	930	3 828	2 73	9843	7 505
	DEM19	2 15	195	3 461	2 76	3687	6 343
	DEM28	2 33	930	4 352	2 44	2046	4 561
	DEM29	2 26	630	4 466	2 70	9843	7 040
	DM10	2 19	348	3 972			
	DM15	2 38	765	4 103	2 59	6648	5 287
	DM16	2 31	237	4 329	2 68	9843	6 242
MEAN		2 2921	3730	3 94629	2 6757	7393	6 67071
STDEV		1039	4154	61521	1274	3339	1 67178

Physio-graphic Region	DEM Name	D A5	Break point	Intercept	D A5	Break point	Intercept
5	DEM9	2 47	9843	2 919			
	DM18	2 35	9843	2 647			
MEAN		2 4100	9843	2 78300			
STDEV		0849	00	19233			
6	DEM6	2 27	3687	3 587			
	DEM7	2 50	1134	2 349	2 73	9843	3 588
	DEM8	2 68	9843	3 331			
MEAN		2 4833	4888	3 08900	2 7300	9843	3 58800
STDEV		2055	4477	65352			
7	DM20	2 33	9843	4 372			
MEAN		2 3300	9843	4 37200			
STDEV							
8	DEM24	2 26	1680	4 876			
	DEM25	2 36	9843	4 225			
	DEM26	2 36	4488	4 535			
	DEM27	2 41	9843	4 376			
MEAN		2 3475	6463	4.50300			
STDEV		0629	4067	27903			
9	DM1	2 08	348	1 427	2.57	5463	4 194
	DM2	2 15	1680	1 719	2 85	9843	7 334
	DM3	2 34	8088	3 665			
	DM4	2 23	1380	3 001			
	DM5	2 20	5463	2 979			
	DM6	2 24	9843	1 726			
	DM7	2 22	2046	2 233	2 80	8088	6 821
	DM8	2 21	9843	2 358			
	DM9	2 12	1380	4 056	2 72	9843	9 556
	DM17	2 31	9843	4 904			
MEAN		2 2100	4991	2 80680	2 7350	8309	6 97625
STDEV		0796	4051	1 13277	1223	2070	2 20213
TOTAL		2 3221	4617	3 70002	2.7225	7764	6 29340
STDEV		1411	3973	1 00285	1114	2734	1 81976

Physio-graphic Region	DEM Name	D A6	Break point	Inter cept	D A6	Break point	Inter cept	D A6	Break point	Inter cept
1	DEM21	2 57	6648	1 858						
	DEM22	2 59	5463	1 785						
	DEM23	2 68	2046	2 338	2 40	6648	183			
MEAN		2 6133	4719	1 99367	2 4000	6648	18300			
STDEV		0586	2390	30043						
2	DEM30	2 30	6648	4 908						
	DEM31	2 34	6648	4 676						
	DEM32	2 28	5463	5 014						
	DEM33	2 31	5463	5 286						
	DEM34	2 31	4488	5 191						
	DEM35	2 30	6648	4 793						
	DEM37	2 24	516	4 836	2 64	6648	7 086			
	DEM39	2 38	6648	3 979						
	DEM40	2 20	6648	4 822						
MEAN		2 2956	5463	4 83389	2 6400	6648	7 08600			
STDEV		0525	2014	37541						
3	DEM1	2 22	195	1 981	2 64	6648	3 423			
	DEM2	2 56	6648	3 439						
	DEM5	2 22	237	2 892	2 69	3030	4 843			
	DEM16	2 38	237	3 498	2 82	6648	5 283			
	DEM17	2 33	1134	1 980						
	DEM20	2 37	630	2 990	2 83	6648	5 416			
	DEM36	2 39	1380	4 627						
	DEM38	2 25	4488	4 175						
	DM11	2 19	1380	4 014						
	DM12	2 22	1134	3 878	2 87	6648	8 462			
	DM13	2 16	516	3 647	2 73	6648	7 172			
	DM14	2 30	516	3 865	2 70	6648	5 819			
MEAN		2 2958	1541	3 41550	2 7543	6131	5 77400			
STDEV		1174	1984	82314	0858	1367	1 63018			
4	DEM3	2 31	2048	4 677						
	DEM4	2 14	516	4 054	2 47	6648	5 601			
	DEM10	2 40	6648	2 363						
	DEM11	2 56	6648	3 137						
	DEM12	2 24	6648	3 584						
	DEM13	2 27	6648	3 037						
	DEM14	2 18	426	4 330	2 66	5687	6 996			
	DEM18	2 19	1380	3 786						
	DEM19	2 35	765	4 079	2 35	1680	3 474	2 66	6648	5 231
	DEM28	2 15	348	4 014	2 77	6648	7 134			
	DEM29	2 30	1680	4 603						
	DM10	2 50	4488	4 569						
	DM15	2 48	6648	4 615						
	DM16	2 45	3030	4 749						
MEAN		2 3229	3423	3 97079	2 5625	4666	5 80125	2 6600	6648	5 23100
STDEV		1378	2722	72183	1882	2131	1 69900			

Physiographic Region	DEM Name	D A6	Break point	Intercept	D A6	Break point	Intercept	D A6	Break point	Intercept
5	DEM9	2 39	3030	3 017						
	DM18	2 29	6648	2 194						
MEAN		2 3400	4839	2 60550						
STDEV		0707	2558	58195						
6	DEM6	2 29	2490	3 [illegible]						
	DEM7	2 63	6648	2 906						
	DEM8	2 49	1134	2 707						
MEAN		2 4700	3424	3 16133						
STDEV		1709	2873	62258						
7	DM20	2 31	2490	4 302						
MEAN		2 3100	2490	4 30200						
STDEV										
8	DEM24	2 34	6648	5 069						
	DEM25	2 27	6648	3 826						
	DEM26	2 25	2490	4 006						
	DEM27	2 31	6648	4 126						
MEAN		2 2925	5608	4 25675						
STDEV		0403	2079	55536						
9	DM1	2 27	3030	1 767						
	DM2	2 32	3030	1 574						
	DM3	2 27	6648	3 112						
	DM4	2 18	630	2 968	2 72	6648	6 163			
	DM5	2 26	3687	3 149						
	DM6	2 27	6648	1 755						
	DM7	2 31	6648	2 078						
	DM8	2 21	6648	2 368						
	DM9	2 20	630	4 350	2 52	6648	6 745			
	DM17	2 33	6648	4 990						
MEAN		2 2620	4425	2 81110	2 6200	6648	6 45400			
STDEV		0514	2537	1 14576	1414	00	41154			
TOTAL		2 3234	3773	3 62410	2 6540	5878	5 58667	2 6600	6648	5 23100
STDEV		1253	2614	1 06069	1562	1640	2 03814			

Physiographic Region	DEM Name	D 51	Break point	Intercept	D 51	Break point	Intercept	D 51	Break point	Intercept
1	DEM21	2 76	2691	2 909						
	DEM22	2 75	4527	2 602						
	DEM23	2 70	4527	2 239						
MEAN		2 7367	3915	2 58333						
STDEV		0321	1080	31539						
2	DEM30	2 46	4527	5 425						
	DEM31	2 28	3147	4 643						
	DEM32	2 35	4527	5 456						
	DEM33	2 36	4527	5 551						
	DEM34	2 57	4527	6 959						
	DEM35	2 43	3678	5 498						
	DEM37	2 58	3873	6 585						
	DEM39	2.53	2427	4 913						
	DEM40	2 25	3492	4 885						
MEAN		2 4233	3858	5 54611						
STDEV		1219	750 8	77089						
3	DEM1	2 43	414	2 144	2 60	813	2 727	2 30	4527	271
	DEM2	2 55	4080	3 654						
	DEM5	2 57	4527	3 057						
	DEM16	2 78	1872	5 770						
	DEM17	2 37	1368	2 025						
	DEM20	2 76	2835	2 909						
	DEM36	2 57	4527	4 986						
	DEM38	2 61	4080	3 840						
	DM11	2 13	1113	3 935						
	DM12	2 43	3678	4 509						
	DM13	2 55	4527	5 230						
	DM14	2 80	4527	5 812						
MEAN		2 5458	3129	3 98925	2 6000	813 0	2 72700	2 3000	4527	27100
STDEV		1910	1541	1 30501						
4	DEM3	2 44	4527	5 548						
	DEM4	2 34	660	4 626	2 76	2076	7 041			
	DEM10	2 47	735	2 398	2 74	4527	3 997			
	DEM11	2 24	111	2 272	2 78	4527	4 220			
	DEM12	2 27	4527	4 079						
	DEM13	2 49	2427	3 639						
	DEM14	2 44	2691	5 390						
	DEM18	2 27	1002	4 425	2 89	4527	6 723			
	DEM19	2 62	1170	4 240	2 67	3315	4 182			
	DEM28	2 43	627	4 813	2 77	4527	6 783			
	DEM29	2 40	1368	5 189						
	DM10	2 12	312	3 911						
	DM15	2 38	660	4 018						
	DM16	2 30	597	3 682						
MEAN		2 3721	1530	4 15857	2 7683	3316	5 82433			
STDEV		1260	1464	97977	0714	1024	1 97[illegible]			

Physio-graphic Region	DEM Name	D SI	Break point	Inter cept	D SI	Break point	Inter cept	D SI	Break point	Inter cept
5	DEM9	2 49	2187	4 119						
	DM10	2 38	4527	3 012						
MEAN		2 4350	3357	3 56550						
STDEV		0778	1655	78277						
6	DEM6	2 31	2835	4 286						
	DEM7	2 24	186	1 327	2 73	4527	3 087			
	DEM8	2 67	4627	3 911						
MEAN		2 4067	2516	3 17467	2 7300	4527	3 08700			
STDEV		2307	2188	1 61107						
7	DM20	2 62	4527	5 250						
MEAN		2 6200	4527	5 25000						
STDEV										
8	DEM24	2 25	1518	5 075	2 60	4527	7 371			
	DEM25	2 48	4527	4 855						
	DEM26	2 29	4527	4 974						
	DEM27	2 29	4527	4 568						
MEAN		2 3275	3775	4 86800	2 6000	4527	7 37100			
STDEV		1034	1504	21928						
9	DM1									
	DM2	2 15	4527	2 958						
	DM3	2 39	1443	4 351						
	DM4	2 26	1368	3 783						
	DM5	2 29	4527	3 810						
	DM6	2 07	4527	1 835						
	DM7	2 70	4527	567						
	DM8	2 08	4527	.133						
	DM9	2 29	1443	4.258						
	DM17	2 42	4527	5 903						
MEAN		2 2944	3491	3 06644						
STDEV		1962	1555	1 88954						
TOTAL		2 4289	2995	4 08300	2 7267	3707	5 34789	2 3000	4527	27100
STDEV		1850	1618	1 42076	0922	1379	2 14615			

Physiographic Region	DEM Name	D 52	Break point	Intercept	D 52	Break point	Intercept	D 52	Break point	Intercept
1	DEM21	2 62	951	2 162	2 29	4527	160			
	DEM22	2 65	3678	1 981						
	DEM23	2 47	312	1 378	2 78	4527	2 527			
MEAN		2 5800	1647	1 84033	2 5350	4527	1 44350			
STDEV		0964	1788	41049	3465	00	1 53230			
2	DEM30	2 16	3492	4 495						
	DEM31	2 42	4527	5 265						
	DEM32	2 38	3492	5 476						
	DEM33	2 43	2691	5 648						
	DEM34	2 35	4527	5 458						
	DEM35	2 44	1686	5 532						
	DEM37	2 47	4527	6 193						
	DEM39	2 46	4527	5 499						
	DEM40	2.39	4527	5 036						
MEAN		2 3889	3777	5 40022						
STDEV		0941	1032	46050						
3	DEM1	2 39	459	2 273	2 61	2076	3 219	2 39	4527	088
	DEM2	2 40	3678	1 477						
	DEM5	2 54	1113	4 351						
	DEM16	2 89	3873	5 528						
	DEM17	2 52	4527	1 934						
	DEM20	2 86	4299	4 807						
	DEM36	2 54	4527	4 928						
	DEM38	2 45	4527	4 294						
	DM11	2 28	1971	4 429						
	DM12	2 26	1299	4 302						
	DM13	2 36	1971	4 363						
	DM14	2 60	4527	5 529						
MEAN		2 5075	3064	4 02542	2 6100	2076	3 21900	2 3900	4527	08000
STDEV		2011	1573	1 36727						
4	DEM3	2 29	1599	5 110	2 74	4527	8 432			
	DEM4	2 45	1443	4 654						
	DEM10	2 28	414	1 476	2 12	4527	-1 570			
	DEM11	2 58	4527	4 508						
	DEM12	2 72	4527	5 163						
	DEM13	2 24	2988	3 791						
	DEM14	2 38	2076	4 878						
	DEM18	2 54	4527	4 516						
	DEM19	2 45	4527	4 940						
	DEM28	2 62	4527	5 665						
	DEM29	2 49	4527	5 575						
	DM10									
	DM15	2 37	1170	4 458						
	DM16	2 40	1170	5 426						
MEAN		2 4469	2925	4 62769	2 4300	4527	3 43100			
STDEV		1416	1647	1 07933	4384	00	7 07348			

Physiographic Region	DEM Name	D S2	Break point	Intercept	D S2	Break point	Intercept	D S2	Break point	Intercept
5	DEM9	2 35	2691	3 290						
	DM18	2 42	4527	2 940						
MEAN		2 3850	3609	3 11500						
STDEV		0495	1298	24749						
6	DEM6	2 25	1056	4 121	2 92	3147	8 961			
	DEM7	2 24	186	1 565	2 7	4527	3 720			
	DEM8	2 51	1233	2 378						
MEAN		2 3333	825 0	2 68800	2 8450	3837	6 34050			
STDEV		1531	560 4	1 30589	1061	975 8	3 70595			
7	DM20	2 16	4527	4 172						
MEAN		2 1600	4527	4 17200						
STDEV										
8	DEM24	2 25	2835	4 808						
	DEM25	2 42	4527	4 703						
	DEM26	2 37	4527	3 511						
	DEM27	2 21	1113	3 866	2 86	4527	8 456			
MEAN		2 3125	3250	4 24700	2 8600	4527	8 45600			
STDEV		0988	1633	66626						
9	DM1	2 35	4527	3 224						
	DM2									
	DM3	2 23	4527	2 103						
	DM4	2 45	4527	3 327						
	DM5	2 54	4527	1 761						
	DM6	2 00	186	1 760	2 53	4527	4 351			
	DM7									
	DM8									
	DM9	3 19	4080	3 791						
	DM17	2 43	4527	6 003						
MEAN		2 3129	3843	3 13843	2 5300	4527	4 35100			
STDEV		1850	1621	1 50244						
TOTAL		2 4169	3108	4 07428	2 6244	4101	4 27289	2 3900	4527	08800
STDEV		1662	1588	1 39808	2686	886 1	3 71981			

Physiographic Region	DEM Name	D S3	Break point	Intercept	D S3	Break point	Intercept	D S3	Break point	Intercept
1	DEM21	2 69	951	2 966	2 30	4527	039			
	DEM22	2 70	2556	3 142						
	DEM23	2 64	2076	2 284						
MEAN		2 6767	1861	2 79733	2 3000	4527	03900			
STDEV		0321	823 8	45319						
2	DEM30	2 62	1776	6 036						
	DEM31	2 36	2076	4 939						
	DEM32	2 32	4527	4 346						
	DEM33	2 33	1776	5 555						
	DEM34	2.47	2304	5 736						
	DEM35	2 29	4527	5 135						
	DEM37	2 44	3678	5 167						
	DEM39	2 56	4527	2 943						
	DEM40	2 32	1443	5 535	2 75	3678	8 478			
MEAN		2 4122	2959	5 04356	2 7500	3678	8 47800			
STDEV		1176	1332	92877						
3	DEM1	2 75	3678	4 183						
	DEM2	2 66	4527	3 952						
	DEM5	2.63	2988	4 563						
	DEM16	2 71	2427	3 540						
	DEM17	2 32	312	1 603	2 76	4527	3 647			
	DEM20	2 57	1299	3 792						
	DEM06	2 52	4080	4 660						
	DEM38	2 22	4299	3 700						
	DM11	2 35	4527	4 335						
	DM12	2 77	4527	5 928						
	DM13	2 26	2988	3 933						
	DM14	2 59	4527	4 603						
MEAN		2 5292	3348	4 06600	2 7600	4527	3 64700			
STDEV		1945	1402	1 00109						
4	DEM3	2 32	1368	4 872						
	DEM4	2 24	4527	4 896						
	DEM10	2 43	1776	3 472						
	DEM11	2 62	4527	2 782						
	DEM12	2 39	4527	2 625						
	DEM13	2 57	1299	2 850						
	DEM14	2 30	858	4 942						
	DEM18	2 18	1233	4 209	2 65	4527	7 457			
	DEM19	2 57	2988	4 045						
	DEM28	2 34	774	4 806	2 86	4527	8 077			
	DEM29	2 35	813	4 807						
	DM10	2 41	1113	4 666						
	DM15	2 32	813	4 221	2 60	4527	5 583			
	DM16	2 43	597	4 709	2 87	2187	7 162	2 20	4527	1 470
MEAN		2 3907	1944	4 13686	2 7450	3942	7 06975	2 2000	4527	1 47000
STDEV		1271	1519	85527	1401	1170	1 06199			

Physio-graphic Region	DEM Name	D 53	Break point	Inter cept	D 53	Break point	Inter cept	D 53	Break point	Inter cept
5	DEM9	2 36	1971	2 665						
	DM18	2 44	1299	3 029	2 60	4527	3 849			
MEAN		2 4000	1635	2 84700	2 6000	4527	3 84900			
STDEV		0566	475 2	25739						
6	DEM6	2 33	2556	4 302						
	DEM7	2 58	4527	3 270						
	DEM8	2 60	4527	3 777						
MEAN		2 5003	3870	3 78300						
STDEV		1504	1138	51603						
7	DM20	2 34	1686	4 154						
MEAN		2 3400	1686	4 15400						
STDEV										
8	DEM24	2 37	3492	5 391						
	DEM25	2 34	3873	4 560						
	DEM26	2 25	2556	4 089						
	DEM27	2 18	774	4 063	2 64	4527	6 954			
MEAN		2 2850	2674	4 52575	2 6400	4527	6 95400			
STDEV		0866	1382	62041						
9	DM1									
	DM2	2 25	4527	2 700						
	DM3	2 38	1872	4 685						
	DM4	2 48	2988	3 409						
	DM5	2 45	4527	5 399						
	DM6	2 27	4527	2 230						
	DM7	2 29	3147	2 865						
	DM8	2 23	4527	1 503						
	DM9	2 32	4527	4 538						
	DM17	2 31	4527	4 336						
MEAN		2 3311	3908	3 51833						
STDEV		0877	901 8	1 29596						
TOTAL		2 4268	2843	4 06040	2 6700	4173	5 69400	2 2000	4527	1 47000
STDEV		1578	1456	1 06314	1727	795 8	2 73555			

Physiographic Region	DEM Name	D S4	Break point	Intercept	D S4	Break point	Intercept
1	DEM21	2 64	2076	2 706			
	DEM22	2 68	2988	2 670			
	DEM23	2 68	1776	2 584			
MEAN		2 6667	2280	2 65333			
STDEV		0231	631 2	06068			
2	DEM30	2 44	2304	5 576			
	DEM31	2 34	2076	4 974			
	DEM32	2 27	4527	5 190			
	DEM33	2 51	2988	6 439			
	DEM34	2 40	1776	5 786			
	DEM35	2 45	1872	5 415			
	DEM37	2 51	2691	5 755			
	DEM39	2 80	2988	4 758			
	DEM40	2 44	4527	6 481			
MEAN		2 4622	2861	5 59711			
STDEV		1481	1042	59607			
3	DEM1	2 63	4527	3 468			
	DEM2	2 79	4527	4 958			
	DEM5	2 56	2988	3 090			
	DEM16	2 75	4527	4 636			
	DEM17	2 47	1971	2 869			
	DEM20	2 50	1066	3 678			
	DEM36	2 49	4527	5 694			
	DEM38	2 27	2691	5 015			
	DM11	2 23	1971	4 047			
	DM12	2 31	2691	4 203			
	DM13	2 47	4527	3 035			
	DM14	2 71	2427	5 698			
MEAN		2 5150	3202	4 19925			
STDEV		1840	1264	1 00442			
4	DEM3	2 36	2427	5 346			
	DEM4	2 37	951	4 874	2 92	2304	8 530
	DEM10	2 43	1518	2 627	2 67	3873	4 271
	DEM11	2 63	4527	2 672			
	DEM12	2 22	2187	3 725			
	DEM13	2 16	414	2 929	2 56	4527	4 782
	DEM14	2 19	312	3 591	2 68	4527	6 274
	DEM18	2 34	2076	4 190			
	DEM19	2 39	774	4 698	2 83	4527	7 223
	DEM28	2 44	735	4 943	2 69	2956	6 265
	DEM29	2 17	537	4 185			
	DM10	2 08	312	3 309			
	DM15	2 28	774	3 948			
	DM16	2 39	358	4 623	2 70	4527	6 401
MEAN		2 3179	1314	3 [illegible]	2 7214	3834	6 24943
STDEV		1444	1164	87359	1177	991 4	1 42830

Physiographic Region	DEM Name	D 54	Break point	Intercept	D 54	Break point	Intercept
5	DEM9	2 17	186	1 827	2 62	4527	3 777
	DM18	2 57	2988	4 394			
MEAN		2 3700	1587	3 11050	2 6200	4527	3 77700
STDEV		2828	1981	1 81514			
6	DEM6	2 53	4527	4 907			
	DEM7	2 64	4527	2 554			
	DEM8	2 53	2427	2 095			
MEAN		2 5667	3827	3 18533			
STDEV		0635	1212	1 50857			
7	DM20	2 29	4527	5 071			
MEAN		2 2900	4527	5 07100			
STDEV							
8	DEM24	2 37	2988	5 059			
	DEM25	2 24	1686	4 136			
	DEM26	2 46	3678	4 762			
	DEM27	2 37	4527	2 590			
MEAN		2 3600	3220	4 13675			
STDEV		0906	1201	1 10059			
9	DM1	2 45	4527	4 415			
	DM2	2 59	4527	3 272			
	DM3	2 19	4527	2.486			
	DM4						
	DM5	2 58	4527	3 454			
	DM6	2 27	4527	1 665			
	DM7	2 31	4527	4 324			
	DM8	2 24	4527	4.118			
	DM9	2 07	2427	3 962			
	DM17	2 38	1443	5 008	2 33	4527	4 184
MEAN		2 3422	3951	3 63378	2 3300	4527	4 18400
STDEV		1750	1169	1.04128			
TOTAL		2 4218	2755	4 11375	2 6667	3988	5 74522
STDEV		1786	1477	1 1814	1657	911 2	1 59417

Physio-graphic Region	DEM Name	D CC 1	Break point	Inter cept	D CC 1	Break point	Inter cept	D CC 2	Break point	Inter cept	D CC 2	Break point	Inter cept
1	DEM21	2 83	8	9 150				2 60	8	8 527			
	DEM22	2 95	7	8 856				2 76	7	9 651			
	DEM23	3 00	8					2 68	7	9 242			
MEAN		2 9267	7 67	9 00300				2 6800	7 33	9 14000			
STDEV		0874	58	20789				0800	58	56890			
2	DEM30	2 12	3	7 783	2 48	7	8 432	2 10	3	7 320	2 47	7	8 026
	DEM31	2 25	7	6 842				2 37	8	7 421			
	DEM32	2 27	7	6 798				2 10	3	7 098	2 45	7	7 767
	DEM33	2 12	3	7 161	2 47	7	7 590	2 11	3	7 554	2 64	8	8 673
	DEM34	2 57	8	7 430				2 48	8	7 680			
	DEM35	2 19	4	7 849	2 87	8	9 599	2 14	4	7 308	2 63	8	8 554
	DEM37	2 20	4	7 152	2 82	7	8 795	2 11	3	7 626	2 49	7	8 360
	DEM39	2 22	5	7 439	2 71	8	8 833	2 09	3	6 930	2 68	8	8 146
	DEM40	2 10	3	6 769	2 40	8	7 366	2 11	3	6 964	2 40	8	7 537
MEAN		2 2267	4 89	7 24700	2 6250	7 50	8 43583	2 1789	4 22	7 32233	2 5371	7 57	8 15186
STDEV		1420	1 96	40783	2005	55	83662	1429	2 17	27758	1101	53	41204
3	DEM1	2 37	5	7 535	3 00	8		2 28	4	8 096	2 87	8	9 438
	DEM2	2 28	3	7 717	2 81	7	8 910	2 21	3	8 091	2 76	8	9 227
	DEM5	2 48	7	8 435				2 46	7	8 622			
	DEM16	2 35	4	8 774	3 00	8		2 26	3	8 974	3 00	8	
	DEM17	2 31	4	8 191	3 00	8		2 35	6	8 724	3 00	8	
	DEM20	2 69	8	8 078				2 35	6	8 446	3 00	8	
	DEM36	2 53	7	8 735				2 53	7	8 594			
	DEM38	2 48	8	8 204				2 12	4	7 358	2 43	8	8 118
	DM11	2 23	5	7 908	2 88	8	9 730	2 10	6	7 564			
	DM12	2 19	4	8 128	2 65	7	9 226	2 34	7	7 775			
	DM13	2 14	5	7 581	2 97	8	10 380	2 16	6	7 768	3 00	8	
	DM14	2 18	4	8 516	3 00	8		2 17	4	7 931	2 93	8	9 828
MEAN		2 3525	5 33	8 15017	2 9137	7 75	9 56150	2 2775	5 25	8 16192	2 8737	8 00	9 15275
STDEV		1656	1 72	41616	1278	46	64170	1342	1 54	50685	1988	00	73338
4	DEM3	2 08	3	7 843	2 40	5	8 506	2 14	5	7 809	2 56	7	8 989
	DEM4	2 10	4	7 705	2 90	8	9 814	2 10	4	8 499	2 48	8	7 456
	DEM10	2 34	4	7 395	3 00	8		2 40	4	8 470	2 84	8	9 645
	DEM11	2 11	3	4 779	3 00	8		2 07	3	5 283	3 00	8	
	DEM12	2 10	3	6 725	2 28	7	7 035	2 09	6	6 402			
	DEM13	2 32	8	6 474				2 11	7	5 867			
	DEM14	2 08	3	7 710	2 55	7	8 668	2 11	4	7 708	2 58	7	8 880
	DEM18	2 00	3		2 55	7	8 497	2 17	5	7 471	2 45	7	8 281
	DEM19	2 65	8	6 947				2 08	3	6 842	2 86	8	8 473
	DEM28	2 10	3	8 030	2 71	7	9 221	2 16	3	8 269	2 60	7	9 074
	DEM29	2 14	4	8 128	2 86	7	9 963	2 12	4	8 086	3 00	8	
	DM10	1 11	4	6 693				1 10	4	7 501			
	DM15	2 13	4	6 789	3 00	8		2 13	4	7 597	2 84	7	9 368
	DM16	2 17	4	6 645	3 00	8		2 15	4	7 479	3 00	8	
MEAN		2 [illegible]	4 14	7 07408	2 7500	7 27	8 81485	2 0664	4 29	7 23450	2 7464	7 55	8 77075
STDEV		[illegible]	1 70	90651	2664	[illegible]	98888	2895	1 14	[illegible]	2159	52	68968

Physiographic Region	DEM Name	D CC 1	Break point	Intercept	D CC 1	Break point	Intercept	D CC 2	Break point	Intercept	D CC 2	Break point	Intercept
5	DEM9	2 40	7	7 660				2 26	6	7 967			
	DM18	2 40	8	7 535				2 43	8	7 974			
MEAN		2 4000	7 50	7 59750				2 3450	7 00	7 97050			
STDEV		0000	71	08839				1202	1 41	00495			
6	DEM6	2 10	3	7 274	2 33	6	7 665	2 10	4	7 454	2 31	6	7 888
	DEM7	2 20	3	4 911	3 00	8		2 14	3	5 518	2 84	6	6 809
	DEM8	2 09	4	4 585	3 00	8		2 11	4	5 186	2 84	7	6 760
MEAN		2 1300	3 33	5 59000	2 7767	7 33	7 66500	2 1167	3 67	6 05267	2 6633	6 33	7 15233
STDEV		0608	58	1 46747	3868	1 15		0208	58	1 22489	3060	58	63758
7	DM20	2 34	8	7 508				2 23	7	6 699			
MEAN		2 3400	8 00	7 50800				2 2300	7 00	6 69900			
STDEV													
8	DEM24	2 10	3	5 344	2 46	6	7 292	2 17	4	6 977	2 38	6	7 385
	DEM25	2 20	4	6 842	3 00	8		2 15	4	7 379	2 63	8	8 581
	DEM26	2 13	4	5 231	2 56	7	6 140	2 36	7	5 928			
	DEM27	2 21	6	6 010				2 11	5	6 259	2 47	8	7 228
MEAN		2 1600	4 25	5 85675	2 6733	7 00	6 71600	2 1975	5 00	6 63575	2 4933	7 33	7 73133
STDEV		0535	1 26	74132	2873	1 00	81459	1112	1 41	66124	1266	1 15	74001
9	DM1	2 03	3	6 264	2 24	8	6 654	2 07	4	6.223	2 29	8	6 785
	DM2	2 02	3	6 215	2 22	6	6.586	2 05	4	5 929	2 15	6	6 147
	DM3	2 10	4	7 244	2 71	7	8 871	2 08	4	7 347	2 32	6	7 853
	DM4	2 08	3	6 191	3.00	8		2 08	4	7 687	2 82	7	9 536
	DM5	2 10	4	6 874	2 50	8	7 843	2 09	4	6 663	2 86	8	9 099
	DM6	2 07	3	6 921	2 36	6	7 471	2 04	3	7 316	2 69	8	8 930
	DM7	2 09	4	6 636	2 48	7	7 628	2 09	4	6 460	3 00	8	
	DM8	2 04	5	4 897	2 77	8	7 343	2.03	3	5 349	2 20	6	5 619
	DM9	2 07	3	6 951	2 40	7	7 603	2 06	3	7 066	2 17	6	7 251
	DM17	2 34	7	7 697				2 33	7	7 700			
MEAN		2 0940	3 90	6 58900	2 5200	7 22	7 49987	2 0920	4 00	6 77400	2 5000	7 00	7 65250
STDEV		0909	1 29	76363	2597	83	71723	0861	1 15	78582	3384	1 00	1 44556
TOTAL		2 2343	4 79	7 17471	2 7085	7 37	8 27361	2 1878	4 74	7 37290	2 6568	7 41	8.17306
STDEV		2696	1 86	1.05326	2662	77	1 11757	2205	1 65	97789	2654	77	1 04697

Physiographic Region	DEM Name	D CC 3	Break point	Intercept	D CC 3	Break point	Intercept
1	DEM21	2.52	8	8.058			
	DEM22	2.59	7	8.984			
	DEM23	2.60	7	8.983			
MEAN		2.5700	7.33	8.67500			
STDEV		.0436	.58	.53434			
2	DEM30	2.08	3	6.333	2.36	7	6.755
	DEM31	2.12	3	7.535	2.37	7	7.931
	DEM32	2.04	3	7.135	2.38	8	7.691
	DEM33	2.12	3	7.685	2.61	8	8.713
	DEM34	2.54	8	8.345			
	DEM35	2.38	8	7.124			
	DEM37	2.10	3	7.288	2.40	6	7.840
	DEM39	2.13	4	6.223	2.73	8	7.690
	DEM40	2.24	5	7.449	2.73	8	9.041
MEAN		2.1944	4.44	7.23522	2.5114	7.43	7.95157
STDEV		.1647	2.13	.65510	.1722	.79	.74695
3	DEM1	2.32	4	8.604	2.90	8	9.914
	DEM2	2.23	4	8.358	2.90	8	10.260
	DEM5	2.57	7	8.752			
	DEM16	2.13	3	8.336	3.00	8	
	DEM17	2.20	5	7.577	3.00	8	
	DEM20	2.23	4	8.653	3.00	8	
	DEM36	2.18	6	6.497			
	DEM38	2.34	7	7.709			
	DM11	2.03	6	7.339			
	DM12	2.89	6	6.972			
	DM13	2.11	5	7.024	3.00	8	
	DM14	2.03	3	6.684	2.82	8	8.329
MEAN		2.2050	5.00	7.70875	2.9457	8.00	9.50100
STDEV		.1525	1.41	.81356	.0728	.00	1.02962
4	DEM3	2.07	4	7.244	2.52	7	8.450
	DEM4	2.10	5	5.992	2.62	8	7.625
	DEM10	2.17	3	7.655	2.63	8	8.664
	DEM11	2.05	4	5.660	3.00	8	
	DEM12	2.10	6	6.426			
	DEM13	2.11	7	5.936			
	DEM14	2.10	3	7.905	2.37	6	8.400
	DEM18	2.24	6	7.589			
	DEM19	2.14	4	7.365	3.00	8	
	DEM28	2.00	3		2.98	8	9.441
	DEM29	2.14	4	7.889	2.71	7	9.338
	DM10	1.07	5	7.876			
	DM15	2.04	4	7.814	2.83	8	9.600
	DM16	2.10	5	7.962	3.00	8	
MEAN		2.0307	4.50	7.17792	2.7560	7.60	8.78829
STDEV		.2826	1.22	.85611	.2213	.70	.70958

Physio-graphic Region	DEM Name	D CC 3	Break point	Inter cept	D CC 3	Break point	Inter cept
5	DEM9	2 34	7	7 983			
	DM18	2 48	8	7 874			
MEAN		2 4100	7 50	7 92850			
STDEV		0990	71	07707			
6	DEM6	2 10	5	7 292			
	DEM7	2 07	3	5 774	2 73	6	7 080
	DEM8	2 32	4	6 531	2 82	7	7 612
MEAN		2 1633	4 00	6 53233	2 7750	6 50	7 34600
STDEV		1365	1 00	.75900	0636	71	37618
7	DM20	2 11	5	6 398			
MEAN		2 1100	5 00	6 39800		–	
STDEV							
8	DEM24	2 11	4	7 141	2 58	8	8 336
	DEM25	2 19	4	7 188	2 51	8	7 915
	DEM26	2 11	3	6 884	2 50	7	7 505
	DEM27	2 .14	5	6 975	2 66	8	8 562
MEAN		2 1375	4 00	7 04700	2 5625	7 75	8 07950
STDEV		0377	82	14197	0741	50	46751
9	DM1	2 07	5	6 597	2 90	8	9 248
	DM2	2 10	5	5 722	2 79	8	8 021
	DM3	2 09	3	7 227	2 51	8	8 101
	DM4	2 20	6	7 500			
	DM5	2 37	6	7 031	3 00	8	
	DM6	2 04	6	5 791			
	DM7	2 10	3	5 805	2 45	7	6 471
	DM8	2 05	4	6 563	2 86	8	9 137
	DM9	2 04	3	7 058	2 17	6	7 290
	DM17	2.30	7	7 503			
MEAN		2 1360	4 80	6 67970	2 6686	7 57	8 04467
STDEV		1158	1 48	69995	2990	79	1 06685
TOTAL		2 1669	4 84	7 25960	2 7092	7 59	8 30897
STDEV		2133	1 59	.85564	2357	69	93018

Physio-graphic Region	DEM Name	D CC 4	Break point	Inter cept	D CC 4	Break point	Inter cept	D' CC 5	Break point	Inter cept.	D CC 5	Break point	Inter cept
1	DEM21	2 60	8	8 327				2 62	7	8 126			
	DEM22	2 65	7	8 786				2 86	7	8 330	2 86	7	8 330
	DEM23	2 65	7	8 754				2 73	7	8 071			
MEAN		2 6333	7 33	8 62233				2 7367	7 00	8 17567	2 8600	7 00	8 33000
STDEV		0289	58	25627				1201	00	13646			
2	DEM30	2 08	3	5 997	2 36	7	6 441	2 08	4	5 748	2 88	8	7 829
	DEM31	2 09	3	7 428	2 32	7	7 804	2 27	6	7 117			
	DEM32	2 26	7	7 512				2 10	4	7 213	2 73	7	8 832
	DEM33	2 09	3	7 443	2 63	8	8 595	2 09	3	7 126	2 85	8	8 817
	DEM34	2 60	8	8 594				2 68	8	7 938			
	DEM35	2 11	4	6 348	2 47	8	7 079	2 11	3	5 983	2 52	8	6 680
	DEM37	2 13	3	6 689	2 56	7	7 566	2 12	3	5 616	2 62	7	6 649
	DEM39	2 13	4	6 090	3 00	8		2 14	3	5 071	3 00	8	
	DEM40	2 12	4	6 990	2 55	7	8 100	2 08	3	6 487	3 00	8	
MEAN		2 1789	4 33	7 01011	2 5557	7 43	7 59750	2 1856	4 11	6 47767	2 8000	7 71	7 76140
STDEV		1668	1 87	83198	2252	53	76125	1944	1 76	93546	1847	49	1 08073
3	DEM1	2 30	4	8 571	2 95	8	10 040	2 24	3	7 858	3 00	8	
	DEM2	2 11	3	7 681	2 88	7	9 126	2 11	3	6 370	2 94	7	7 905
	DEM5	2 14	3	7 824	3 00	8		2 16	3	6 923	3 00	8	
	DEM16	2 27	3	7 993	3 00	8		2 33	3	5 894	3 00	8	
	DEM17	2 11	4	6 926	3 00	8		2 13	3	5 751	3 00	8	
	DEM20	2 38	4	8 618	3 00	8		2 28	3	7 098	3 00	8	
	DEM06	2 19	5	6 199				2 14	4	5 480	3 00	8	
	DEM38	2 15	7	6 310				2 16	6	[illegible]139			
	DM11	2 02	5	7 341				2 02	4	[illegible]	3 00	7	
	DM12	2 03	5	6 848				2 0[illegible]	4	6 806	3 00	8	
	DM13	2 07	5	6 437	3 00	8		2 0[illegible]	4	6 208	3 00	8	
	DM14	2 12	5	5 870	3 00	8		2 [illegible]7	5	5 186	3 00	8	
MEAN		2 1575	4 42	7 21817	2 9787	7 87	9 58300	2 1500	3 75	6 41933	2 9945	7 82	7 90500
STDEV		1098	1 18	92932	0436	35	64630	0984	97	79609	0181	40	
4	DEM3	2 07	4	6 925	2 67	7	8 519	2 08	4	6 477	2 83	7	8 362
	DEM4	2 05	3	5 529	2 20	6	5 792	2 07	4	5 525	2 74	8	7 288
	DEM10	2 11	3	7 508	2 55	7	8 374	2 00	3	7 484	2 47	6	7 975
	DEM11	2 12	3	5 808	2 37	6	6 283	2 62	8	8 547			
	DEM12	2 26	7	7 393				2 11	3	6 714	2 46	6	7 381
	DEM13	2 30	8	6 804				2 39	7	8 169			
	DEM14	2 13	4	8 019	2 49	6	8 757	2 16	4	7 378	3 00	7	
	DEM18	2 14	[illegible]	7 107	3 00	8		2 00	5		3 00	8	
	DEM19	2 20	4	7 947	3 00	8		2 57	8	8 533			
	DEM28	2 27	5	6 734	3 00	8		2 04	3	5 609	3 00	8	
	DEM29	2 15	4	7 166	2 75	7	8 768	2 13	4	6 448	3 00	8	
	DM10	1 10	4	8 223				1 10	4	7 742			
	DM15	2 11	3	7 992	2 77	8	9 [illegible]	2 13	4	7 731	2 93	8	9 820
	DM16	2 16	4	8 371	3 00	8		2 26	3	7 752	2 89	8	9 480
MEAN		2 0836	4 36	7 25207	2 7091	7 18	7 98329	2 1329	4 71	7 23962	2 8329	7 40	8 38433
STDEV		2926	1 50	85774	2816	87	1 37390	3526	1 73	1 00747	2118	84	1 06191

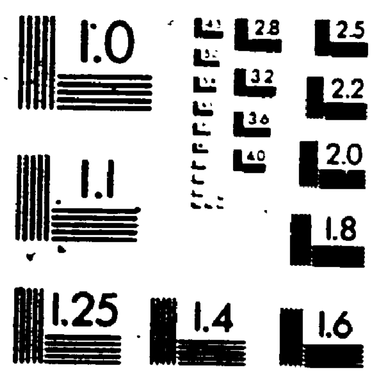
1.0
2.8
2.5
3.2
2.2
3.6
4.0
2.0
1.1
1.8
1.25
1.4
1.6

Physio-graphic Region	DEM Name	D CC 4	Break point	Inter cept	D CC 4	Break point	Inter cept	D CC 5	Break point	Inter cept	D CC 5	Break point	Inter cept
5	DEM9	2 18	4	7 247	2 81	7	8 852	2 14	3	5 777	2 90	7	7 306
	DM18	2 57	8	7 167				2 70	8	6 042			
MEAN		2 3750	6 00	7 20700	2 8100	7 00	8 85200	2 4200	5 50	5 90950	2 9000	7 00	7 30600
STDEV		2758	2 83	05657				3960	3 54	18738			
6	DEM6	2 08	4	7 394	2 24	6	7 740	2 06	4	7 382	2 47	7	8 439
	DEM7	2 27	3	8 243	2 70	6	9 220	2 53	7	8 650			
	DEM8	2 67	8	8 862				2 35	5	7 227	2 89	7	8 604
MEAN		2 3400	5 00	8 16633	2 5150	6 00	8 48450	2 3133	5 33	7 75300	2 6800	7 00	8 56650
STDEV		3012	2 65	73700	3889	00	1 05298	2371	1 53	78068	2970	00	18031
7	DM20	2 19	7	6 340				2 30	7	6 129			
MEAN		2 1900	7 00	6 34000				2 3000	7 00	6 12900			
STDEV													
8	DEM24	2 12	4	7 286	2 47	7	8 156	2 18	7	6 978			
	DEM25	2 12	8	6 354				2 12	6	5 710			
	DEM26	2 13	4	7 257	2 33	7	7 684	2 11	4	7 157	2 40	7	7 774
	DEM27	2 19	5	7 333	2 60	8	8 477	2 15	5	7 167	3 00	8	
MEAN		2 1400	4 75	7 05750	2 4667	7 33	8 10567	2 1400	5 50	6 75295	2 7000	7 50	7 77400
STDEV		0337	96	47004	1350	58	39889	0316	1 29	70041	4243	71	
9	DM1	2 10	3	5 907	2 67	7	7 042	2 10	4	4 400	2 66	7	5 820
	DM2	2 09	3	5 312	2 27	6	5 628	2 03	5	4 775	2 90	8	7 391
	DM3	2 07	3	6 508	2 56	8	7 643	2 05	3	5 049	2 81	8	7 369
	DM4	2 06	3	6 685	2 23	6	7 006	2 03	3	6 078	2 66	7	7 674
	DM5	2 07	3	5 714	2 47	6	6 466	2 13	4	4 636	3 00	8	
	DM6	2 02	5	5 408				2 04	4	5 098			
	DM7	2 05	4	4 972	2 75	8	7 323	2 11	5	5 020	2 78	8	7 283
	DM8	2 04	4	6 597	2 26	7	7 212	2 07	4	6 322	2 29	7	6 855
	DM9	2 03	4	6 756	2 21	7	7 211	2 04	4	5 758	2 16	7	6 004
	DM17	2 26	6	6 796				2 26	6	5 633			
MEAN		2 0790	3 80	6 06560	2 4275	6 87	6 94137	2 0860	4 20	5 27690	2 6575	7 50	6 90657
STDEV		0684	1 03	68440	2143	83	62668	0707	92	63891	2920	53	71913
TOTAL		2 1703	4 59	7 09041	2 6545	7 25	7 80355	2 1903	4 60	6 57821	2 8248	7 55	7 74612
STDEV		2209	1 61	96365	2839	78	1 09996	2518	1 60	1 10694	2264	59	99414

Physiographic Region	DEM Name	D Div1	Break point	Intercept	D Div2	Break point	Intercept	D Div3	Break point	Intercept
1	DEM21	2.65	6	18.330	2.57	6	15.420	2.67	6	15.910
	DEM22	2.74	6	17.726	2.77	5	17.550	2.57	5	15.970
	DEM23	2.85	6	17.180	2.63	5	16.420	2.59	5	16.070
MEAN		2.7465	6.00	17.07862	2.6567	5.33	16.46333	2.6100	5.33	15.98333
STDEV		1002	00	70343	1026	58	1.06566	0529	58	08083
2	DEM30	2.23	5	13.340	2.22	6	12.840	2.28	6	12.270
	DEM31	2.20	6	12.140	2.26	6	12.890	2.23	5	13.090
	DEM32	2.15	5	11.730	2.21	5	12.600	2.24	6	12.910
	DEM33	2.26	6	12.700	2.20	4	13.900	2.38	6	14.160
	DEM34	2.37	4	13.210	2.22	5	12.570	2.32	4	13.810
	DEM35	2.24	5	13.460	2.21	5	12.780	2.20	6	12.180
	DEM37	2.46	6	14.610	2.19	6	12.730	2.26	6	13.120
	DEM39	2.31	6	13.484	2.29	6	13.379	2.32	6	12.302
	DEM40	2.15	6	12.453	2.21	6	13.582	2.25	6	12.886
MEAN		2.2625	5.44	13.01410	2.2228	5.44	13.03012	2.2752	5.67	12.96975
STDEV		1026	73	86154	0307	73	47277	0558	71	68281
3	DEM1	2.38	5	13.700	2.42	6	14.540	2.55	6	15.700
	DEM2	2.37	5	13.900	2.37	6	14.290	2.44	6	14.960
	DEM5	2.44	6	14.730	2.44	6	14.980	2.42	6	14.730
	DEM18	2.46	5	15.280	2.60	6	16.460	2.48	5	15.260
	DEM17	2.41	5	14.460	2.32	6	14.590	2.26	6	13.260
	DEM20	2.58	6	14.890	2.40	6	14.710	2.31	5	14.520
	DEM36	2.20	5	12.530	2.23	6	13.220	2.19	5	12.660
	DEM38	2.22	6	12.070	2.23	6	12.520	2.24	6	12.040
	DM11	2.30	6	12.064	2.11	6	13.830	2.17	6	12.528
	DM12	2.29	6	13.603	2.38	6	13.595	2.41	6	12.979
	DM13	2.27	6	13.168	2.15	6	13.675	2.16	6	13.365
	DM14	2.32	6	14.266	2.28	6	13.292	2.29	6	13.702
MEAN		2.3527	5.58	13.79674	2.3271	6.00	14.14185	2.3268	5.75	13.88361
STDEV		1093	51	98439	1375	00	1.02675	1299	45	1.09581
4	DEM3	2.17	5	13.250	2.18	6	13.130	2.14	5	12.520
	DEM4	2.18	5	13.020	2.14	6	11.650	2.22	6	11.640
	DEM10	2.42	6	13.730	2.52	6	15.310	2.27	5	13.390
	DEM11	2.25	3	10.290	2.24	4	10.900	2.18	5	11.120
	DEM12	2.18	6	12.060	2.07	6	11.200	2.08	6	11.230
	DEM13	2.34	6	12.430	2.10	6	10.800	2.08	6	10.690
	DEM14	2.22	5	13.230	2.24	6	13.340	2.19	5	13.260
	DEM18	2.20	4	13.110	2.15	5	12.640	2.07	4	12.140
	DEM19	2.53	6	12.525	2.15	4	12.030	2.22	5	12.890
	DEM28	2.30	5	14.070	2.39	6	14.610	2.33	5	14.090
	DEM29	2.20	5	13.560	2.17	5	13.370	2.21	5	13.390
	DM10	2.26	6	12.638	2.19	5	13.534	2.15	5	13.708
	DM15	2.27	6	12.636	2.19	6	13.657	2.16	6	13.740
	DM16	2.29	6	12.642	2.20	6	13.384	2.17	6	13.665
MEAN		2.2725	5.29	12.79937	2.2097	5.50	12.82536	2.1764	5.29	12.67653
STDEV		1024	91	90832	1168	76	1.35924	0732	61	1.12383

Physio-graphic Region	DEM Name	D Div1	Break point	Inter cept	D Div2	Break point	Inter cept	D Div3	Break point	Inter cept
5	DEM9	2 46	6	14 130	2 25	6	13 550	2 25	6	13 450
	DM18	2 42	6	13 456	2 44	6	14 203	2 47	6	13 864
MEAN		2 4394	6 00	13 79321	2 3434	6 00	13 87672	2 3600	6 00	13 65682
STDEV		0291	00	47629	1322	00	46205	1556	00	29248
6	DEM6	2 27	6	13 060	2 14	5	12 600	2 08	4	12 160
	DEM7	2 36	6	12 403	2 42	4	11 930	2 25	4	11 590
	DEM8	2 04	4	9 200	2 14	4	10 360	2 36	4	12 590
MEAN		2 2240	5 33	11 55430	2 2333	4 33	11 63000	2 2300	4 00	12 11333
STDEV		1659	1 15	2 06519	1617	58	1 14074	1411	00	50163
7	DM20	2 30	6	12 657	2 26	6	12 772	2 20	6	12 706
MEAN		2 2971	6 00	12 65697	2 2623	6 00	12 77196	2 2007	6 00	12 70558
STDEV										
8	DEM24	2 13	4	11 680	2 25	6	12 630	2 17	5	12 480
	DEM25	2 58	6	14 580	2 26	6	13 150	2 23	4	12 730
	DEM26	2 25	6	10 990	2 26	6	11 520	2 19	4	12 240
	DEM27	2 19	4	11 340	2 12	6	11 300	2 11	5	11 070
MEAN		2 2875	5 00	12 14750	2 2225	6 00	12 15000	2 1750	4 50	12 29500
STDEV		2011	1 15	1 64595	0685	00	88502	0500	58	32542
9	DM1	2 22	6	11 642	2 21	6	13 132	2 18	6	10 836
	DM2	2 21	6	11 521	2 16	6	12 789	2 15	6	10 556
	DM3	2 24	6	13 640	2 25	6	12 997	2 21	6	13 085
	DM4	2 26	6	12 181	2 15	6	13 954	2 31	6	13 080
	DM5	2 23	6	12 302	2 21	6	14 139	2 37	6	12 490
	DM6	2 23	6	12 018	2 14	6	11 787	2 14	6	10 625
	DM7	2 25	6	12 614	2 29	6	13 312	2 17	6	12 237
	DM8	2 20	6	10 469	2 20	6	11 411	2 12	6	11 200
	DM9	2 17	6	12 145	2 10	6	12 698	2 16	6	12 582
	DM17	2 30	6	13 695	2 36	6	14 015	2 27	6	13 524
MEAN		2 2324	6 00	12 22570	2 2068	6 00	13 02345	2 2076	6 00	12 02141
STDEV		0358	00	96123	0761	00	91163	0822	00	1 11883
TOTAL		2 3099	5 55	13 08393	2 2661	5 67	12 27876	2 2601	5 48	13 01286
STDEV		1517	73	1 49702	1434	63	1 38940	1338	71	1 30871

Physio-graphic Region	DEM Name	D Div4	Break point	Inter cept	D Div5	Break point	Inter cept
1	DEM21	2 55	6	15 080	2 62	6	15 210
	DEM22	2 53	6	15 400	2 47	4	16 460
	DEM23	2 69	6	16 190	2 53	5	14 310
MEAN		2 5900	6 00	15 55667	2 5400	5 00	15 32667
STDEV		0872	00	57134	0755	1 00	1 07974
2	DEM30	2 28	6	12 030	2 14	5	10 930
	DEM31	2 20	6	12 860	2 26	5	12 730
	DEM32	2 22	6	12 920	2 10	4	12 170
	DEM33	2 26	6	13 220	2 10	4	12 090
	DEM34	2 26	6	13 460	2 29	6	12 840
	DEM35	2 13	4	11 420	2 35	6	12 180
	DEM37	2 06	4	10 990	2 17	5	11 370
	DEM39	2 30	6	12 757	2 26	6	11 201
	DEM40	2 21	6	12 003	2 05	6	11 906
MEAN		2 2129	5 56	12 40666	2 1917	5 22	11 93527
STDEV		0765	88	84022	1023	83	65757
3	DEM1	2 47	6	15 270	2 37	4	14 050
	DEM2	2 17	3	18 250	2 17	3	11 640
	DEM5	2 25	4	13 460	2 21	3	12 320
	DEM16	2 71	6	15 180	2 96	4	14 740
	DEM17	2 12	4	11 940	2 25	3	11 310
	DEM20	2 44	6	15 150	2 37	3	13 240
	DEM06	2 26	5	12 360	2 24	5	11 250
	DEM08	2 20	6	12 420	2 24	5	12 130
	DM11	2 06	6	12 298	2 18	6	13 025
	DM12	2 23	6	13 306	2 19	6	12 438
	DM13	2 10	6	11 665	2 22	6	12 132
	DM14	2 26	6	12 406	2 33	6	11 539
MEAN		2 2724	5 33	13 65042	2 3110	4 50	12 48452
STDEV		1847	1 07	1 94847	2157	1 31	1 09506
4	DEM3	2 10	5	11 920	2 12	4	11 500
	DEM4	2 13	6	10 640	2 05	4	10 260
	DEM10	2 22	5	13 050	2 32	6	13 450
	DEM11	2 29	6	11 670	2 60	6	15 590
	DEM12	2 25	6	12 930	2 24	5	12 370
	DEM13	2 29	6	12 540	2 34	6	14 040
	DEM14	2 17	5	13 290	2 40	5	13 960
	DEM18	2 09	6	11 950	2 08	5	11 450
	DEM19	2 30	6	13 860	2 37	6	14 400
	DEM28	2 24	5	12 230	2 11	4	10 660
	DEM29	2 14	4	12 260	2 15	4	11 590
	DM10	2 19	6	13 986	2 25	6	13 235
	DM15	2 18	6	13 716	2 27	6	13 448
	DM16	2 20	6	14 104	2 34	6	13 088
MEAN		2 1993	5 57	12 72474	2 2588	5 21	12 78863
STDEV		0695	65	1 01655	1526	89	1 53253

Physio-graphic Region	DEM Name	D Div4	Break point	Inter cept	D Div5	Break point	Inter cept
5	DEM9	2 18	4	12 510	2 46	5	12 460
	DM18	2 61	6	13 995	2 59	6	12 950
MEAN		2 3429	5 00	13 25261	2 52274	5 50	12 70478
STDEV		2303	1 41	1 05020	0887	71	34617
6	DEM6	2 11	6	12 410	2 09	5	12 280
	DEM7	2 59	6	15 600	2 39	6	14 710
	DEM8	2 50	6	15 330	2 40	5	13 470
MEAN		2 4000	6 00	14 44667	2 2933	5 33	13 48667
STDEV		2551	00	1 76896	1762	58	1 21509
7	DM20	2 24	6	11 684	2 25	6	11 589
MEAN		2 2404	6 00	11 68426	2 2500	6 00	11 58885
STDEV							
8	DEM24	2 22	6	12 810	2 23	6	12 520
	DEM25	2 17	6	11 630	2 11	5	10 670
	DEM26	2 22	6	12 820	2 11	4	12 130
	DEM27	2 23	6	12 940	2 15	5	12 310
MEAN		2 2100	6 00	12 55000	2 1500	5 00	11 90750
STDEV		0271	00	61617	0566	82	84025
9	DM1	2 22	6	12 092	2 26	6	11 787
	DM2	2 17	6	11 191	2 22	6	12 364
	DM3	2 23	6	12 777	2 20	6	11 040
	DM4	2 14	6	12 436	2 25	6	12 653
	DM5	2 20	6	11 665	2 23	6	10 875
	DM6	2 12	6	10 969	2 20	6	12 328
	DM7	2 27	6	11 817	2 26	6	11 904
	DM8	2 19	6	12 576	2 20	6	13 005
	DM9	2 08	6	11 423	2 10	6	11 258
	DM17	2 32	6	12 594	2 30	6	10 988
MEAN		2 1937	6 00	11 95410	2 2219	6 00	11 82031
STDEV		0723	00	63777	0526	00	75798
TOTAL		2 2526	5 66	12 95780	2 2706	5 21	12 50938
STDEV		1385	74	1 46511	1633	97	1 30947

Physiographic Region	DEM Name	Dividers results 1	2	3	4	5	Equipaced polygon results 1	2	3	4	5
				Individual contour lines							
1	DEM21	1 25	1 16	1 20	1 18	1 16	1 34	1 30	1 27	1 29	1 29
	DEM22	1 16	1 20	1 20	1 20	1 28	1 22	1 28	1 28	1 29	1 32
	DEM23	1 18	1 22	1 20	1 18	1 26	1 23	1 29	1 31	1 26	1 37
MEAN		1 1967	1 1933	1 2000	1 1867	1 2333	1 2633	1 2900	1 2867	1 2800	1 3267
STDEV		0473	0306	0 0000	0115	0613	0666	0100	0208	0173	0404
2	DEM30	1 16	1 16	1 09	1 08	1 17	1 24	1 26	1 19	1 18	1 38
	DEM31	1 13	1 19	1 18	1 16	1 16	1 20	1 27	1 23	1 22	1 24
	DEM32	1 17	1 19	1 31	1 16	1 18	1 26	1 29	1 40	1 25	1 24
	DEM33	1 17	1 15	1 16	1 16	1 38	1 28	1 23	1 26	1 28	1 27
	DEM34	1 40	1 17	1 20	1 21	1 27	1 57	1 22	1 26	1 34	1 24
	DEM35	1 20	1 13	1 14	1 20	1 14	1 29	1 22	1 21	1 25	1 20
	DEM37	1 18	1 22	1 13	1 18	1 16	1 32	1 27	1 20	1 19	1 19
	DEM39	1 15	1 18	1 28	1 10	1 10	1 26	1 28	1 36	1 22	1 13
	DEM40	1 18	1 16	1 20	1 12	1 16	1 31	1 19	1 33	1 21	1 28
MEAN		1 1933	1 1722	1 1878	1 1522	1 1911	1 3033	1 2478	1 2700	1 2378	1 2411
STDEV		0800	0264	0705	0441	0839	1064	0338	0755	0494	0692
3	DEM1										
	DEM2										
	DEM5	1 17	1 16	1 22	1 19	1 15	1 27	1 27	1 27	1 26	1 21
	DEM16	1 19	1 22	1 21	1 18	1 26	1 20	1 29	1 29	1 28	1 32
	DEM17	1 19	1 23	1 15	1 18	1 15	1 26	1 28	1 25	1 16	1 18
	DEM20	1 26	1 29	1 18	1 14	1 16	1 36	1 30	1 27	1 25	1 24
	DEM36	1 20	1 22	1 30	1 10	1 18	1 32	1 30	1 30	1 25	1 19
	DEM38	1 23	1 15	1 16	1 23	1 16	1 28	1 16	1 27	1 15	1 17
	DM11	1 10	1 11	1 01	1 08	1 04	1 65	1 25	1 09	1 12	1 10
	DM12	1 14	1 15	1 06	1 03	1 02	1 22	1 22	1 10	1 11	1 11
	DM13	1 10	1 16	1 07	1 07	1 00	1 17	1 21	1 16	1 11	1 08
	DM14	1 16	1 15	1 13	1 17	1 18	1 23	1 22	1 22	1 10	1 20
MEAN		1 1740	1 1840	1 1490	1 1350	1 1300	1 3050	1 2500	1 2200	1 1790	1 1800
STDEV		0517	0538	0860	0662	0827	1323	0464	0818	0725	0715
4	DEM3	1 20	1 16	1 13	1 10	1 20	1 26	1 22	1 16	1 13	1 15
	DEM4	1 11	1 13	1 16	1 11	1 09	1 24	1 23	1 23	1 13	1 12
	DEM10	1 15	1 20	1 25	1 21	1 36	1 23	1 30	1 28	1 26	1 24
	DEM11	1 06	1 13	1 07	1 13	1 21	1 16	1 17	1 13	1 14	1 30
	DEM12	1 15	1 08	1 17	1 21	1 20	1 21	1 15	1 26	1 31	1 30
	DEM13	1 13	1 06	1 05	1 20	1 21	1 23	1 13	1 13	1 34	1 21
	DEM14	1 14	1 15	1 16	1 18	1 18	1 19	1 20	1 26	1 30	1 27
	DEM18	1 18	1 18	1 12	1 17	1 12	1 24	1 25	1 23	1 18	1 15
	DEM19	1 14	1 18	1 10	1 20	1 25	1 19	1 23	1 28	1 29	1 37
	DEM28	1 16	1 23	1 24	1 20	1 06	1 26	1 39	1 30	1 23	1 18
	DEM29	1 14	1 16	1 16	1 17	1 20	1 24	1 26	1 23	1 24	1 27
	DM10	1 20	1 25	1 20	1 21	1 22	1 24	1 30	1 25	1 30	1 42
	DM15	1 24	1 20	1 19	1 18	1 18	1 32	1 34	1 29	1 22	1 24
	DM16	1 14	1 13	1 16	1 22	1 21	1 17	1 24	1 25	1 45	1 29
MEAN		1 1529	1 1600	1 1543	1 1779	1 1921	1 2271	1 2436	1 2343	1 2514	1 2507
STDEV		0434	0528	0575	0387	0717	0414	0720	0560	0901	0852

Physiographic Region	DEM Name	Dividers results 1	2	3	4	5	Equipaced polygon results 1	2	3	4	5
		Individual contour lines									
5	DEM9	1 22	1 17	1 17	1 19	1 14	1 27	1 22	1 29	1 24	1 18
	DM18	1 24	1 18	1 20	1 12	1 08	1 30	1 22	1 22	1 23	1 20
MEAN		1 2300	1 1750	1 1850	1 1550	1 1100	1 2850	1 2200	1 2550	1 2350	1 1900
STDEV		0141	0071	0212	0495	04[illegible]	0212	0 0000	0495	0071	0141
6	DEM6										
	DEM7	1 16	1 17	1 18	1 25	1 25	1 21	1 25	1 22	1 33	1 33
	DEM8	1 10	1 20	1 19	1 23	1 19	1 17	1.25	1 29	1 35	1 27
MEAN		1 1300	1 1850	1 1850	1 2400	1 2200	1 1900	1 2500	1 2550	1 3400	1.3000
STDEV		0424	0212	.0071	0141	0424	0283	0 0000	0495	0141	0424
7	DM20	1 17	1 15	1.11	1 08	1 04	1 27	1 27	1 26	1 20	1 12
MEAN		1 1700	1 1500	1 1100	1 0800	1 0400	1 2700	1 2700	1.2600	1 2000	1 1200
STDEV											
8	DEM24	1 17	1 18	1 10	1 17	1 08	1 25	1 23	1 21	1 30	1 14
	DEM25	1 14	1 30	1 17	1 12	1 10	1 26	1 46	1 27	1.26	1 24
	DEM26	1 27	1 39	1 28	1 12	1 16	1 33	1 42	1 34	1 25	1 19
	DEM27	1 13	1 16	1 15	1 18	1 16	1 32	1 27	1 23	1 22	1 28
MEAN		1 1775	1 2575	1 1750	1 1475	1 1250	1 2900	1 3450	1 2625	1.2575	1 2125
STDEV		0640	1078	0759	0320	0412	0408	1121	0574	0330	0608
9	DM1	1 11	1 11	1 13	1 18	1 14	1 16	1 15	1 16	1 18	1 18
	DM2	1 08	1 13	1 12	1 08	1 02	1 13	1 12	1 13	1 12	1 22
	DM3	1 34	1 10	1 14	1 13	1 09	1 18	1 22	1 18	1 17	1 22
	DM4	1 23	1 12	1.09	1 14	1 30	1 28	1 30	1 17	1 18	1 26
	DM5	1 15	1 09	1 11	1 12	1 14	1 22	1 19	1 16	1 16	1 14
	DM6	1 14	1 23	1 02	1 02	1 03	1 24	1 32	1 08	1 07	1 11
	DM7	1 11	1 08	1 06	1 01	1 02	1 05	1 14	1 13	1 10	1 06
	DM8	1 01	1 00	1 04	1 07	1 06	1 09	1 06	1 10	1 15	1 13
	DM9	1 26	1 17	1 21	1.14	1 04	1 25	1 23	1 26	1 17	1 10
	DM17	1 25	1 26	1 18	1 21	1 14	1 28	1 26	1 31	1 20	1 23
MEAN		1 1680	1 1290	1 1100	1 1100	1 0980	1 1980	1 1990	1 1680	1 1500	1 1650
STDEV		0995	0752	0598	0648	0868	0656	0827	0700	0408	0664
TOTAL		1 1725	1 1709	1 1562	1 1515	1 1562	1 2565	1 2471	1 2324	1 2213	1 2193
STDEV		0652	0623	0670	0565	0846	0891	0700	0717	0770	0813

Appendix 2

Contour plots of the DEMs

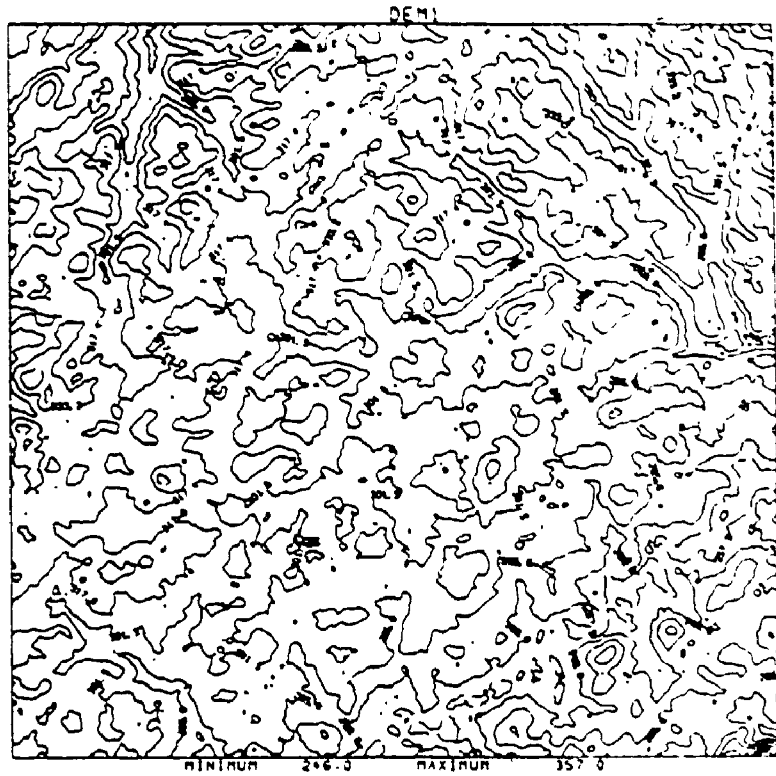
DEM1
MINIMUM 246.0
MAXIMUM 357.0

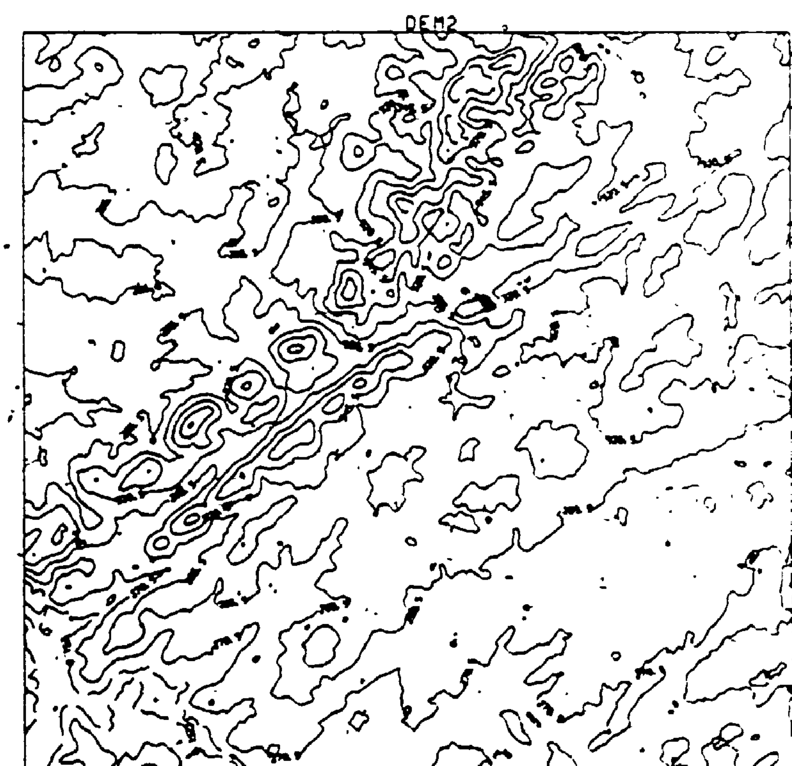
DEM2
MINIMUM 233.0
MAXIMUM

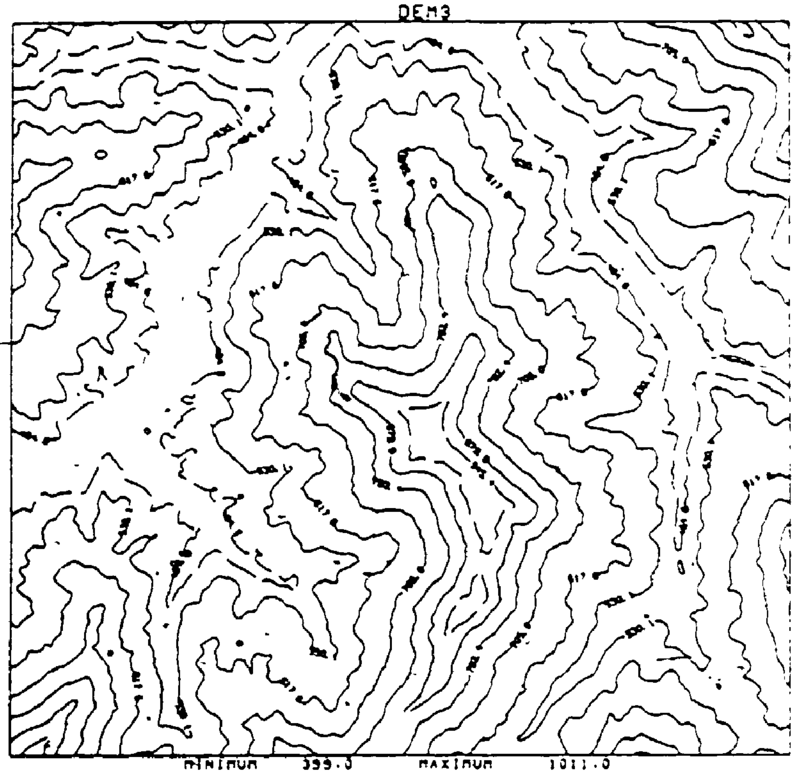
DEM3
MINIMUM 399.0 MAXIMUM 1011.0

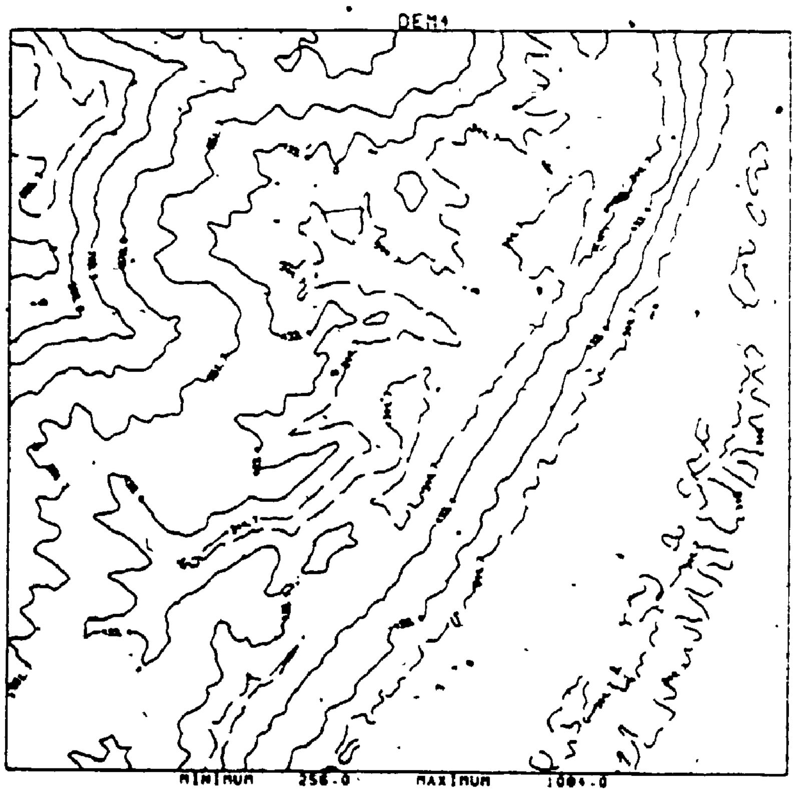
DEM4
MINIMUM 256.0 MAXIMUM 1004.0

DEM5

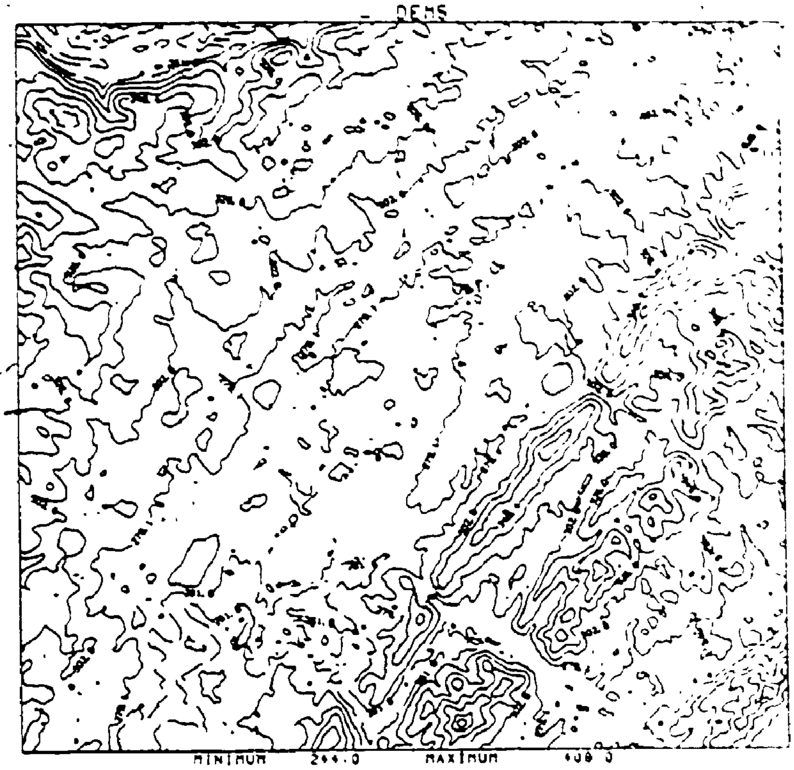

DEM6

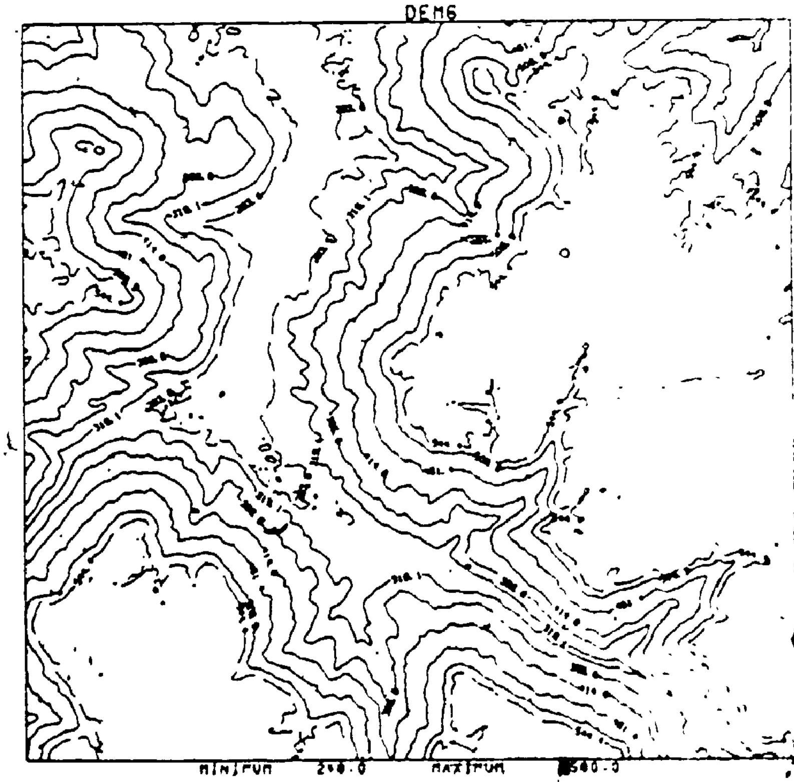

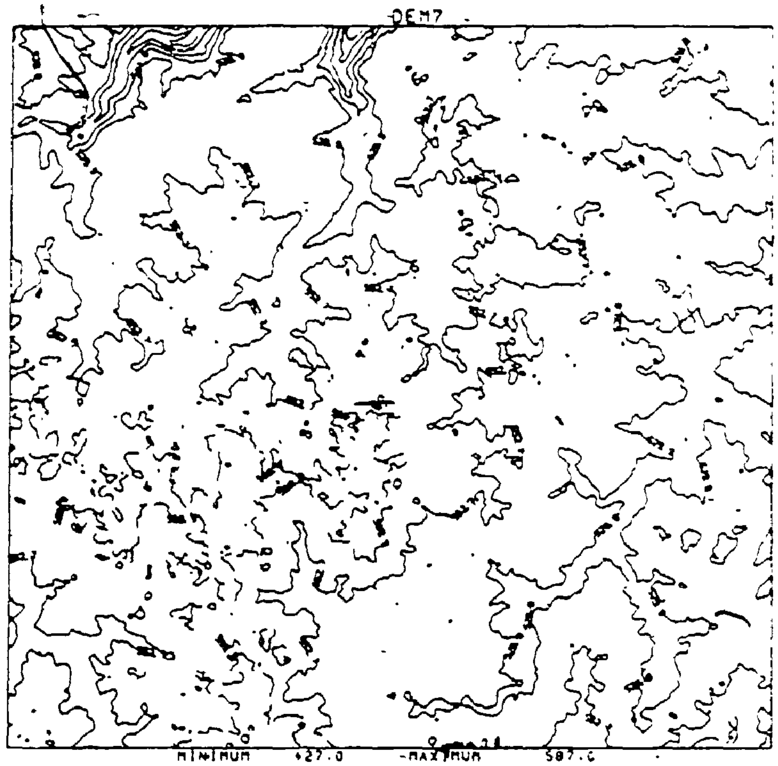
DEM7
MINIMUM 427.0
MAXIMUM 587.0

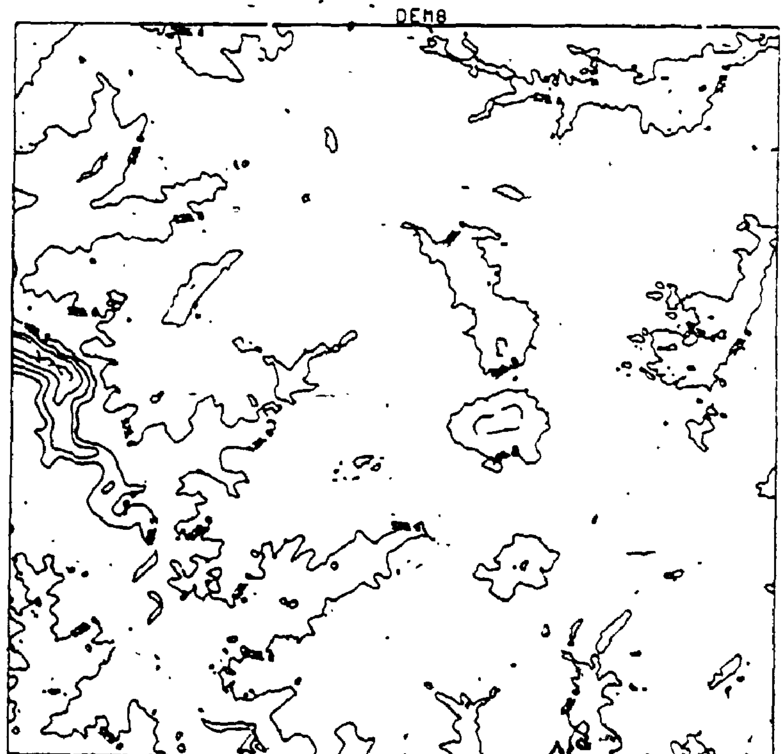
DEM8
MINIMUM 367.0
MAXIMUM 620.0

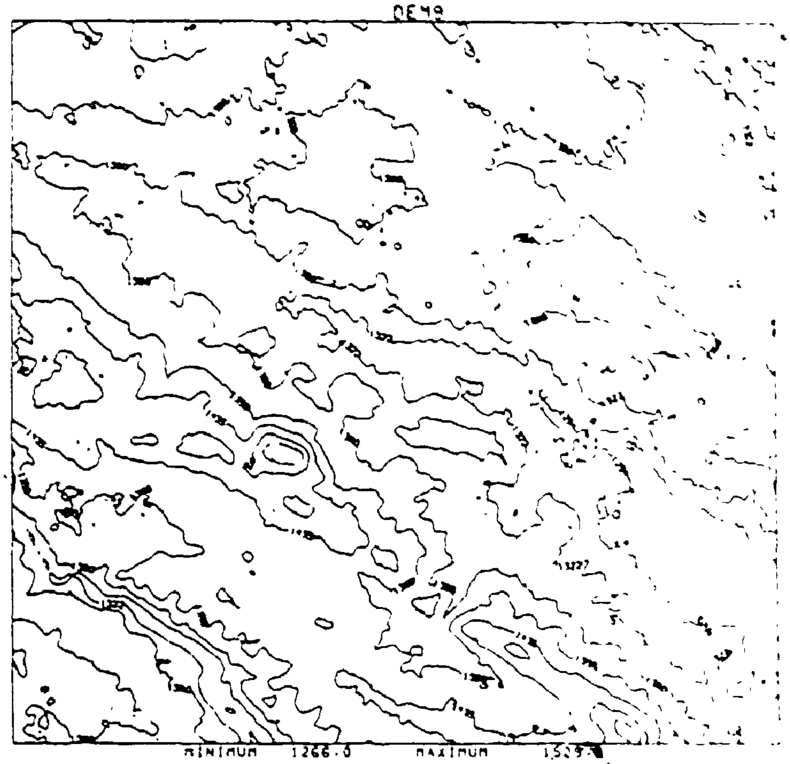
DEM9
MINIMUM 1266.0 MAXIMUM

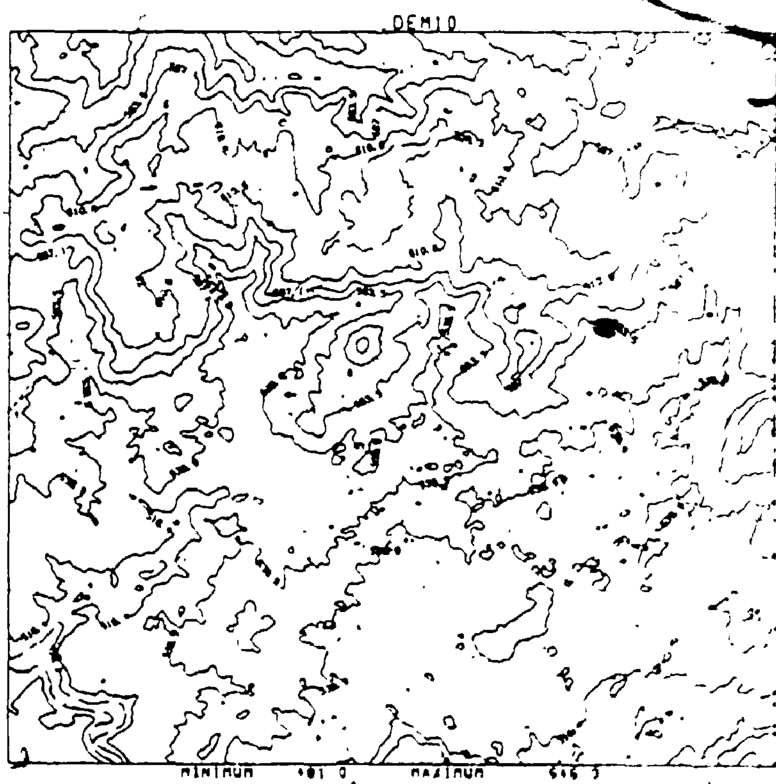
DEM10
MINIMUM MAXIMUM

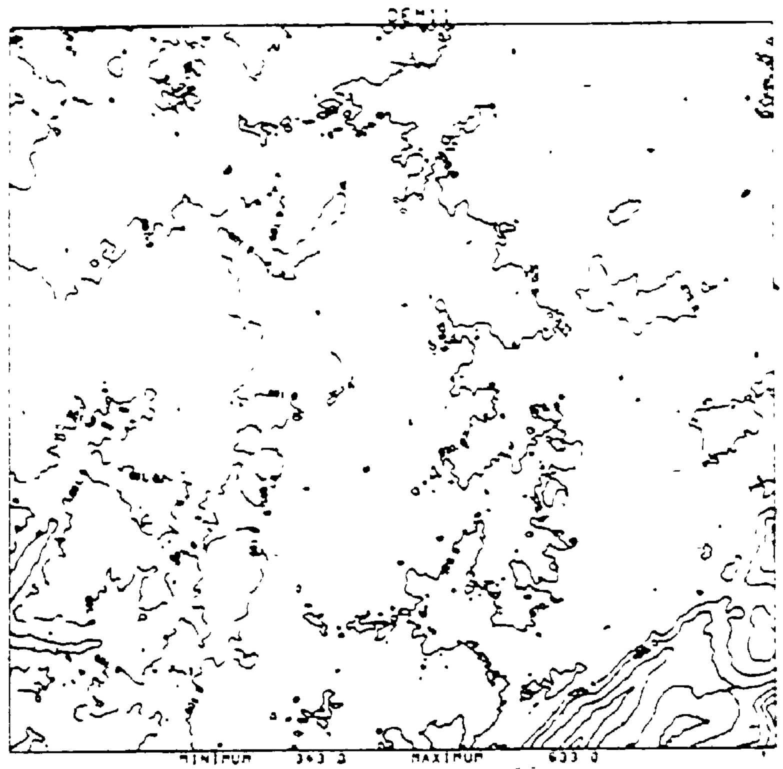
DEM11
MINIMUM 343.0 MAXIMUM 633.0

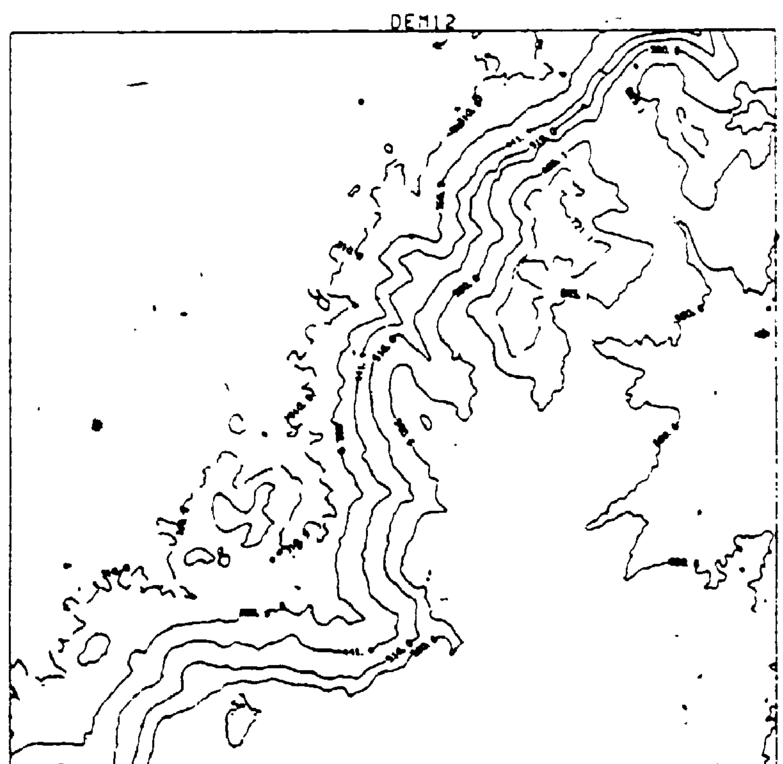
DEM12
MINIMUM 255.0 MAXIMUM

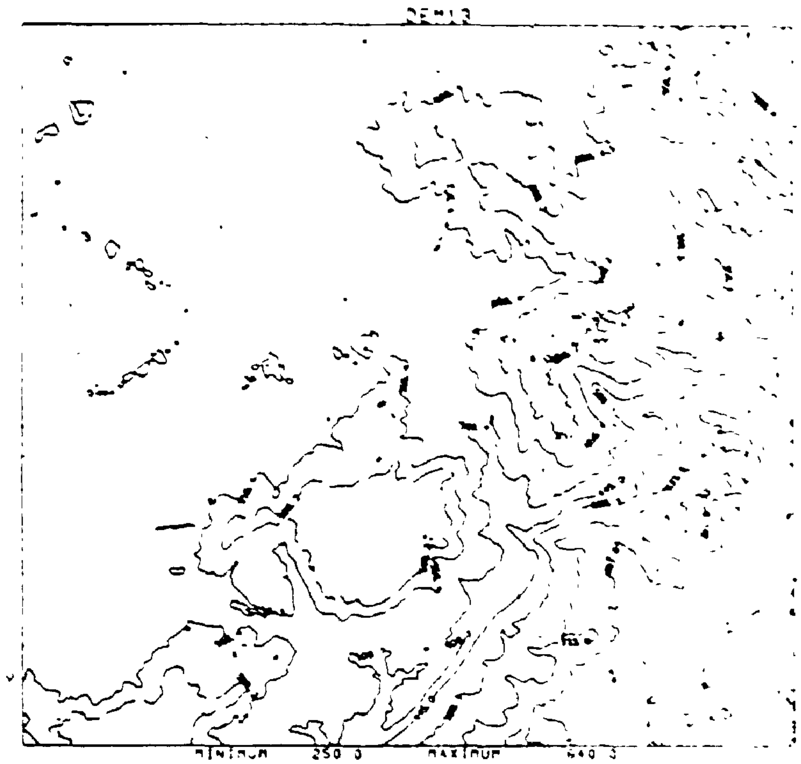
DEM13
MINIMUM
250.0
MAXIMUM

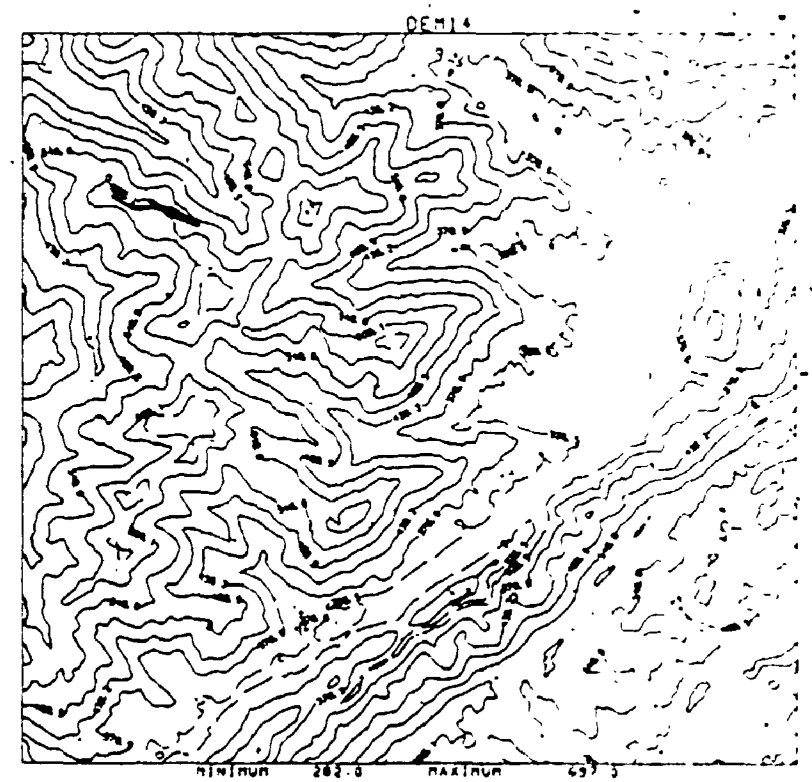
DEM14
MINIMUM
282.0
MAXIMUM

DEM16

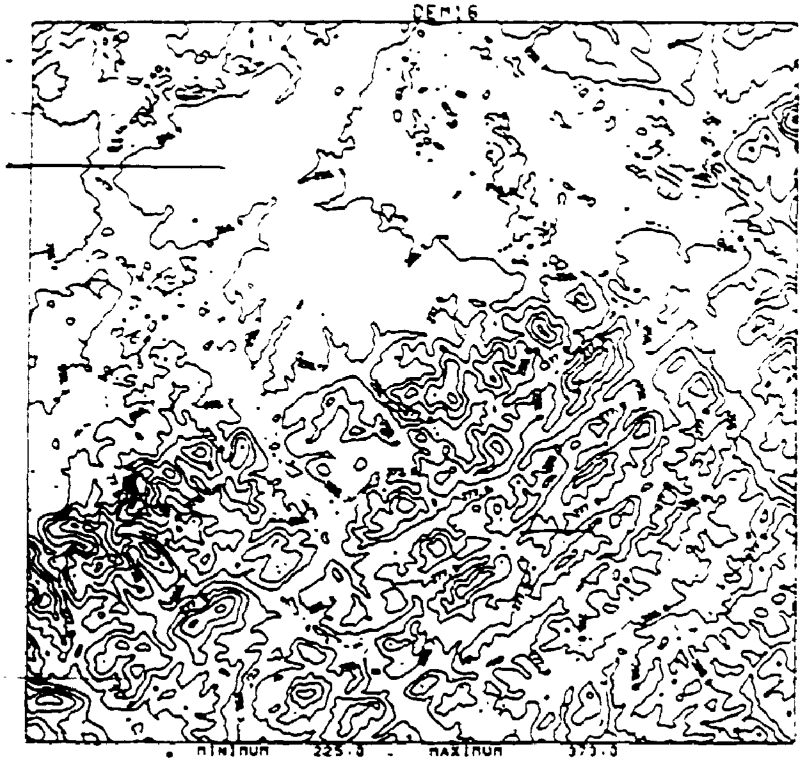

DEM17

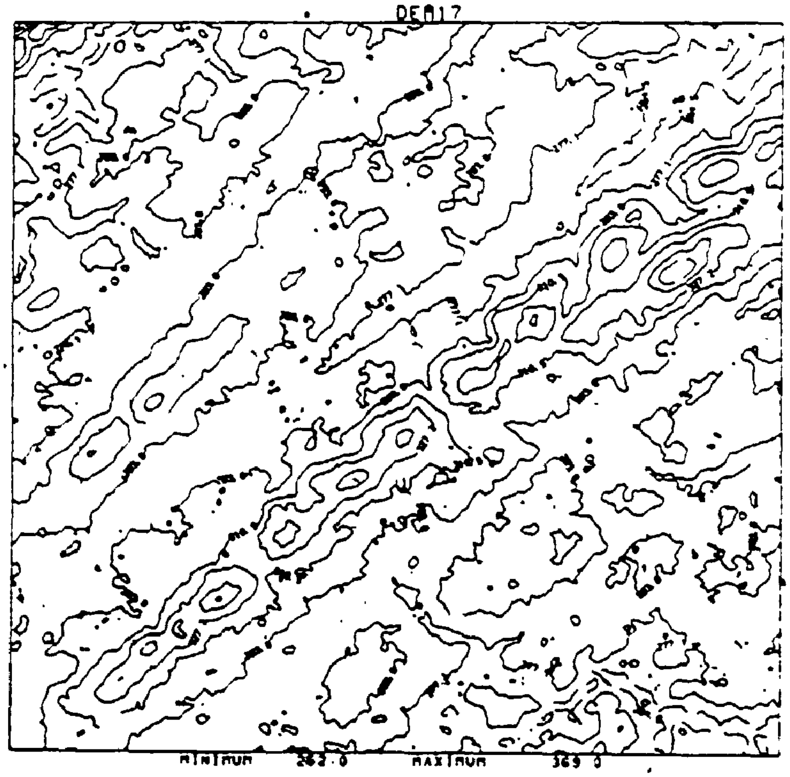

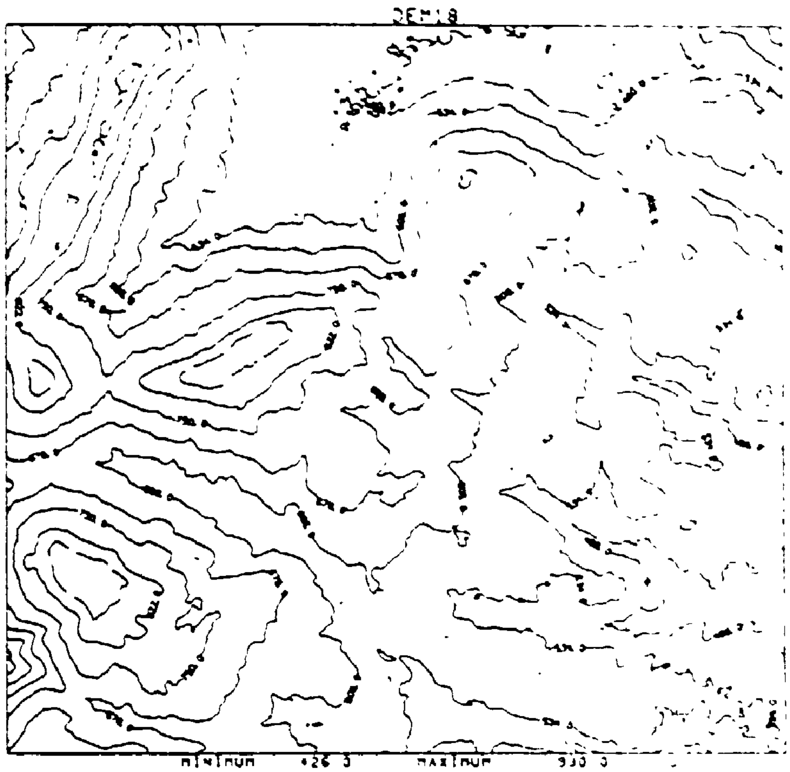
DEM18
MINIMUM 426.0 MAXIMUM 930.0

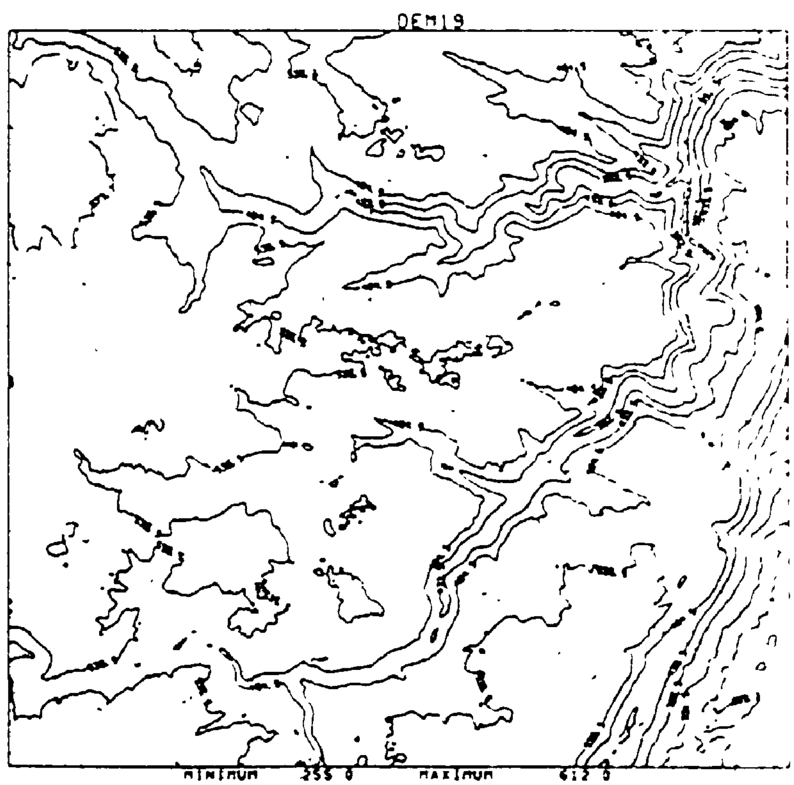
DEM19
MINIMUM 255.0 MAXIMUM 612.0

DEM20

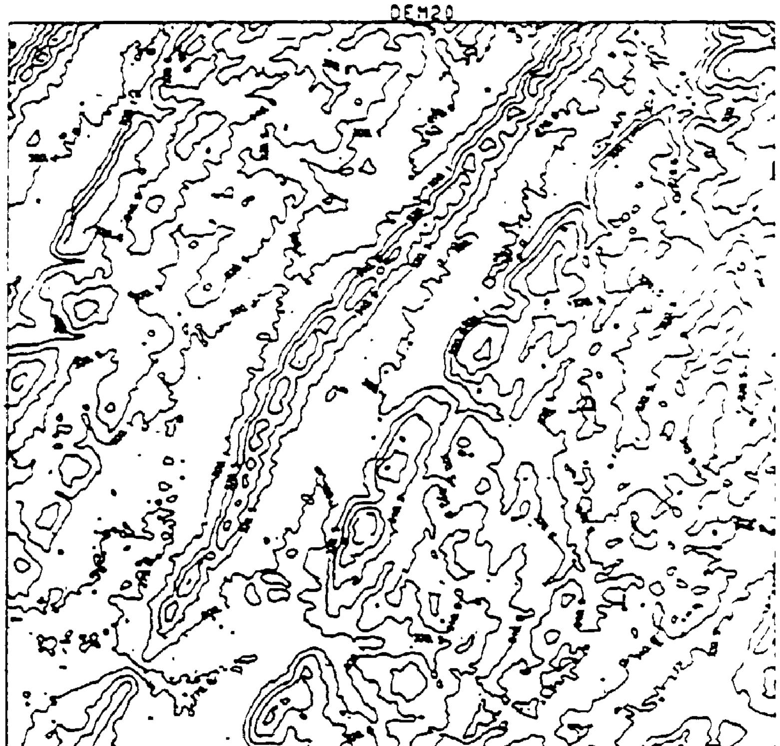

MINIMUM 245.0 MAXIMUM 392.0

DEM21

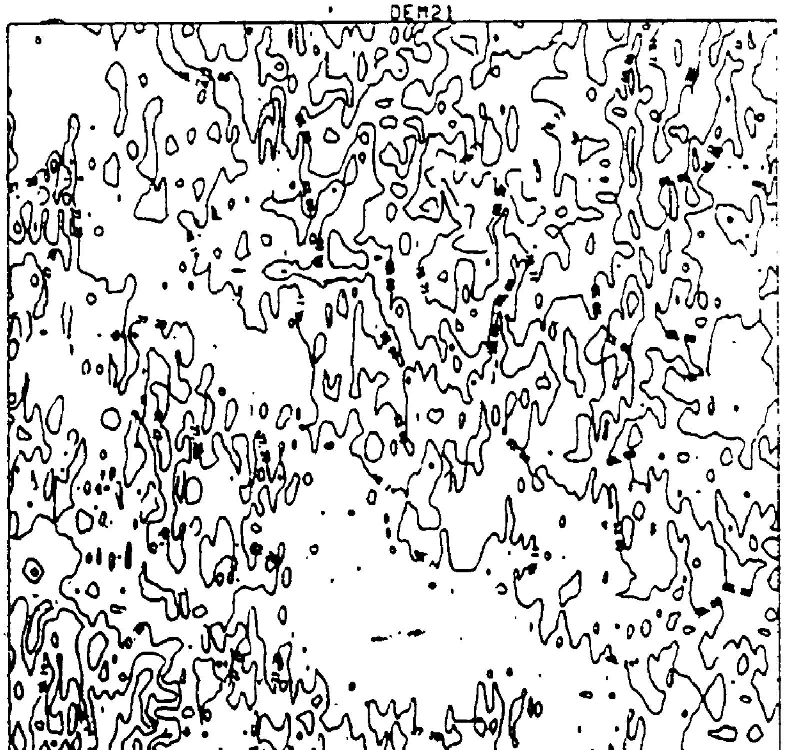

MINIMUM 0.0 MAXIMUM 38.0

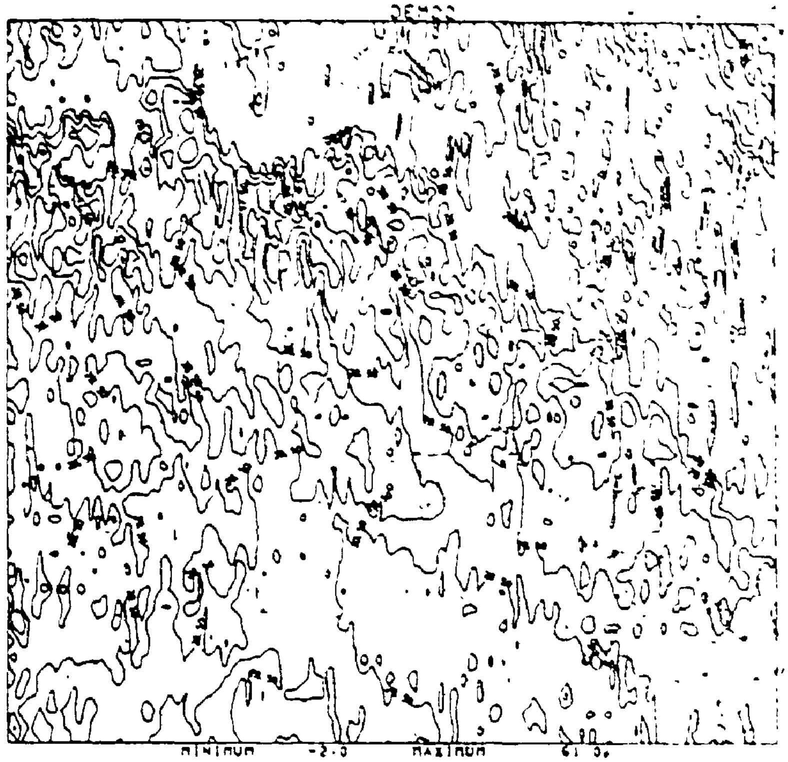
MINIMUM -2.0 MAXIMUM 61.0

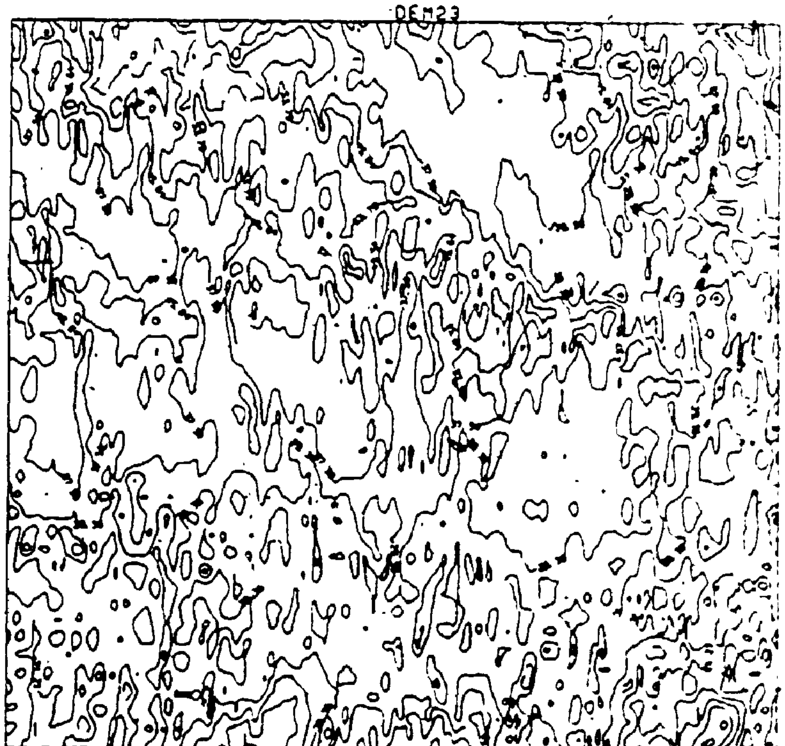
DEM23
MINIMUM 9.0 MAXIMUM 66.0

DEM24

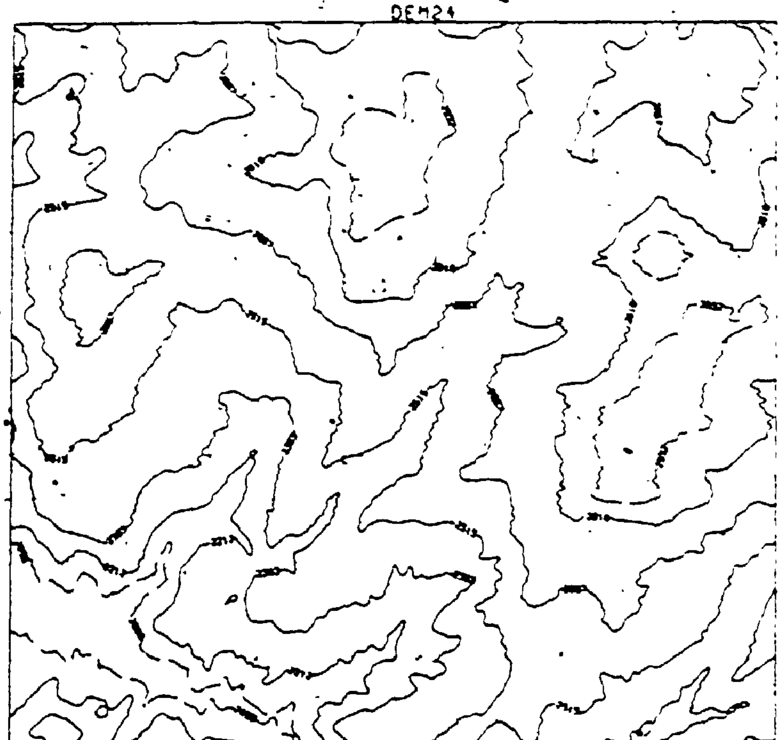

DEM25

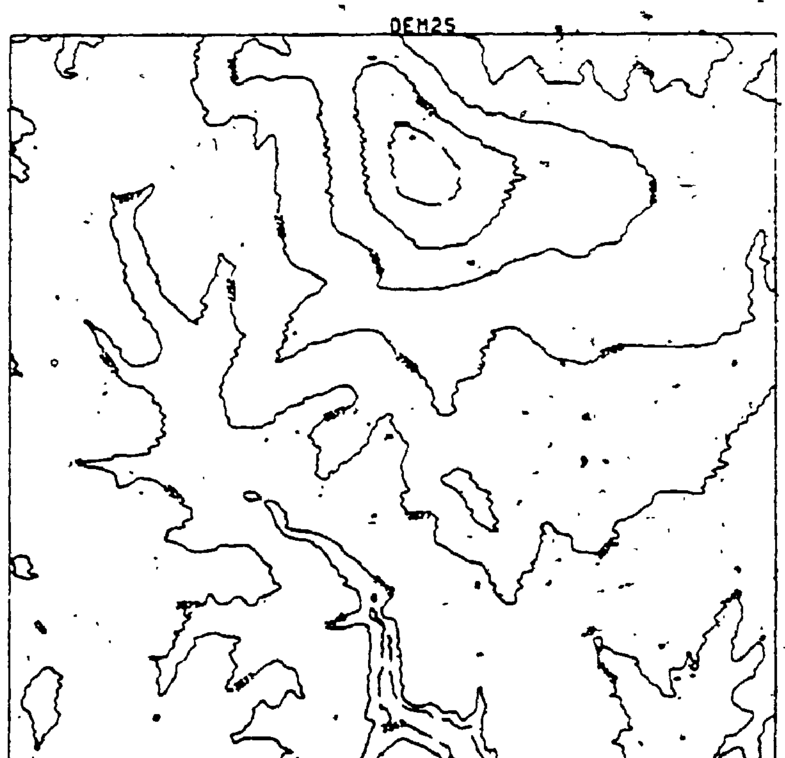

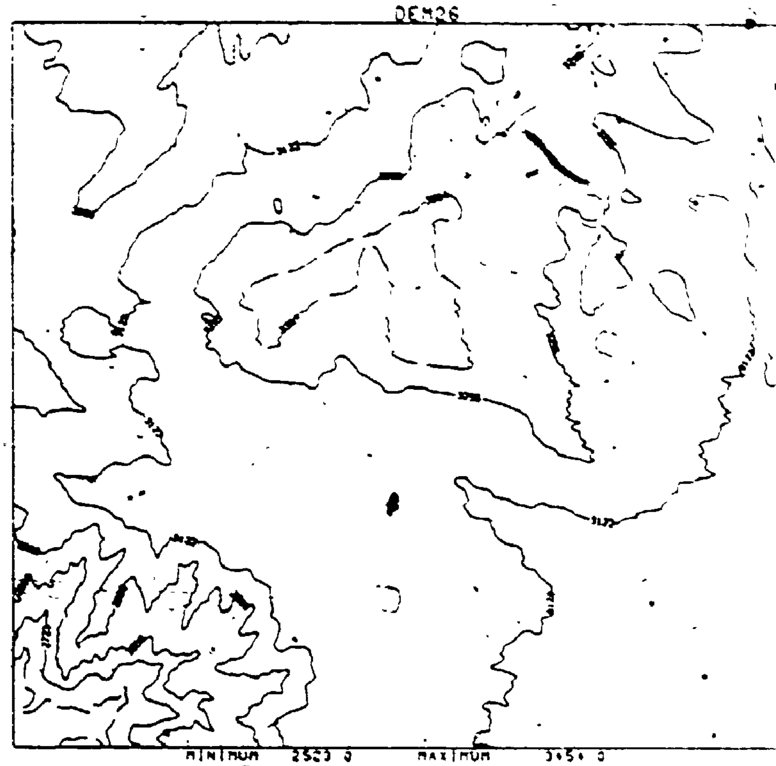
DEM26
MINIMUM 2523.0 MAXIMUM 3454.0

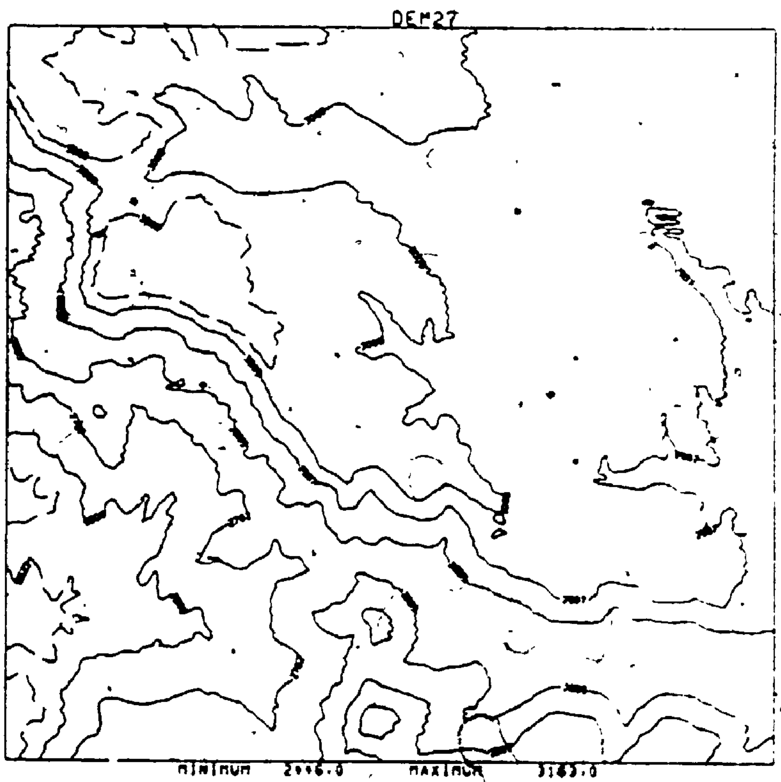
DEM27
MINIMUM 2996.0 MAXIMUM 3183.0

DEM28

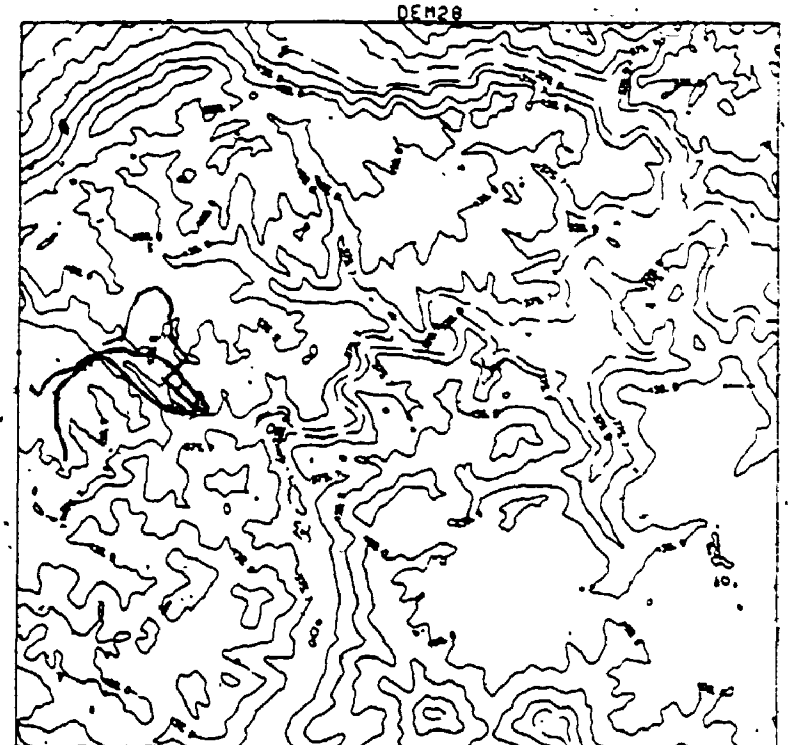

MINIMUM 284.0 MAXIMUM 712.0

DEM29

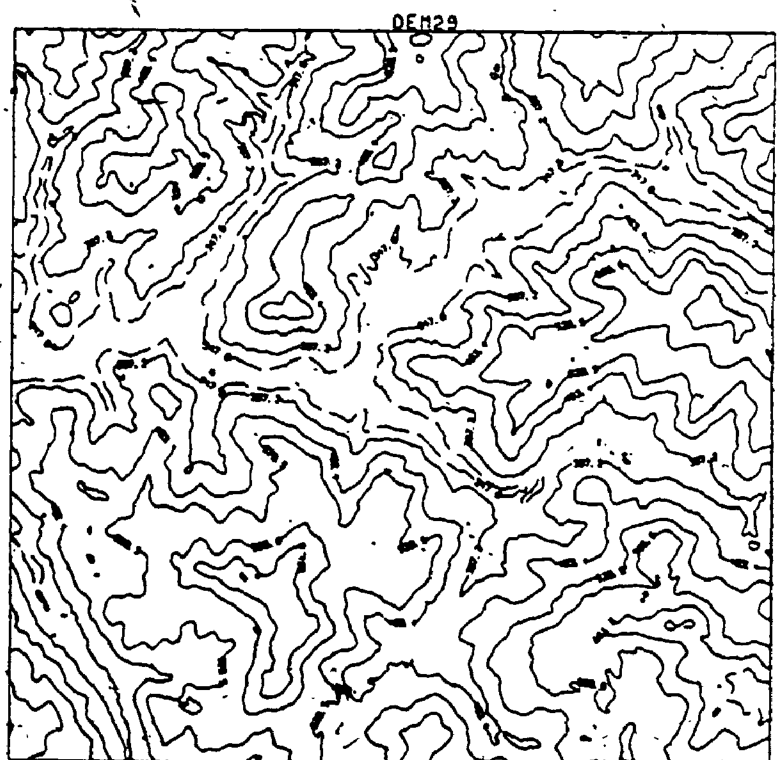

MINIMUM 298.0 MAXIMUM 761.0

DEM30

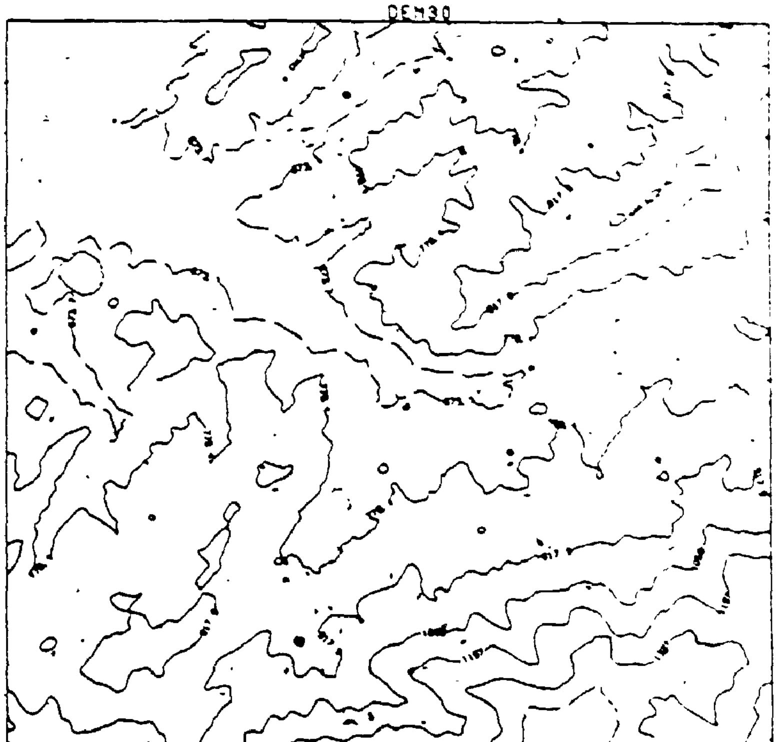

MINIMUM 565.0 MAXIMUM 1546.0

DEM31

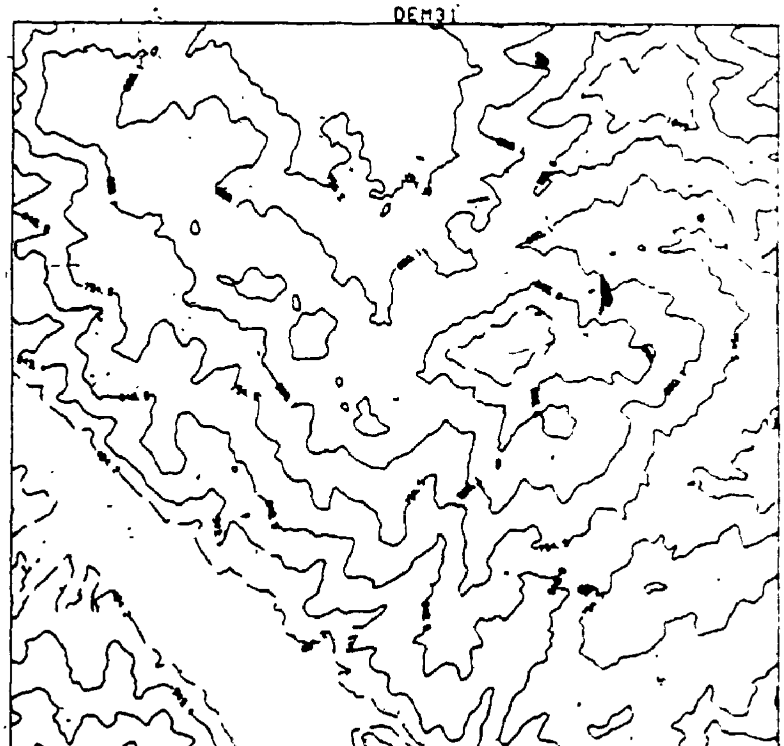

MINIMUM 385.0 MAXIMUM 1124.0

DEM32

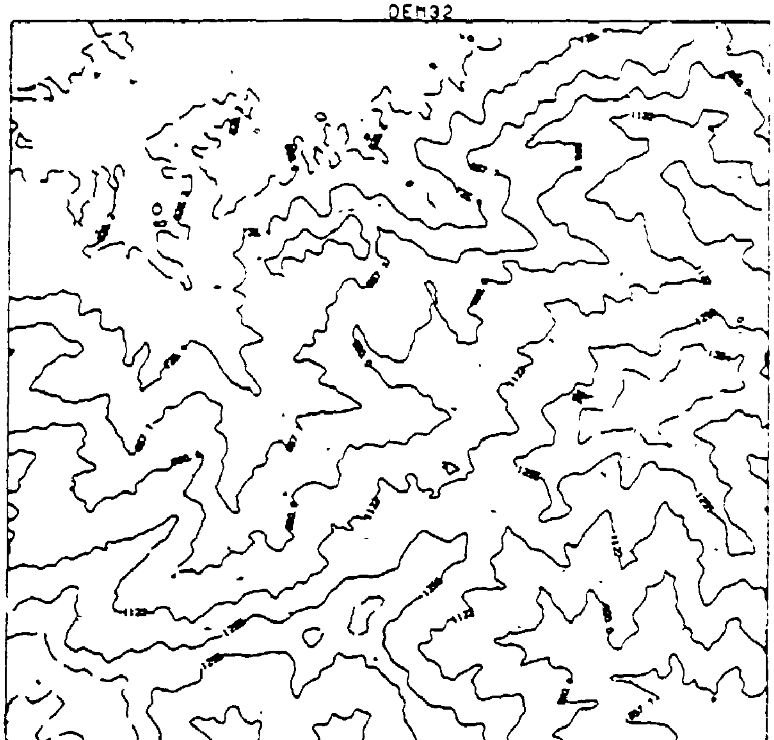

MINIMUM 527.0 MAXIMUM 1453.0

DEM33

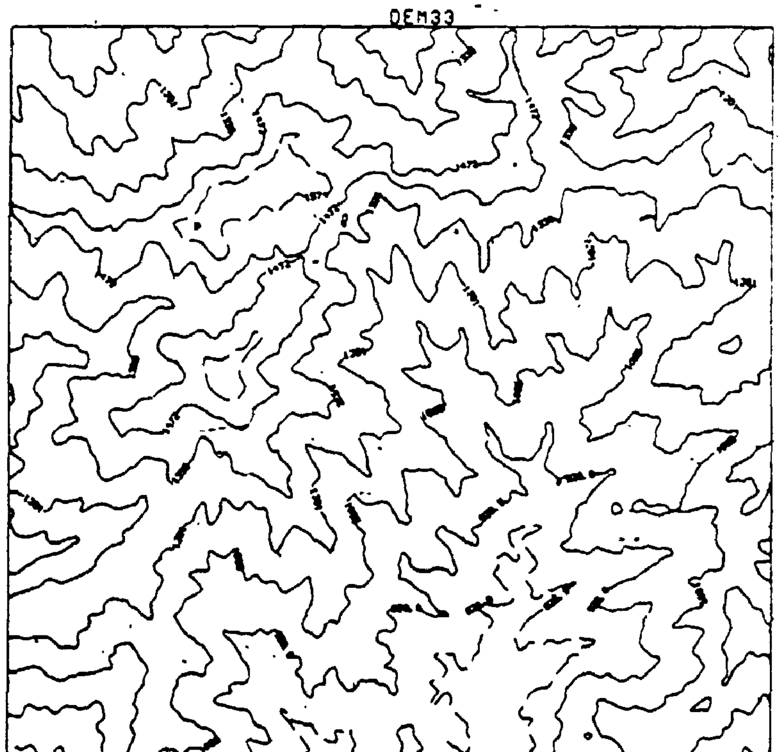

MINIMUM 725.0 MAXIMUM 1676.0

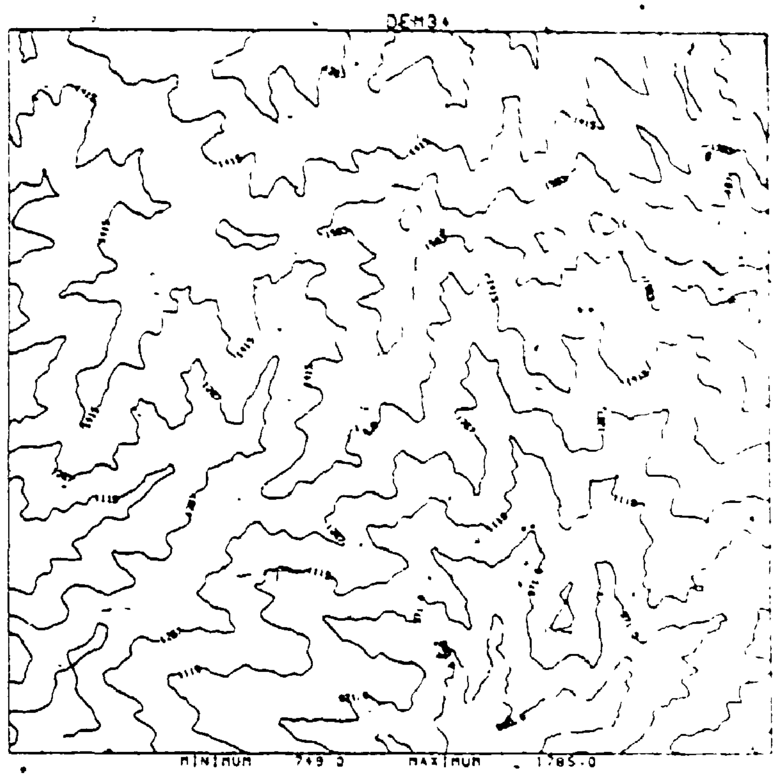
DEM34
MINIMUM 749.0 MAXIMUM 1785.0

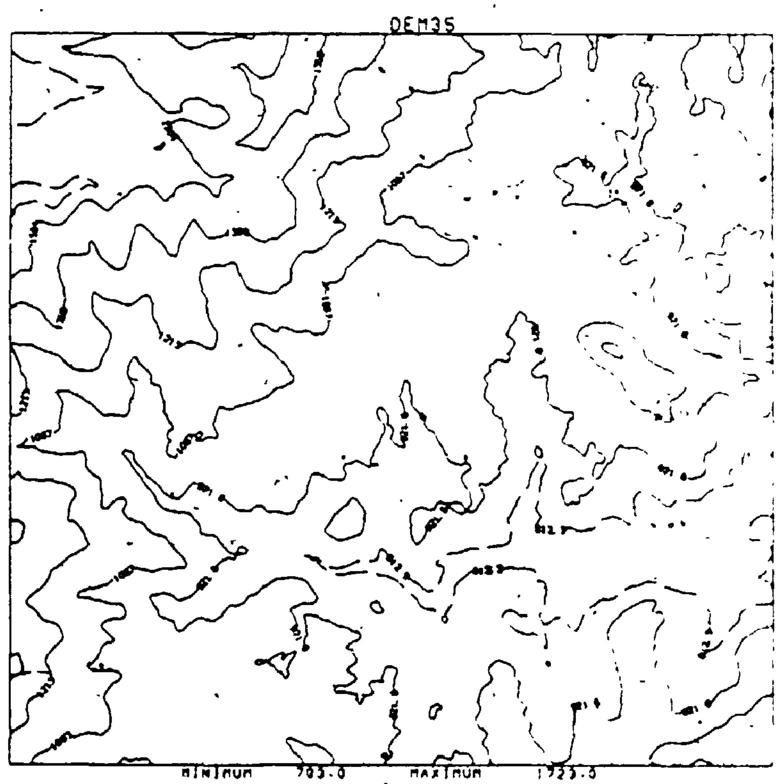
DEM35
MINIMUM 703.0 MAXIMUM 1723.0

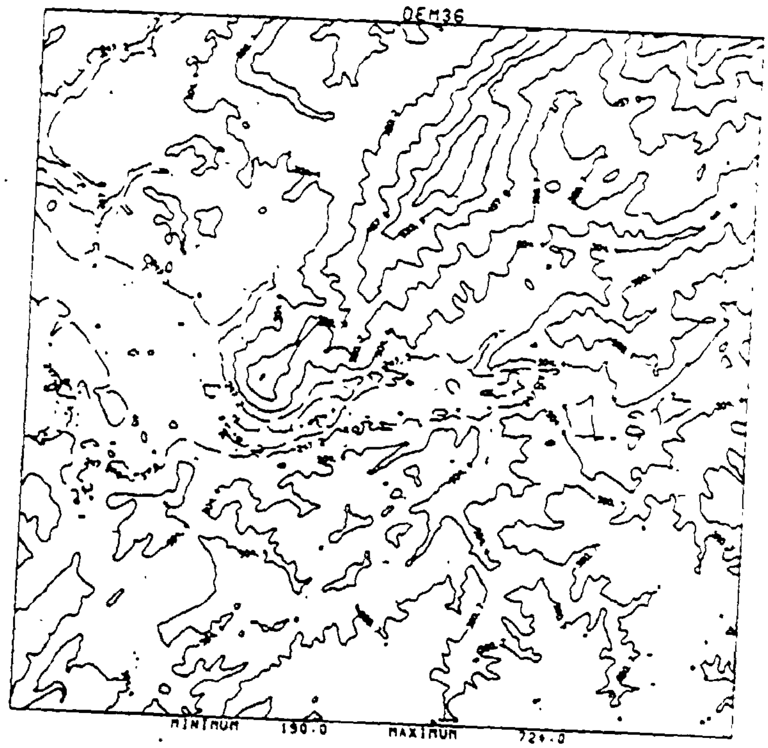
DEM36
MINIMUM 190.0 MAXIMUM 724.0

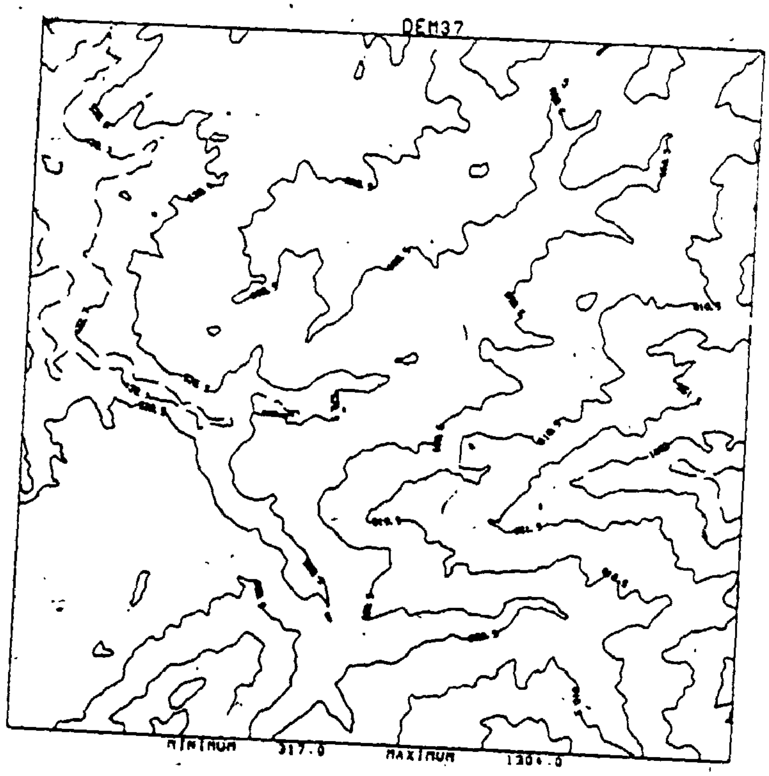
DEM37
MINIMUM 317.0 MAXIMUM 1304.0

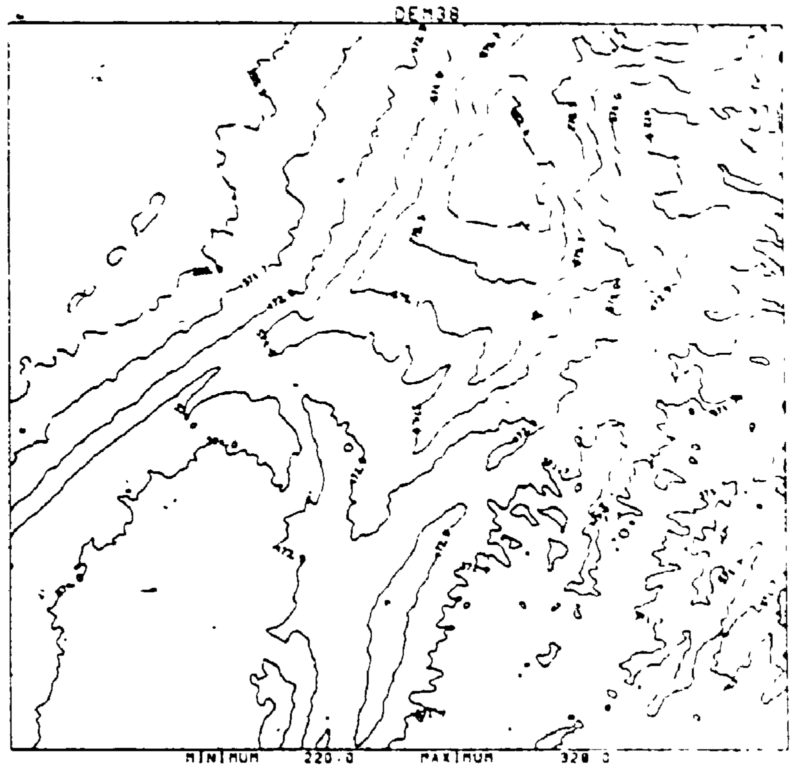
DEM38
MINIMUM 220.0
MAXIMUM 320.0

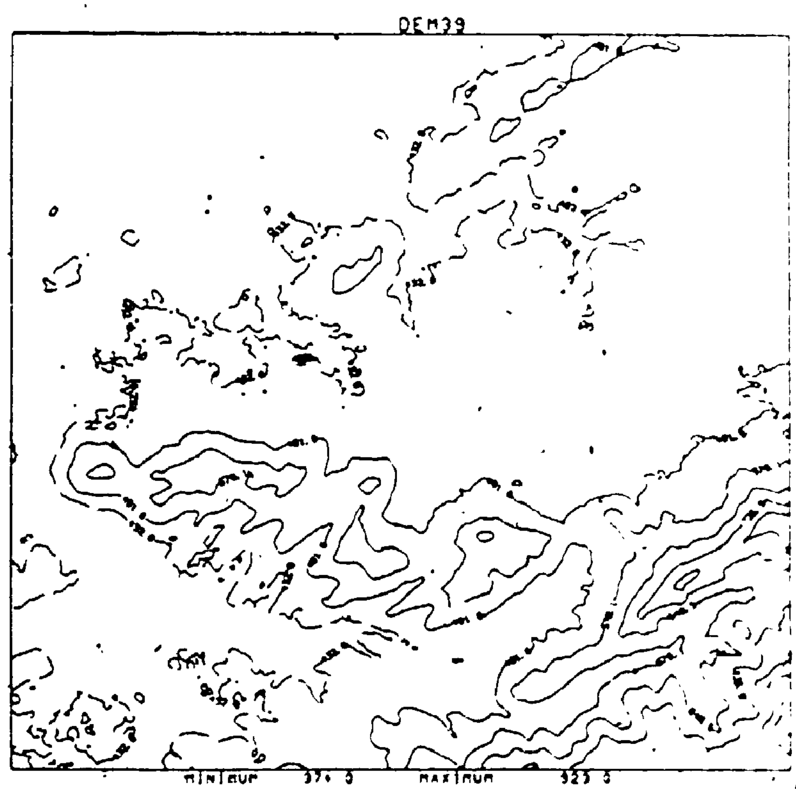
DEM39
MINIMUM
MAXIMUM

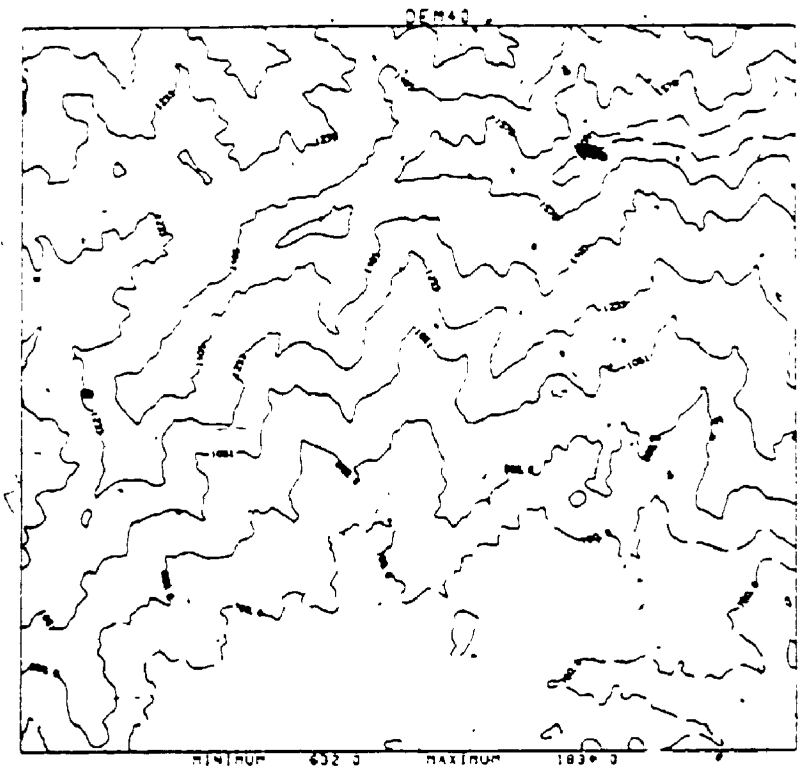
DEM40
MINIMUM 632.0 MAXIMUM 1834.0

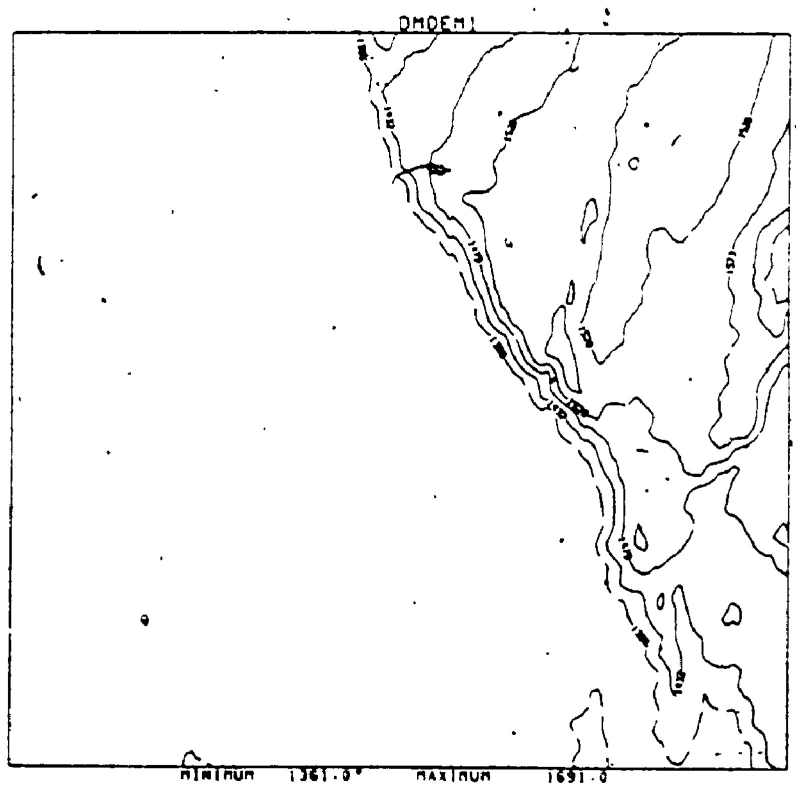
DMDEM1
MINIMUM 1361.0 MAXIMUM 1691.0

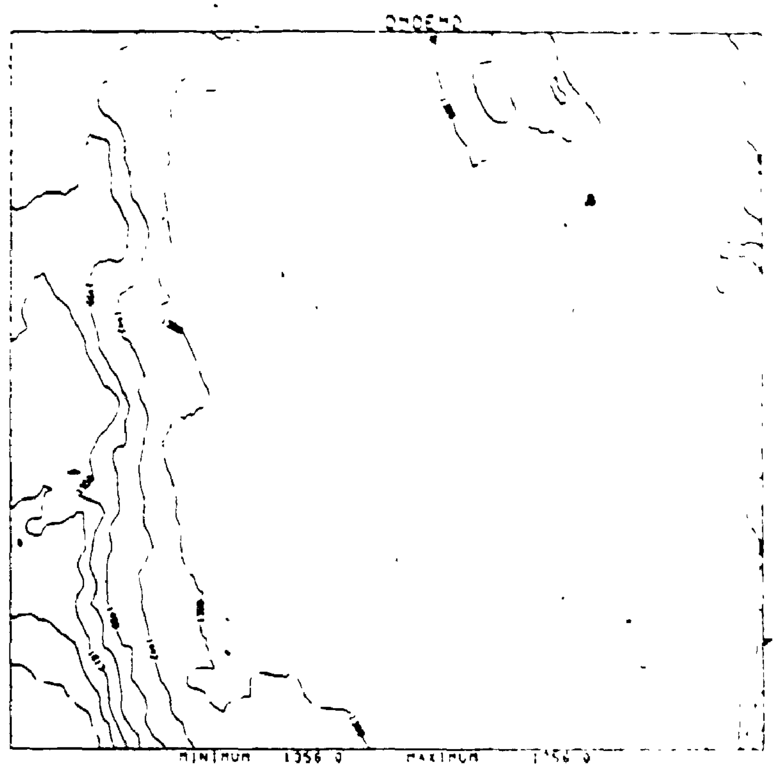
MINIMUM 1356.0
MAXIMUM

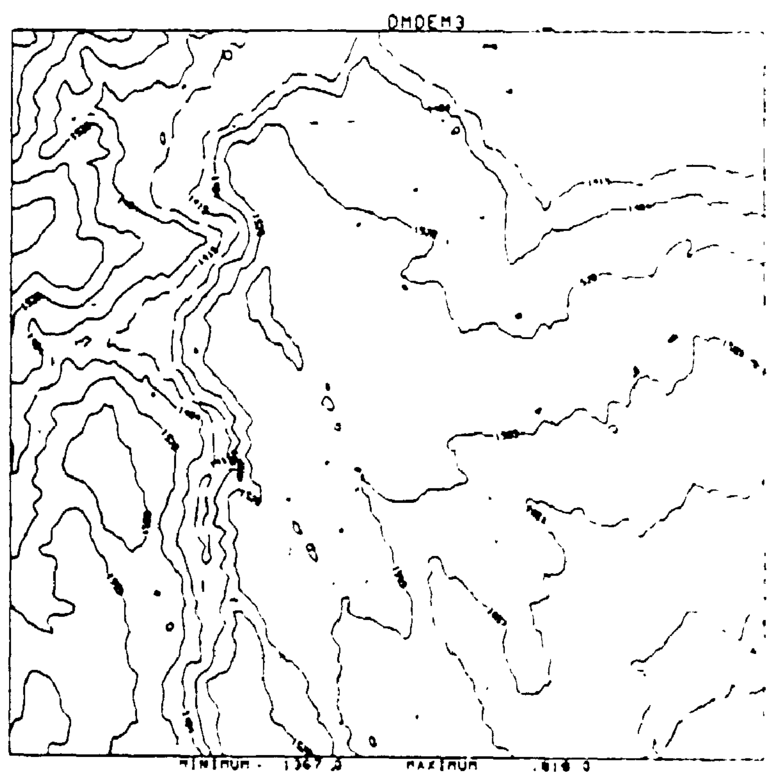
DMDEM3
MINIMUM 1367.0
MAXIMUM

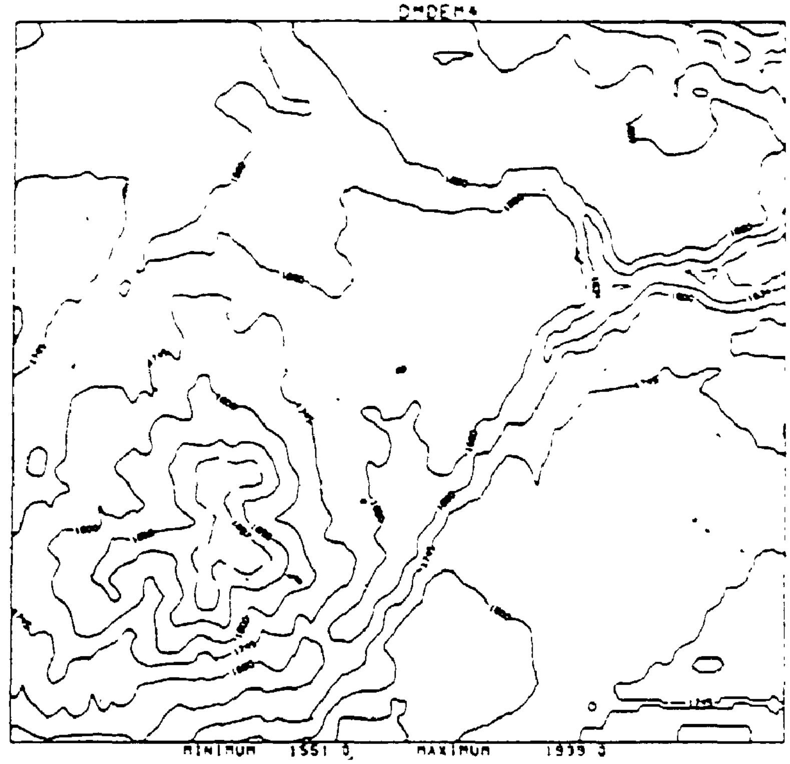
DMDEM4
MINIMUM 1551.0 MAXIMUM 1939.0

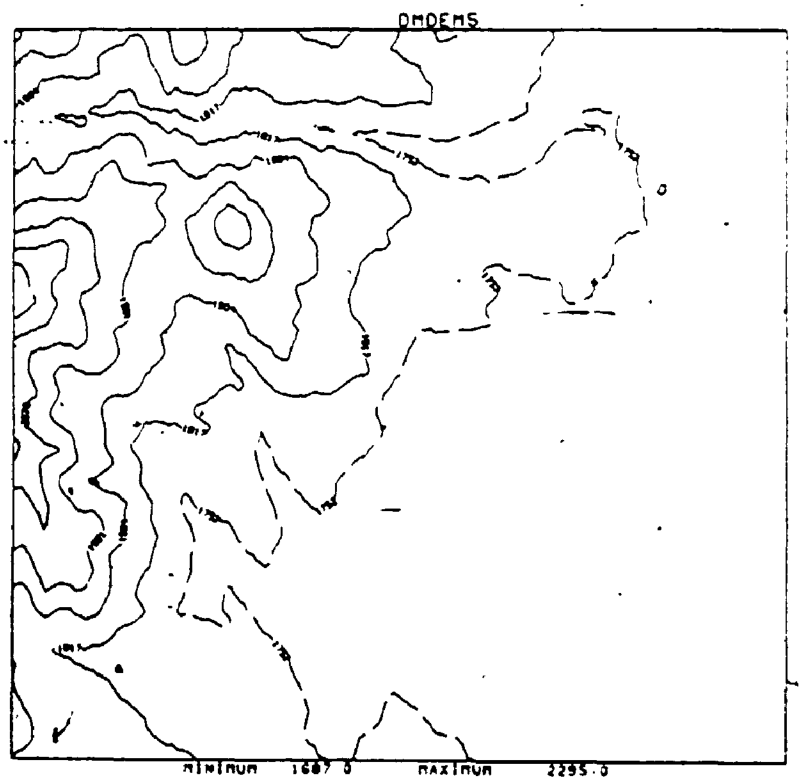
DMDEM5
MINIMUM 1687.0 MAXIMUM 2295.0

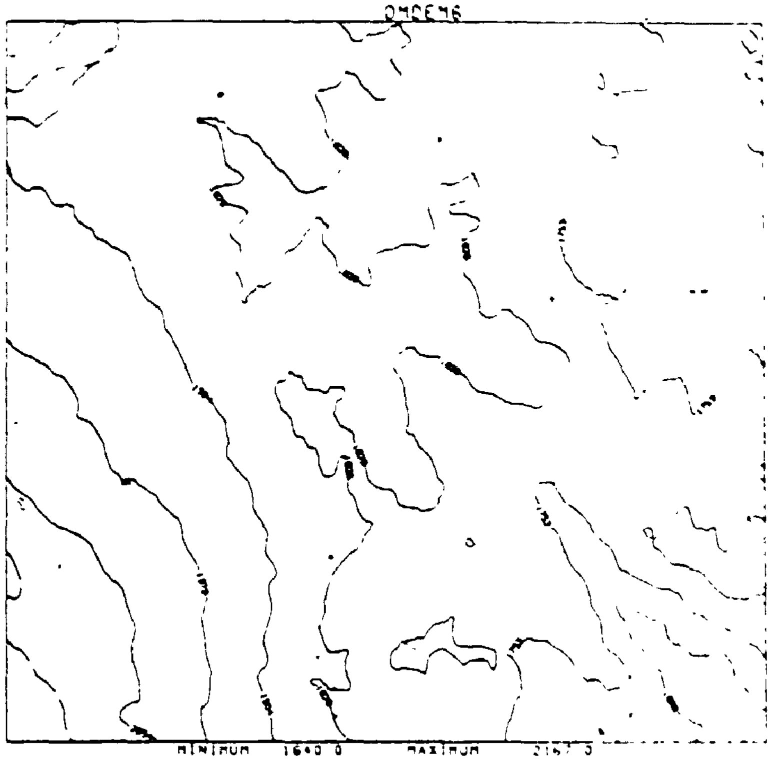

DMDEM6
MINIMUM 1640.0 MAXIMUM 2167.0

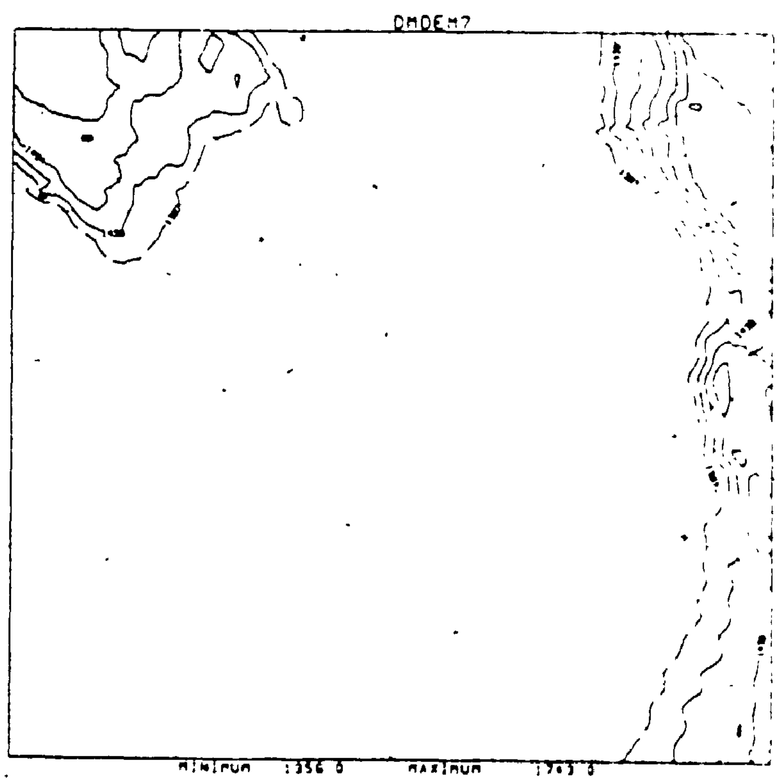

DMDEM7
MINIMUM 1356.0 MAXIMUM 1743.0

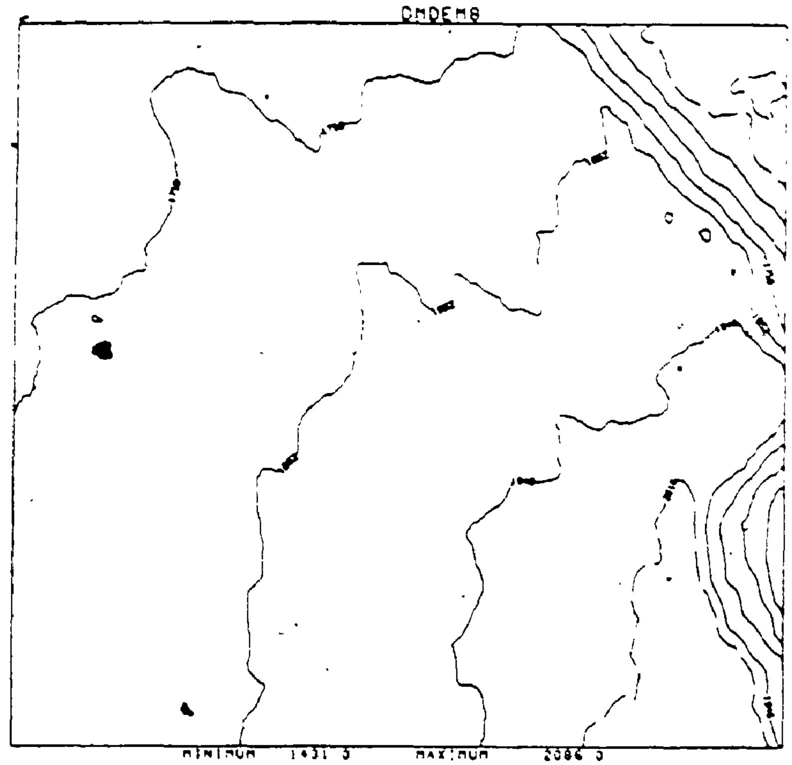
DMDEM8
MINIMUM 1431.3 MAXIMUM 2086.3

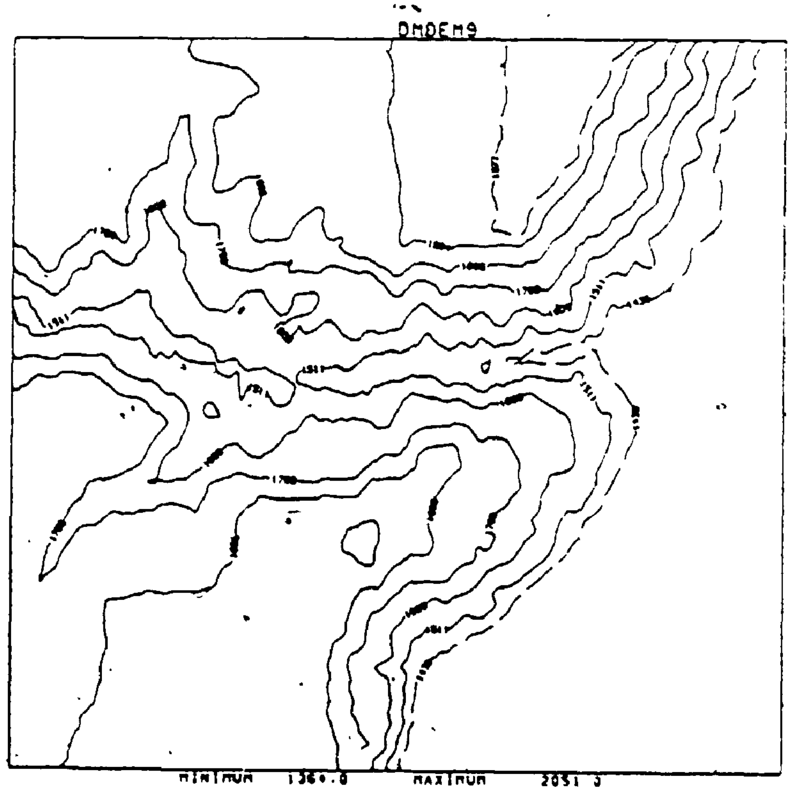
DMDEM9
MINIMUM 1364.0 MAXIMUM 2051.3

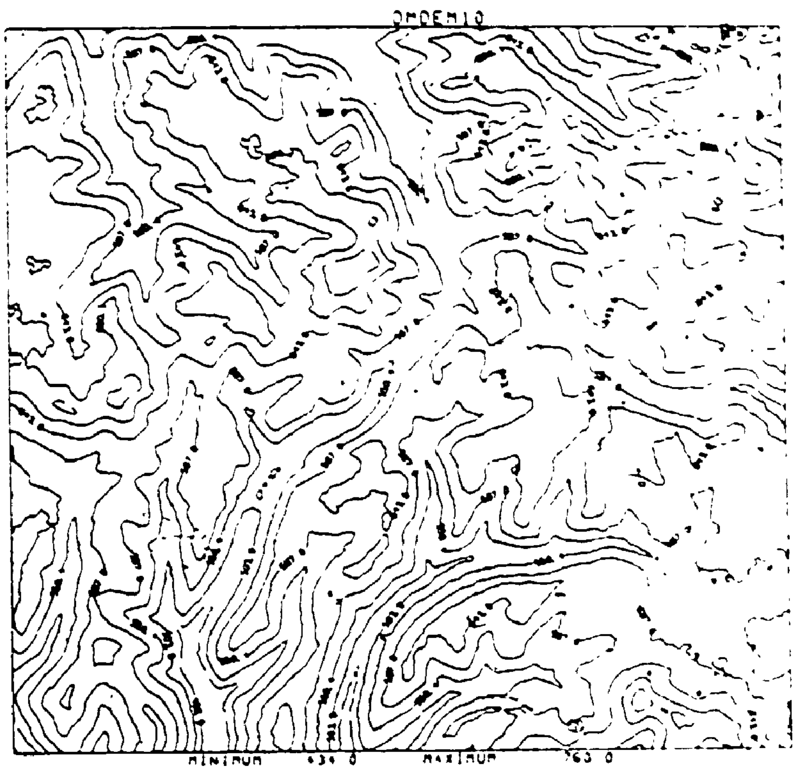
DMDEM10
MINIMUM 434.0
MAXIMUM 763.0

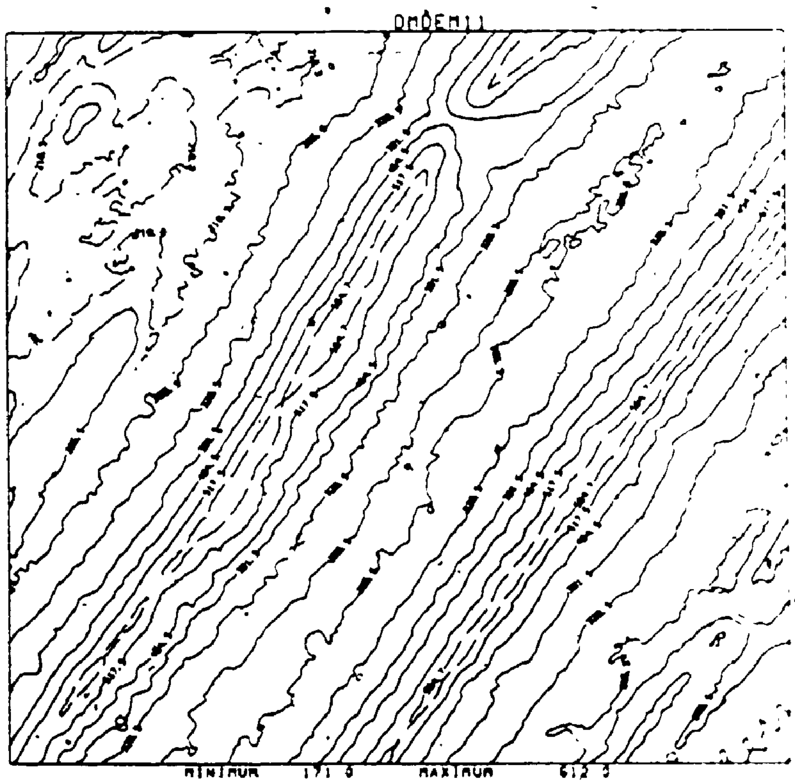
DMDEM11
MINIMUM 171.0
MAXIMUM 612.0

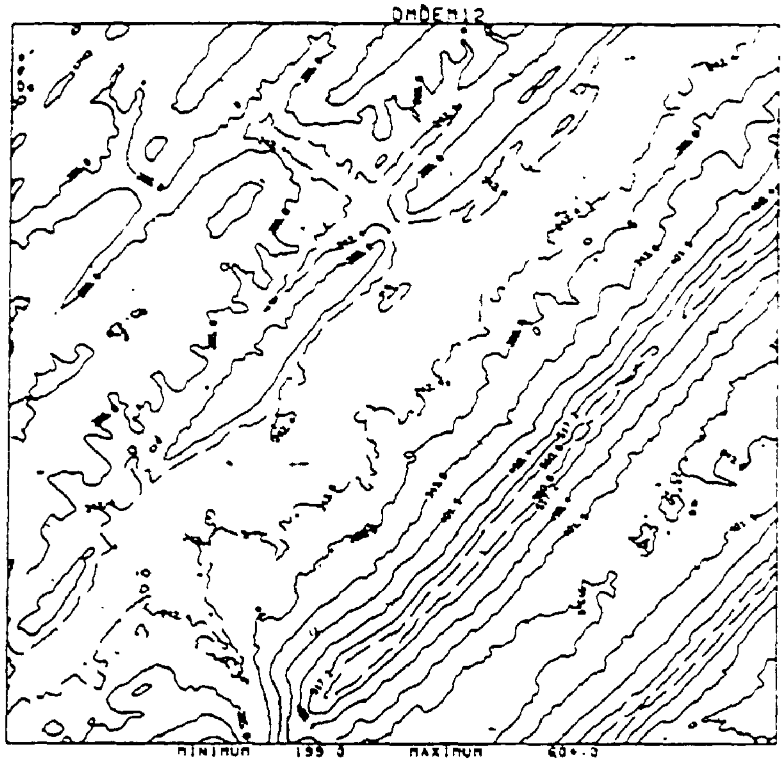
DMDEM12
MINIMUM 199.0 MAXIMUM 604.0

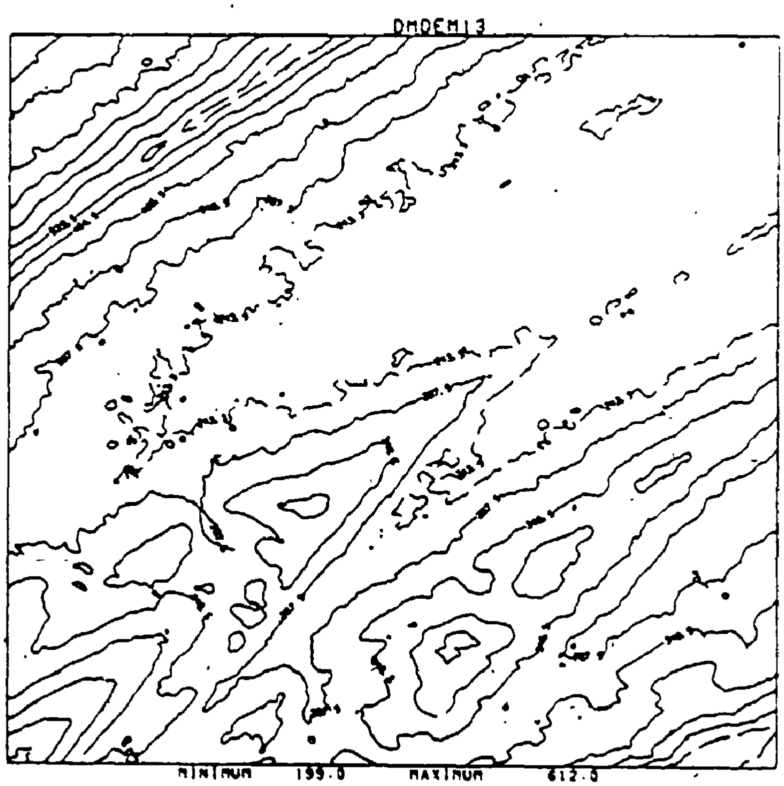
DMDEM13
MINIMUM 199.0 MAXIMUM 612.0

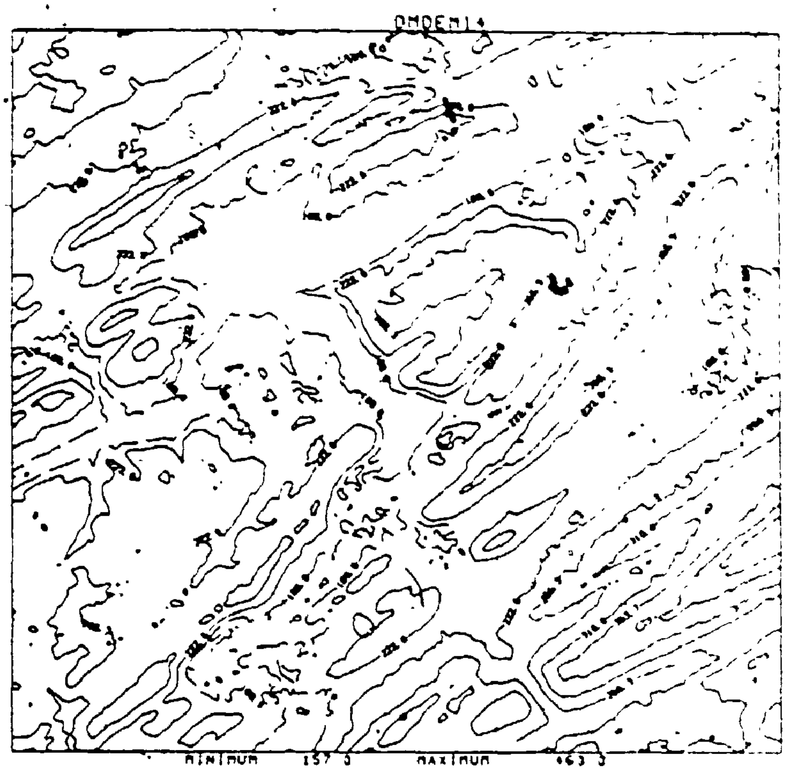
DMDEM14
MINIMUM 157.0
MAXIMUM 463.0

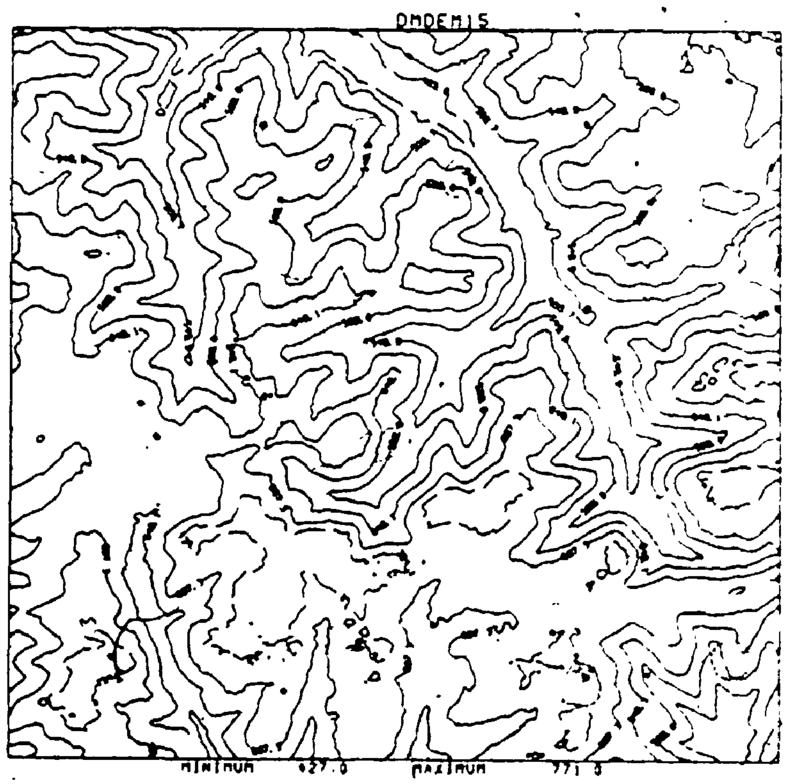
DMDEM15
MINIMUM 427.0
MAXIMUM 771.0

DMDEM16

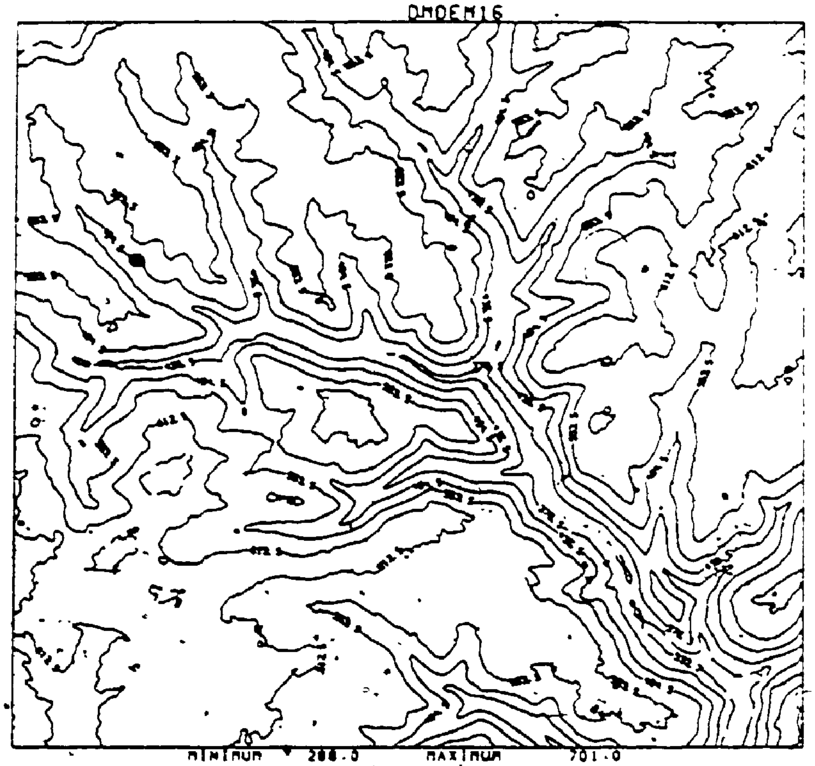

MINIMUM 288.0 MAXIMUM 701.0

DMDEM17

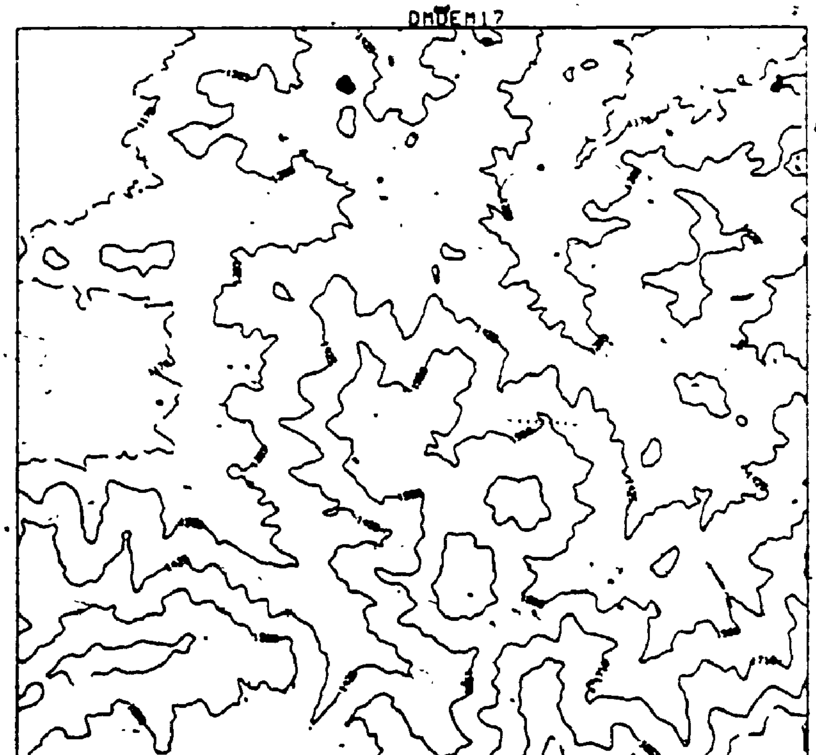

MINIMUM 1069.0 MAXIMUM 2066.0

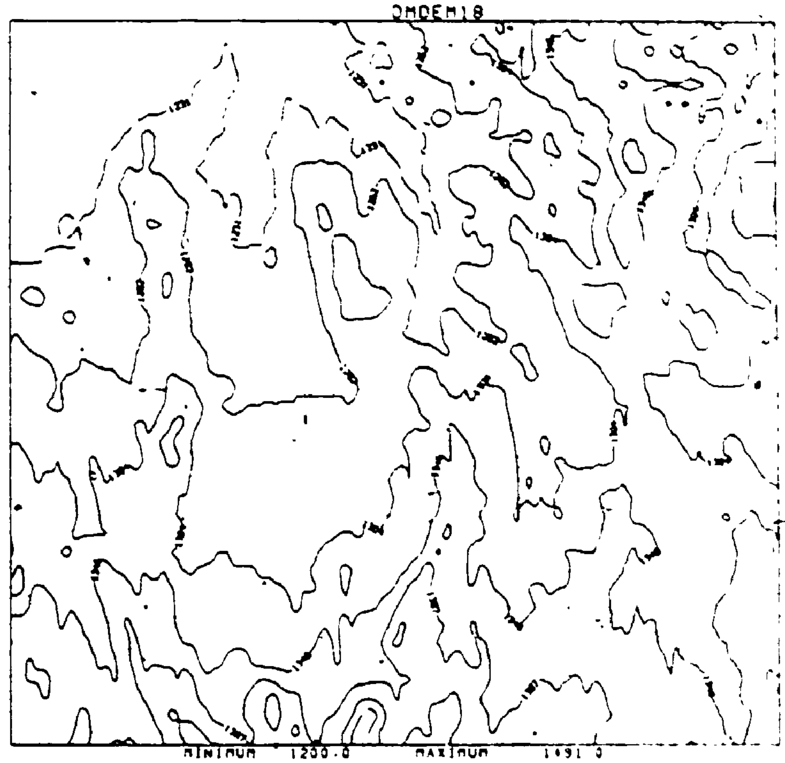

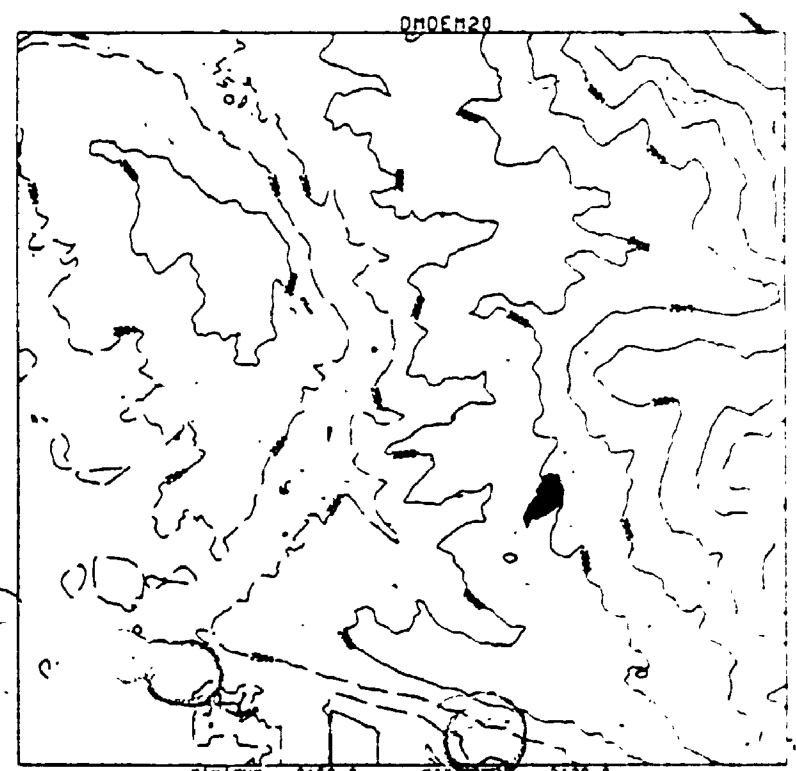

Bibliography

Adler, R. J., 1981. **The geometry of random fields.** New York: John Wiley & Sons.

Agterberg, F. P., 1974. **Geomathematics.** Amsterdam: Elsevier.

Agterberg, F. P., 1982. **Recent developments in geomathematics.** Geo-Processing 2: 1-32.

Aharony, Amnon, 1984. **Percolation, fractals, and anomalous diffusion.** Journal of Statistical Physics 34(5/6): 931-939.

Ahnert, Frank, 1984. **Local relief and the height limits of mountain ranges.** Am. Jour. of Science 284: 1035-1055.

Albers, Donald J., G. L. Alexanderson (eds.), 1985. **Mathematical people.** Boston: Birkhauser.

Albinet, G., G. Searby and D. Stauffer, 1986. **Fire propagation in a 2-D random medium.** Le Journal de Physique 47: 1-7.

Amedeo, D., R. G. Golledge, 1975. **An introduction to scientific reasoning in geography.** New York: John Wiley & Sons, Inc.

Anderle, R., 1987. **Fractal properties of talus slopes.** Paper presented at AAG Annual convention, Portland, OR., 1987.

Anonymous, 1985. **Index to Digital Line Graph (DLG) and Digital Elevation Model (DEM) data.** Reston, VA.: National Cartographic Information Center, U.S.G.S.

Arlinghaus, Sandra Lach, 1985. **Fractals take a central place.** Geografiska Annaler 67B (2): 83-88.

Armstrong, M., L. Hopkins, 1983. **Fractal enhancement for thematic display of topologically stored data.** Proc. Auto-Carto Six, pp. 309-318.

Armstrong, A. C., 1986. **On the fractal dimensions of some transient soil properties.** J. of Soil Science 37: 641-652.

Aviles, C. A., C. H. Scholz and J. Boatwright 1987. **Fractal analysis applied to characteristic segments of the San Andreas fault.** Journal of Geophysical Research 92(B1): 331-344.

Band, Lawrence E., 1986. **Topographic partition of watersheds with digital elevation models.** Water Resources Research 22(1): 15-24.

Barnsley, M. F., S. Demko, 1985. **Iterated function systems and the global construction of fractals.** Proc. R. Soc. Lond. A 399: 243-275.

Bassett, K., R. J. Chorley, 1971. **An experiment in terrain filtering.** Area 3: .

Batty, Michael, 1985. **Fractals -- geometry between dimensions.** New Scientist 4: 31-35.

Batty, Michael, Paul Longley, 1986. **The fractal simulation of urban structure.** Environment and Planning A 18: 1143-1179.

Berry, M. V., J. H. Hannay, 1978. **Topography of random surfaces.** Nature 273: 573.

Berry, M. V., Z. V. Lewis, 1980. **On the Weierstrass-Mandelbrot fractal function.** Proc. R. Soc. Lond. A 370: 459-484.

Boyce, R. B., W. A. V. Clarke, 1964. **The concept of shape in geography.** Geographical Review 54: 561-572.

Bracewell, Ronald N., 1978. **The Fourier transform and its applications.** New York: McGraw-Hill.

Bradbury, R. H., R. E. Reichelt and D. G. Green, 1983. **Fractal dimension of a coral reef at ecological scales.** Mar. Ecol. Progr. Ser. 10: 169-171.

Bradbury, R. H., R. E. Reichelt and D. G. Green, 1984. **Fractals in ecology: methods and interpretation.** Mar. Ecol. Progr. Ser. 14: 295-296.

Brown, S. R., C. H. Scholz, 1985. **Broad bandwidth study of the topography of natural rock surfaces.** Journal of Geophysical research 90: 12,575-12,582.

Brunsden, D., J.C. Doornkamp, D.K.C. Jones, 1978. **Applied geomorphology: A British perspective.** Oxford: Oxford University Press.

Brunsden, D., J. B. Thornes, 1979. **Landscape sensitivity and change.** Trans. of the Inst. of British Geog. NS 4: 463-484.

Burgess, T. M., Webster, R., 1980a. **Optimal interpolation and isarithmic mapping of soil properties I the semi-variogram and punctual kriging.** J. of Soil Science, 31: 315-331.

Burgess, T. M., Webster, R., 1980b. **Optimal interpolation and isarithmic mapping of soil properties II Block kriging.** J. of Soil Science, 31: 333-341.

Burrough, P. A., 1981. **Fractal dimensions of landscapes and other environmental data.** Nature 294: 240-242.

Burrough, P. A., 1983a. **The application of fractal ideas to geophysical phenomena.** Paper presented at a conference organized by the Institute of Mathematics and its Applications 8 June 1983.

Burrough, P. A., 1983b. **Multiscale sources of spatial variation in soil. I. The application of fractal concepts to nested levels of soil variation.** J. Soil Science 34: 577-597.

Burrough, P. A., 1983c. **Multiscale sources of spatial variation in soil. II. A non-Brownian fractal model and its application in soil survey.** J. Soil Science 34: 599-620.

Burrough, P. A., 1985. **The application of fractal ideas to geophysical phenomena.** Bull. of the Inst. Math.

Burroughs, William, 1986. **Randomness rules the weather.** New Scientist 111 (1516): 36-40.

Carpenter, Loren C., 1980. **Computer rendering of fractal curves and surfaces.** SIGGRAPH '80 Conference Proceedings, July, 1980, Seattle, WA.

Chambers, J. M., W. S. Cleveland, B. Kleiner, and P. A. Tukey, 1983. **Graphical methods for data analysis.** Boston: Duxbury Press.

Charlier, Roger H., 1968. **Quantitative analysis, geometrics and morphometrics.** Zeitschrift fur Geomorphologie 12(4): 375-387.

Chorley, R. J., 1969. **The drainage basin as the fundamental geomorphic unit.** In: Chorley, R. J. (ed.) 1969. Water, Earth and Man. London: Methuen & Co. Ltd., pp 77-99.

Chorley, R. J. (ed.), 1972a. **Spatial analysis in geomorphology.** London: Methuen & Co.

Chorley, R. J., 1978. **Bases for theory in geomorphology.** IN: Embleton, C., D. Brunsden and D. K. C. Jones 1978.

Chorley, R. J., B. A. Kennedy, 1971. **Physical geography: A systems approach.** London: Prentice Hall.

Chung, K. L., 1979. **Elementary probability theory with stochastic processes.** New York: Springer-Verlag.

Church, M., D. M. Mark, 1980. **On size and scale in geomorphology.** Prog. Phys. Geog. 4: 342-390.

Clark, Isobel, 1979. **Practical Geostatistics.** London: Applied Science Publishers Ltd.

Clark, N. N. 1986. **Three techniques for implementing digital fractal analysis of particle shape.** Powder Technology 46: 45-52.

Clarke, Keith C., 1986. **Computation of the fractal dimension of topographic surfaces using the triangular prism surface area method.** Computers and Geosciences 12: 713-722.

Clarke, Keith C., 1987. **Scale-based simulation of topography.** Auto-Carto 8: 680-688.

Cox, N., 1977. **Allometric change of land forms: Discussion and reply.** Geol. Soc. Am. Bull. 88: 1199-1202.

Craig, Richard, 1978. **A computer program for the simulation of landform erosion.** Computers and Geosciences 6: 111-142.

Cressie, Noel, Douglas M. Hawkins, 1980. **Robust estimation of the variogram:** I. Math. Geology 12: 115-125.

Culling, W. E. H., 1981. **Stochastic processes.** in Wrigley and Bennett, 1981, pp. 202-211.

Culling, W. E. H., 1985. **Equifinality: Chaos, Dimension and Pattern - The Concepts of Non-linear Dynamical Systems Theory and their Potential for Phys.Geo.** Geography Discussion Papers, New Series No. 19, London School of Economics, London.

Culling, W. E. H., 1986a. **On hurst phenomena in the landscape.** Transaction, Japanese geomorphological union 7: 221-243.

Culling, W. E. H., 1986b. **Highly erratic spatial variability of soil-pH on Iping Common, West Sussex.** Catena 13: 81-89.

Culling, W. E. H., Mark Datko, 1987. **The fractal geometry of the soil-covered landscape.** Earth surface processes and landforms 12: 369-385.

Curl, R. L., 1986. **Fractal dimensions and geometries of caves.** Math. Geology 18: 765-784

Cushman, John H., 1986. **On measurement, scale and scaling.** Water Resources Research 22(2): 129-134.

Dalrymple, J. B., R. J. Blong and A. J. Conacher, 1968. **An hypothetical nine unit landsurface model.** Z. fur Geomorphologie 12: 60-76.

Davidson-Arnott, R. G. D., 1981. **Computer simulation of nearshore bar formation.** Earth Surface Processes and Landforms 6: 23-34.

Davis, John C., 1986. **Statistical and data analysis in geology (2nd ed.).** New York: John Wiley & Sons.

Dell'Orco, P., M. Ghiron, 1983. **Shape representation by rectangles preserving their fractality.** Proc. Auto-Carto Six, pp. 299-308.

Demko, Stephen, Laurie Hodge and Bruce Naylor, 1985. **Construction of fractal objects with iterated function systems.** ACM Siggraph 19(3): 271-276.

Derbyshire, E., K. J. Gregory and J. R. Hails, 1979. **Geomorphological processes.** Folkestone, England: Wm Dawson & Sons Ltd.

Dewdney, A. K., 1985. **Computer recreations.** Scientific American 253: 16-24.

Diaconis, P., B. Efron, 1983. **Computer-intensive methods in statistics.** Scientific American 248(5): 116-130.

Douglas, D. H., 1986. **Experiments to locate ridges and channels to create a new type of digital elevational model.** Cartographica 23(4): 29-61.

Dutton, G. H., 1981. **Fractal enhancement of cartographic line detail.** Amer. Cartog. 8: 23-40.

Dyreson, D., 1978. **Review of Fractals: Form, chance and dimension.** Professional Geographer 30: 420-421.

Eastman, J. Ronald, 1985. **Single-pass measurement of the fractal dimension of digitized carto- graphic lines.**

Elassal, A. A., V. M. Caruso, 1983. **USGS digital cartographic standards. Digital Elevation Models.** U. S. Geological Survey Circular 895-B.

Ellis, T. J., D. Profitt, D. Rosen and W. Rutkowski, 1978. **Measurement of the lengths of digitized curved lines.** College Park, Maryland: Univ. of Maryland Computer Science Center.

Embleton, C., D. Brunsden and D. K. C. Jones (eds.), 1978. **Geomorphology: Future problems and future prospects.** Oxford: Oxford University Press.

Embleton, C., J. B. Thornes (eds.), 1970. **Process in geomorphology.** London: Edward Arnold.

Evans, I. S., 1987. **The Morphometry of specific landforms.** in: Gardiner, V. (ed.), 1987 International Geomorphology 1986 Part II, N.P.: John Wiley & Sons Ltd.

Evans, I. S., 1972. **General geomorphometry, derivatives of altitude, and descriptive statistics. in Chorley, 1972a, p. 1790.**

Falconer, K. J., 1985. **The geometry of fractal sets.** Cambridge: Cambridge University Press.

Feunekes, U., I. R. Methven, 1986. **A cellular fire growth model.** Unpublished paper.

Fournier, A., D. Fussell, 1980. **Stochastic modelling in computer graphics.** SIGGRAPH '80 Conference Proceedings, July, 1980, Seattle, Wa.

Fournier, A., D. Fussell and L. Carpenter, 1982a. **Computer rendering of stochastic models.** Comm. ACM 25: 371-384.

Fournier, A., D. Fussell and L. Carpenter, 1982b. **Author's reply to Comment on computer rendering of fractal stochastic models by B. B. Mandelbrot.** Comm. ACM 25: 583-584.

Fox, Christopher G., Dennis E. Hayes, 1985. **Quantitative Methods for Analyzing the Roughness of the Seafloor.** Reviews of Geophysics 23(1): 1-48.

Frank, Andrew U., Bruce Palmer and Vincent B. Robinson, 1986. **Formal methods for the accurate definition of some fundamental terms in physical geography.** Proceedings, Second International Conference on Spatial Data Handling pp. 583-599.

Frederisksen, Poul, Ole Jacobi and Kurt Kubik, 1985. **A review of current trends in terrain modelling.** ITC Journal 1985-2: 101-106.

Freeman, H., G. G. Pieroni (eds), 1980. **Map data processing.** New York: Academic Press.

Freiberger, W., U. Grenander, 1977. **Surface patterns in theoretical geography.** Computers in Geosciences 3: 547-578.

Frolov, Y. S., D. H. Maling, 1969. **The accuracy of area measurements by point counting techniques.** Cartographic Journal 6: 21-35.

Gardner, M., 1976. **Mathematical games: In which "monster" curves force redefinition of the word "curve".** Scientific American 235(6): 124-133

Gardner, M., 1978. **Mathematical games: White and brown music, fractal curves and one-over-f fluctuations.** Scientific American 237(4): 16-32.

Geisel, T., 1982. **Chaos, randomness and dimension.** Nature 298: 322-323.

Gerrard, A. J., 1984. **Multiple working hypotheses and equifinality in geomorphology: comments on the recent article by Haines-Young and Petch.** Trans. Inst. Br. Geogr. N. S. 9: 364-366.

Gierhart, J. W., 1954. **Evaluation of methods of area measurement.** Surveying and Mapping 14: 460-465.

Gilbert, L. E., 1987. **Are topographic data sets fractal?.** Paper presented at MGUS-87, Redwood City, Ca., 1987.

Gloss, G. H., 1972. **Introduction to thematic cartography.** Course notes, Dept. of Survey Engineering, U.N.B.

Goodchild, M. F., 1979. **The Theory of Kriging: Review and Interpretation.** Unpublished Manuscript: Dept. Geography, University of California.

Goodchild, M. F., 1980a. **The effects of generalization in geographical data encoding in Freeman and Pieroni (1980), pp. 191-205.**

Goodchild, M. F., 1980b. **Fractals and the accuracy of geographical measures.** Mathematical Geology 12(2): 85-98.

Goodchild, M. F., 1981. **PlusX Manual.** Department of Geography, The University of Western Ontario.

Goodchild, M. F., 1982. **The fractional Brownian process as a terrain simulation model.** Modelling and Simulation 13: 1133-1137.

Goodchild, M. F., 1983. **Scientific geography: Utility or elegance?.** The Pittsburgh Geographical and Regional Science sessions Newsletter 1: 12-13.

Goodchild, M. F., 1985. **Questions, tools or paradigms: Scientific geography in the 1980's.** Ontario Geography 25: 3-12.

Goodchild, M. F., 1987. **Lakes on fractal surfaces: A null hypothesis for lake-rich landscapes.** Paper presented at MGUS-87, Redwood City, CA., 1987.

Goodchild, M. F.; A. W. Grandfield, 1983. **Optimizing raster storage: An examination of four alternatives.** Auto Carto 6 2: 400-407.

Goodchild, M. F., B. Klinkenberg, M. Glieca, M. Hasan, 1985. **Statistics of hydrologic networks on fractional brownian surfaces.** Modeling and Simulation 16: .

Goodchild, M. F., D. M. Mark, 1987. **The fractal nature of geographic phenomena.** Annals of the association of American Geographers 77: 265-278.

Goudie, A. (ed.), 1981. **Geomorphological techniques.** London: Allen & Unwin.

Grassberger, P., 1984. **Chaos and diffusion in deterministic cellular automata.** Physica D 10: 52-58.

Gregory, K. J., E. H. Brown, 1966. **Data processing and the study of land form.** Zeitschrift fur Geomorphologie 10: 237-263.

Grenander, U., 1975. **Dynamic models of geomorphological patterns.** Math. Geology 7: 267-278.

Griffin, Mark W., 1987. **A rapid method for simulating three-dimensional fluvial terrain.** Earth surface processes and landforms 12: 31-38.

Hack, J. T., 1957. **Studies of longitudinal stream profiles in Virginia and Maryland.** United States Geological Survey Professional Paper 294B: 45-94.

Haines-Young, R. H., J. R. Petch, 1980. **The challenge of critical rationalism for methodology in physical geography.** Prog. Phys. Geog. 4: 63-78.

Haining, R. P., 1981. **Spatial and temporal analysis: Spatial modelling.** in Wrigley and Bennett 1981, pp. 86-91.

Håkanson, Lars, 1978. **The length of closed geomorphic lines.** Mathematical geology 10: 141-167.

Harbaugh, J. W., G. Bonham-Carter, 1970. **Computer simulation in Geology.** New York: John Wiley.

Hardy, R. L., 1977. **Least squares prediction.** Photogrammetric Engineering and Remote Sensing 43(4): 475-492.

Hartmann, W. K., 1977. **Cratering in the solar system.** Scientific American 237(1): 84-99.

Harvey, D., 1969. **Explanation in Geography.** London: Edward Arnold.

Heil, Richard J., Susan M. Brych, 1978. **The digital terrain model: a tool for quantifying terrain characteristics.** Proceedings, ACSM Fall Convention pp. 156-171.

Hettner, Alfred, 1972. **The surface features of the land. Problems and methods of geomorphology.** (Translated and with a preface by Philip Tilley) London: The MacMillan Press Ltd.

Hill, F. S. Jr., S. E. Walker, Jr., 1982. **On the use of fractals for efficient map generation.** Proceedings, Graphics Interface '82, Toronto, Ont., 17-21 May, 1982.

Hobson, R. D., 1972. **Surface roughness in topography: Quantitative approach. in Chorley, 1972a, p. 221-245.**

Housen, K. R., R. M. Schmidt, 1983. **Crater Ejecta Scaling Laws: Fundamental forms based on dimensional analysis.** Journal of Geophysical Research 88(B3): 2485-2499.

Hugus, Marc K., David M. Mark, 1984. **Spatial data processing for digital simulation of erosion.** Technical papers, 1984 ASP-ACSM Fall Convention, pp. 683-693.

Hutchinson, John E., 1981. **Fractals and self similarity.** Indiana University Mathematics Journal 30(5): 713-747.

Jeffery, Tom, 1987. **Mimicking mountains.** Byte 12: 337-344.

Journel, A.G., 1985. **Geostatistics: Models and tools for the earth sciences.** Mathematical Geology 18(1): 119-140.

Journel, A. G., Ch. J. Huijbregts, 1978. **Mining geostatistics.** London: Academic Press.

Kadanoff, Leo P., 1986. **Fractals: Where's the physics?.** Physics Today, February, 1986.

Kagan, Y. Y., 1981. **Spatial distribution of earthquakes: the three-point moment function.** Geophys. J. R. astr. Soc. 67: 697-717.

Kagan, Y. Y., L. Knopoff, 1980. **Spatial distribution of earthquakes: the two-point correlation function.** Geophys. J. R. astr. Soc 62: 303-320.

Kauffman, S. A., 1984. **Emergent properties in random complex automata.** Physica D 10: 145-156.

Kaye, B. H., 1985. **Harmonious rocks, infinite coastlines and fineparticle science.** mimeograph of forthcoming publication.

Kennedy, Stephen K., Wei-Hsiung Lin, 1986. **Fract -- A fortran subroutine to calculate the variables necessary to determine the fractal dimension of closed forms.** Computers and geosciences 12: 705-712.

Kent, Clement, Jonathon Wong, 1982. **An index of littoral zone complexity and its measurement.** Can. J. Fish Aquat. Sci 39: 847-853.

King, C. A. M., M. J. McCullagh, 1971. **A simulation model of a complex recurved spit.** J. Geol. 79: 22-37.

Kirkby, M. J., 1986. **A two-dimensional simulation model for slope and stream evolution.** unpublished paper.

Kirkby, M. J., 1987. **The hurst effect and its implications for extrapolating process rates.** Earth surface process and landforms 12: 57-67.

Krige, D. G., 1966. **Two-dimensional weighted moving average trend surfaces for ore valuation.** Journal of the S. African Inst. of Mining & Metallurgy: Symposium - Mathematical Statistics & Computer Applications in Ore Evaluation.

Krumbein, W. C., 1976. **Probabilistic modeling in geology. in Merriam, 1976, pp. 39-54.**

Lauzon, J. P., D. M. Mark, L. Kikuchi, and J. A. Guevara, 1985. **Two-dimensional run-encoding for quadtree representation.** Computer vision, graphics and image processing 30: 59-69.

Lavenda, Bernard, 1985. **Brownian Motion.** Scientific American 252(2): 70-85.

Laverty, Martin, 1987. **Fractals in karst.** Earth Surface Processes and Landforms 12: 475-480.

Lawrence, G. R. P., 1979. **Cartographic methods (2nd ed.).** New York: Methuen & Co. Ltd.

Le Mehaute, Alain, 1984. **Transfer processes in fractal media.** Journal of Statistical Physics 36(5/6): 665-676.

Levi, Barbara G., 1986. **New global fractal formalism describes paths to turbulence.** Physics Today, April, pp.17-18.

Lovejoy, S., 1982. **Area-perimeter relation for rain and cloud areas.** Science 216: 185-187.

Lovejoy, S., B. B. Mandelbrot, 1985. **Fractal properties of rain, and a fractal model.** Tellus 37(A): 209-232.

Lovejoy, S., D. Schertzer, 1985. **Generalized scale invariance in the atmosphere and fractal models of rain.** Water Resources Research 21(8): 1233-1250.

Lovejoy, S., D. Schertzer, 1986. **Scale invariance, symmetries, fractals, and stochastic simulations of atmospheric phenomena.** Bulletin American Meteorological Society 67: 21-32.

Lovejoy, S., D. Schertzer, 1987. **Extreme variability, scaling and fractals in remote sensing analysis and simulation.** IN: J. P. Muler (ed.)

Lovejoy, S., D. Schertzer, P. Ladoy, 1986. **Fractal characterisation of inhomogeneous geophysical measuring networks.** Nature 319: 43-44.

Lovejoy, S., D. Schertzer and A. A. Tsonis, 1987. **Functional box-counting and multiple elliptical dimensions in rain.** Science 235: 1036-1038.

Maling, D.H., 1968. **How long is a piece of string?.** Cartographic Journal 5: 147-156.

Mandelbrot, B. B., 1963. **New methods in statistical economics.** The Journal of Political Economy 71(5): 421-440.

Mandelbrot, B. B., 1967. **How long is the coast of Britain? Statistical self-similarity and fractional dimension.** Science 156: 636-638.

Mandelbrot, B. B., 1975a. **Stochastic models for the Earth's relief, the shape and the fractal dimension of coastlines, and the number-area rule for islands.** Pr. of the Nat. Academy of Sciences USA 72: 3825-3828.

Mandelbrot, B. B., 1975b. **On the geometry of homogeneous turbulence, with stress on the fractal dimension of the isosurface of scalars.** J. Fluid Mechanics 72: 401-416.

Mandelbrot, B. B., 1977. **Fractals: Form, chance and dimension.** San Francisco: Freeman.

Mandelbrot, B. B., 1978. **The fractal geometry of trees and other natural phenomena.** Lecture Notes in Biomathematics 23: 235-249.

Mandelbrot, B. B., 1981. **Scalebound or scaling shapes: A useful distinction in the visual arts and in the natural sciences.** Leonardo 14: 45-47.

Mandelbrot, B. B., 1982. **Comment on computer rendering of fractal stochastic models.** Comm. ACM 25: 581-583.

Mandelbrot, B. B., 1983. **The fractal geometry of nature.** San Francisco: Freeman.

Mandelbrot, B. B., 1984a. **Squig sheets and some other squig fractal constructions.** Journal of Statistical Physics 36(5/6): 519-543.

Mandelbrot, B. B., 1984b. **Fractals in Physics: Squig Clusters, Diffusions, Fractal Measures, and the Unicity of Fractal Dimensionality.** Journal of Statistical Physics 34(5/6): 895-929.

Mandelbrot, B. B., 1984c. **On fractal geometry, and a few of the mathematical questions it has raised.** Proceedings of the International Congress of Mathematicians, August 16-24, 1983, pp. 1661-1675.

Mandelbrot, B. B., 1984d. **Additional perspectives on fractals.** College Math Journal 15(2): 115-119.

Mandelbrot, B. B., 1984e. **The Construction of Random Fractals: A Survey and a List of Open Problems.** Stochastic Processes and Their Applications 17(1): 11.

Mandelbrot, B. B., 1985. **Continuous interpolation of the complex discrete Map z z(1-z), and related topics.** Physica scripta T9: 59-63.

Mandelbrot, B. B., 1986a. **Self-Affine fractal dimensions.** Proceedings of the Sixth Triest International Symposium on Fractals in Physics p. 3-15.

Mandelbrot, B. B., 1986b. **Multifractals and fractals.** Physics Today, Sept., pp. 11-12.

Mandelbrot, B. B., Dann E. Passoja and Alvin J. Paullay, 1984. **Fractal character of fracture surfaces of metals.** Nature: 308: 721-722.

Mandelbrot, B. B., John W. Van Ness, 1968. **Fractional Brownian motions, fractional noises and applications.** Siam Review 10(4): 422-437.

Mandelbrot, B. B., James R. Wallis, 1968. **Noah, Joseph, and Operational Hydrology.** Water resources research (4)5: 909-918.

Mann, C. John, 1970. **Randomness in nature.** Geological Society of America Bulletin 81: 95-104.

Mark, D. M., 1975. **Geomorphometric parameters: A review and evaluation.** Geografiska Annaler, Series A 3: 165-177.

Mark, D. M., 1978. **Comments on Freiberger and Grenander's "Surface patterns in theoretical geography".** Computers and Geosciences 4: 371372..

Mark, D. M., 1979a. **Topology of ridge patterns: Randomness and constraints.** Geol. Soc. Am. Bull. 90: 164-172.

Mark, D. M., 1979b. **Review of Fractals: Form, chance and dimension.** GeoProcessing 1: 202-204.

Mark, D. M., 1980. **On scales of investigation in geomorphology.** Can. Geog. 24: 81-82.

Mark, D. M., 1983. **Automated detection of drainage network from digital elevation models.** Auto-Carto 6 (2): 288-298.

Mark, D. M., 1984. **Fractal dimension of a coral reef at ecological scales: a discussion.** Mar. Ecol. Progr. Ser. 14: 293-296.

Mark, D. M., P. B. Aronson, 1984. **Scale-dependent fractal dimensions of topographic surfaces: An empirical investigation, with applications in geomorphology.** Math. Geol.

Mark, D. M., M. Church, 1977. **On the misuse of regression in earth science.** Math. Geol. 9: 63-75.

Mark, D. M., M. F. Goodchild, 1982. **Topological model for drainage networks with lakes.** Water Resources Research 18: 275-280.

Mark, D. M., J. P. Lauzon, 1984. **Linear quadtrees for geographic information systems.** Proceedings, Int. Symp. on Spatial Data Handling, Aug 20-24, Zurich, Switzerland.

Mark, D. M., J. P. Lauzon, 1985. **Approaches for Quadtree-base geographic information systems at continental or global scales.** Auto-carto 7: 355-364.

Mather, P. M., 1972. **Areal classification in geomorphology. in Chorley, 1972a, pp. 305-322.**

Mather, P. M., 1979. **Theory and quantitative methods in geomorphology.** Progress in Physical Geography 3(4): 471-487.

Matheron, G., 1973. **The intrinsic random functions and their applications.** Adv. Appl. Prob. 5: 439-468.

May, R. R., 1975. **Patterns of species abundance and diversity.** IN: Cody, M. L. and J. M. Diamond (eds.) 1975. Ecology and evolution of communities. Madison: University of Wisconsin.

McBratney, A. B., R. Webster, 1986. **Choosing functions for semi-variograms of soil properties and fitting them to sampling estimates.** J. of Soil Science 37: 617-639.

McClure, M., 1985. **Computer illusions: Fractals make mathematical magic in the movies.** Popular computing 4(3): 49-52.

McCullagh, Patrick, 1978. **Modern Concepts in Geomorphology.** Oxford: Oxford University Press.

McDermott, J., 1984. **Geometrical forms known as fractals find sense in chaos.** Smithsonian 14(9): 110-117.

Merriam, D. F. (ed.), 1976. **Random processes in geology.** New York: Springer-Verlag.

Miyazima, Sasuke, H. Eugene Stanley, 1987. **Intersection of two fractal object: Useful method of estimating the fractal dimension.** Physical Review B 35(16): 8898-8900.

Monkhouse, F. J., H. R. Wilkinson, 1973. **Maps and Diagrams (3rd ed.).** London: Methuen & Co. Ltd.

Monmonier, Mark S., 1982. **Computer-assisted cartography: Principles and prospects.** Englewood Cliffs, N.J.: Prentice-Hall, Inc.

Morse, D. R., J. H. Lawton, M. M. Dodson and M. H. Williamson., 1985. **Fractal dimension of vegetation and the distribution of arthropod body lengths.** Nature 314: 731-733.

Moss, M. R., 1983. **Landscape synthesis, landscape processes and land classification: Some theoretical and methodological issues.** GeoJournal 7(2): 145-153.

Moultrie, W., 1970. **Systems, computer simulation, and drainage basins.** Illinois Geog. Soc. Bulletin 12: 29-35.

Muller, J.-C., 1986. **Fractal dimension and inconsistencies in cartographic line representations.** The Cartographic Journal 23: 123-130.

Muller, J.-C., 1987. **Fractal and automated line generalization.** The Cartographic Journal 24: Preprint.

Muller, J. P. (ed.), 1987. **Digital Image Processing In Remote Sensing.** Taylor and Francis, London.

Nittmann, Johann, H. Eugene Stanley, 1986. **Tip splitting without interfacial tension and dendritic growth patterns arising from molecular anisotropy.** Science 321: 663-668.

Nortcliff, Stephen, 1980. **Spatial analysis of soil.** Progress in Physical Geography 8(2): 261-269.

O'Callaghan, J. F., D. M. Mark, 1984. **The extraction of drainage networks from digital elevation data.** Computer vision, graphics and image processing 28: 323-344.

O'Neill, Michael P., David M. Mark, 1985. **The Use of Digital Elevation Models in Slope Frequency Analysis.** Pittsburgh Conference on Modeling and Simulation, pp. 1-8.

O'Neill, Michael P., David M. Mark, 1987. **On The Frequency Distribution of Land Slope.** Earth Surface Processes and Landforms 12: 127-136.

Oommen, John B., R. L. Kashyap, 1983. **Scale preserving smoothing of islands and lakes.** Auto-Carto 6 (2): 243-251.

Orbach, R., 1984. **Dynamics of fractal structures.** Journal of Statistical Physics 36(5/6): 735-748.

Orbach, R., 1986. **Dynamics of fractal networks.** Science 231: 814-819.

Orey, S., 1970. **Gaussian sample functions and the Hausdorff dimension of level crossings.** Z. fur Wahrscheinlichkeitstheorie 15: 249-256.

Pattison, W. D., 1964. **The four traditions of geography.** J. Geog. 63: 211-216.

Pavlidis, T., 1978. **A review of algorithms for shape analysis.** Computer graphics and image processing 7: 243-258.

Peitgen, H.-O., P. H. Richter, 1986. **The beauty of fractals.** Berlin: Springer-Verlag.

Pentland, Alex P., 1983. **Fractal-based description.** Proc. of IJCAI 83: 973-981.

Pentland, Alex P., 1984. **Fractal-based description of natural scenes.** IFFE PAMI 6(6): 661-674.

Perkal, J., 1966. **On the length of empirical curves (Trans. by R. Jackowski from Zastoscwania Matematyki 3: 257-286,1958).** Michigan InterUniversity Comm. of Math. Geog. Disc. Paper No.10.

Pfeifer, Peter, David Avnir and Dina Farin, 1983. **Ideally Irregular Surfaces, of Dimension Greater Than Two, in Theory and Practice.** Surface Science 126: 569-572.

Philip, G. M., D. F. Watson, 1986a. **Matheronian Geostatistics--Quo Vadis?.** Mathematical Geology 18(1): 93-117.

Philip, G. M., D. F. Watson, 1986b. **"Matheronian Geostatistics--Quo Vadis?".** Mathematical Geology 18(5): 501-509.

Pielou, E. C., 1977. **Mathematical ecology.** New York: John Wiley & Sons.

Pike, R. J., 1986. **Variance spectra of representative 1: 62,500-scale topographies: A terrestrial calibration for planetary roughness at 0.3 km to 7.0 km.** Lunar and Planetary Sciences 17: 668-669.

Pike, R. J., 1987a. **The geometric signature: Quantifying landslide-terrain types from Digital Elevational Models.** Paper present at the MGUS-87 conference, Redwood City, CA., 1987.

Pike, R. J., 1987b. **Information content of planetary terrain: Varied effectiveness of parameters for the Earth.** Lunar and Planetary Science 18: 778-779.

Pike, R. J., 1987c. **Toward geometric signatures for planetary terrain: An assessment of the Earth at 1: 24,000 scale.** Lunar and Planetary Science 18: 780-781.

Pike, R. J., W. J. Rozema, 1975. **Spectral analysis of landforms.** Annals of the AAG 65: 499-516.

Pitty, A. F., 1968. **Some comments on the scope of slope analysis based on frequency distributions.** Zeitschrift fur Geomorphologie 12: 350-355.

Pitty, A. F., 1971. **Introduction to geomorphology.** London: Methuen & Co Ltd.

Pollack, Andrew, 1985. **Math Technique Turns Chaos Into Order.** New York Times, Tuesday, January 22.

Power, W. L., T. E. Tullis, S. R. Brown, G. N. Boitnott, and C. H. Scholz, 1987. **Roughness of natural fault surfaces.** Geophysical Research Letters 14: 29-32.

Preston, K., 1984. **Four-dimensional logical transforms: Data processing by cellular automata.** Physica D 10: 205-212.

Price, W. E., 1976. **A random-walk simulation model of alluvial-fan deposition in Merriam, 1976, pp. 55-62.**

Raisz, E. 1957. **Landforms of the United States.** Cambridge, Mass.: Self published.

Richardson, L. F., 1961. **The problem of contiguity: An appendix to 'Statistics of deadly quarrels'.** General Systems Yearbook 6: 139-187.

Ripley, B. D., 1981. **Spatial statistics.** New York: John Wiley & Sons.

Robinson, Arthur H., Barbara B. Petchenik, 1976. **The nature of maps.** Chicago: The University of Chicago Press.

Ross, Benjamin, 1986. **Dispersion in fractal fracture networks.** Water Resources Research 22(5): 823-827.

Roy, Andre, Ginette Gravel and Celine Gauthier, 1987. **Measuring the Dimension Of Surfaces: A Review And Appraisal Of Different Methods.** Proceedings Auto-Carto 8: 68-77.

Sager, Thomas W., 1982. **Nonparametric maximum likelihood estimation of spatial patterns.** Annals of Statistics 10: 1125-1136.

Sander, Leonard M., 1986. **Fractal growth processes.** Nature 322: 789-794.

Saperstein, Alvin M., 1984. **Chaos -- a model for the outbreak of war.** Science 309: 303-305.

Savigear, R. A. G., 1965. **A technique of morphological mapping.** Annals AAG 55: 514-538.

Sayles, R. S., T. R. Thomas, 1976. **Surface topography as a nonstationary random process.** Nature 271: 431-434.

Sayles, R. S., T. R. Thomas, 1978. **Sayles and Thomas reply.** Nature 273: 573.

Schenck, Jr., Hilbert, 1963. **Simulation of the Evolution of Drainage-Basin Networks with a Digital Computer.** Journal of Geophysical Research 68(20): 5739-5745.

Scholz, C. H., C. A. Aviles, 1986. **The fractal geometry of faults and faulting.** Earthquake Source Mechanics (Geophysical Monograph 37) M. Ewing Ser. 6.

Schwarz, H., H. E. Exner, 1980. **The implementation of the concept of fractal dimension on a semi-automatic image analyser.** Powder Technology 27: 207-213.

Scott, R. M., M. P. Austin, 1971. **Numerical classification of land systems using geomorphological attributes.** Australian Geographical Studies 9: 33-40.

Seginer, I., 1969. **Random walk and random roughness models of drainage networks.** Water Resources Research 5: 591-607.

Shelberg, M. C., H. Moellering and N. S. Lam, 1982. **Measuring the fractal dimensions of empirical cartographic curves.** Proc. AutoCarto V/ ISPRS IV Symposium, pp. 481-490.

Shelberg, M. C., H. Moellering and N. S. Lam, 1983. **Measuring the fractal dimensions of surfaces.** Proc. Auto-Carto Six, pp. 319-328.

Shelberg, M. C., H. Moellering, 1983. **IFAS: a program to measure fractal dimensions of curves and surfaces.** Proceedings ACSM, 43: 483-492.

Skoda, G., 1987. **Fractal dimension of rainbands over hilly terrain.** Meteorol. Atmos. Phys. 36: 74-82.

Small, R. J., 1978. **The study of landforms: A textbook of geomorphology (2nd ed).** Cambridge: Cambridge University Press.

Smart, J. S., C. Werner, 1976. **Applications of the random model of drainage basin composition.** Earth Surface Processes 1: 219-233.

Smart, J. S., 1968. **Statistical Properties of Stream Length.** Water Resources Research 4(5): 1001-1014.

Sorensen, P. R., 1984. **Fractals.** Byte 9(10): 157-172.

Speight, J. G., 1971. **Log-normality of slope distributions.** Zeitschrift fur Geomorphologie 15: 290-311

Sprunt, B. F., 1972. **Digital simulation of drainage basin development in Chorley, 1972a, pp. 371-389.**

Steinhaus, H., 1954. **Length, Shape and Area.** Colloquium Mathematicum 3: 1-13.

Steinhaus, H., 1969. **Mathematical Snapshots (3rd American ed.).** New York: Oxford University Press.

Steyn, D. G., K. W. Ayotte, 1985. **Application of two-dimension terrain height spectra to mesoscale modeling.** J. of Atmospheric Sciences 42: 2884-2887.

Strahler, Arthur N., 1952. **Hypsometric (Area-altitude) analysis of erosional topography.** Bull. of the Geological Soc. Am. 63: 1117-1142.

Thornes, J. B., 1978. **The character and problems of theory in contemporary geomorphology.** IN: Embleton, C., D. Brunsden and D. K. C. Jones 1978.

Thornes, J. B., 1979. **Processes and interrelationships, rates and changes in Embleton and Thornes, 1979, pp. 378-387.**

Thornes, J. B., D. Brunsden, 1977. **Geomorphology and Time.** London: Methuen.

Waymire, Ed, 1985. **Scaling limits and self-similarity of precipitation fields.** Water Resources Research 21(8): 1271-1281.

Webster, R., T.M. Burgess, 1980. **Optimal Interpolation and Isarithmic Mapping of Soil Properties III Changing Drift and Universal Kriging.** Journal of Soil Science 31: 505-524.

Werner, Christian, 1982. **The distribution of tributaries in drainage networks according to Horton, Shreve, and nature.** Modeling and Simulation 13: 1139-1145.

Werner, Christian, 1982. **Analysis of Length Distribution of Drainage Basin Perimeter.** Water Resources Research 18(4): 997-1005.

Werritty, A., 1972. **The topology of stream networks. in Chorley, 1972, p. 167-196.**

Wheeler, J. O., 1978. **Bibliography on geographic thought, philosophy, and methodology.** Occasional Paper No. 3, University of Georgia, Athens, Georgia.

White, Ellen R., 1985. **Assessment of Line-Generalization Algorithms Using Characteristics Points.** The American Cartographer 12(1): 17-27.

Whittle, P., 1954. **On stationary processes in the plane.** Biometrika 41: 434-449.

Williams, P. W., 1972. **The analysis of spatial characteristics of karst terrains in Chorley, 1972a, p. 167-196.**

Willson, S. J., 1984. **Growth rates and fractional dimensions in cellular automata.** Physica D 10: 69-74.

Wilson, E. Bright, 1986. **One hundred years of physical chemistry.** American Scientist 74: 70-77.

Woldenberg, M. J. (ed.), 1985. **Models in geomorphology.** Winchester, Mass.: Allen & Unwin, Inc.

Wolfram, S., 1984. **Universality and complexity in cellular automata.** Physica D 10: 1-35.

Woronow, A., 1981. **Morphometric consistency with the Hausdorff-Besicovitch dimension.** Math. Geology 13: 201-216.

Wrigley, N., R. J. Bennett (eds.), 1981. **Quantitative geography: A British view.** London: Routledge & Kegan Paul.

Young, G. S., R. A. Pielke and R. C. Kessler, 1984. **A comparison of the terrain height variance spectra of the Front Range with that of a hypothetical mountain.** J. of the Atmospheric Sciences 41: 1249-1250.

Young, G. S., R. A. Pielke, 1983. **Application of terrain height variance spectra to mesoscale modeling.** J. of the Atmospheric Sciences 40: 2555-2560.

Zar, J. H., 1968. **Calculation and miscalculation of the allometric equation as a model in biological data.** Bioscience 18: 1118-1120.

Zar, J. H., 1984. **Biostatistical Analysis, second edition**. Englewood Cliffs, N. J.: Prentice-Hall, Inc.

Zevenbergen, Lyle W., Colin R. Thorne, 1987. **Quantitative Analysis of Land Surface Topography.** Earth Surface Processes and Landforms 12: 47-56.